



Doctoral Thesis

Form-Driven Design of Bending-Active Tensile Structures in Architecture

Author(s):

Boulic, Léa

Publication Date:

2019

Permanent Link:

<https://doi.org/10.3929/ethz-b-000421084> →

Rights / License:

[In Copyright - Non-Commercial Use Permitted](#) →

This page was generated automatically upon download from the [ETH Zurich Research Collection](#). For more information please consult the [Terms of use](#).

DISS. ETH NO. 26473

Form-Driven Design of Bending-Active Tensile Structures in Architecture

A thesis submitted to attain the degree of
DOCTOR OF SCIENCES of ETH ZURICH
(Dr. sc. ETH ZURICH)

presented by
LÉA, CAROLINE, CÉLESTINE BOULIC

Diplôme d'Ingénieur, École Centrale de Nantes
Diplôme d'État d'Architecte, École Nationale Supérieure d'Architecture de Nantes

born on 18.06.1990
citizen of France

accepted on the recommendation of
Prof. Dr. Joseph Schwartz (ETH Zurich)
Prof. Dr. Juan José Castellón (Rice University)

2019

Contents

Abstract	v
Zusammenfassung	vii
Résumé	ix
1 Introduction	1
1.1 Material-driven hybrid structural systems	1
1.2 Research overview	11
2 Research Framework	15
2.1 Research context	15
2.2 Research scope	45
3 Structural Model	51
3.1 Bending-active beams in 2D space	51
3.2 Shaping bending-active beams by adjusting their bending stiffness	62
3.3 Shaping bending-active beams with external restraining forces .	74
3.4 On the extension to 3D space	87
4 Design Approach	99
4.1 Form-driven design approach	99
4.2 Graphical construction of restraining cable nets	105
4.3 Geometric patterns of restraining cables	119
4.4 Form-finding of restraining cable nets	125
5 Design Application	139
5.1 A bending-active tensile sun-shading façade system	140
5.2 Application of the form-driven design approach	143
5.3 Geometric studies	146
5.4 Parametric models	151
5.5 Material investigation	156

5.6 Observations	163
6 Conclusion	165
6.1 Contributions	165
6.2 Limitations and further developments	169
6.3 Overview and final discussion	172
References	177
List of Figures	193
Acknowledgments	201

Abstract

Resulting from the reciprocal interaction of slender beams, which are actively bent, and cables or membranes, which are pre-stressed, bending-active tensile structures attract growing interest due to their various qualities. These structures have expressive curved shapes, are lightweight and can be assembled quickly, thus allowing the construction of innovative small and medium-scale structures such as temporary pavilions. Their equilibrium geometry, however, is complex and difficult to predict. The form-finding methods currently available for the design of bending-active tensile structures generally limit the designer's influence on the final equilibrium geometry and make the design process less intentional. In order to overcome this restriction and achieve seamless integration of architectural and structural design, this research introduces a novel approach to the design of bending-active tensile structures in architecture.

The proposed approach allows to define the bending-active beams directly in their equilibrium geometry thus providing the designer explicit control on the overall geometry of the bending-active tensile structures. This is made possible by breaking up the complex problem of form-finding bending-active tensile structures into simpler sub-problems, and successively addressing the equilibrium of the bending-active beams and that of the pre-stressed cables or cable nets. The control of the overall geometry of the bending-active tensile structures is achieved with a twofold strategy. On the one hand, through the differentiation, along the beams' axis, of their bending stiffness; on the other hand, through the control of the forces applied on the beams' axis via the pre-stressed restraining cables.

In the present work, a novel structural model of slender beams is first defined based on a simplified mechanical model and the use of form and force diagrams. This structural model facilitates the understanding of the mechanisms involved in the static equilibrium of a bending-active beam in 2D space. It thus makes it possible to control its static equilibrium, particularly from a geometric standpoint. Moreover, a form-driven design approach is formulated and its different procedures are elaborated. In particular, the equilibrium of the bending-active beams in their desired equilibrium geometry is analysed by means of the introduced structural model, and several specific graphical and numerical methods are developed to address the equilibrium of the cables and cable nets connected to them. Finally, the potential of the approach is demonstrated in a real archi-

tectural context by the design of a bending-active tensile structure that acts as a sun-shading system for the glazed façade of an office building.

Zusammenfassung

Biegeaktive, zugbeanspruchte Strukturen basieren auf dem wechselseitigen Zusammenwirken schlanker Balken, welche aktiv gebogen und mit Seilen oder Membranen vorgespannt werden. Aufgrund ihrer vielfältigen Eigenschaften stossen sie auf ein stetig wachsendes Interesse. Diese Strukturen sind geprägt von ausdrucksstarken gekrümmten Formen, ausserdem sind sie äusserst leicht und schnell zusammenbaubar, was die Realisierung innovativer kleiner und mittlerer Konstruktionen, wie temporäre Pavillons, ermöglicht. Ihre Gleichgewichtsgeometrie ist jedoch komplex und schwer vorhersehbar. Die derzeit verfügbaren Formfindungsmethoden für den Entwurf biegeaktiver, zugbeanspruchter Strukturen begrenzen allgemein den Einfluss des Entwerfers auf die endgültige Gleichgewichtsgeometrie, so dass der Entwurfsprozess nur bedingt kontrollierbar erscheint. Um diese Einschränkung zu überwinden und eine nahtlose Integration von architektonischem und tragwerkstechnischem Entwurf zu erreichen, stellt die vorliegende Forschung einen neuen Ansatz für den Entwurf biegeaktiver, zugbeanspruchter Strukturen in der Architektur vor.

Der vorgeschlagene Ansatz erlaubt es, die biegeaktiven Balken direkt in ihrer Gleichgewichtsgeometrie zu definieren, wodurch der Entwerfer eine explizite Kontrolle über die globale Geometrie von biegeaktiven, zugbeanspruchten Strukturen erhält. Dies wird ermöglicht, indem das komplexe Problem der Formfindung von biegeaktiven, zugbeanspruchten Strukturen in einfachere Teilprobleme zerlegt wird und das Gleichgewicht für die biegeaktiven Balken und die vorgespannten Seile oder Seilnetze nacheinander erzeugt wird. Die Kontrolle der globalen Geometrie wird mit einer Doppelstrategie erreicht. Einerseits durch die Differenzierung der Biegesteifigkeit entlang der Balkenachse, andererseits durch die gezielte Kontrolle der Kräfte, die über die vorgespannten Seile auf die Balkenachse wirken.

In der vorliegenden Arbeit wird zunächst ein neuartiges Tragwerksmodell von schlanken Balken definiert, das auf einem vereinfachten mechanischen Modell und der Verwendung von Lage- und Kräfteplänen basiert. Dieses Modell erleichtert das Verständnis der Phänomene, die zur Erzeugung des statischen Gleichgewichts eines biegeaktiven Balkens in zwei Dimensionen wirken. Es ermöglicht somit die Kontrolle des statischen Gleichgewichts von einem geometrischen Standpunkt aus. Darüber hinaus wird ein formorientierter Entwurfsansatz formuliert und dessen unterschiedlichen Verfahren detailliert dargestellt.

Das eingeführte Tragwerksmodell wird insbesondere zur Erzeugung des Gleichgewichts von biegeaktiven Balken verwendet, während verschiedene, speziell entwickelte grafische und numerische Methoden dazu dienen, das Gleichgewicht mit den verbindenden zugbeanspruchten Elementen zu untersuchen. Das Potenzial des Ansatzes wird schliesslich in einem realen architektonischen Kontext durch den Entwurf einer biegeaktiven, zugbeanspruchten Struktur für ein Sonnenschutzsystem einer verglasten Bürogebäudefassade vorgeführt.

Résumé

Issues de l'interaction réciproque de poutres élancées initialement droites et activement fléchies et de câbles ou de membranes tendus, les structures tendues à flexion active font l'objet d'un intérêt grandissant du fait de leurs diverses qualités. Légères, rapidement assemblées, à l'esthétique aérienne et dotées de formes courbes expressives, elles permettent la construction de structures innovantes de petite et moyenne échelle telles que des pavillons temporaires. Leur géométrie est néanmoins complexe et difficilement prédictible. Les méthodes de recherche de forme actuellement disponibles pour la conception des structures tendues à flexion active tendent à restreindre l'influence du concepteur sur la géométrie d'équilibre des structures générées et à rendre le processus de conception peu intentionnel. Dans le but de dépasser cette limitation et de réussir une intégration plus forte l'une à l'autre des conceptions architecturale et structurelle, cette recherche introduit une nouvelle approche de conception des structures tendues à flexion active en architecture.

En décomposant le problème complexe de recherche de forme des structures tendues à flexion active en sous-problèmes plus simples, et en abordant successivement l'équilibre des poutres activement fléchies et celui des éléments tendus, l'approche proposée permet de définir les poutres activement fléchies directement dans leur géométrie d'équilibre et fournit ainsi au concepteur un contrôle explicite de la géométrie globale des structures tendues en flexion active. Ce contrôle s'opère selon une double stratégie : d'une part, par la différenciation, le long de l'axe des poutres, de leur raideur de flexion, et d'autre part, par le contrôle des efforts exercés sur l'axe des poutres par les éléments tendus.

Dans le travail ici présenté, un nouveau modèle structurel des poutres élancées est d'abord défini à partir d'un modèle mécanique simplifié et de l'utilisation de diagrammes de forme et de forces. Ce modèle structurel facilite la compréhension des mécanismes impliqués dans l'équilibre statique d'une poutre activement fléchie dans le plan et permet ainsi d'en contrôler l'équilibre statique, notamment du point de vue géométrique. Dans un deuxième temps, une approche de conception dite axée sur la forme est formulée et ses différentes procédures sont détaillées. En particulier, le modèle structurel introduit sert à résoudre l'équilibre des poutres activement fléchies, tandis que plusieurs méthodes graphiques et numériques sont spécifiquement développées pour aborder l'équilibre des éléments tendus qui leur sont connectés. Enfin, le potentiel de l'approche est démontré

dans un contexte architectural réel par la conception d'une structure tendue à flexion active ayant pour fonction la protection solaire des façades vitrées d'un bâtiment de bureau.

1. Introduction

1.1 Material-driven hybrid structural systems

As a consequence of the distinction between the disciplines of architecture and engineering, form and structure tend to be addressed independently during the architectural design process: first the geometric definition of forms, often without real structural consideration and emanating above all from a purely formal process, and then the structural analysis of the defined forms. In this context, on the one hand, the constructed form does not express how the forces flow within the structure and, on the other hand, large sections of material are often required to withstand the bending stresses that are generated. In this sense, the geometric description of the form takes precedence over its physical and structural reality and the material is often considered as a secondary and passive instance in the design process, attributed to geometrically defined elements and serving the form to meet mechanical and aesthetic requirements.

Material-driven structural forms Another design approach is possible, in which form and structure are considered jointly and equally, as in natural systems, whose form results from the translation of the physical laws that underlie them. Inspired by this observation, particularly with regard to biological organisms (studies by D'Arcy Thompson (Thompson 1917) and Robert Le Ricolais (Le Ricolais 1973) among others), a growing interest in structural morphology (Motro 2009) has developed over the 20th century among architects and engineers. The understanding of the fundamental relationships between the form of a structure and the forces that act on it or can be transferred by it has been the starting point for many explorations and advances in the field of structural systems, breaking with the structural typologies that existed until then. In particular, intense and prolific research in structural morphology has led to alternative principles of lightweight construction according to which a structural system derives its strength from its specific form and not from the accumulation of matter.

If Vladimir Shukhov's projects of tensile roofs and hyperbolic towers at the beginning of the 20th century were the precursors of this research in structural morphology, it is from the 1950s onwards that the most remarkable lightweight

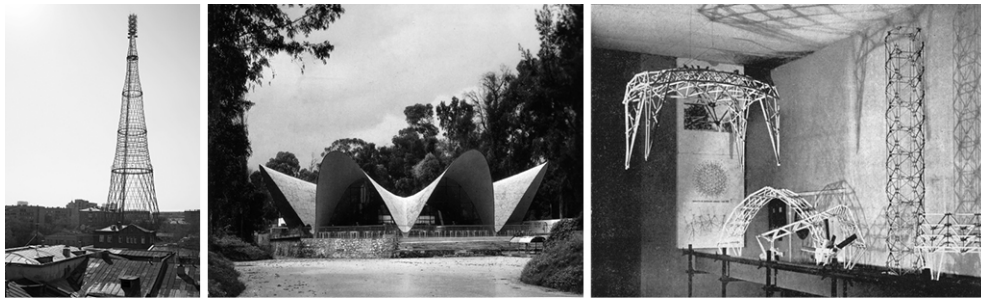


Figure 1.1: Lightweight structures – (from left to right) Hyperbolic tower by Vladimir Shukhov (1922), *Los Manantiales* shell structure by Félix Candela (1958) and models by Robert Le Ricolais (1945).

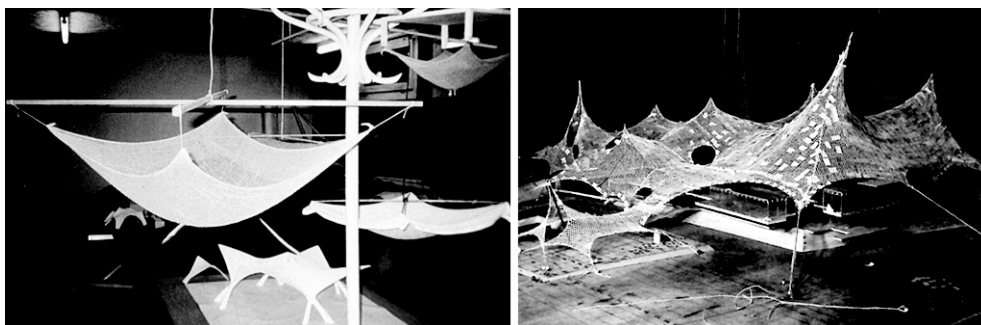


Figure 1.2: Physical form-finding models – (left) Hanging models by Heinz Isler (1981) and (right) textile membranes and rope nets model for the *German Pavilion 67* by Frei Otto (1965).

structures have been built by figures like Buckminster Fuller, Félix Candela, Heinz Isler and Frei Otto (Figure 1.1). Their interdisciplinary teams of architects and engineers have contributed to the development of structural concepts based on the equilibrium of forces and the optimum use of the specific capacities of materials and, consequently, to the necessary form-finding techniques. There, the use of the physical model, as already initiated in the 1900s by Antoni Gaudí with his network of hanging chains for the design of the stone church of Colònia Güell (Huerta 2006), proved to be successful. By deforming flexible bodies under the effect of a force field, the forms of innovative structures emerge on their own as a result of the flow of forces (Figure 1.2). Frei Otto's contribution is exemplary in introducing this paradigm shift in which an approach based on a process of form emergence replaces a top-down design approach: it is then the material, its specific mechanical properties, that informs the structure and its geometry. In this way, the design is not imposed on the material, but rather the result of the interaction between material, geometry and boundary conditions.

Lightweight tensile structures Frei Otto's work on tensile roof structures marked a breakthrough in the generation of lightweight structures and provides an eloquent example of this new design approach and the role of physical models. His extensive research in the field of tensile structures supported by masts and

Übersicht der aus Selbstbildungsprozessen hervorgehenden Konstruktionen geordnet nach den sie erzeugenden Kräften
Overview of the structures which develop from self-forming processes, classified according to the generating forces

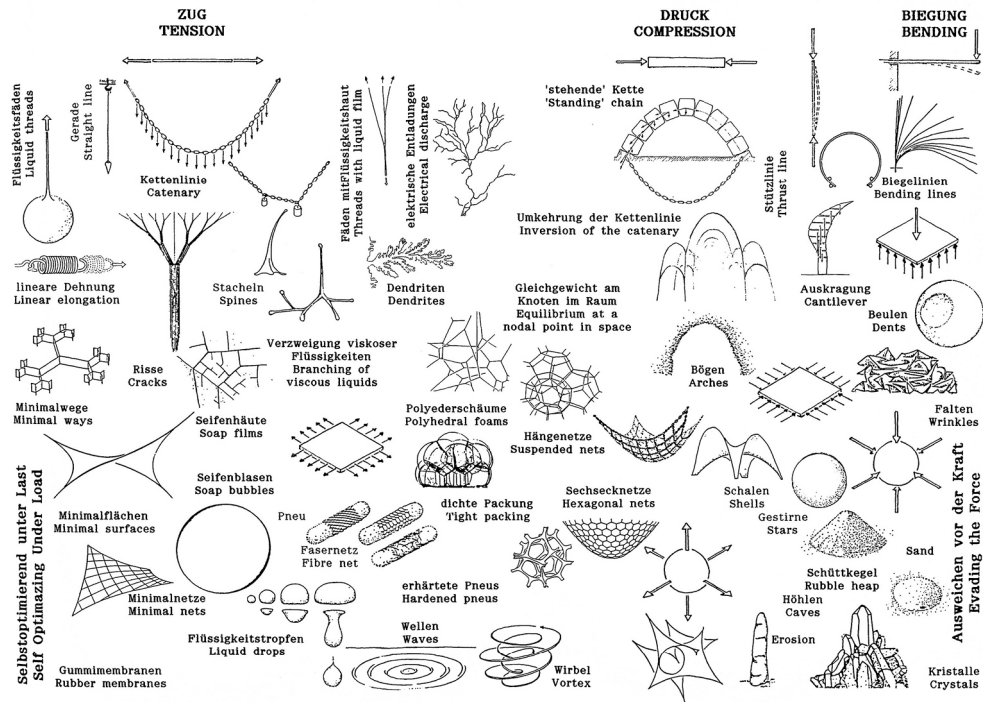


Figure 1.3: Classification of self-forming processes according to the generating forces by Frei Otto (Gass 1990)

cables was grounded on tensile stresses (Roland 1965). Always preferable to compression and bending, which induce structures with thick structural members, tension leads indeed to thin and lightweight constructions. Built from textile membranes or cable nets, tensile structures are surface structural systems with an anticlastic curvature. They are characterised by their ability to resist external loading through an increased tension in their doubly curved surface, which is in turn resisted by compression and bending in the supporting elements. The geometry of a tensile surface is determined by the magnitude of the forces which flow in it, but at the same time, these forces can only be calculated from the surface's geometry. No mathematical equation can explicitly define the geometry of a tensile surface and the vicious circle between forces and geometry can only be solved by a very large number of complex and iterative calculations, much too complex for the computers then available in the 1960s and 1970s. The *German Pavilion 67* in Montreal (1967) designed by Frei Otto and Rolf Gutbrod and the roofs of the *Munich Olympic Park* (1972) designed with Günther Behnisch and Fritz Auer are two emblematic structures that have made Frei Otto famous. They were entirely designed from a meticulous work on physical form-finding scale models to determine the distribution of forces and to measure the equilibrium geometry to be enlarged at real scale.

Bending as a self-forming process Frei Otto's studies on physical models were not limited to tensile structures, and throughout the second half of the 20th century, he and his team at the Institute for Lightweight Structures at the University of Stuttgart conducted extensive research on abiotic self-forming processes (Gass 1990). Just like tension and compression, he identifies bending as the generating force of a self-forming processes (Figure 1.3). Indeed, under the action of bending and provided they are sufficiently elastic, slender structural elements deform without breaking. The curved geometries they adopt derived from their geometric and material characteristics and the forces to which they are subjected. The structures so generated are very lightweight due to the slenderness of their bent elements. The curved geometry causes an increase in the structural stiffness of the bent elements allowing the activation of their very thin sections. Such intentional use of bending for structural and formal purposes was later referred to as "active bending" (Lienhard 2014). This formation process is widely implemented empirically and pragmatically as a structural principle in many vernacular architectural constructions which use plant stems (branches, reeds, bamboos and other grass species) to create arches and shells (Figure 1.4).

For his part, Frei Otto was mainly interested in active bending as a means of erecting and forming grid-shell structures from flat grids of slender linear beams. The overall geometry of these grid-shells, which is doubly curved, was established independently from the bending phenomenon, by hanging chain models, as in the case of the timber structure of the *Multihalle Mannheim*, designed by Frei Otto in collaboration with Edmund Happold in 1975 (Burhardt 1978). Active bending remained then for some decades outside the field of structural engineering, due to a lack of appropriate numerical methods and tools and probably also to a mistrust of such structures among engineers. Recently, driven by the development of new simulation methods and digital design tools and a growing interest in design approaches where the shape emerges from the properties of the building materials (Menges 2012), active bending has received increasing attention, specifically in academia. In particular, the research of the ITKE Institute of the University of Stuttgart, including the doctoral research of Julian Lienhard (Lienhard 2014), has led to the design of several small and medium-scale pavilions which, thanks to their prospective nature, contributed to establishing the structural and architectural potential of structures using bending as a formation strategy.

Hybrid structural systems The introduction of active bending as a structural principle in the field of structural engineering and academia has been achieved partly through research aimed at integrating flexible elements into tensile structures (Barnes 2000, Adriaenssens and Barnes 2001, Off 2010). In fact, often in the design of tensile structures, supporting structural elements additional to the membranes or the cable nets are involved, principally in the form of rigid masts and cables. The masts are then subjected to compressive forces that compensate



Figure 1.4: Bending as a self-forming process – (right) Construction of a traditional mudhif house from plant stems (Iraq) and (left) *Elastica* curve by Euler (Euler 1744)

for the tensile forces acting in the membranes or the cable nets. The integration of flexible elements within membranes and cable nets thus ensures the necessary compressive forces for their tensioning. This co-action principle between tensile and compressive elements is the same, for example, as that used by the tensegrity structures (Figure 1.5) developed by Kenneth Snelson and Buckminster Fuller (Marks 1960, 55-64; Fuller 1975, 369-411): the introduction of compressive elements into a continuum of membranes or cables allows very lightweight structures to be put under tension, which can then be risen and cover large spans. Membranes integrating flexible elements and tensegrity structures are defined as hybrid structures according to the classification of structural systems proposed by Heino Engel (Engel 1967); “the redirection of forces is effected through the co-action of two or several – in their structural function basically equipotent – mechanisms from different structures “families””.

Hybrid bending-active tensile structures Bending-active tensile structures (Slabbinck et al. 2017), also known as “textile hybrids” (Ahlquist et al. 2013), are defined as the co-action of bending-active elements, which play the role of compressive elements, and tensile elements within the same structural system. The slenderness of the bending-active elements necessary for their bending and the restraining effect of the tensile elements leads to very lightweight structures. The *Oval Intention* geodesic dome tent put on the market by *The North Face* company in 1975 and whose design was based on the ideas and assistance of Buckminster Fuller (Hamilton 2017) can be considered as one of the first structures where the mutual interaction between actively bent and pre-stressed elements is intentionally addressed in the sense of Hengel’s co-action principle (Figure 1.6).

The simplicity and economy of means by which curved forms can be produced, the performance, adaptability and lightness of bending-active tensile structures as well as their formal expressiveness are reasons that explain the interest they arouse. Yet, few bending-active tensile architectural structures have been designed and built outside academia. The reason for this lack of enthusiasm cer-



Figure 1.5: Lightweight hybrid structural systems – (left) Tensegrity sphere hold by Buckminster Fuller (1979) and (right) membrane tensegrity *Temporary Pavilion* in Noda Kazuhiro Kojima + Kojima Laboratory, Tokyo University of Science (2011) (*Temporärer Pavillon in Noda / Temporary Pavilion in Noda* 2012).



Figure 1.6: Hybrid bending-active tensile structures – (left) *Geodome 4* tent by the North Face company (2018), (right) *Isoropia* structure by CITA and collaborators (2018).

tainly stems, on the one hand, from the reluctance of architects and engineers who have limited knowledge and experience with these structures and, on the other hand, from the challenges associated with the design and formation process which must be simulated through a non-linear and complex analysis and requires appropriate numerical methods and digital tools (Kelly et al. 2001).

Form-designing versus form-finding and form-steering The design of bending-active tensile structures, like that of any other structural system whose geometry can only be established by means of a form-finding process, raises the question of the role of the designer and his/her degree of influence on the formation process. Form-finding, whether analog or digital, must indeed be understood as a deterministic process during which the definition of a set of conditions, both related to the structural system itself (material properties, cross-sections, stress states, topology, etc.) and to its environment (support conditions, loads, etc.), leads to a specific geometry. Faced with the uniqueness

of this solution and the superiority of the physical rules that determine it, what influence can the designer have on the structure's geometry?

Frei Otto himself expressed his doubts about the use of form-finding models in the design of an architectural project:

"It is extremely difficult to apply self-forming processes for architectural design. Although the experiment constitutes a very direct way of achieving the form, which, by its very nature, has already undergone an optimisation process, design work can only be seen in relation to the complexity of a building task and the integration of the building into its surroundings and into society. [...] Siegfried Gass says it, and I would like to emphatically stress this point: The use of physical experiments in the design field does not itself lead to humane or natural architecture. As with geometrical or computational optimisation methods, the experiments only constitute an aid. They are instruments for those of us who know how to use them, nothing more." (Otto 1990)

As a matter of fact, beyond its primary supporting function, a structure must also fulfil other purposes, including its spatial, programmatic, environmental, symbolic, aesthetic functions, in relation to the specificities of a given context. More broadly, the design of an architectural project involves the integration of multiple dimensions, some of which are not directly quantifiable in a purely objective manner. In line with Frei Otto's comments, but pointing more specifically to bending-active structures, and therefore also to bending-active tensile structures, Lienhard et al. even talk about a submission of the designer:

"Despite the apparent freedom of formal expressions that the built examples show [...], all bending-active structures rely on physical form defining mechanisms which design intentions have to subordinate to." (Lienhard, Alpermann, Gengnagel and Knippers 2013)

Yet, during a form-finding process, it is possible to steer the equilibrium geometry of the structure towards a result that satisfies the desired architectural intentions (Kilian 2014). By manipulating the various parameters of the structural system, the resulting form and force distribution can be influenced. In particular, it is relatively easy, in a digital and parametric environment, to vary the support conditions, loads, mechanical properties of the system, topology, etc. In this way, the designer actively explores different design variations and can steer the form-finding process towards a result that is close to the expected geometry. However, due to the non-linear nature of the structural system, this form-steering process is far from being straightforward and must be operated by means of successive attempts. If the structural system is sensitive, a slight change in the parameters can lead to a significantly different state of equilibrium, making the steering process tedious. In this blind search, new forms that were not yet thought of may emerge, but at the same time there is a risk that the designer may lose his/her control over the design process.

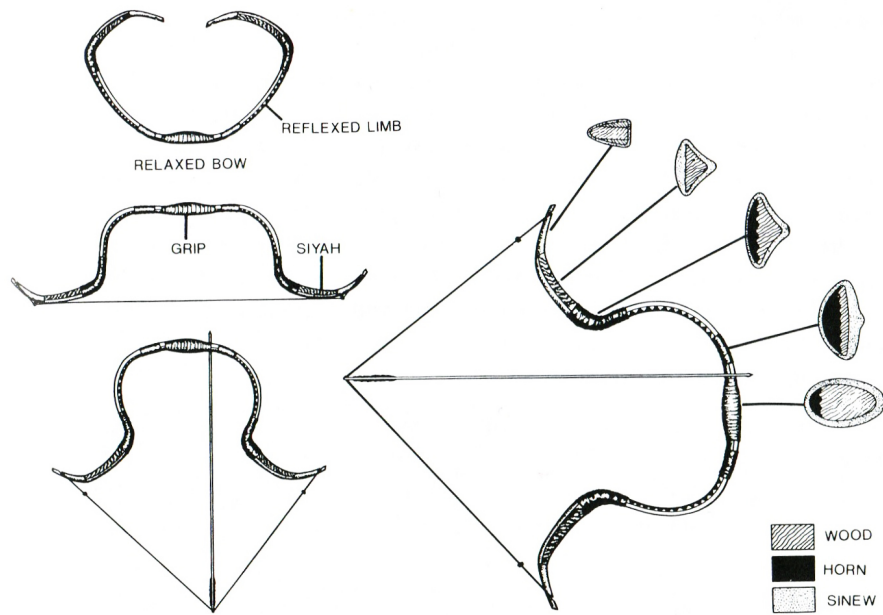


Figure 1.7: Asian composite bow illustrating how a differentiated bending stiffness along the limb of the bow affects its form in relation to functional aspects (Bergman and McEwen 1997).

Material and geometric differentiation More specifically, in the context of material-based design, as in the case of active bending, controlling the structure's geometry can be achieved by interfering with its mechanical and geometric characteristics, i.e. by assigning the structure its mechanical and geometric characteristics in an appropriate and differentiated manner (Menges 2012). For instance, such a differentiation strategy is developed in a natural way by biological systems which, through principles of heterogeneity, anisotropy and hierarchy, manage to integrate elegantly formal, structural and functional needs (Lienhard et al. 2015).

The tailoring opportunities offered by the new computer-assisted manufacturing methods allow the introduction into structural systems of non-standard elements with non-uniform geometric and physical characteristics. The possibility of a heterogeneous differentiated design driven by the distribution and specification of materials, which breaks with a conventional, homogeneous modular design driven by the logic of material assembly, is then introduced (Oxman 2012). This paradigm shift opens the way for design processes in which material is actively used as a mediator between form and structure. Therefore, the structural and formal potential embodied in materials – too often underestimated by common design processes – can be fully exploited. With the introduction of material and geometric differentiation, the range of possible form-found design solutions is expanded, but, in return, the number of parameters on which to act increases, which makes the process of form-steering more tedious, even impossible, to conduct.

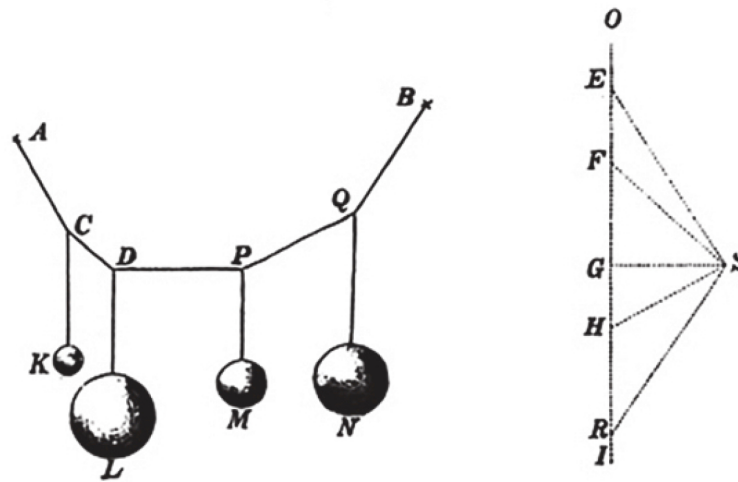


Figure 1.8: Static equilibrium of weights hanging on a cable analysed through graphic statics – Form and force diagrams (Varignon 1725).

With regard to active bending, composite bows are a good example to illustrate how a differentiated distribution of the manufacturing materials along the limb allows to control the curvature of a bent element in relation to its function and behaviour (Figure 1.7) (Beukers and van Hinte 2005). Very advanced composite systems which certainly took hundreds of years to develop, composite bows consist of a slender strip of wood – or a laminate of more than one – to which are glued on the outer side lengths of elastic animal tendon and on the inner side strips of compressible animal horn (Bergman and McEwen 1997).

Structural design with graphic statics Introducing differentiated geometric and mechanical properties within a self-formed structure can support to control its form. However, understanding the role of the form of a structure on its static behaviour and on the distribution of the forces acting on it appears as a fundamental condition to be able to negotiate their formal and structural aspects and thus achieve the convergence of architectural and structural design.

With this regard, graphic statics, a vector-geometric illustration of the distribution of forces in a structure, contributes to an understanding of the formative effect of active forces within a supporting structure. Graphic statics, which “has for its object the deduction of the principles of statics and the solution of static problems by means of geometrical constructions” (Malcolm 1914, p.3), was formalised by Karl Culmann (1821-1881), a professor at the time at ETH Zurich. It is grounded on the reciprocal relationship between two diagrams: the form diagram, representing the geometry of the structure, and the force diagram,

representing the equilibrium of the internal and external forces acting on the structure (Stevin 1586, Varignon 1725, Culmann 1866, Cremona 1872).

By reducing the internal forces of a structure to compression and tension, graphic statics allows the visual representation of the internal force flow as means of a strut and tie model. The visual expression of this structural information that is both intuitive and understandable to the designer does not represent an excessive simplification of the physical condition. Rather, this view of structural systems is mathematically precise thanks to the lower bound theorem of the theory of plasticity and linear algebra and satisfies the standards of engineering. Concurrently, the use of resultant forces and internal force flow encourages a unified understanding of the interplay of form and load-bearing capacity and provides graphic statics a creative strength over numerical methods.

Overall, more oriented towards the conception of form than form-finding and other numerical methods, graphic statics is a strong approach to design which supports an integral and holistic understanding of architectural and structural design.

1.2 Research overview

Bending-active tensile structures have expressive curved shapes, are lightweight and can be assembled quickly, thus allowing the construction of innovative small and medium-scale structures such as temporary pavilions. Resulting from the reciprocal interaction of slender beams, which are actively bent, and cables or membranes, their equilibrium geometry, however, is complex and difficult to predict. The current methods used for the design of bending-active tensile structures are based on form-finding approach in which the final equilibrium geometry of the structures is searched for. These methods generally limit the designer's influence on the final equilibrium geometry and tend to make the design process less intentional and intuitive.

Research focus Motivated by a seamless integration of architectural and structural design, the primary aim of this research is to introduce a novel approach for the design of bending-active tensile structures in architecture.

Embracing both the physical mechanisms and the formal aspect of design, the proposed approach intends to give the designer more explicit and intuitive control over the final equilibrium geometry of bending-active tensile structures and consequently facilitate the integration of geometry-related criteria into their design. Grounded on a graphical methodology for the structural modelling of bending-active beams, such form-driven design approach aims to be an alternative and complementary approach to existing form-finding methods, especially in the early conceptual stage of the design where the simplicity and transparency of graphical methods prove to be very valuable.

In order to achieve a more intentional design of bending-active tensile structures in architecture, this research investigates, on the one hand, the relation between the physical form-defining mechanisms and the resulting spatial configurations and, on the other hand, the role of material as mediator between both. In particular, this research focuses on the introduction of gradient of geometric and material properties as a means to integrate these two structural and formal aspects. The idea is to strengthen and activate the role of material as a mediator between form and forces, geometry and physical phenomenon, and thus, to give the designer additional control onto the design process through material related parameters.

Thesis structure The rest of this thesis is organised in five chapters:

Chapter 2 – *Research Framework* – outlines the research context within which the proposed design approach for bending-active tensile structures in architecture has been formulated, by exposing its theoretical background and a literature review. Moreover, the scope of the present work is delineated and

the research process undertaken for the development of the proposed design approach for bending-active tensile structures in architecture is highlighted.

Chapter 3 – *Structural Model* – describes the structural model on which the form-driven design approach is built. In particular, this structural model allows to describe the static equilibrium of bending-active beams and is based on a graphical methodology and a simplified mechanical model. From there, a twofold strategy is proposed to shape bending-active beams into target equilibrium geometries.

Chapter 4 – *Design Approach* – introduces the proposed form-driven approach for the design of bending-active tensile structures consisting of bending-active beams and pre-stressed cables and cable nets. After a description of the form-driven approach itself, different graphical and numerical methods are developed for the generation of pre-stressed cables and cable nets in equilibrium with the bending-active beams.

Chapter 5 – *Design Application* – focuses on a case study which was used as a design experiment to test the applicability of the developed design approach in a real architectural context. In particular, this chapter presents the form-driven design of bending-active tensile structure for façade sun-shading.

Chapter 6 – *Conclusion* – provides a summary of the various contributions of this research, presents the current limitations and proposes suggestions for future developments. It finally reflects on the overall content of the thesis.

Related publications Part of this thesis has been published in scientific journals and presented in international conferences by the author:

Boulic, L. and Schwartz, J.: 2017, Graphic Statics Principles for the Design of Actively Bent Elements Shaped with Restraining Systems, *Proceedings of the IASS Annual Symposium 2017*, Hamburg, Germany.

Boulic, L. and Schwartz, J.: 2018, Design Strategies of Hybrid Bending-Active Systems Based on Graphic Statics and a Constrained Force Density Method, *Journal of the International Association for Shell and Spatial Structures* **59**(4), 267–275.

Boulic, L.: 2020, Graphical Method for the Construction of Pairs of 3D Skew Funiculars in Equilibrium with Coplanar Loads and Controlled Supports' Positions, *Structural Concrete*, (accepted for publication).

Boulic, L., D'Acunto, P., Bertagna, F. and Castellón, J.: 2020, Form-Driven Design of a Bending-Active Tensile Façade System, *International Journal of Space Structures*, (accepted for publication).

2. Research Framework

2.1 Research context

This section outlines the context of this research. First, bending-active tensile structures are introduced based on definitions, classifications and build examples. Then, the non-linear equations that govern the static equilibrium and the large deflection of bending-active beams are presented. Finally, a review of the existing numerical and graphical methods for the modelling of bending-active beams and bending-active tensile structures is made.

2.1.1 Bending-active tensile structures

Definition of bending-active structures Bending, when related to a rigid structure subjected to external loads, is synonymous with deflections that can compromise the functionality of the structure or cause its collapse. Structural members are then given large cross-sections to minimise the deformation of the structure. On the contrary, “active bending” refers to the intentional use of large elastic deformations for structural and formal purposes. Respectively, the term “bending-active” characterises a vast range of structural systems which make use of large deformations as a “self-forming” (Gass 1990), “form-defining” and “self-stabilising” strategy (Lienhard 2014). Bending-active structures take advantage of the capacity of slender flexible structural elements, which are, in most cases, initially straight or flat, to elastically deform and bend into curved geometries. Strains within the actively bent elements remain infinitesimal but, due to the elements’ slenderness, it results in large deformations.

As such, in this context, the notion of active bending refers more to a strategy of form definition than to a particular type of structure. The behaviour of bending-active structures under loads cannot indeed be generalised to any specific and inherent mechanism just as no generic geometric definition of these systems can be established. Nevertheless, all bending-active structures have in common certain characteristics which derive from the elastic deformations upon which they are based. First, bending-active structures are lightweight structures. This is due to the fact that the actively bent elements must necessarily be thin and slender in order to bend without breaking. Second, owing to the reversible nature of the elastic deformations, bending-active structures have a capacity to store

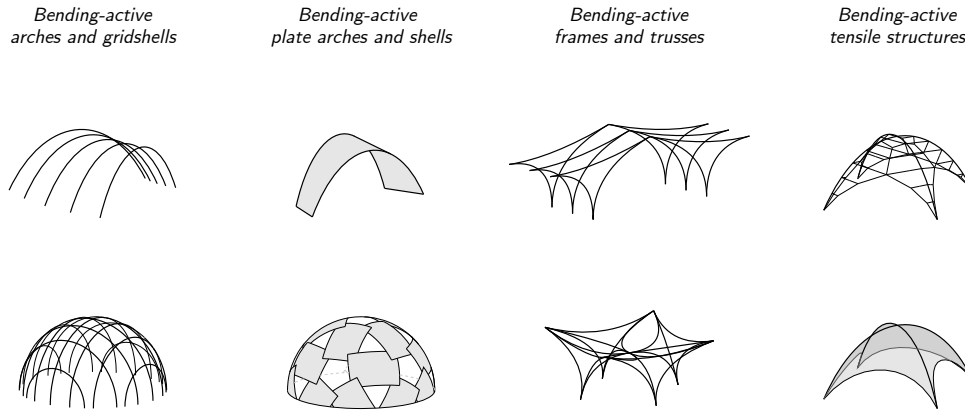


Figure 2.1: Classification of bending-active structures according to their typology.

elastic energy and, potentially, to dissipate it. This is the principle on which the bow, for example, is based. Third, bending-active structures gain structural stiffness through bending. At the level of the slender elements, curved shapes have a higher structural height than straight or flat shapes, and the residual stresses that occur have a stiffening effect. At the global level, the load-bearing capacity of bending-active structures relies more on the activation of their overall geometry than on the activation of the very thin cross-sections. In particular, the generation of double curved surfaces or the combination of bending-active elements with tensile restraining elements are the main strategies for stiffening bending-active structures. Finally, bending-active structures have in common the relative simplicity, rapidity and economy of their assembly process.

Classification of bending-active structures Active bending does not refer to a particular type of structures in itself, and different typologies can be distinguished among the bending-active structures (Figure 2.1).

Most of the built bending-active structures belong to well-known classical structural typologies such as the arches, the grid-shells, or the trusses. Active bending has indeed proved to be an efficient way to build such typologies, in particular with advantages in the construction process and in the efficient use of material.

Arched structures are the most straightforward application of active bending as a construction principle (Figure 2.3) and are behind many vernacular constructions worldwide (Cataldi 1997). The choice of elastically deformed elements for construction is then mainly motivated by economic reasons and manufacturing constraints. Traditional techniques for the construction of huts and temporary and mobile shelters generally make use of natural stems (branches, bamboo stems, grass bundles) that are elastically bent for the construction of arches but also grid-shell structures in the form of domes (Cataldi 1997). Such vernac-



Figure 2.2: Vernacular bending-active structures – (*left*) Traditional mudhif collective house by Madans people in Iraq, (*right*) traditional hut by Dorze people in Ethiopia.



Figure 2.3: Bending-active arched structures – (*left*) *Forest Pavilion* by nArchitects (2011), (*right*) *AA/ETH Pavilion* by the Architectural Association (EmTech) and the Chair of Structural Design ETH Zurich (2011).



Figure 2.4: Bending-active grid-shells – (*from left to right*) Mannheim Multihalle by Carlfried Mutschler & Partners, Frei Otto and Ove Arup & Partners (1975), *Pannikar Pavilion* by CODA (2014), *UWE Pavilion* by the University of West of England and Format Engineers (2016).



Figure 2.5: Bending-active shells – (*from left to right*) Geodesic *Plydome* by Buckminster Fuller (1957), *ICD/ITKE Research Pavilion 2010* by ICD/ITKE, University of Stuttgart (2010), *Bend9 Pavilion* by Riccardo La Magna (2016).



Figure 2.6: Bamboo bending-active frames and trusses – (left) Sports hall in Thailand by Chiangmai Life Architects and Construction (2017), (left) Conference hall in Da Nang by in Vietnam by Vo Trong Nghia (2015).

ular constructions include for instance the traditional mudhif collective houses by Madans people in Iraq (Frey 2010), the traditional hut by Dorze people in Ethiopia (Figure 2.2) or more recently the *Bamboo Structure Project* in Iran by Rai Studio (2009) (*Bamboo Structure Project / Pouya Khazaeli Parsa* 2010).

Bending-active grid-shells, also referred to as elastic grid-shells, consist of linear elements which are bent and assembled into a regular or irregular double curved grid (Figure 2.4). Widely represented in vernacular constructions, bending-active grid-shells are also used for the realization of modern architectural constructions of medium and large scale including, among several others, the *Savill Garden Gridshell* by Buro Happold & Glen Howells Architects (2006) (Harris and Roynon 2008), the *Downland Gridshell* by Buro Happold and Edward Cullinan Architects (2002) (Harris et al. 2003) or the temporary constructions of the *Toledo Timber Grid-shell* (2012) (Pone et al. 2013) and the *Ephemeral Cathedral of Créteil* (2013) (Du Peloux et al. 2016)). The pioneering project of the *Multihalle Mannheim*, built in 1974 and designed by Carlfried Mutschler and Partners, Frei Otto, Ove Arup and Partners (Burhardt 1978), remains the most outstanding modern application of active bending to the field of architectural construction. In order to increase the structural stiffness of bending-active grid-shells, additional bracing slats or cables arranged diagonally with respect to the grid are sometimes added after the erection process.

The use of slender plywood or metal plate elements makes it possible to build bending-active plate structures in the form of shells and arches (Figure 2.5). The continuous and double curved surface of the bending-active plate shells provides them with a geometrical stiffness and allows the loads to be transferred by membrane action. Exemplary projects include the *Plydome* structures by Buckminster Fuller (1957) (Marks 1960, 210-213), the *ICD/ITKE Pavilion 2010* (Fleischmann and Menges 2011), the *ICD/ITKE Pavilion 2015-2016* (Bechert et al. 2016), the *Studio One Research Pavilion 2017* (Schleicher et al. 2017), the structures *Bend9* and *Berkley Weave* (La Magna et al. 2016) and the robotically sewed timber shells *Demonstrators A and B* (Alvarez et al. 2018). The structural stiffness of bending-active plate arches can be achieved by an increase in their

structural height, which can result from the assembly of several arched plates together (*ETH/AA Pavilion* (D'Acunto and Kotnik, 2013)) (Figure 2.3), the twisting of long single plates (*Polycentric Pavilion* (nARCHITECTS 2016)) or the braiding of several long plates together (*Timber Fabric* structures (Hudert and Weinand 2011, Sistaninia et al. 2013)).

Finally, flexible linear elements can be bent and assembled into frame- or truss-like structures resulting in bending-active frame and truss structures. Two-dimensional bending-active frames and trusses are mainly found in recent bamboo constructions in Southeast Asia, as evidenced by numerous projects of Vietnamese architect Vo Trong Nghia (*Wind and Water* bar (Fearson 2012), conference hall in Da Nang (Kwok 2015a), Naman beach bar (Kwok 2015b), bamboo club and café in Vinh city (Purpura 2018)) or by the bamboo sports hall in Thailand by Chiangmai Life Architects and Construction (Mairs 2017) (Figure 2.6). Additionally, several research projects investigate the assembly of linear elastic elements into bundles in order to generate three-dimensional frame structures (Bessai 2013, Tamke et al. 2013).

Beyond these classical typologies, the formal possibilities offered by active bending open the design space to innovative and hybrid typologies incorporating an enormous potential of topologically complex spatial configurations. New types of structural systems explore the hybridisation of actively bent elements with pre-stressed tensile elements resulting in so-called “bending-active tensile (hybrid) systems”¹, or equally “textile hybrids” (Lienhard and Knippers 2015) (Figure 2.7).

Eventually, as opposed to static bending-active systems, kinetic bending-active systems take advantage of the elastic deformations on which they are based to reversibly bend and unfold during their operation time. Such kinetic structures have applications in particular in façade sun-shading actuated systems (Lienhard et al. 2011, Knippers et al. 2012, Lienhard, Riederer, Jungjohann, Oppe and Knippers 2013, Körner et al. 2018) and temporary structures (Tornabell et al. 2014).

1. There is no unified terminology in the research community to describe such newly studied hybrid structures. In the literature, they are successively named “hybrid bending-active constructions” (De Laet et al. 2013), “textile hybrids” (Ahlquist 2015, Lienhard and Knippers 2015), “hybrid structures” (Alpermann and Gengnagel 2012, Lienhard, Alpermann, Gengnagel and Knippers 2013), “bending active tensile membrane hybrid structure” (Deleuran et al. 2015) and “form-active hybrid structures” (Quinn et al. 2016). (Slabbinck et al. 2017) propose a classification of these “bending-active tensile hybrid structures” and a corresponding terminology, but the latter has not been commonly adopted to date. In particular, in the proposed classification, different terms are introduced according to the degree of interdependency between the tensile form-active elements and the bending-active elements, “bending-active tensile structures” denoting structures with a low interdependency compared to so-called “bending-active tensile hybrid structures” which display a higher interdependency. In this thesis, “bending-active tensile structures” will be used independently of this distinction, considering that, in all these hybrid structural systems, there is an interaction between the distinct bending-active and tensile elements. Therefore, the term hybrid is implicit.



Figure 2.7: Bending-active tensile structures – (from left to right) *Isoropia* structure by CITA, Royal Danish Academy of Fine Arts, and collaborators (2018), Hybrid structure by MPDA19 Studio 2, BarcelonaTech (2019), *Form Follows Tension* installation by Chair of Structural Design, Technische Universität München (2015).

The above paragraphs are not intended to be an exhaustive list of all architectural precedents for the application of the principle of active bending. More complete inventories can be found in (Lienhard, Alpermann, Gengnagel and Knippers 2013, Lienhard and Gengnagel 2018, Liuti et al. 2018).

Material for bending-active structures The capacity of a structural element to bend without breaking depends, on the one hand, on its slender geometry and, on the other hand, on the mechanical properties of the material it is made of. In particular, a suitable material for active bending applications should display the following characteristics: (1) a high stiffness to provide the structure with its final stiffness and to prevent it from deforming, (2) a high bending strength (yield strength) to provide bending capacity, and (3) a high tenacity to facilitate handling on site during the structure erection. Considering these three criteria and those of affordability, environmental footprint and durability, (Kotelnikova-Weiler et al. 2013) concluded that the best suitable materials are Glass Fibre Reinforced Polymer (GFRP), Natural Fibre Reinforced Polymer (NFRP) and timber. In a further comparison between different timber species, (Lienhard 2014, 33-36) highlighted that bamboo stands out thanks to its remarkable qualities that make it perform similar to GFRP. This explains in particular why bamboo is so widely used in vernacular architecture for the construction of bending-active structures.

Definition of bending-active tensile structures Bending-active tensile structures are “hybrid systems” (Engel 1967), which are based on the combination of bending-active elements and tensile elements into single unified structural systems (Figure 2.8). Pre-stressing forces are introduced in the tensile elements by the bending-active elements, which serve as a supporting and shape-defining structure for the tensile elements and tend to react to their bending deformation. In particular, these pre-stressing forces are needed to create the doubly curved geometry of the form-active tensile elements, namely the membranes and the

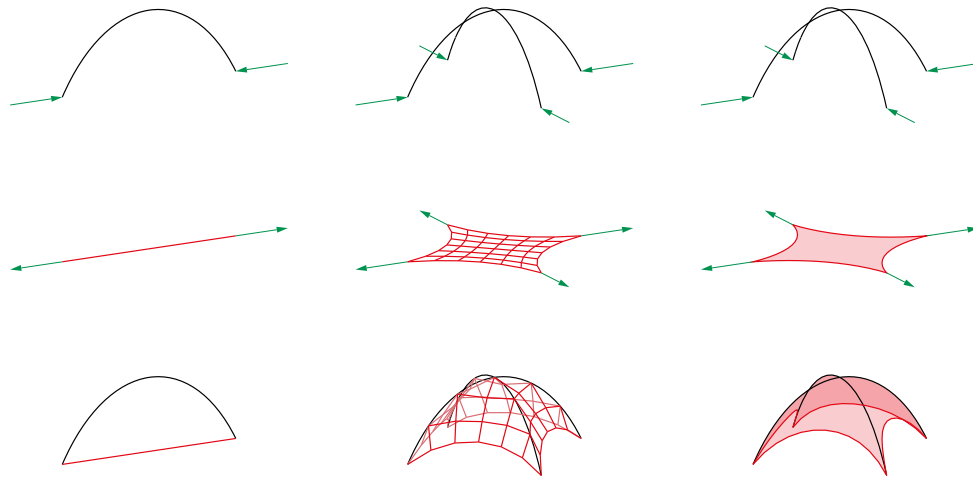


Figure 2.8: Reciprocal interaction between bending-active elements and tensile elements (cables, cable-nets and membranes) in a bending-active tensile structural system.

cable-nets. In turn, the forces applied by the tensile elements onto the bending-active elements are responsible for their bending and determine their bent geometry. Bending-active tensile structures benefit from such reciprocal interaction and perform better than the same elements considered separately. On the one hand, the tensile elements enhance the overall stiffness of the bending-active elements through a restraining and stabilising effect. When the bending-active elements to which they are connected are subjected to applied loads, they tend to prevent their deformation by a loads transfer. On the other hand, the integration of bending-active elements within tensile structures allows a wider variety of the structures' boundary conditions than in conventional tensile structures, opening up the range of design possibilities to membranes with free standing edges, with a reduced number of intermediate supports needed, etc..

Classification of bending-active tensile structures The hybridisation of bending-active elements and tensile elements offers new formal and structural possibilities. The diversity of bending-active tensile projects developed in recent years reflects the exploration of these possibilities, which has been facilitated by new developments in simulation techniques and numerical tools. While the use of GFRP tubes as slender flexible beams has, in practice, become widespread in bending-active tensile structures (with rare exceptions in which the flexible elements are metal or bamboo rods or plywood strips), different types of tensile elements are in use in bending-active tensile structures. A series of bending-active tensile prototypes and built projects is briefly presented here, classified according to the nature of the restraining tensile elements: coated woven membranes, knitted membranes and cables.

A first category of built bending-active tensile structures makes use of coated woven membranes, which are traditionally used for the construction of conven-

tional tensile structures. It is the case, in particular, of the prototypical reinforced membrane structure *Bat-Sail*, which integrates flexible battens into a structural membrane (Off 2010), the permanent sun-shading structure in Marrakech by the University of Stuttgart (Lienhard and Knippers 2012) or the self-stressed prototypical canopy designed at the Vrije Universiteit Brussel (De Laet et al. 2013) (Figure 2.9). Additional examples include structural building components in the form of arches and columns composed of bending-active linear elements restrained with a membrane (Alpermann and Gengnagel 2012, 2013), the temporary pavilion *Textile Hybrid M1* (Lienhard, Ahlquist, Menges and Knippers 2013) or the sculptural hanging structure exhibited during the annual symposium of the International Association of Shell and Spatial Structures in Hamburg in 2017 (Lienhard et al. 2017). The conventional membranes used in these projects are woven and the weaving technique only allows the manufacturing of flat pieces of low elasticity fabric. Considering that the double curved surfaces of form-active tensile structures are not developable, i.e. they cannot be flattened in a plane without deformation, the use of coated woven membranes in tensile structures requires cutting and sewing together fabric panels. In addition, wrinkles are likely to occur in the membrane if it is not stretched properly, which can occur for example if the pattern, cutting or assembly is not precise enough (Lienhard et al. 2017).

A second category built bending-active tensile projects involves knitted membranes as tensile elements. Due to the manufacturing technique they derive from, knitted membranes have several advantages over woven membranes. On the one hand, knitted membranes are much more extensible than woven membranes. In particular, this high elasticity can be taken advantage of in static bending-active tensile structures, in which it limits the risk of wrinkles, or in kinetic structures, in which the membranes successively adopt different geometries and prestressing states and can remain stretched in the different configurations (Aldinger et al. 2018, Puystiens et al. 2019a,b). On the other hand, it is possible to vary the structure of the knit and to tailor and adapt knitted membranes to the requirements of each project. Firstly, it is possible to produce non-developable surfaces in single pieces directly and thus avoid cutting and assembling different parts. Secondly, the membrane can have different mechanical characteristics at different locations of the structure such as elasticity gradient within the membrane and reinforcement of certain areas. These last two aspects have been explored in particular in the *Semi-Toroidal* (Ahlquist and Menges 2013) and *Mobius Rib Knit* (Ahlquist 2015) textile hybrid prototypes, developed at the ICD, University of Stuttgart in 2012 and at the Taubman College of Architecture in 2014. Ultimately, it is also possible to integrate connection details into the knitted membranes in the form of sheaths, pockets, holes or any other detail, which facilitate the assembly of the membranes with the bending-active elements or the cables (Tamke et al. 2016, Ramsgaard Thomsen et al. 2019). Most recent research projects on bending-active tensile structures have been investigating such

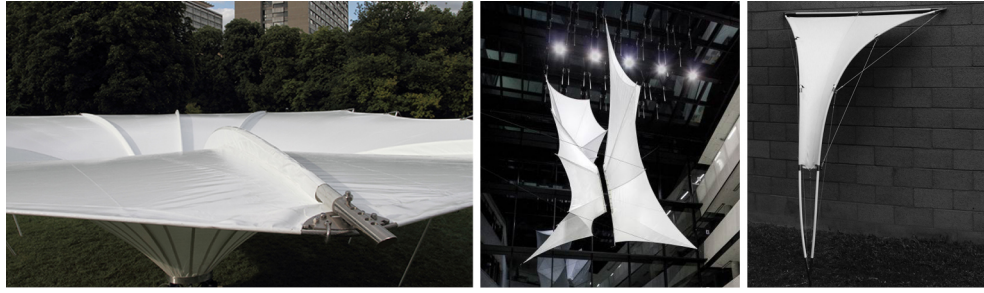


Figure 2.9: Bending-active tensile structures with coated woven membranes – (from left to right) Permanent umbrella in Marrakech by the Institute of Building Structures and Structural Design, University of Stuttgart (2011), bending-active textile hybrid sculpture by Lienhard in Hafen City University Hamburg (2017), and modular self-tensioned bending-active canopy by the Vrije Universiteit Brussel (2013).



Figure 2.10: Bending-active tensile structures with a bespoke knitted membrane – (left) *sensoryPLAYSCAPE (v1.0)* by Taubman College of Architecture and Urban Planning, University of Michigan (2015), and (middle and right) *Hybrid Tower* by CITA, The Royal Danish Academy of Fine Arts (2014).

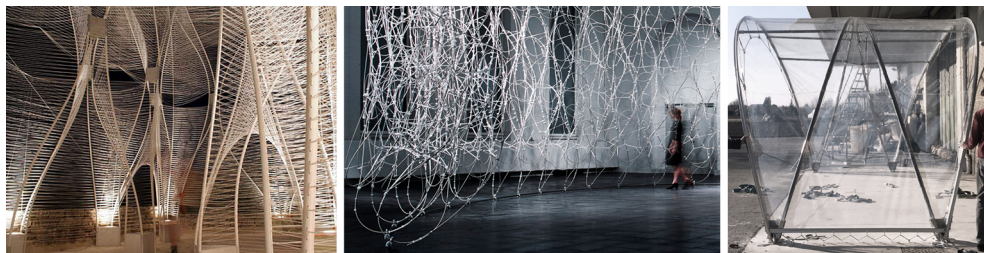


Figure 2.11: Bending-active elements restrained with cables – (from left to right) *Windshape* installation by nArchitects (2006), *Lace Wall* installation by CITA, The Royal Danish Academy of Fine Arts (2016) and *TemporActive Pavilion* by Politecnico di Milano (2019).

knitted membranes' potentialities as evidenced by the *Hybrid Towers* (Deleuran et al. 2015, Thomsen et al. 2015) (Figure 2.10) and the *Isoropia* installation at 2018 Venice Biennale Danish Pavilion (La Magna et al. 2018). A challenging aspect though of the tailoring of knitted membranes is to integrate into the form-finding simulations the highly differentiated material behaviour which result from such non-standard tensile elements.

A last category of built bending-active tensile structures employs cables as a means to bend and brace the bending-active elements (Figure 2.11). Unlike membranes, which have a biaxial stress state, cables only allow uniaxial loads transfer and can usually take higher forces than membranes. Notable prototypical works are the *Windshape* ephemeral structure (nARCHITECTS 2006), the 6m high self-standing *Hybrid Tower*² (Quinn et al. 2016), and the module-based self-standing *Lace Wall* (Tamke et al. 2017). Additional examples include structural building components in the form of restrained arches in which flexible poles are restrained with radial cables connected to a bottom prestressing cable (Alpermann and Gengnagel 2012, Mazzola et al. 2019).

Besides, tensile restraining systems of different kinds can be brought together within the same bending-active tensile structure. Particularly, membranes and cables can be used in combination, as shown for example by the *Hybrid Towers* (Deleuran et al. 2015, Thomsen et al. 2015), *Isoropia* (La Magna et al. 2018) and the VUB's canopy (De Laet et al. 2013) projects.

Challenges associated with the design of bending-active tensile structures

The diversity of new forms that emerges from the bending-active tensile structures could suggest a simple and smooth design process. On the contrary, these new formal and structural possibilities have as their counterpart a complex design and simulation process. The coupling of bending-active elements and tensile elements induces indeed a complex formation process guided by complex reciprocal interactions. Moreover, for both bending-active structures and tensile structures, it is not possible to formulate in advance a geometrical description of the structure at equilibrium. This is well known in the field of tensile structures: the geometry of the structure at equilibrium is the result of a close interaction between form, forces, material characteristics and boundary conditions. This is why the design process is referred to as form-finding.

The problem of determining the equilibrium geometry of tensile structures has been solved since the 1970s by various numerical form-finding methods such as the Finite Element Method (Haug 1972, Haber and Abel 1982), the Force Density Method (Linkwitz and Schek 1971, Schek 1974) and the Dynamic Relaxation (Day 1965, Barnes 1975, 1980). Since then, a large number of tensile structures have been realised thanks to these different calculation methods, which have been continuously improved.

On the contrary, digital tools for the simulation of elastic curves, which allow an extensive exploration of bending-active structures in the architectural and structural field, have only been developed relatively recently, driven in particular by developments in the field of computer graphics. One of the main difficulties

2. The design of the tower was developed by the author as a participant to the *Smartgeometry2016* workshop (Gothenburg, Sweden) based on a modelling pipeline provided by the workshop tutors.

when simulating the deformation process of elastic elements comes from the non-linearity of their structural behaviour.

Apart from the recent numerical form-finding methods, which allow an integral approach to bending-active structures based on their mechanical behaviour, other empirical and geometric approaches have been used to address the design of bending-active structures (Lienhard, Alpermann, Gengnagel and Knippers 2013). However, they have a reduced scope of application due to their limitation in predicting the equilibrium geometry of the structures.

The empirical approach consists in addressing bending-active structures through physical experiments only and the structures' geometry and behaviour are empirically established from the experience acquired over the centuries. This approach is at work in many examples of bending-active constructions found in vernacular architecture. Especially in cultural and geographical contexts where the tradition of bamboo construction is strong, this behaviour-based approach is still in use for the design of large contemporary structures such as those designed by Vietnamese architects Vo Trong Nghia (Fearson 2012, Kwok 2015b,a, Purpura 2018).

The geometric approach takes advantage of the geometrical similarities that some elastic curves share with well-known mathematical curves, in particular the arc of a circle and the parabola/catenary (Gass 1990). Thus, bending is used as a means of approximating geometries established separately, in an analytical way or through hanging chain form-finding models. Richard Buckminster Fuller was the first one to use the elastic properties of building materials to build geometrical shapes with architectural potential. As part of his research on geodesic domes, he constructed a series of *Plydome* structures (1957) whose semi-spherical shape is materialised by a set of plywood plates interconnected at the topological vertices of the dome (Marks 1960). Its methodology, purely geometrical but nevertheless rigorous, is based on the circular geometry (arc of circle) that a flexible element takes under pure bending. A few years later, Frei Otto became interested in elastic grid-shells and in 1974, in collaboration with the Büro Happold, he built a project that will remain emblematic: the *Multihalle Mannheim* (Burhardt 1978). This double curved grid-shell is produced by the elastic deformation of a lattice of straight elements assembled flat and subjected to external loads during the erection process. The double curved geometry of the grid-shell has been established by an analogue model of hanging chains in order to obtain a structure in compression-only under its self-weight (Figure 2.12). Indeed, it is then observed that a bent element takes, under certain conditions, a shape similar to the catenary shape of a suspended chain. Thus, in the case of the *Multihalle Mannheim*, bending allowed the erection and realisation of an approximate funicular shape and the form-finding tool used is classic and does not involve bending. In the decades that followed, a number of other elastic grid-shells were constructed using a similar approach: the *Savill Garden Gridshell* by Büro Happold & Glen Howells Architects (2006) (Harris and Roynon 2008),

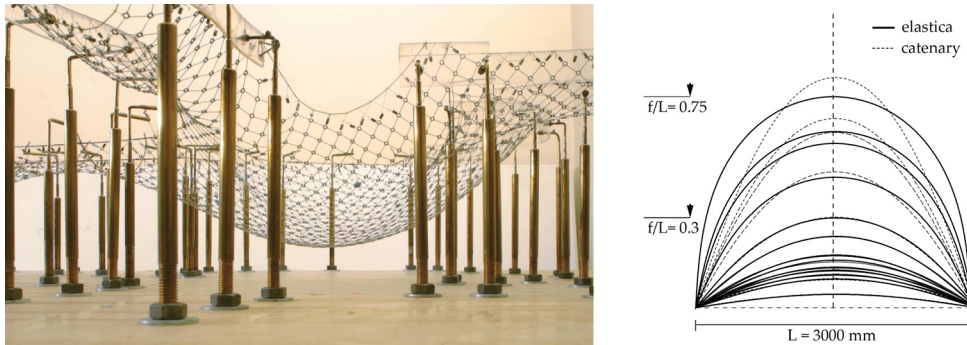


Figure 2.12: Form-finding of the *Multihalle Mannheim* elastic grid-shell – (left) Hanging chain model (1975) and (right) comparison between *Elastica* and catenary curves (Lienhard 2014).

the *Downland Gridshell* by Buro Happold and Edward Cullinan Architects (2002) (Harris et al. 2003). To date, they are, with the vernacular architectural projects mentioned above, the only large scale architectural projects built on the principle of active bending. Besides, the equilibrium geometry of elastic elements under bending correspond to a geometry that minimise the bending potential energy and the curvature of the bent elements. Based on this observation and on the properties of geodesic lines to be minimal curvature curves on a surface, another geometry-based approach consists in bending elements along the geodesic lines of a free form surface to generate bending-active free-form shells (Pirazzi and Weinand 2006).

In the context of architectural and structural design, however, the consideration of the mechanical behaviour of slender elastic elements is necessary to define the equilibrium geometry of bending-active (tensile) systems and to assess internal forces. This requires the elaboration of physical and mathematical models describing the large deformation of slender elastic elements.

2.1.2 Modelling elastic curves

Predicting and describing the deformation of slender elastic beams or rods under loads has been a challenging problem for scientists from the 17th century. The so-called *Elastica* problem was first posed by Bernoulli (1694) and its solving was tightly bound to the development of infinitesimal and variational calculus. Later on, after the development of the theory of elasticity and of the beam theory, the problem was formulated in the way it is known in structural mechanics nowadays.

The next paragraphs are structured as follows. First, the definition and description of slender beam elements are given. Then, the problem of slender elastic beams under large deformations and infinitesimal strains is formulated in the case of plane deformations, highlighting the geometrical non-linearity of the structural response. Particularly, the analytical solution of the deflection curve in the case of the *Elastica* problem is presented, as proposed by Euler and Bernoulli. Finally, the constitutive equations of the three-dimensional (3D) static equilibrium of a slender beam are expressed for a general load case and the resulting torsional and flexural moments acting on the beams are specified in the context of the theory of rod elements.

Slender beams In structural mechanics, a beam is a three-dimensional body with two dimensions which are small compared to the third one. It is modelled in the elastic theory by finite planar surfaces, called cross sections, such that the set of cross sections' centroids is a continuous curve (Figure 2.13). This curve is referred to as the centroidal axis of the beam or, equally, as its axis, and is the main dimension of the beam. Besides, the cross sections are normal to the centroidal axis and vary slowly and continuously. Several theories have been developed to describe the behaviour of beams under external loads. The classical beam theory, known as the Euler-Bernoulli's beam theory, neglects shear deformation effects and assumes that, over deformation, the cross sections remain normal to the deflection curve of the centroidal axis, behave as rigid body and therefore remain plane.

A slender beam³ is a beam with at least one of its cross sections' characteristic dimensions which is very small compared to the main dimension (i.e. the beam's length). When the slender beam is such that its two cross sections' characteristic dimensions are very small compared to the beam's length, the slender beam can then be described as a rod and the Kirchhoff and Clebsch's theory of thin and inextensible elastic rods under finite displacements can apply (Dill

3. Sometimes equally referred to as *spline beams* or *splines* in the literature (Adriaenssens and Barnes 2001, Barnes et al. 2013, Van Mele et al. 2013). In the field of manufacturing, a spline is a thin and flexible piece of wood or metal used to draw smooth curves, mainly used in timber workshops by stair manufacturers and carpenters or formerly in naval, aerospace and automotive manufacturing workshops.

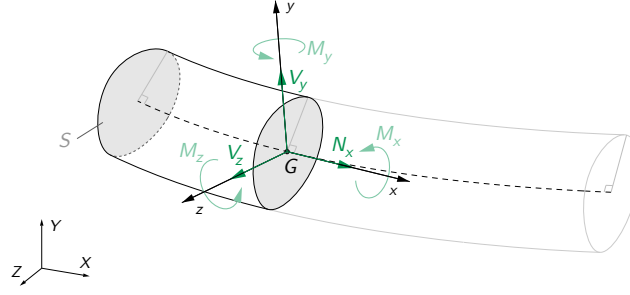


Figure 2.13: Force-couple action at the cross section of an Euler-Bernoulli beam.

1992). It is then assumed the following Kirchhoff-Love hypotheses: (i) cross sections remain plane, undistorted, and normal to the axis of the rod; (ii) the transverse stress is zero; (iii) the bending moments and the twisting moment are proportional to the components of curvature and twist of the axis.

With regard to the context of active bending, in the rest of this thesis, structural elements described as beams will always refer to slender beams. Besides, when slender beams will be described as rods, it will be to highlight that they have a cross section whose characteristic dimensions are very small in relation to their length. Assuming the elastic behaviour of the slender beams over deformation, the deflection curves of their axis will be referred to as their elastic curve.

A beam under Euler-Bernoulli's hypothesis to be subjected to the action of forces and torques is considered as shown in Figure 2.13. The deflection curve of its centroidal axis is described by the continuous function $\boldsymbol{\gamma}(s) = (X(s), Y(s), Z(s))$ in the global coordinate system $(\mathbf{X}, \mathbf{Y}, \mathbf{Z})$ where s is the curvilinear abscissa along the centroidal axis of the beam. A local coordinate system $(\mathbf{x}(s), \mathbf{y}(s), \mathbf{z}(s))$ is associated to each cross section's centroid $G(s)$ such that the axis $\mathbf{x}(s)$ is tangent to the deflection curve of the beam and that $\mathbf{y}(s)$ and $\mathbf{z}(s)$ are the cross-sectional principal axes. This frame follows the cross section upon deformation and is called a material frame. The resultant force and resultant moment acting on the cross section at its centroid G can be expressed as the following force-couple system:

$$\{\boldsymbol{\tau}_{int}\} = \left\{ \begin{array}{cc} N_x & M_x \\ V_y & M_y \\ V_z & M_z \end{array} \right\}_{G, (x, y, z)} \quad (2.1)$$

In the case of a two-dimensional (2D) beam loaded in the plane (\mathbf{X}, \mathbf{Y}) of its centroidal axis, the cross sections are only subject to a normal force N_x along \mathbf{x} , a shear force V_y along \mathbf{y} and a bending moment M_z around \mathbf{z} acting at their centroid G . Thus, the force-couple system at the cross section simplifies to:

$$\{\boldsymbol{\tau}_{int}\} = \left\{ \begin{array}{cc} N_x & 0 \\ V_y & 0 \\ 0 & M_z \end{array} \right\}_{G, (x, y, z)} \quad (2.2)$$

Theoretical development of 2D elastic curves The study of elastic curves was initiated over the end 17th century with the so-called *Elastica*⁴ problem. This problem addresses the deformation of slender elastic beams bending under normal compressive force. The history of the development of the *Elastica* curves has been extensively reported by (Levien 2008) and is shortly recounted below.⁵

At the end of the 17th century, the mathematician Jakob Bernoulli analysed the shape of the deflection curve of a slender elastic beam. Based on infinitesimal calculus, he formulated the equations and solved the theoretical problem of the elastic curve of a vertical slender beam fixed at its lower end and loaded with a conservative vertical load at the upper end (Bernoulli 1694) (Figure 2.14(c)). He related the local curvature of the deflection curve to the local bending moment. Fifty years later, under the instigation of his nephew Daniel Bernoulli, Euler approached the problem through variational calculus and posed the equations of various fundamental cases of bending (Euler 1744). He related the *Elastica* problem to a problem of curvature/energy minimisation. He finally identified the governing parameters of bending relative to geometry and material, and related the local curvature to the local bending moment through a new mechanical quantity, the “flexural rigidity”. A modern and synthetic formulation of the Euler’s *Elastica* problem and its analytical solutions based on complete elliptic integrals of first and second kind can be found in (Timoshenko and Gere 1961, 76-82). Finally, Navier, often considered as the founder of the general theory of elasticity and of modern structural analysis, developed the general differential equation of the elastic curve of bent beams (Navier 1826). He identified the influence played by the modulus of elasticity E and, with the moment of inertia I (initially referred as J by Navier), he introduced the governing geometric parameter of the cross section of the beam.

Given the global coordinate system (\mathbf{X}, \mathbf{Y}) shown in Figure 2.14(c), the deflection of an elastic beam obeys the following differential equation:

$$\frac{Y''}{(1 + Y'^2)^{(3/2)}} = \frac{M_z}{EI_z} = \kappa_z \quad (2.3)$$

where the prime denotes differentiation with respect to the parameter X . The right term of equation (2.3) describes the local bending curvature κ_z . I_z is the principal moment of inertia of the cross section around the principal axis \mathbf{Z} , normal to the plane of deformation. EI_z , originally referred to as “flexural rigidity” by Euler, is defined as the bending stiffness of the cross section of the beam. In order to make this solution applicable in engineering design, several simplifications are usually introduced relative to the geometry and loading of the considered structural element. For common beams with small deflections

4. *Elastica* means thin strips in Latin.

5. Additionally, (Schwartz 2010) gives a larger overview on the historical development of the concept of bending in material and mechanical engineering, including the development of elastic and plastic bending.

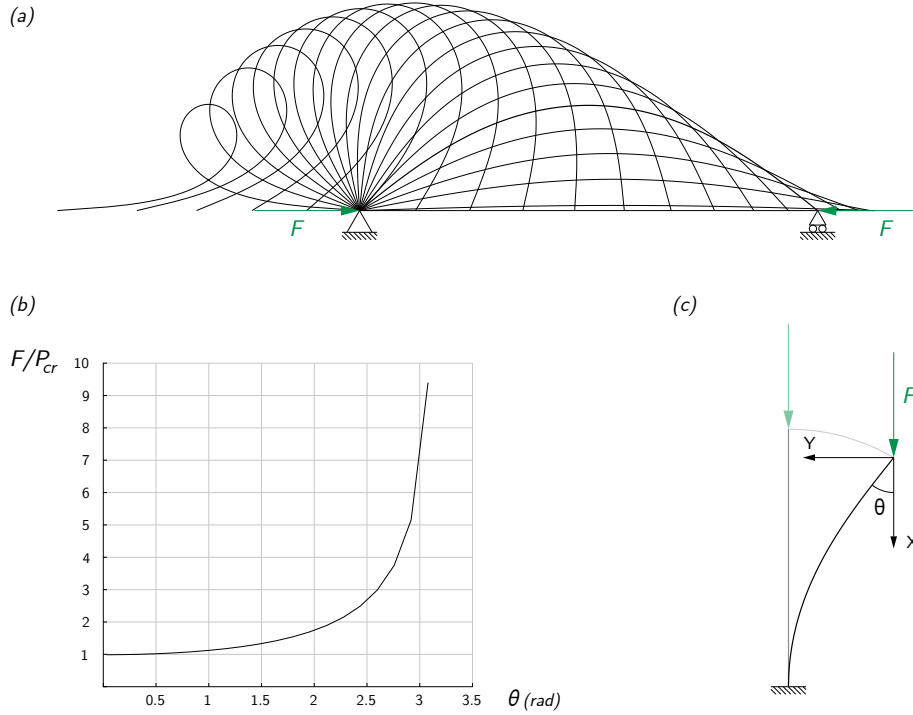


Figure 2.14: *Elastica* curves – Simply supporter slender elastic beam with an actuating force F at its sliding support. While bending, the beam gains structural stiffness, in the sense that the more the beam bends, the larger the actuating force F must be to induce a same given variation of angle θ . P_{cr} is the so-called Euler critical actuating force triggering the buckling of the beam.

compared to their length, the term Y'^2 can be neglected and the equation is linearised to the well-established formulation in classical structural mechanics:

$$Y'' = \frac{M_z}{EI_z} = \kappa_z \quad (2.4)$$

In the common cases of beams without considerable normal compressive forces, the equilibrium conditions are formulated assuming an undeformed centroidal axis of beam, and the deflections are calculated using equation (2.4). The so-called first order theory is generally used in structural design to calculate structures not affected by instability problems.

For slender structural elements under considerable normal compressive forces, the equilibrium conditions have to be formulated considering the deformed centroidal axis of the beam (or column) using (2.3). The so-called second order theory is generally used in structural design for stability analysis. In the case of a simply supported beam with uniaxial load, the solution of equation (2.4) leads to the critical Euler load P_{cr} under which the beam starts to buckle (i.e. to deform out of the axis of the load). The elastic deflection curve in the first mode is sinusoidal.

The linearisation of equation (2.4) leads in first order theory as well as in second order theory to an unchanged length of the beam i.e. distance between the supports.

For slender structural elements subjected to large deformations as for instance the slender beams of bending-active structures, the equilibrium conditions have to be formulated considering the deformed centroidal axis of the beam, using the non-linearised formula (2.3). The so-called third or higher order theories consider the effect that due to the considerable deformations the distance between the supports is decreasing with increasing deflections (Figure 2.13(a)).

In the context of bending-active structures, under the condition that they are externally statically undetermined, buckling can be regarded as a phenomenon of labile equilibrium rather than structural instability leading to collapse. If the elastic deformation capacity of the material is provided, slender beams keep on deforming elastically without breaking.

The above relationship between the local bending curvature κ_z of a beam and the bending moment M_z (Equation (2.3)) can equally be found by isolating a differential segment of a bi-dimensional Euler-Bernoulli beam (Figure 2.15).

The local coordinate system $(G, \mathbf{x}, \mathbf{y}, \mathbf{z})$ is chosen such that the axis \mathbf{x} is tangent to the deflection curve of the beam's axis at the cross section's centroid G and that the axes \mathbf{y} and \mathbf{z} are the principal axes of the cross section, in such a way that $\int_S y dS = \int_S z dS = \int_S yz dS = 0$ and that the axis \mathbf{y} belongs to the oscillating plane of the segment. By definition, the bending moment M_z at the centroid G around the axis \mathbf{z} is:

$$M_z = \int_S \sigma_x y dS \quad (2.5)$$

where S is the cross section area. According to the theory of elasticity, the axial stress σ_x is proportional to the axial strain ϵ_x and is given by:

$$\sigma_x = \epsilon_x E \quad (2.6)$$

where E is the modulus of elasticity of the cross section. Besides, as a plane cross section remains plane and normal to the deflection curve over deformation, the axial normal strain ϵ_x is distributed linearly over the cross-section such that:

$$\epsilon_x = \epsilon_G + \kappa_z y \quad (2.7)$$

where κ_z is the local bending curvature. Finally, as a result of axes \mathbf{y} and \mathbf{z} chosen such that $\int_S y dS = \int_S z dS = \int_S yz dS = 0$, the combination of equations (2.5), (2.6) and (2.7) gives:

$$M_z = E \epsilon_G \int_S y dS + E \kappa_z \int_S y^2 dS = E I_z \kappa_z \quad (2.8)$$

where I_z is the principal moment of inertia of the cross section around axis \mathbf{z} , also called second moment of area.

Torsion and the general case of 3D elastic curves In the general case of a slender beam deforming under loads in 3D space, a bending moment $\mathbf{M}_y(s)$ around axis \mathbf{y} and a torsional moment $\mathbf{M}_x(s)$ around axis \mathbf{x} may additionally act at the cross sections' centroid G , as well as a shear force $\mathbf{V}_z(s)$ along \mathbf{z} . At any point of the curve $\boldsymbol{\gamma}(s) = (X(s), Y(s), Z(s))$, a curvature vector $\boldsymbol{\kappa}(s)$ can be defined. It is normal to the oscillating plane of the deflection curve at that point and is defined as:

$$\boldsymbol{\kappa}(s) = \frac{\boldsymbol{\gamma}'(s) \wedge \boldsymbol{\gamma}''(s)}{\|\boldsymbol{\gamma}'(s)\|^3} \quad (2.9)$$

where the prime denotes differentiation with respect to the parameter s . As shown in Figure 2.16, the curvature vector $\boldsymbol{\kappa}(s)$ can be decomposed into two orthogonal components, $\boldsymbol{\kappa}_y$ and $\boldsymbol{\kappa}_z$, parallel to \mathbf{y} and \mathbf{z} respectively.

Within the scope of the Kirchhoff's theory of rods, the bending moments and the twisting moment are assumed to be proportional to the components of curvature and twist of the axis (Audoly and Pomeau 2010). The bending moment \mathbf{M}_f at the centroid due to combined bending can then be defined as:

$$\mathbf{M}_f = \mathbf{M}_y + \mathbf{M}_z = EI_y \boldsymbol{\kappa}_y + EI_z \boldsymbol{\kappa}_z \quad (2.10)$$

If the cross section of the beam is quadratic or circular, the bending moment \mathbf{M}_f and the curvature vector $\boldsymbol{\kappa}$ are both aligned along the same direction. On the contrary, in the case of rectangular or elliptic cross sections, \mathbf{M}_f and $\boldsymbol{\kappa}$ are, in general, not aligned. As for the torsional moment $\mathbf{M}_t = \mathbf{M}_x$, it is assumed to be proportional to the twist $\boldsymbol{\tau}_x$ of the cross sections around the axis and is given by $\mathbf{M}_t = GJ\boldsymbol{\tau}_x$, where G is the shear modulus and J is the polar moment of inertia of the section. Finally, the vector of the resultant internal moments \mathbf{M} can be written as:

$$\mathbf{M} = EI_y \boldsymbol{\kappa}_y + EI_z \boldsymbol{\kappa}_z + GJ\boldsymbol{\kappa}_x \quad (2.11)$$

For non-circular cross sections, the torsional moment around the axis \mathbf{x} has to be calculated directly from the shear stresses acting on the cross sections as

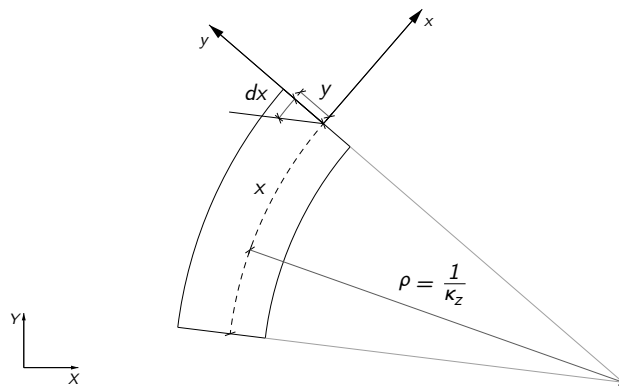


Figure 2.15: Differential segment of a Euler-Bernoulli beam in the plane.

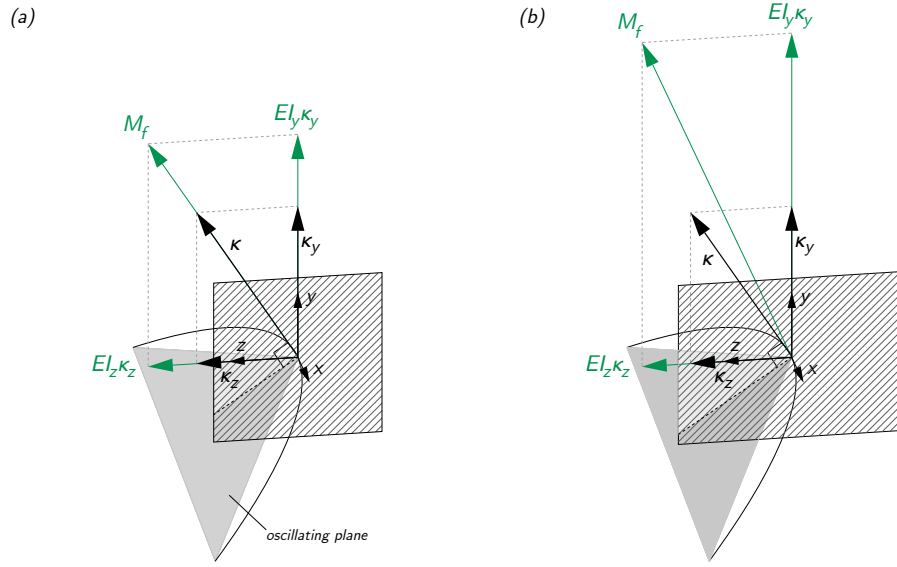


Figure 2.16: Bending moment and curvature vectors in the case of quadratic (a) and rectangular (b) cross sections.

follows:

$$M_x = \int_S (y\tau_{yz} + z\tau_{zy}) dS \quad (2.12)$$

The rotation of the cross sections around the centroidal axis of a structural element caused by torsion affects the bending stiffness of its cross sections and can result in a significant out-of-plane deformation of its centroidal axis. In the context of bending-active structures, this deformation process, although due to twisting, is equally referred to as “active bending” as the deformations are elastic and reversible and the structural elements, and more generally the structures, gain structural stiffness through it.

For certain bending-active structures, their geometry at static equilibrium is deeply governed by the effect of torsion. In particular, torsion has a non-negligible impact on structural systems comprised of elements with sections non radially symmetric to their main axis, such as flat slender beams, and can strongly drive the design of such structures. The case of a single flat beam bent into an *Elastica* and whose ends are then twisted in opposite direction is a clear illustration of this out-of-plane deflection and is reported in (Slabbinck et al. 2017). Within topologically more complex bending-active structures, torsion can also arise due to the interconnection of bending-active elements to each other and affect the overall equilibrium geometry and stresses. The physical interaction of flat beams to each other, whether a rigid connection (over faces for example) or a contact-only connection (curved edge against curved edge), induces constraints on the twisting degree of freedom of the flat beams’ cross sections and thus torsion in the flat beams. This is the case of grid-shell structures made of rectangular cross section timber beams as shown in (Lefevre et al. 2017) and,

even more significantly, for structures made of wide strips of plywood that are interlaced. The twisted interlaced structures made from flexible timber strips of the *Radical Wood Pavilion Shanghai 2012* by Aalto University, Finland (Niranen 2013), and of the different *Timber Fabric* structures by IBOIS Institute, EPFL (Nabaei et al. 2013, Sistaninia et al. 2013), are some relevant examples. Through torsion, these interlaced structures increase their structural depth and their overall structural stiffness. The wider the single flat beams, the more torsion has a predominant effect onto the outcome geometry, and the less the bending beam theory is applicable. In particular, in the case of bending-active plate structures, new mechanical models have to be defined where bending and torsion are considered in a consistent way (La Magna et al. 2016).

2.1.3 Numerical methods for the form-finding of bending-active structures

Finding an analytical solution to the non-linear partial differential equations that govern the large deflection of a slender beam under external loads is rarely possible, except for a limited number of relatively simple situations. For instance, an analytical solution of the deflection curve can be found in the case of the Euler's *Elastica*, a straight regular beam vertically clamped at one end and subject to a vertical force at its free end (Timoshenko and Gere 1961, 76-82), or for a straight regular beam clamped at one end and subject to a force and a moment at the other end (Zhang and Chen 2013). In the general case of slender elements subjected to any boundary conditions, whether kinematic or static, or with non-regular material and geometrical characteristics, numerical methods are used to obtain an approximation of the deflection curves.

Essentially, numerical methods approximate the solution of a problem through discretisation: the original problem, which is continuously defined, is replaced by a discrete problem whose solution can be found more easily. Moreover, when the solution cannot be calculated directly, numerical methods involve an iterative solution process. So-called numerical incremental methods make use of iterations to advance a solution through a sequence of intermediate steps until a convergence state is reached. The iteration steps can be compared to small time increments, although they usually do not connect to a realistic time-dependent process. Numerical incremental methods are often referred to as being explicit or implicit. When the calculation of the system configuration at step $n + 1$ is based on its configuration at step n , the method is said to be explicit. On the contrary, when the calculation of the system configuration at step $n + 1$ entails solving an equation related to steps n and $n + 1$, the method is said to be implicit. Implicit methods make it possible to model time-depend phenomena more precisely since the intermediate configurations are much closer to each other. However, in return, they are costlier in terms of calculation than explicit methods. In practice, regarding bending-active structures, the choice of an explicit or implicit resolution method mainly depends upon the problem to be solved.

On the one hand, for design-oriented problems in which more emphasis is placed on the geometric configuration of the structure at equilibrium, after the formation process, than on stresses and deformations, explicit methods are reported as more advantageous (D'Amico et al. 2016). Indeed, as the history of the structure since its original unstressed configuration does not matter much, the intermediate configurations leading to the equilibrium do not necessarily need to be close to each other. Accordingly, the time variable has no physical meaning, as well as the masses and stiffness parameters involved in the method's algorithm which refer only to the numerical process itself and will be likely set according to prescribed design parameters and/or numerical stability issues (D'Amico et al.

2016). Additionally, the initial configuration of the structure can be far from equilibrium.

On the other hand, implicit methods are preferred when a physical simulation of the structure's behaviour under prescribed forces or displacements is needed, for instance in order to simulate the construction process and track the deformation path or to assess the structure's behaviour under prescribed loads. In such a case, intermediate configurations of the systems need to be close to each other as the simulation is influenced by inherited stress state and that the simulation may not involve large displacements any more (unless the loads are again very large). Besides, masses and stiffness parameters are physically meaningful. In general, implicit methods are considered harder to implement and require extra computation but there are usually much more stable and so larger time steps can be implemented.

Overall, the choice of an appropriate numerical method, together with a mechanical model – which provides the governing equations – and an appropriate kinematic description in the form of a system of variables, also referred as degrees of freedom (DoFs) – which allows for the description in space of the position and orientation of each cross section of the discretised slender element, forms the numerical modelling framework.

Various numerical methods can be found in the literature for the solution of the non-linear partial differential equations describing the equilibrium of bending-active structures. The main numerical methods which are currently in use for the design of bending-active structures, both in academia and practice, are:

- Dynamic Relaxation Method (Day 1965) with 3-DoF beam models (Adriaenssens and Barnes 2001, Barnes et al. 2013), with 4-DoF beam models (Du Peloux et al. 2015), with 6-DoF beam models (D'Amico et al. 2014), and in combination with the Force Density Method (Van Mele et al. 2013).
- Projective Constraint-based Solver (within *Kangaroo2* plugin (Piker n.d.)) (Quinn et al. 2016, Bauer et al. 2018).
- Particle-Spring Systems in the form of custom programmed software environments (Ahlquist et al. 2015, Suzuki and Knippers 2017, Suzuki et al. 2018).
- Finite Element Method with non-linear solvers and meshed-based (Lienhard et al. 2014) or iso-geometric-based (Bauer et al. 2017) discretization methods.

Additional methods include gradient-based optimisation algorithms (Nabaei et al. 2015, Cuvilliers et al. 2018, Rombouts et al. 2018).

These distinct numerical methods offer significant differences in terms of implementation, convergence, and interactivity with the designer and the choice of a method over the others depends on the nature of the problem to be solved.

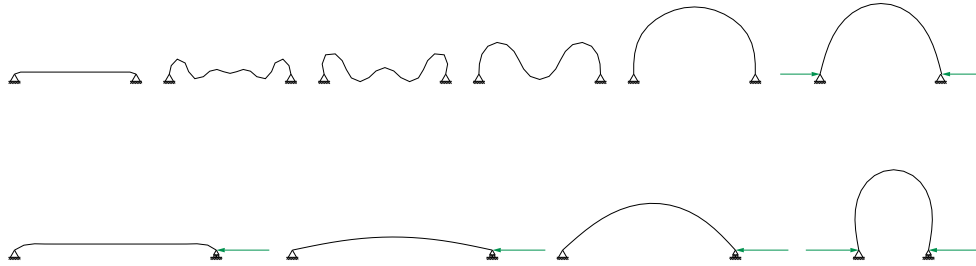


Figure 2.17: Form-finding of *Elastica* curves with the dynamic relaxation method – Successive geometries of the beam throughout the form-finding process, from an initial arbitrary configuration to the equilibrium configuration. Successive geometries of the beam from an initial arbitrary configuration to its equilibrium configuration.

In particular, for design-oriented problem, modelling frameworks based on the dynamic relaxation method, on *Kangaroo2*'s projection-based solver and on particle-spring systems will be favoured, while modelling frameworks based on the implicit finite element method will be chosen for physical simulations. The four methods are briefly described below and discussed afterwards.

Dynamic Relaxation Method Among the numerical methods for the design of bending-active structures, the dynamic relaxation method is probably the most favoured one. The dynamic relaxation method is a numerical iterative method for solving mechanical problems based on a set of nonlinear equations. It is grounded on a pseudo dynamic process and was proposed by Day and by Otter in the 1960s (Otter and Day 1960, Day 1965). Static equilibrium is regarded as the limit state of strongly damped vibrations: from a given arbitrary and inaccurate initial configuration, each node of the structure incrementally oscillates until, due to artificial damping, the structure comes to rest in a static equilibrium (Figure 2.17). Although based on different mechanical models and kinematic descriptions (3DoFs, 3DoFs + two boundary conditions, 4DoFs or 6DoFs), a large number of computational frameworks for the form-finding of bending-active structures rely on the dynamic relaxation method (Adriaenssens and Barnes 2001, Douthe et al. 2006, Barnes et al. 2013, D'Amico et al. 2014, Du Peloux et al. 2015, D'Amico et al. 2016, Bessini et al. 2017, Lefevre et al. 2017). The different contributions are reviewed in (Lázaro et al. 2018). Dynamic relaxation is often favoured over other methods owing to its reported simple implementation and good convergence. Besides, since the dynamic relaxation method is equally suitable for the form-finding of cables nets and membranes (Day and Bunce 1969, Barnes 1975, 1999), the form-finding of bending-active tensile structures can naturally be achieved with this method (Barnes 1999, Adriaenssens and Barnes 2001). Alternatively, the force density method, initially proposed for the form-finding of cable nets by Schek (Schek 1974), can be implemented in the

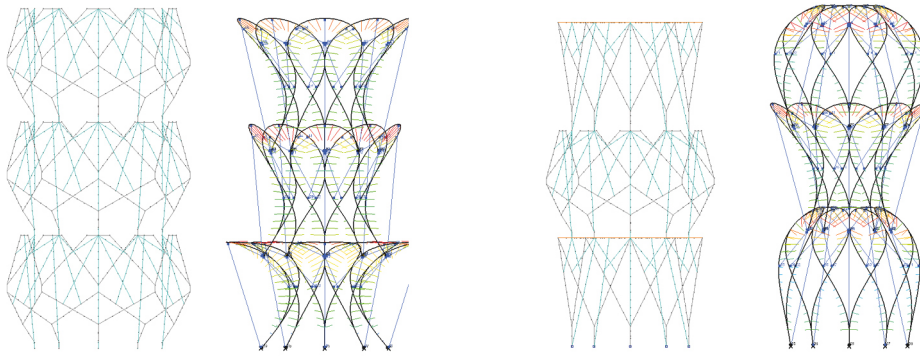


Figure 2.18: Design exploration of bending-active tensile structures with *Kangaroo2*'s solver in *Rhinoceros 3D* CAD modelling software environment – Form-found equilibrium geometry of the structures and their arbitrary original configuration.

dynamic relaxation algorithm to form-find bending-active tensile structures (Van Mele et al. 2013).

Projective Constraint-based Solver With an algorithm resembling the kinetic damping of the dynamic relaxation method, the projective constraint-based solver of *Kangaroo2* (Piker n.d.), a plugin developed by Piker for the visual programming environment *Grasshopper* (Rutten 2009) integrated to *Rhinoceros 3D* CAD modeling software environment (Robert McNeel & Associates n.d.), offers a user-friendly interface able to address many form-finding problems including the one of bending-active and tensile structures (Figure 2.18). As reported in (Bauer et al. 2018) and (Cuvilliers et al. 2018), instead of adopting the standard force-based approach to calculate the acceleration, velocity and ultimately position of the nodes, as in the dynamic relaxation method, the algorithm of *Kangaroo2*'s solver makes use of projections. Goal functions are defined for all the nodes and they return target positions where nodes are projected and that correspond to their closest zero energy state. More precisely, the new position of a node is obtained by its projection onto the barycentre of the target positions of each goal function that affects the node, weighted by their relative strength. It results that the new position remains within the convex hull defined by the distinct target positions, avoiding problems of large acceleration vectors, divergence and instability which might come along with the dynamic relaxation method. Little information is communicated by the developer onto the algorithm itself but according (Cuvilliers et al. 2018), the projective constraint-based solver used would be derived from the Shape-Up algorithm (Bouaziz et al. 2012) developed in the field of computer graphics for geometry processing. In the currently available version of *Kangaroo2* (version 2.4.2 at the time of the research), the solver operates on 3DoF vertices and the goal function related to bending behaviour does not consider orientation or anisotropy of the cross section neither torsion.

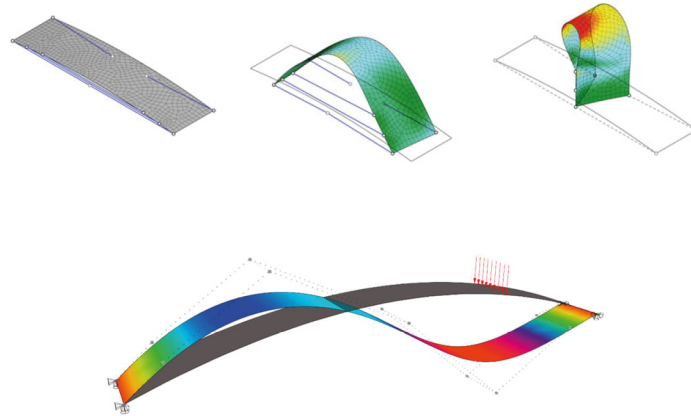


Figure 2.19: Form-finding of bending-active plate structures based on a finite element analysis – (top) Classical mesh-based approach with *SoFiSTiK*'s software and (bottom) isogeometric-based approach with *Kiwi!3D* plugin for *Grasshopper*.

In particular, the goal function related to bending derive from (Adriaenssens and Barnes 2001). Goals functions for prestressing membranes and cables can also be implemented, allowing the design of bending-active tensile structures (Quinn et al. 2016) (Figure 2.18).

Particle-spring systems Similar as well to the dynamic relaxation method, particle-spring systems, which originate from the computer graphics industry, can also be used for structural form-finding applications (Kilian and Ochsendorf 2005). In particular, particle-spring systems are mainly popular among architects through custom programmed software environments such as *springFORM* (Ahlquist et al. 2015), *ElasticSpace* (Suzuki and Knippers 2017) or *Iguana* (Suzuki et al. 2018). Although they offer a high degree of interaction during the design process, these programs are not as widespread as *Kangaroo2* software.

Finite Element Method Very different from the three methods mentioned above, the finite element method can also be used to address the equilibrium of bending-active structures. The finite element method is a general method for numerically solving partial differential equations of boundary value problems. It has indeed established itself as an essential tool in the field of structural analysis, and its versatility makes it widely applied to a diverse variety of technical problems. A matrix approach, the finite element method is based on the discretisation of the object to be analysed into a number of simple and finite elements, through the generation of a mesh. A weak problem formulation and a linearisation on each element of the partial differential equations in the form of a linear matrix equation are then used to calculate an approximate solution of the equations at the mesh vertices. Unlike the dynamic relaxation method, which uses an iterative integration scheme, the finite element method is a matrix approach, that uses in its most common implementation (linear static problems) a single operation

to solve a system of linear algebraic equations. Applied to the calculation of solids and structures, the finite element method makes it possible to calculate the displacements of mesh nodes by solving the linear matrix equation (force displacement relationship): $\mathbf{F} = \mathbf{k}\boldsymbol{\delta}$, where \mathbf{F} represents the force vector, \mathbf{k} the system stiffness matrix (established from the stiffness matrix of each of the finite elements), and $\boldsymbol{\delta}$ the unknown nodal displacement vector.

In the case of active-bending structures, due to the large displacements they undergo, a geometric non-linear analysis must be performed. As a consequence, the acting loads must be applied following an incremental procedure, and the quantities involved in the problem updated throughout the loading process. In particular, at each step of the calculation, the initial state of the structure is inherited from the previous deformed state and the stiffness matrix is updated.

Various incremental procedures can be used to bring slender elements into their elastically deformed shapes. For structures with low complexity, a simple way is to perform a number of linear supports displacements as illustrated in (D'Acunto and Kotnik 2013). Alternatively, for structures with higher complexity and for which incremental supports displacements is no longer possible, (Lienhard et al. 2014) proposed a form-finding procedure in which virtual ultra-elastic contracting cable elements pull associated points from an initially planar system into an elastically deformed configuration. In both cases, the incremental loading procedure mimics the assembly and erection process of the structure.

If bending-active structures are form-found through the deformation process of defined elements, this approach cannot be applied to the form-finding of membranes since their original configuration geometry is only known after the form-finding process. In relation to this problem and to the need to initialise the geometry of form-active tensile elements, (Dieringer et al. 2013, Philipp and Bletzinger 2013) make use of the Update Reference Strategy (Bletzinger and Ramm 1999) to carry out configuration updates during the form-finding process of bending-active tensile structures.

As an alternative to the classical mesh-based approach to finite element method, (Bauer et al. 2017) highlight the potential of using isogeometric analysis (Hughes et al. 2005), a subgroup of finite element methods, to simulate building process such as the bending of slender elastic elements. The isogeometric analysis allows structural analysis to be directly integrated into a computer-aided design environment (Bauer et al. 2017, Längst et al. 2017). Contrary to the above mesh-based finite element method in which the structure under analysis is discretised into finite elements and the calculation performed onto the vertices of the elements, the isogeometric analysis operates the finite element analysis directly onto the control points of the NURBS curves, which serve for the geometry description of the elements. The main advantage of the isogeometric analysis is that the same mathematical geometry description is used during the design and the structural analysis, making model conversions no longer required.

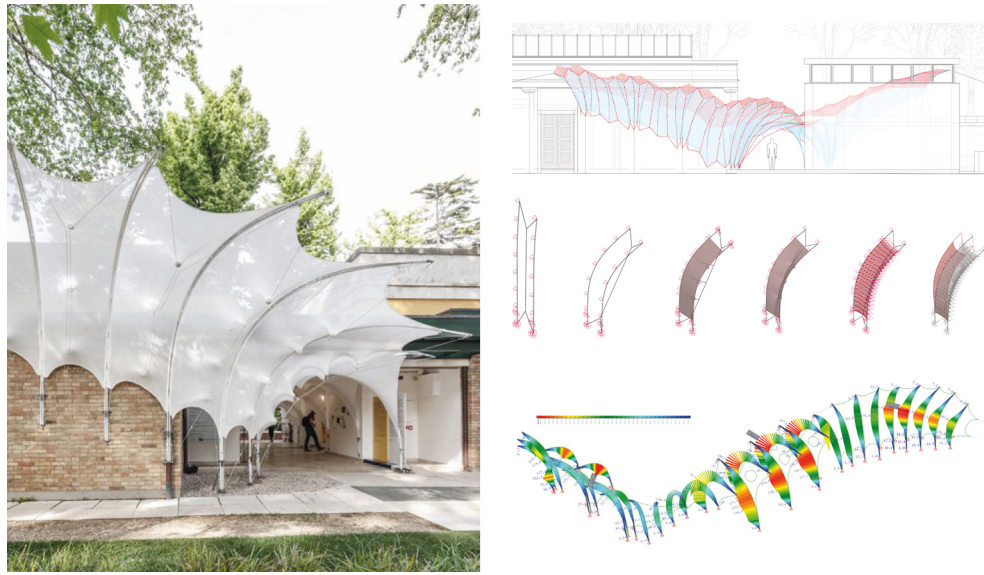


Figure 2.20: Design of *Isoropia* structure by CITA, Royal Danish Academy of Fine Arts, and collaborators (2018) – (from top to bottom) Distinct modelling methods and environments *Kangaroo2*, *Kiwi!3D* and *SOFiSTiK* successively used during the design process.

Diversity and complementarity of the numerical form-finding methods

The wide range of numerical methods and associated modelling tools which have been developed and released over the last decade can be explained by the fact that they are not all used for the same purposes. Indeed, each of them offers specific and relevant strengths with respect to the modelling of bending-active structures and displays advantages and disadvantages relating to accuracy, speed, user interfacing and design interactivity. Therefore, the different methods and associated tools do not exclude each other but, on the contrary, are complementary and can advantageously be combined during the design process.

A comparison between three distinct software environments for the design and simulation of two exemplary bending-active structures, namely *SOFiSTiK*'s Finite Element Method solver (*SoFiSTiK AG n.d.*) with an active bending module for the simulation of large deflections (implicit method), *Kiwi!3D* new plugin for *Grasshopper* based on Isogeometric Analysis (implicit method) and *Kangaroo2* and its projective constraints-based solver (explicit method) have been made by (Bauer et al. 2018). It highlights that Finite Element tools provide more precise simulations but in return present limitations in terms of exploratory design in a context of parametric modelling. In particular, the form-finding process, which has to operate on the original unstressed configuration of the elements, needs to be replicated for each design iteration, which makes real time interactions hard to implement, even impossible. Besides, the resort to Finite Element tools requires not only familiarity with the numerical method that they are based on but also a good control over the numerical parameters involved in

the incremental loading procedure, which makes their use difficult for uninitiated designers.

This is a reason why, even if the explicit finite element methods can be used for design-oriented problems, implicit software environments based on a projective constraint-based solver or on particle-spring systems are favoured during the early exploratory phase of the design of bending-active structures. Although less precise, these latter environments display the great advantage of providing users with interactive interfaces allowing design exploration. In particular, *Kangaroo2* is valued for its high level of interactivity, accessibility and customisability since it provides users with an unequalled freedom to script goal functions to suit their own requirements, and with the possibility to create a design, explore topological variations and modify accordingly based on real-time feedback on the structural performance (Quinn et al. 2016, Bauer et al. 2018). In this way, finite elements methods are rather dedicated to the precise form-finding and structural evaluation of structures which are first generated with tools based on explicit methods.

A demonstrative example of the complementarity of the distinct methods and modelling tools is the design workflow of *Isoropia* (Figure 2.20), a bending-active tensile installation built at the Danish Pavilion as part of the 2018 Venice Biennale (La Magna et al. 2018). The same distinct modelling environments as those considered in (Bauer et al. 2018) were used to form-find and analyse the structural behaviour of the structure, each of them being involved within the design at the stage for which it was the most appropriate. Specifically, a first stage of the design consisted in a large series of design iterations with the use of *Kangaroo2*. An interactive design modelling pipeline (Quinn et al. 2016) gave the designers the possibility to quickly explore topological variations and modify the geometry on the go based on structural and architectural requirements. In a second stage, the results for the first form-finding stage were evaluated with respect to displacements and stresses under common design load cases, while the erection process was also considered. This evaluation process was performed with *Kiwi!3D*, which favourably and seamlessly combines *NURBS* modelling with physical simulations, and implied a sequential calculation. Eventually, a detailed analysis of the structural behaviour of the canopy was performed at the latest stage of the development process with the use of *SOFiSTiK*, providing a deepest insight into the global behaviour of the structure and into the critical areas of the elements and therefore prevent potential failure. The authors concluded that breaking down the workflow between different tools was particularly effective and beneficial for the speed of execution of the project.

An additional example demonstrating how tools and methods can complement each other is the design process of the *Textile Hybrid M1* (Lienhard, Ahlquist, Menges and Knippers 2013) which involved in a first instance, as an explorative tool, a software environment based on particle-spring systems (namely *springFORM* (Ahlquist et al. 2015)), and once the global topology of the sys-

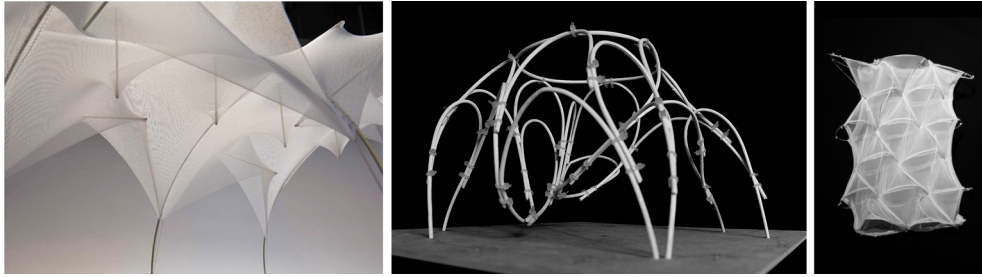


Figure 2.21: Physical models used as a generative driver of the design of bending-active structures – (from left to right) Conceptual model of the arched roof of *Isoropia* structure by CITA, Royal Danish Academy of Fine Arts, and collaborators (2018), exploration of bending-active arched structures by IACC and CITA (2014) and explorative model for the design of the installation *Lace Wall* by CITA, Royal Danish Academy of Fine Arts (2016).

tem was defined used *SOFiSTiK* to precisely form-find the structures, evaluate its behaviour under loads and generate the cutting pattern of the prestressing membrane.

It should also be noted in that these projects, as in many others, additionally to numerical tools, physical models and experiments keep on playing an important role as a generative driver of the design process and often contribute to define the essential concepts of the design (Figure 2.21).

2.1.4 Graphical method for the modelling of first order elastic curves

Although not valid for the large deflections of bending-active beams, graphic statics has proven to be effective at modelling elastic curves within the scope of the first order theory. Mainly known for the geometric construction of funiculars and arches in equilibrium with given loads, graphic statics makes it also possible to graphically find the bending moment diagram and the deflection curve of continuous beams under loads (Ritter and Culmann 1900, Wolfe 1921) (Figure 2.22). The corresponding graphical procedure involves the geometric construction of funicular polygons, which correspond in terms of graphical integration to a second integral of the loads, as demonstrated by Massau (1878-1887) (Tournès 2003). First, the bending moment diagram of the beam is built as a funicular in equilibrium with the actual loads acting on the beam. Then, a second funicular in equilibrium with the bending moments acting on the beam taken as a distributed load is constructed. This second funicular corresponds to the deflection curve of the beam by a scaling factor, which depends on the scales of the form diagram and the force diagram and on geometric parameters such as the position of the poles in the force diagram.

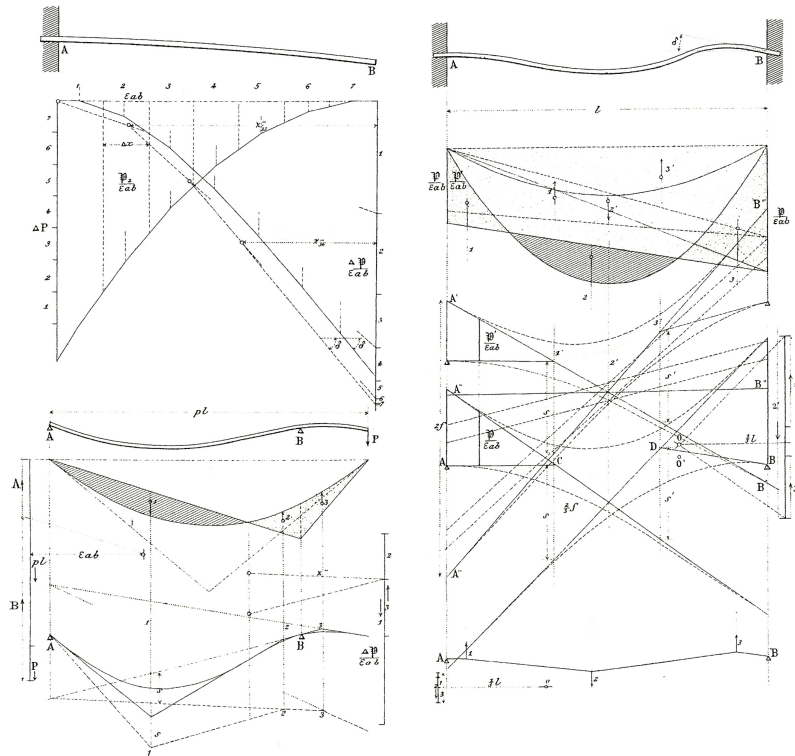


Figure 2.22: Bending moment diagram and first order elastic curve of slender beams with the graphic statics method by Karl Culmann (Addis 2007).

2.2 Research scope

2.2.1 Problem statement

Discussion on existing approaches One of the difficulties associated with the design of bending-active tensile structures is to define the structures' geometry at equilibrium, particularly due to the geometric nonlinearity of the bending phenomenon (Lienhard 2014, 15–21). The numerical methods which are currently used to predict their equilibrium geometry are mainly based on form-finding algorithms. These complex algorithms are effective, on the one hand, in determining the structures' equilibrium geometry from given boundary conditions and parameters related to the structures and, on the other hand, in analysing the structures' behaviour under loads (Section 2.1.3). However, despite the diversity and complementarity of the existing form-finding methods and the related digital tools, there is a persistent need of a better integration of the designer's intuition in the design process (Slabbinck et al. 2017). One of the reasons is that form-finding methods have the disadvantage of offering only an indirect control over the final equilibrium geometry of the bending-active tensile structures. This control is generally achieved by steering the form-found structures towards an expected output through an iterative adjustment of the parameters that serve as inputs for the form-finding algorithm (Kilian 2014). However, confronted with the complex reciprocal equilibrium which underlies bending-active tensile structures and opaque numerical form-finding processes, the designer often lacks of an intuitive design strategy to implement the mental idea he/she has formed of the object to be designed and consequently integrate into the design architectural, programmatic, structural and manufacturing aspects. More specifically, the designer is confronted with the fact that he/she cannot explicitly control the equilibrium geometry of bending-active tensile structures. Yet, the possibility to adjust explicitly their geometry, in particular through the control of the equilibrium geometry of the actively bent elements, may appear as particularly relevant to foster the intuitive and intentional design of bending-active tensile structures and ultimately provide an integral response to the structural, architectural, and geometry-related aspects of their design.

Research questions The design of bending-active tensile structures cannot be released from the physical laws that govern their equilibrium. Faced with these objective laws, the designer seems to see his/her initiative and influence limited in the design process. The intention of this research is to question **how far it is possible to preserve the leading role of the designer in the design of bending-active tensile structures in architecture.**

On the one hand, it is a matter of offering the designer a means of controlling the geometry of bending-active tensile structures in order to help him/her implementing his/her design intention. This can be achieved by developing a

simplified and easily comprehensible structural model that brings out the reciprocal dependencies between geometry, forces and physical material quantities at work in bending-active tensile structures. More specifically, based on the evidence of graphic statics being an efficient, simple and transparent tool for the consistent structural design of equilibrated architectural forms, the research explores **how graphical methods can support the design of bending-active tensile structures composed of bending-active beams and pre-stressed cables and cable nets** and ultimately overcome some of the limitations of the current form-finding methods, for instance by giving emphasis to the final equilibrium geometry.

On the other hand, on the basis of this simplified structural model, design strategies that take advantage of the reciprocal interactions between geometry-force-material have to be established in order to support the designer in his/her role. In the context of a material-based design process such as active bending, the research investigates **how the possibility to specify and control inherent material properties in a structural design to match a desired equilibrium geometry can be implemented in the design of bending-active tensile structures**.

2.2.2 Research objective and methodology

With the intention to overcome some of the limitations of the existing form-finding methods, the primary goal of this research is to define a design approach that connects simply and transparently, yet accurately, the geometric and structural dimensions of bending-active tensile structures and foster their intentional design. In an alternative and complementary way to form-finding approaches, the proposed approach is form-driven and aims to support the designer in materialising consistently his/her conceptual intentions and in integrating more easily to the design geometry-based criteria, especially during the early conceptual stage of the design.

Grounded on the definition of a simplified structural model for slender elastic beam and on the use of graphical methods, the proposed form-driven design approach investigates strategies to enforce the bending-active beams of a bending-active tensile structure to match a target equilibrium geometry through the adaptation of the beams' bending stiffness and the restraining effect of pre-stressed cables and cable nets. In particular, the role of material as a mediator between form and forces, geometry and physical laws, is asserted and activated, providing the designer additional lever to influence the design process and integrate both the mechanical conditions of the bending-active beams and the specific target equilibrium geometry.

The development of the proposed form-driven design approach for bending-active tensile structures in architecture is the outcome of three main research phases:

1. Structural Model In a first step, a new mechanical model for slender elastic beams was defined (Chapter 3). This simplified model (Boulic and Schwartz 2017) describes the internal and external forces acting on a slender beam that is elastically deformed in its plane of symmetry and therefore only subjected to bending (no torsional forces) (Section 3.1). The application of graphic statics' principles, more specifically the use of a force diagram to represent static equilibrium of a structural system, led to the visualisation of certain relationships between the curved equilibrium geometry of a bending-active beam and the internal and external forces acting on it. In particular, based on the analysis of the force diagram, two graphical strategies to enforce a bending-active beam to bend into a specific target geometry were highlighted: on the one hand, the adjustment of the beam's bending stiffness along its axis to match the target curvature of the bent beam (Section 3.2) (Boulic and Schwartz 2018), and, on the other hand, the application of additional restraining forces onto the beam's axis by a post-tensioning restraining system (Section 3.3) (Boulic and Schwartz 2017). Finally, the use and extension of the same mechanical model for the modelling of bending-active beams in 3D space subjected to torsional forces was discussed (Section 3.4).

2. Design Approach In a second step, the design approach itself, whose foundations are based on the results provided by the above structural model, was developed (Chapter 4). This approach is intended for the design of bending-active tensile structures composed of slender beams elastically bent in their plane of symmetry and connected together by three-dimensional pre-stressed cables and cable nets (Boulic and Schwartz 2018). Whereas existing form-finding methods address the equilibrium of bending-active tensile structures globally, the form-based design approach establishes their equilibrium geometry by decoupling the equilibrium of the bending-active beams and that of the pre-stressed elements. This decoupling allows to consider the bending-active beams directly in their target equilibrium geometry, while the conditions leading to such a geometric configuration of equilibrium of the bending-active beams inform the equilibrium geometry of the pre-stressed elements (Section 4.1).

On the one hand, the above structural model was used for the equilibrium of the bending-active beams. On the other hand, different methods, both graphical and numerical, were developed for the generation of restraining cables and cable nets enforcing the equilibrium of the bending-active beams in their target geometry. First, a fully graphical method (Boulic 2020) was developed to generate bending-active tensile structures composed of a single bending-active beam restrained by a 3D cable net deriving from the geometric transformation of an original 2D tensile restraining system (Section 4.2). Second, specific geometric configurations of bending-active beams and cables were proposed to create bending-active tensile structures composed of several bending-active beams (Section 4.3). Third, in order to develop bending-active tensile structures with a

more complex and less constrained configuration, an extension of the force density method (Schek 1974) was formulated for the form-finding of pre-stressed cable nets under constraints (Section 4.4) (Boulic and Schwartz 2018).

3. Design Application In a final step, a specific bending-active tensile structure was designed in order to test the applicability of the proposed form-driven approach to a real and complex design context and illustrate the approach' potential (Chapter 5). More specifically, this case study consisted in the design of an external sun-shading façade system whose sun-shading performances are directly influenced by its geometry. An integral design framework was introduced to take into account and integrate to the design various architectural, structural, functional and constructibility criteria directly related to the geometry of the bending-active tensile sun-shading structure.

3. Structural Model

This Chapter proposes a novel structural scheme to model the static equilibrium of bending-active beams deforming elastically in 2D space. It is based on a simplified mechanical model of the internal forces which act on the beams and on the implementation of the graphic statics principles to address the static equilibrium of the beams.

3.1 Bending-active beams in 2D space

The content of Section 3.1 has been partly published in (Boulic and Schwartz 2017).

3.1.1 Mechanical model of bending-active beams

A simplified mechanical model is introduced to describe the behaviour of slender and elastic beams undergoing in 2D space large displacements and infinitesimal elastic strains. More specifically, this model applies to bending-active beams – and equally to bending-active rods – with a plane of symmetry which is also the plane of the external loading. As a result, the deformations occur in that plane of symmetry due to bending moments which are normal to that plane and there is no torsion around the beams' axis. Normal sections of the bending-active beams are considered to remain plane, undistorted and normal to the beams' axis after deformation. In particular, the model is described for bending-active beams whose axis is straight in the undeformed configuration, corresponding to a zero initial curvature of the beams.

Discrete modelling of a continuous bending-active beam Consider a slender linear beam defined by its axis and with $(O, \mathbf{x}, \mathbf{y})$ as plane of symmetry (Figure 3.1). The curved and continuous axis of the beam is discretised into linear bars and nodes and the internal and external forces acting on the continuous axis are translated into discrete forces acting at the nodes. In particular, the beam's axis is discretised into N bars, which can be of different size (the more refine the discretisation, the more accurate the modelling will be), and in $N + 1$ nodes. l_i stands for the length of bar i and θ_i for its orientation in relation to the reference axis \mathbf{x} . The distance between nodes $i - 1$ and $i + 1$ is $l_{i-1,i+1}$ and El_i is

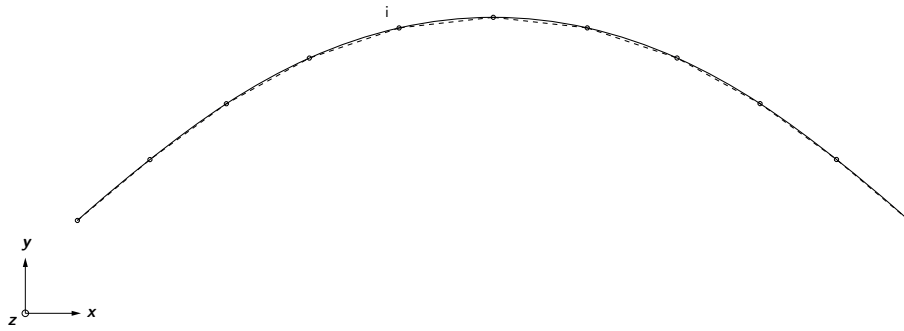
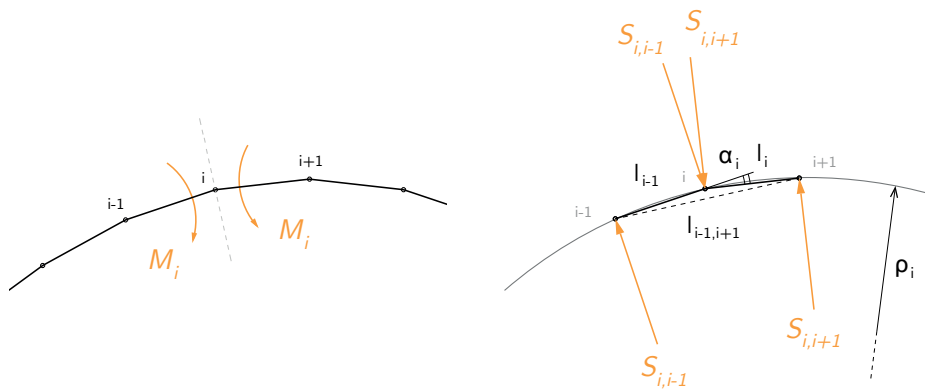
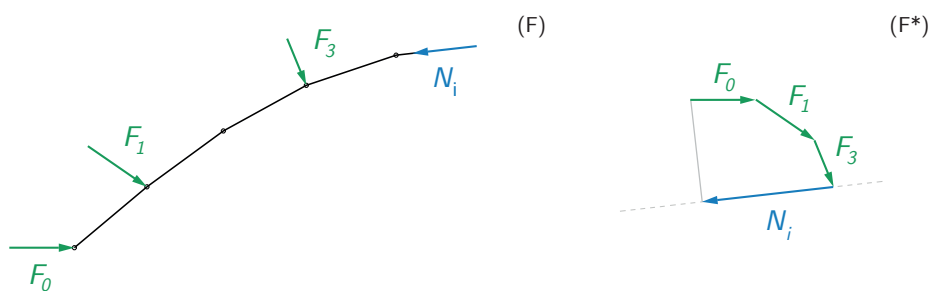


Figure 3.1: Discretisation of a bending-active beam.

Figure 3.2: Discrete shear bending forces in a discretised bending-active beam – Three consecutive nodes ($i-1, i, i+1$) and the pairs of shear forces equivalent to the bending moment acting on the central node i .Figure 3.3: Axial forces in a bending-active beam – Free body diagram of the beam (F) and force diagram representing its global equilibrium (F^*). Forces represented as green vectors are external forces; blue vectors correspond to compressive axial forces while red vectors would correspond to tensile axial forces.

the bending stiffness of the beam around the axis \mathbf{z} at node i such that $(\mathbf{x}, \mathbf{y}, \mathbf{z})$ is an orthogonal coordinate system. The angle α_i is defined as being $\theta_i - \theta_{i-1}$.

As proposed by (Adriaenssens and Barnes 2001), internal forces acting at the beam's nodes are of two natures: shear bending forces and axial forces.

Shear bending forces Bending moments acting on a continuous beam can indeed be translated into discrete forces acting at the nodes of the discretised beam (Adriaenssens and Barnes 2001). Under the assumption that three consecutive nodes $(i-1, i, i+1)$ are close enough, they are assumed to lie on a circle which radius is the radius of curvature of the beam's axis at node i (Figure 3.2). The radius of curvature ρ_i of the beam's axis, and hence the bending moment \mathbf{M}_i at node i , can be directly deduced from the nodes' relative position:

$$\rho_i = \frac{l_{i-1,i+1}}{2 \sin \alpha_i} \quad (3.1)$$

$$M_i = \frac{EI_i}{\rho_i} = EI_i \frac{2 \sin \alpha_i}{l_{i-1,i+1}} \quad (3.2)$$

The bending moment \mathbf{M}_i is translated into two couples of shear forces $(\mathbf{S}_{i,i-1}, -\mathbf{S}_{i,i-1})$ and $(\mathbf{S}_{i,i+1}, -\mathbf{S}_{i,i+1})$ applied respectively at nodes $(i-1, i)$ and $(i, i+1)$. According to the free body diagrams of bar $(i-1)$ and bar (i) , which must fulfil equilibrium, the magnitude of the shear forces is respectively:

$$S_{i,i-1} = EI_i \frac{2 \sin \alpha_i}{l_{i-1} l_{i-1,i+1}} \quad (3.3)$$

$$S_{i,i+1} = EI_i \frac{2 \sin \alpha_i}{l_i l_{i-1,i+1}} \quad (3.4)$$

The shear forces $(\mathbf{S}_{i,i-1}, -\mathbf{S}_{i,i-1})$ and $(\mathbf{S}_{i,i+1}, -\mathbf{S}_{i,i+1})$ act normal to the bars, in opposite direction as illustrated in Figure 3.3.

Axial forces Unlike in (Adriaenssens and Barnes 2001) where the axial forces in the bars depend on the cross-sectional area A of the bars and on their modulus of elasticity E , in the proposed mechanical model, axial forces are material-independent and are deduced from the global equilibrium of a free body diagram of the beam (Figure 3.3). As a result, it is assumed that the beam preserves its original length while bending. This assumption is in line with the hypothesis of infinitesimal elastic strains. The axial force \mathbf{N}_i in bar i can be obtained simply from a force diagram, by projecting along \mathbf{u}_i the inverse of the resultant force of the external forces \mathbf{F}_j acting on the nodes of the free-body diagram of the beam, with \mathbf{u}_i to the unite vector along bar i pointing in the direction of node $i+1$ from node i :

$$\mathbf{N}_i = -\left(\sum_{j=0}^i \mathbf{F}_j \cdot \mathbf{u}_i\right) \mathbf{u}_i \quad (3.5)$$

Moments External moments acting on the beam are also translated into equivalent pairs of forces ($F_{M_{ext}}, -F_{M_{ext}}$) applied at two consecutive nodes perpendicularly to the bar and in opposite direction. The magnitude of the forces corresponding to a moment M_{ext} applied on bar i is given by:

$$F_{M_{ext}} = \frac{M_{ext}}{l_i} \quad (3.6)$$

3.1.2 Graphic statics principles applied to bending-active beams

Nodal equilibrium Following the principles of graphic statics, for a bending-active beam to be in equilibrium, to all its nodes in the form diagram (F) must correspond a closed polygon of forces in the force diagram (F^*) (Figure 3.4). For each of the nodes, all the internal and external forces acting on it are drawn end-to-end (clock-wise) in the force plan where they must form a closed polygon.

Graphical construction of a bending-active beam in equilibrium By constructing sequentially and alternately its form and force diagrams, it is possible to graphically construct a discretised bending-active beam in equilibrium, node by node. This sequential process is based on the fact that the equilibrium of node i defines the position of node $i + 2$ in relation to the position of node $i + 1$ (Figure 3.5). In this way, an entire bending-active beam in equilibrium can be defined from the position of its nodes 0 and 1 and the external loads acting at node 0. By changing the position of node 1 of the beam and/or the loads acting at node 0, a large family of bending-active beams in equilibrium can be generated (Figure 3.6).

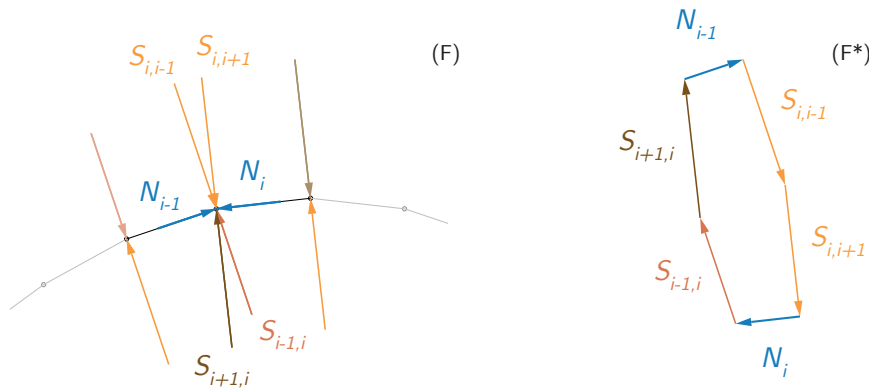


Figure 3.4: Nodal equilibrium – Form (F) and force (F^*) diagrams of a beam's node i . Different orange tones are used in order to highlight the distinct pairs of shear bending forces acting at node i . In this example, only internal forces are acting at node i (shear bending forces and axial forces) and external loads such as self-weight are not considered.

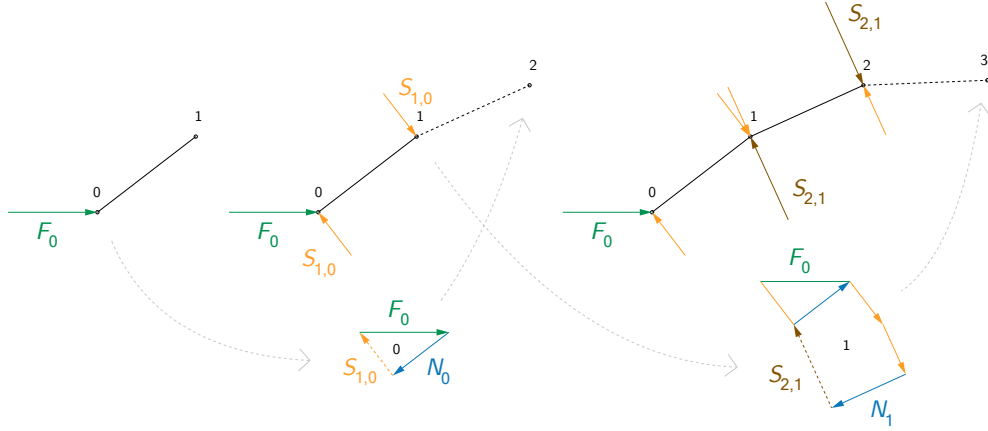


Figure 3.5: Node-by-node construction of a bending-active beam in equilibrium – Sequential graphical construction involving alternately the form diagram and the force diagram of the beam.

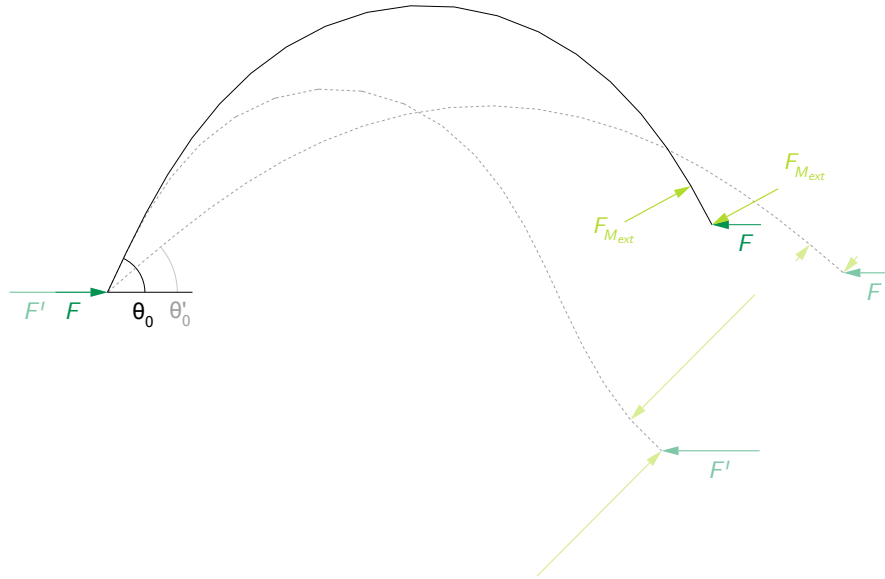


Figure 3.6: Generation of family of bending-active beams in equilibrium based on the boundary conditions at node 0: orientation θ_0 of the first beam's segment and external load \mathbf{F} .

In case that the equilibrium geometry of the actively bent beam has to fulfil specific boundary conditions (either static or kinematic), the generative parameters of the beam, namely the orientation θ_0 of the first bar of the beam (i.e. the position of node 1 in relation to node 0) and the external loads acting at node 0, have to be iteratively adjusted until the conditions are met. This iterative process can be implemented in a digital environment, where the node-by-node graphical construction of the beam can be automatised. Optimisation algorithms

can then be used to find the set of above generative parameters that lead to the equilibrium of the beam under the imposed boundary conditions.

Test case: the *Elastica* beam In order to validate the proposed modelling framework, it has been benchmarked with the numerical method of the dynamic relaxation (Day 1965, Adriaenssens and Barnes 2001). The comparison was carried out for the case of Euler's *Elastica* beam for which an analytical expression of the deformed shape is known (Timoshenko and Gere 1961, 76–82). The test considers a straight beam of length $l = 2m$, pin-ended to two supports $1.4m$ apart, which corresponds to a span/length ratio of 0.7 (Figure 3.7). The beam has a uniform circular cross section of diameter $15mm$ and a modulus of elasticity $E = 26GPa$. The self-weight of the beam is neglected.

For the proposed graphical method, as explained above, the force \mathbf{F} acting at node 0 and the inclination θ_0 of the beam at its end have been iteratively adjusted until the beam reaches the imposed location of its supports. Figure 3.7(a)-(b) shows the form and force diagrams of the beam finally obtained.

Regarding the algorithm of the dynamic relaxation, it was implemented in the form of a Python scripting code in the CAD software environment Rhinoceros (Adriaenssens and Barnes 2001, Douthe et al. 2006).

The bent geometry of the beam, in particular its inclination θ_0 at its ends and the dimensionless quantity F^2/EI , are compared for the different methods and for different refinements N of the discretisation of the beam's axis (Figure 3.7). The results are summarised in Table 3.1. It can be observed that the proposed graphical method is as close to the analytical solution as the dynamic relaxation method. As naturally expected, the difference to the analytical solution decreases with the refinement of the discretisation. Overall, these results validate the precision of the proposed graphical method and its ability to describe the behaviour of bending-active beams in 2D space.

Besides, an upper limit of the shortening of the beam due to its bending can easily be calculated for the graphically constructed *Elastica* beam. Given that the magnitude of the axial forces along the beam's axis is lower or equal to that of the external force \mathbf{F} , the shortening of the axis of the above 2m long beam is lower or equal to 0.15mm. This validates the assumption that the beam preserves its initial length while bending and that axial forces can be considered as independent from the mechanical properties of the beam.

Normalised force diagram and effect of scaling Consider the form and force diagrams of a bending-active beam in equilibrium. Normalised forces can be introduced. They correspond to the actual forces acting on the beam, divided by a scaling factor, which can be the bending stiffness of the beam EI or a nominative bending stiffness value EI^* in case that the beam has a non-constant bending-stiffness along its axis. The normalised force diagram of the beam can be assembled from the normalised forces. It actually corresponds to a scaled

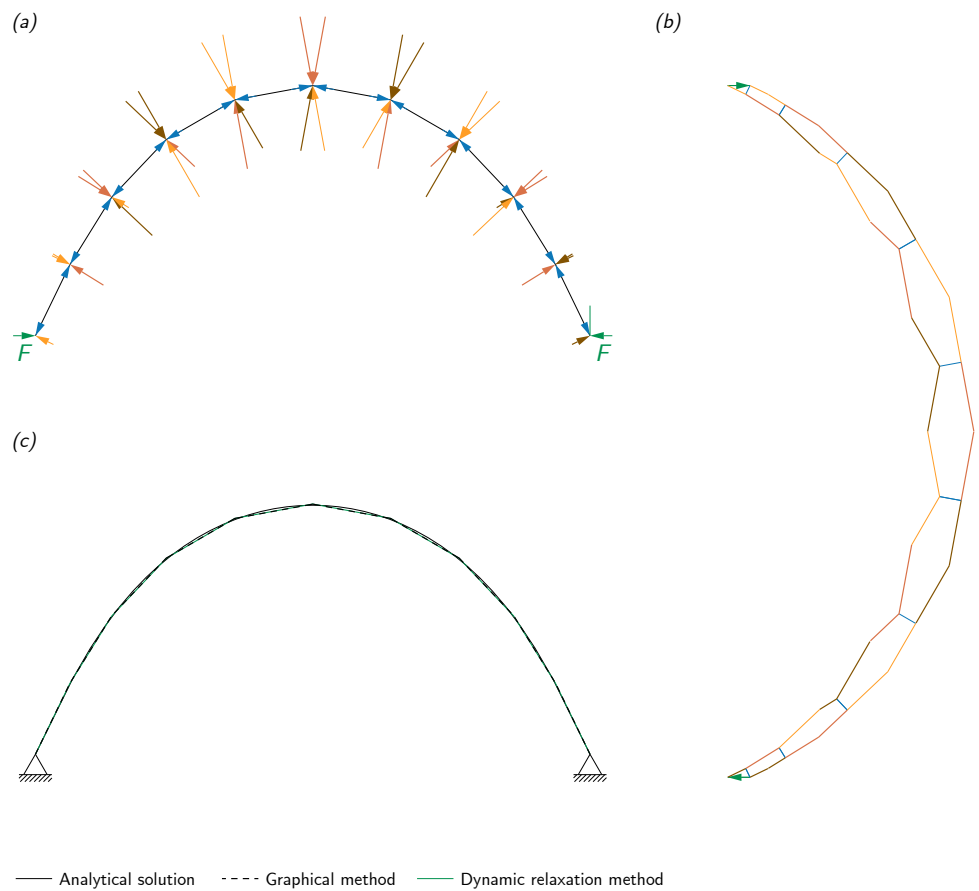


Figure 3.7: *Elastica* beams obtained by means of different methods – For a same span/length ratio of 0.7, geometry of the beam obtained with the graphical method (a)(b) compared with of the geometry form-found with the numerical algorithm of the dynamic relaxation and the analytical solution of the *Elastica* (c).

Table 3.1: Geometric comparison of the *Elastica* beams obtained by means of different methods, including the proposed graphical method.

	N	θ_0 (°)	Fl^2/EI	Calculated s/l
Analytical solution	-	64.89	11.65	0.700
Graphical method	10	64.09	11.52	0.6998
	20	64.70	11.62	0.6999
	100	64.84	11.65	0.6982
Dynamic relaxation	10	64.05	11.51	0.700
	20	64.61	11.61	0.6994

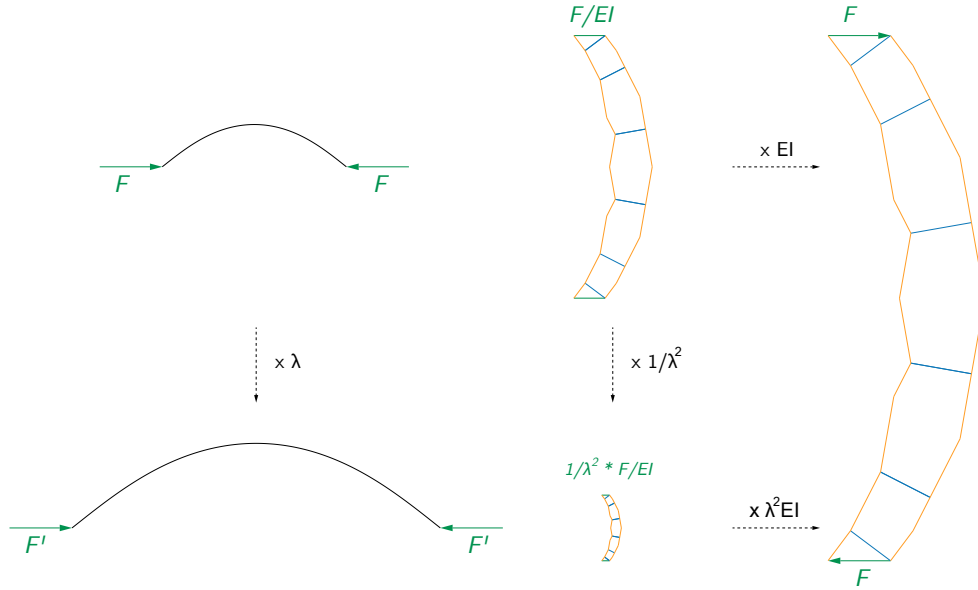


Figure 3.8: Normalised force diagram and effect of scaling – Form diagrams (F) (left), normalised force diagrams (F^*) (middle) and absolute force diagram (F^*) (right). A beam with a bending stiffness EI is bent under the prestressing force F . As the geometry of the beam is scaled by a factor λ in the form plan (F), the shear forces are scaled by a factor $1/\lambda^2$ in the force plan (F^*). In order to equilibrate this new scaled beam, the new bending stiffness EI' and the new prestressing force F' must verify $F'/EI' = 1/\lambda^2$. This can be obtained for example by the following configurations: $(F' = F/\lambda^2; EI' = EI)$, $(F' = F; EI' = EI/\lambda^2)$ and $(F' = F/\lambda; EI' = \lambda EI)$.

version of the actual force diagram (Figure 3.8). Considering normalised forces instead of the actual forces has no influence on the bent geometry of the beam.

Normalised force diagrams help to understand better the effect of scales on the bending-active beams. In particular, in those cases in which the self-weight of the beams is neglected, if the scale of the form diagram of a bending-active beam is changed, the new and original beams share the same normalised force diagram. In that way, the relative magnitude of absolute forces and the relative bending stiffness of the two beams can be deduced from the relative normalising and scaling of their force diagrams. This property is illustrated Figure 3.8. More generally, this aspect of the proposed graphical modelling framework allows to visualise how, the bending stiffness of a beam can have no direct influence on its bent equilibrium geometry (on the contrary gradients of bending stiffness do) while it impacts the magnitude of the forces acting on the beam, similarly as for the analytical solution of the *Elastica* beam (Timoshenko and Gere 1961, 76–82). When the effect of self-weight is neglected, this consideration makes it possible to address the equilibrium of a bending-active beam first with arbitrarily normalised forces and then integrate back the material properties. The corresponding actual forces acting on the beam can be retrieved by scaling its force diagram by the appropriate factor, without affecting the geometry of the

beam. Scaling effects on bending-active structures have been discussed in a broader context in (Lienhard and Knippers 2013).

On the limitation of using graphic statics to form-find bending-active beams

One of the specificities of graphic statics, which constitutes its strength compared to other structural design methods, is the existence of reciprocal relationships between the form and force diagrams of a structure as successively established by (Stevin 1586), (Varignon 1725), (Culmann 1866) and (Cremona 1872). In particular, these reciprocal relationships allows to modify the form diagram of a structure by altering its force diagram and vice versa. These reciprocal relationships are explicitly at play in the design of the funicular structures of an arch or a cable subjected to external loads (Figure 3.9 (left)). For these structures, specific geometric transformations of their force diagrams make it possible to generate new funicular shapes all in equilibrium with the same external loads. In particular, moving the pole of the funicular's force diagram along a line parallel to the virtual line connecting the supports of the funicular results in funiculars of different height.

When the reciprocal relationships between the form and force diagrams of a structure become too complex, numerical calculations need to be involved for the reciprocal geometric transformation of the form and force diagrams. This is for example the case in the procedure presented above for the graphical construction of a bending-active beam in equilibrium under specific boundary conditions and in which the parameters governing the equilibrium geometry of the beam have to be searched in an iterative manner. Indeed, in the case of the equilibrium of bending-active beams, this research could not establish explicit reciprocal relationships between their form and force diagrams. One reason is that the internal forces involved in the equilibrium of the beams, namely the shear bending forces, are “active” forces which cannot be calculated prior the equilibrium geometry of the beams is established as they depend on it in a non-linear way – the position of a point i influences the shear bending forces applying at nodes $(i - 2, i - 1, i, i + 1, i + 2)$. The elastic curve of the axis of a bending-active beam can be regarded as a funicular curve in equilibrium with the “active” discrete bending forces (Figure 3.9 (right)). Figure 3.9 illustrates for example how in the case of a funicular structure, the external loads for which the structure is designed remain unchanged during the form-finding exploration, while the discrete bending forces equilibrating an actively-bent beam vary for various geometric configuration of beams. Therefore, in the case of bending-active beams, the force diagram only cannot be the starting point for the construction of the form diagram as it is done for the form-finding of funiculars for example.

On how graphic statics is intended to be used Alternatively, in the rest of this thesis, the graphical representation of the principles of static equilibrium which is the force diagram is used as a design and analysis tool to deduce what are

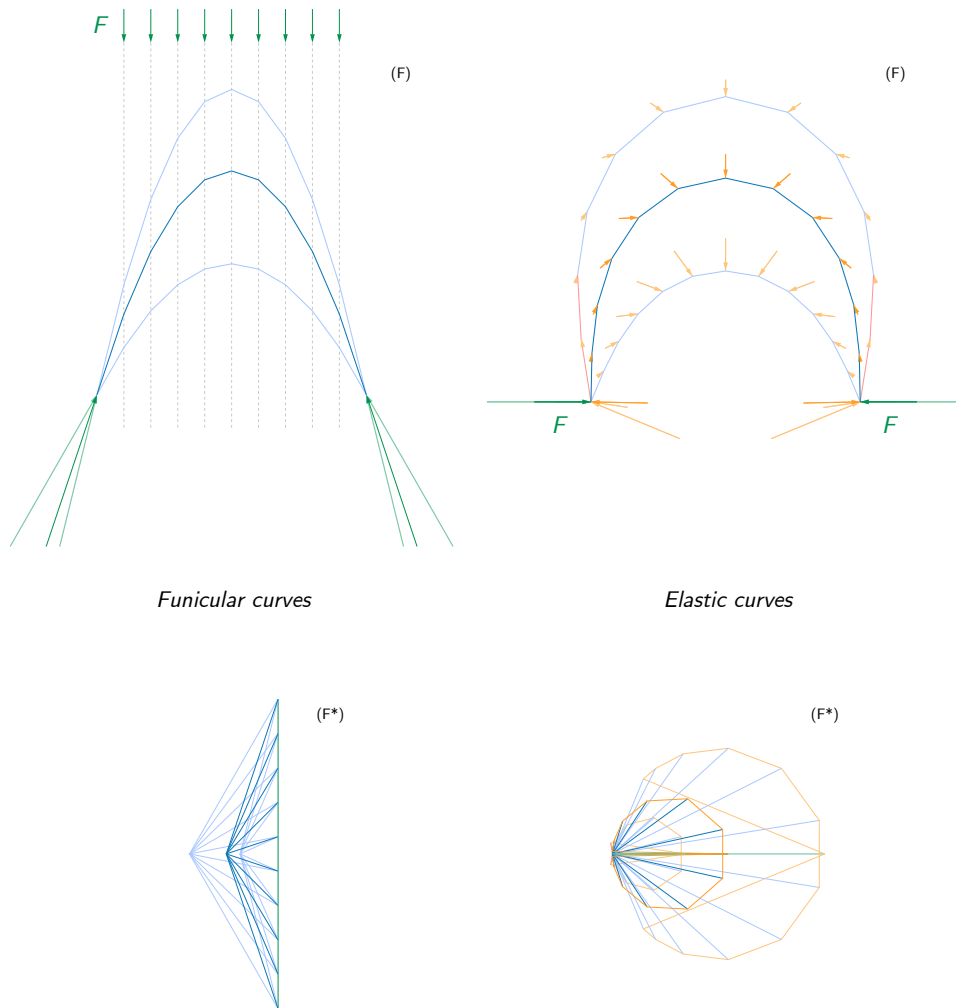


Figure 3.9: Funicular curves and elastic curves – Discrete bending forces (in orange) are represented as the resultant force of all the shear bending forces acting at each node.

the conditions that make a bending-active beam reach the static equilibrium in a target geometry which is defined beforehand by the designer. Any plane curve can indeed be discretised and analysed as an bending-active beam according to the modelling scheme proposed in Section 3.1 (Figure 3.10). For a given set of external loads and a given distribution of bending stiffness along the beam's axis, nodal forces are calculated and assembled in a force diagram. It is most likely that the bending-active beam is not in equilibrium in the considered configuration and that the polygons of forces of the force diagram are not closed. Additional forces are required in order to enforce the beam to be in equilibrium in the target geometry under the considered loads and boundary conditions.

Based on the visual representation of static equilibrium and on manipulations of force diagrams, the rest of Chapter 3 proposes a form-driven methodology

which allows to equilibrate bending-active beams into target curved geometries by means of, on the one hand, redistributing internally the shear bending forces through a controlled variation of the bending stiffness along their axis (Section 3.2) and, on the other hand, applying externally additional restraining forces on the beams' axis (Section 3.3). In both cases, the target geometries of the bending-active beams is first defined as plane continuous curves by the designer based on his/her design intentions and on design requirements and then, the conditions required for their equilibrium in the target geometries are developed based on static equilibrium. Starting from the deformed geometry of the beams, the proposed methodology represents a reverse approach to the form-finding approaches presented in Section 2.1.3 where the bent geometry is searched for (Figure 4.1). In an early phase of the design, this approach intends to support a more intentional and controlled design of the bending-active structures and take advantage of graphic statics as a powerful design and analysis tool.

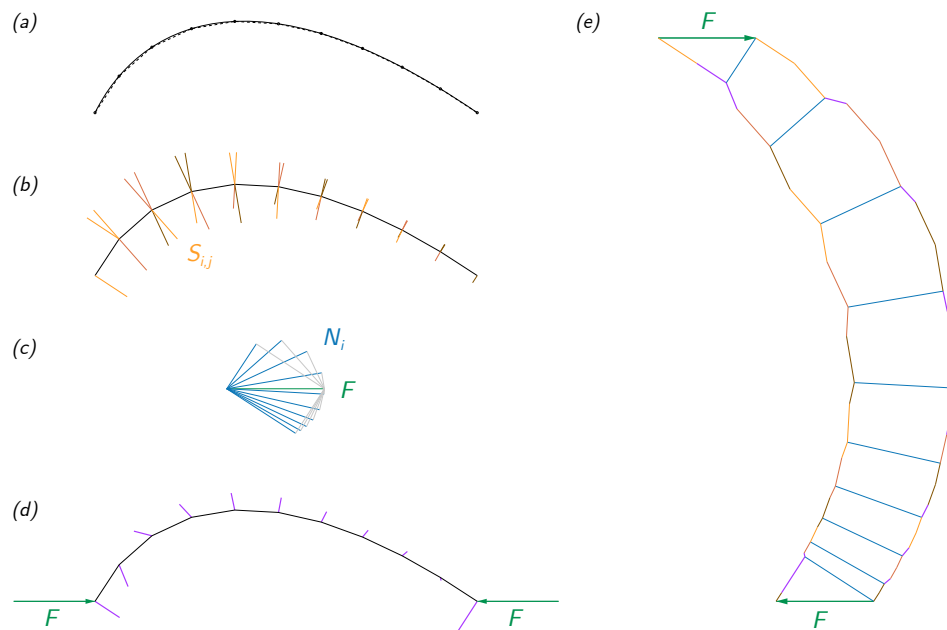


Figure 3.10: Analysis a bending-active beam in its target equilibrium geometry – The beam is out of equilibrium in the considered bent geometry and under the given boundary conditions since the polygons of forces of its force diagram do not close. Additional forces (in purple) are necessary to close the polygons.

3.2 Shaping bending-active beams by adjusting their bending stiffness

The curvature of a bending-active beam and its bending stiffness are locally related with each other as described by Equation 2.3. By precisely controlling and varying the bending stiffness along the beam's axis, it is possible to enforce the beam to bend into a target equilibrium geometry. In nowadays context of digital fabrication, the production of beams with bespoke bending stiffness is made possible. Structural elements with a cross section that varies along the beam's axis can be manufactured (Brütting et al. 2017) as well as structural elements with gradient of material properties (Bechert et al. 2016).

(Nicholas and Tamke 2012, Tamke et al. 2012) have illustrated in an experimental and empirical way how adjusting the bending stiffness of flexible elements can be used to match a target geometry. An analytical use of the curvature-bending stiffness relationship has been made by (Bechert et al. 2016), under the assumption of constant bending moment, for the design of initially planar plywood strips whose bent shape is pre-programmed into their bespoke laminate. In order to retrieve more accurate bending stiffness values, (Brütting et al. 2017) analytically calculate the local bending moment along the axis of a pinned-end flat beam from the forces acting at the beam's ends.

Here, a simple graphical procedure is proposed in Section 3.2.1 based on the mechanical model of bending-active beams presented in Section 3.1.1 and on the manipulation of force diagrams. This procedure applies for any support conditions and loads acting on a beam as long as they are compatible with the global and local equilibrium of the beam. These global and local conditions of equilibrium relate to the beam's bent geometry. They are formulated generally in Section 3.2.2 and explicitly specified in the case of a beam loaded at its ends only in Section 3.2.3.

The content of Section 3.2 has been partly published in (Boulic and Schwartz 2018).

3.2.1 Graphical procedure

Consider a bending-active beam in its target equilibrium geometry, it is discretised and loaded at its nodes. The internal forces acting at each node of the beam – the axial forces \mathbf{N}_i and the shear bending forces $\mathbf{S}_{i,j}$ – can be calculated from the nodes' position, a nominative bending stiffness of the beam at its nodes and the external forces acting on the beam, according the mechanical model presented in Section 3.1.1.

The equilibrium of each node of the beam is studied through the corresponding polygon of forces in the force diagram. Very likely, the polygons of forces do not close because the internal and external forces acting at the beam's nodes are not in equilibrium for the given target equilibrium geometry. By adjusting

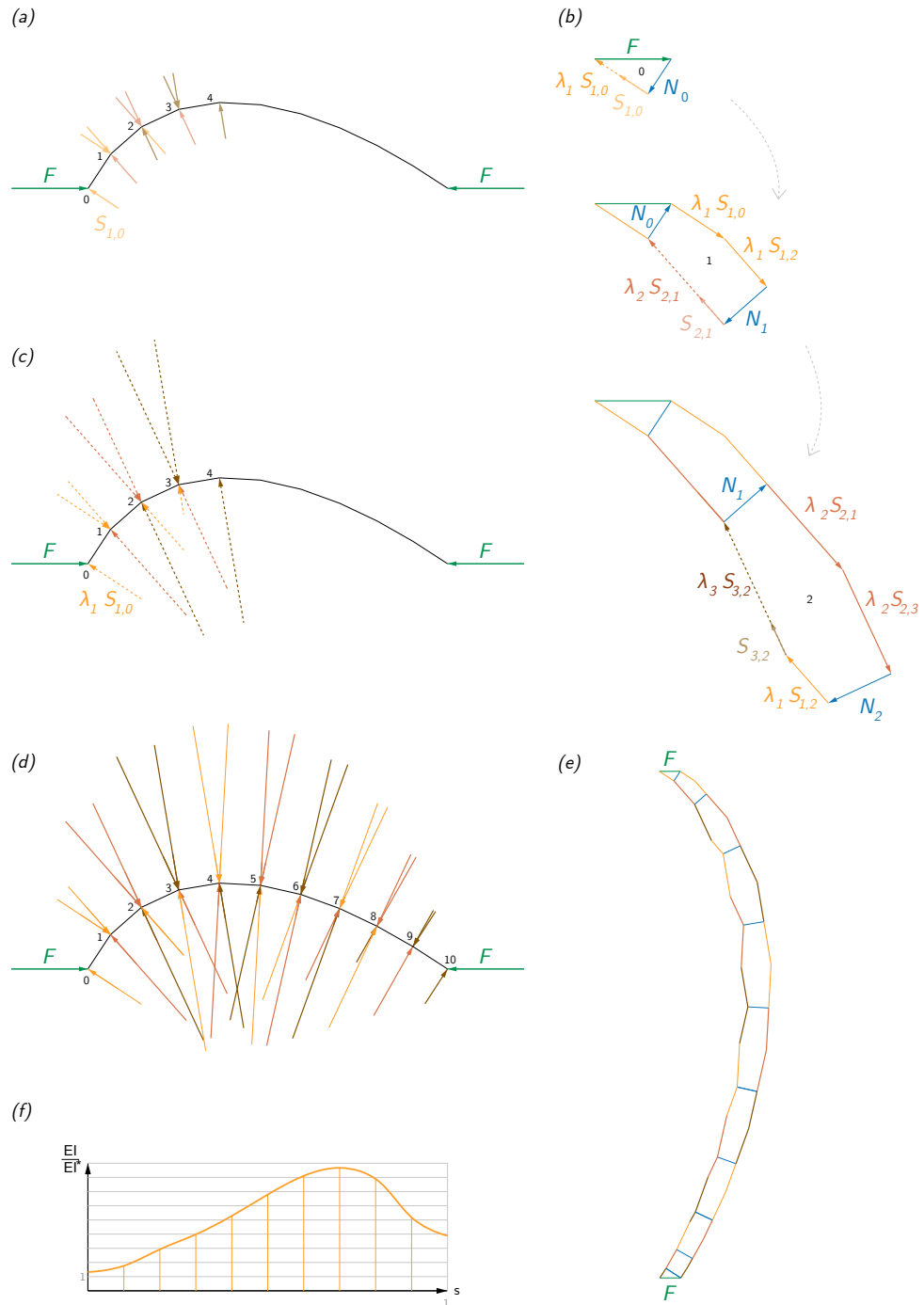


Figure 3.11: Calculation of the adjusted bending stiffness EI along the beam's axis by means of manipulation of the beam's force diagram – Shear bending forces for a nominative constant EI value (a) and for the adjusted EI (c); Iterative manipulation of force diagram (b), complete force diagram (e) and resulting shear bending forces (d); Distribution along the beam's axis of the adjusted EI to match the target equilibrium geometry and the given loads (f).

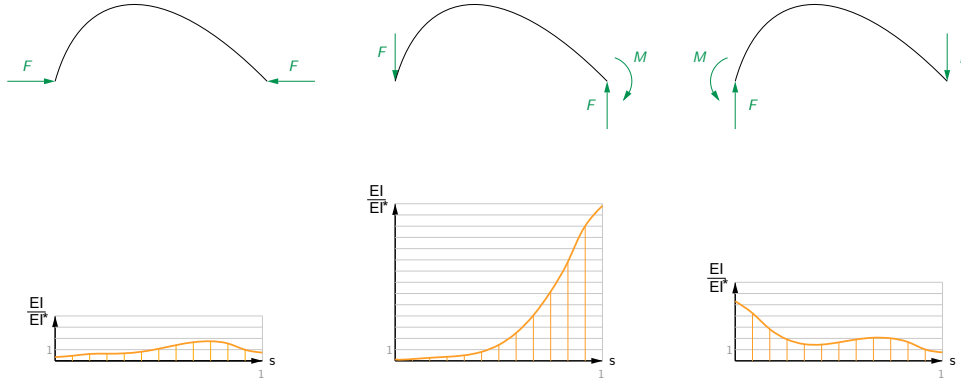


Figure 3.12: Influence of the beam's support conditions on the distribution of the bending stiffness EI along the beam's axis.

the bending stiffness of the beam at its nodes, it is possible to extend or shrink the shear bending forces and, ultimately, close the polygons of forces.

The beam's bending stiffness that corresponds to the target equilibrium geometry, the external loads and the support conditions is calculated node by node, through an iterative graphical procedure which is illustrated in Figure 3.11. Given that the previous nodes are in equilibrium, at node i , the shear bending force $S_{i+1,i}$ needs to be multiplied by a factor λ_{i+1} in order to close the polygon of forces of node i . λ_{i+1} relates to the variation of bending stiffness, in relation to the nominative bending stiffness, which is required at node $i+1$ to satisfy the equilibrium of node i . When considering the equilibrium of node $i+1$, the shear bending forces $S_{i+1,i}$ and $S_{i+1,i+2}$ are multiplied by λ_{i+1} and the shear bending force $S_{i,i+1}$ is multiplied by λ_i . As shown in Figure 3.11, this node-by-node graphical procedure is initiated at node 0. After all the polygons of forces of the force diagram have been rebuilt, the non-uniform distribution of bending stiffness along the beam's axis is found.

3.2.2 General conditions on the external loads

Given a target equilibrium geometry of the bending-active beam, different support conditions and external loads can be considered which result in different non-uniform distributions of bending stiffness along the beam's axis (Figure 3.12). This aspect can be taken advantage of in a design perspective as the same curved geometry can be materialised by many different bending-active beams. However, a bending stiffness distribution cannot be found for any support condition and external loads. The beam must be a statically determined system and the loads be consistent with the target equilibrium geometry.

Consider the case of a bending-active beam supported at its ends on supports which can transfer to the beam punctual forces and moments in the form of torques or forces. In order to generate a statically determined system of external

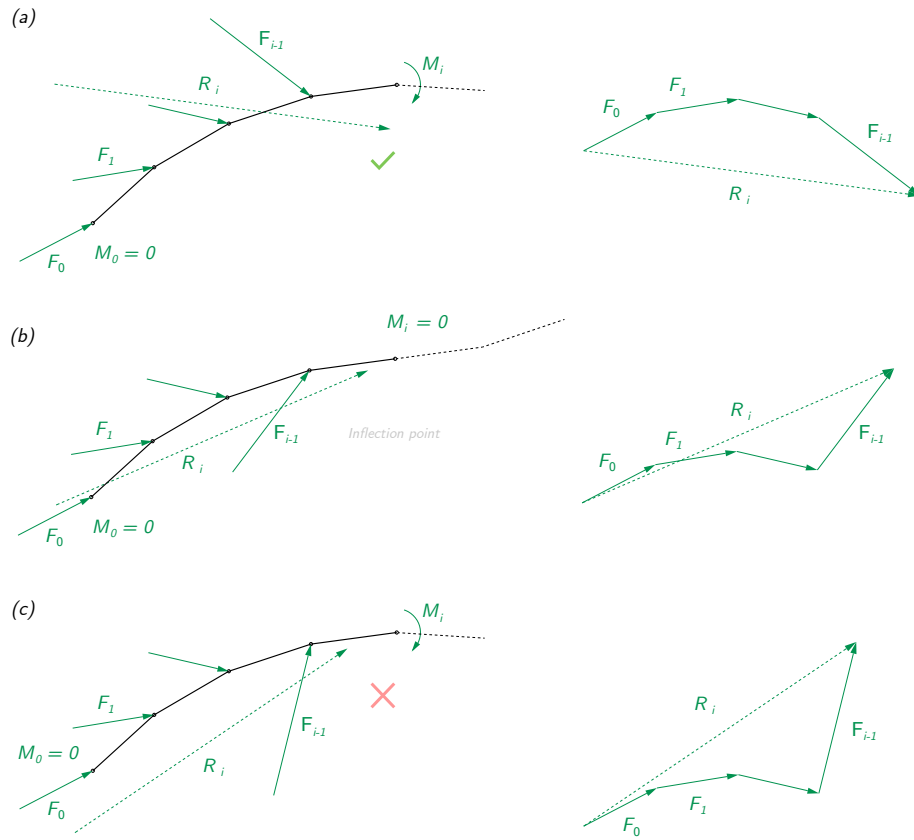


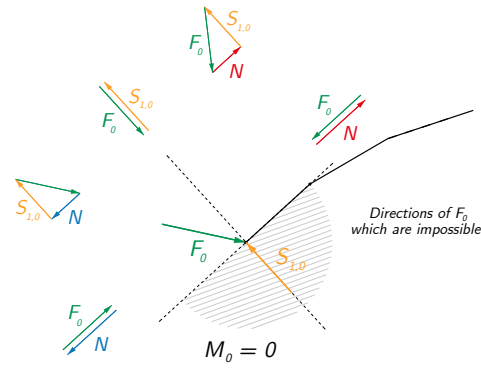
Figure 3.13: Equilibrium conditions of a bending-active beam sub-system in relation to its local curvature.

forces compatible with the bent geometry of the beam, the external forces acting on the beam must satisfy, on the one hand, the global equilibrium of the beam and, on the other hand, the local equilibrium of the beam with its internal forces. This means that the external forces must meet global and local conditions, which translates into a restricted range of inclination and magnitude of each of the external forces relatively to the other ones.

- First, the resultant force of the external forces acting on the beam must be null as well as the resultant moment of the external forces and external moments acting on the beam. This last condition should be verified at any node of the beam's axis and in particular, at its ends, where it is supported.
- Second, these two conditions must also be respected for any sub-system of the beam. More specifically, the orientation of the bending moment generated at the end of any beam's sub-system must be compliant with the orientation of the beam's curvature at that node. In particular, in the case of a node being an inflection point of the beam's axis curve, the external forces and external moments acting on the beam must verify that the bending moment is null at that node (Figure 3.13).

- Third, the equilibrium of the nodes 0 and 1 at the beam's ends provides local conditions on the external forces and external moments acting at those nodes. In particular, the corresponding polygons of forces in the diagram of forces must close. Figure 3.14 shows under which conditions (orientation of the external force \mathbf{F}_0 acting at node 0, presence of an external torque ($\mathbf{F}_M, -\mathbf{F}_M$) acting at node 0 or not, its direction), it is possible to close the polygon of forces of node 0 by changing the magnitude of $\mathbf{S}_{1,0}$, i.e. adjusting the bending stiffness of node 1.

(a) $M_0 = 0$



(b) $M_0 \neq 0$

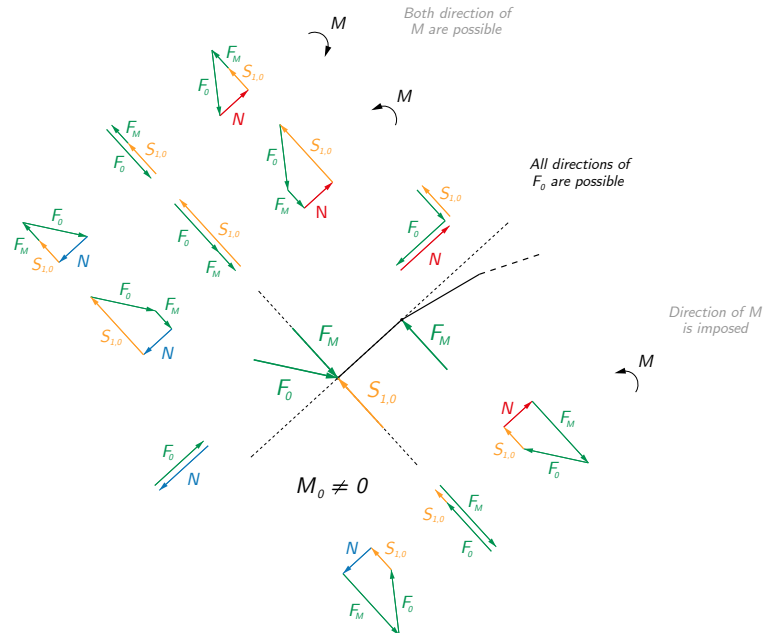


Figure 3.14: Local equilibrium conditions at the end of a bending-active beam. Possible orientation of the external load and moment acting at the end node in relation to the target equilibrium geometry of the beam.

3.2.3 Conditions on the external actions in the case of a beam loaded at its ends only

In the specific case of a beam loaded at its ends only (no loads applied along its axis), the aforementioned conditions can be expressed more explicitly in relation to the bent geometry of the beam. Depending on the support conditions and on the target equilibrium geometry of the beam, the target equilibrium geometry limits, even defines in a unique way, the feasible orientation of the loads at its supports which meet both the global and local conditions of equilibrium.

Figure 3.15 presents nine possible configurations, considering different support conditions and the presence or not of inflection points along the beam. In the case of configurations 1, 4, 5, 7, 8 and 9, the beam can only be in equilibrium if the reaction forces are inclined along one specific direction, directly related to the bent geometry of the beam (alignment of supports and/or inflection point(s)). This relates to the fact that inflection points and rotation-free supports correspond to a null bending moment. Regarding configurations 2, 3 and 6, global and local conditions of equilibrium are fulfilled as long as the inclination of the reactions forces remains between limit angles which are related to the beam's bent geometry as well (represented as green dashed areas in the different illustrations). The definition of the limit angles emerges from the integration of the different ranges of feasible orientation which emanate from the various local and global conditions, and is further detailed through the various examples presented below. Because the beam is only loaded at its ends, the reaction force at one end is the reverse of the reaction force at the other end.

Configuration 1 The first example to be considered corresponds to configuration 1 in Figure 3.15 and is a bending-active beam which is pinned at both ends A and B and bends without inflection point. Because of the pin connections, the bending moment at ends A and B is null and the force \mathbf{F} acting on end A must therefore generate a moment which is null at end B . Consequently, the force \mathbf{F} must be aligned to the line connecting A and B . The equilibrium of any sub-system of the beam implies that \mathbf{F} is oriented towards end B . This corresponds to the classical configuration of the *Elastica* and the calculation of the corresponding non-uniform bending stiffness distribution along the beam's axis is illustrated in Figure 3.11.

Configuration 2 The second example is depicted in Figure 3.16 and considers a pinned-fixed beam which bends without inflection point. It corresponds to configuration 2 in Figure 3.15. Two distinct conditions required for the equilibrium of the beam need to be fulfilled: first, the local condition of equilibrium at pinned end A , which involves the tangent line to the beam at A (Figure 3.14(a)) ; and

second, the global condition of equilibrium at end B in relation to the direction of the external bending moment M_B .

Configuration 3 The third example is a beam fixed at both ends which bends without inflection point. It corresponds to configuration 3 in Figure 3.15 and is illustrated in Figure 3.17. The external bending moments M_A and M_B acting at ends A and B have been chosen such that they have the same direction. The direction of the force F acting on the beam's ends is constrained by two conditions of equilibrium. The first condition that must be fulfilled is the global moment equilibrium of the beam at end B . The second condition relates to the local equilibrium of forces at end A as depicted in Figure 3.14(b): the orientation of the external bending moment M_A in relation to the orientation of the beam's curvature at end A imposes an additional constraint on the feasible orientation of force F .

Configuration 6 The fourth example considers a beam fixed at both ends whose deformed geometry displays an inflection point. Such configuration is similar to configuration 6 in Figure 3.15 and is illustrated in Figure 3.18. The beam can be subdivided into two sub-systems, from the inflection point I to each end of the beam. As the inflection point coincides to a null bending moment, each sub-system corresponds to a beam in configuration 2 and its feasible support

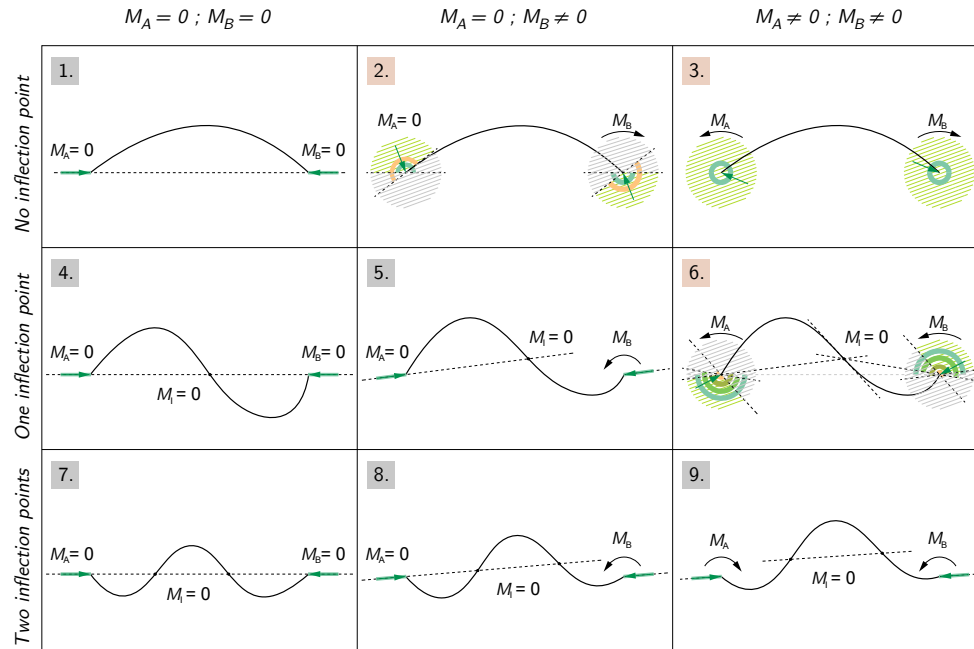


Figure 3.15: Different possible bent geometries taken by of a slender beam loaded at its ends only in relation to the different support conditions.

conditions can be analysed accordingly. In addition to these various conditions imposed on the direction of force \mathbf{F} , an additional global condition should be fulfilled emerging from the global equilibrium of the moments acting on the beam. It derives from the identical direction of the external bending moments \mathbf{M}_A and \mathbf{M}_B and, in addition to limit the direction of force \mathbf{F} , it governs the values of \mathbf{M}_A , \mathbf{M}_B and \mathbf{F} in respect to each other.

Two interconnected beams The fifth example presented in Figure 3.19 consists of two beams which are fixed at one of their ends and whose other free ends are tangentially connected together. One of the beams displays an inflection point in its bent configuration, while the other beam not. In addition to the conditions imposed by the equilibrium of each of the beam considered separately, further conditions emerge from the global equilibrium of the whole system as detailed further in Figure 3.19.

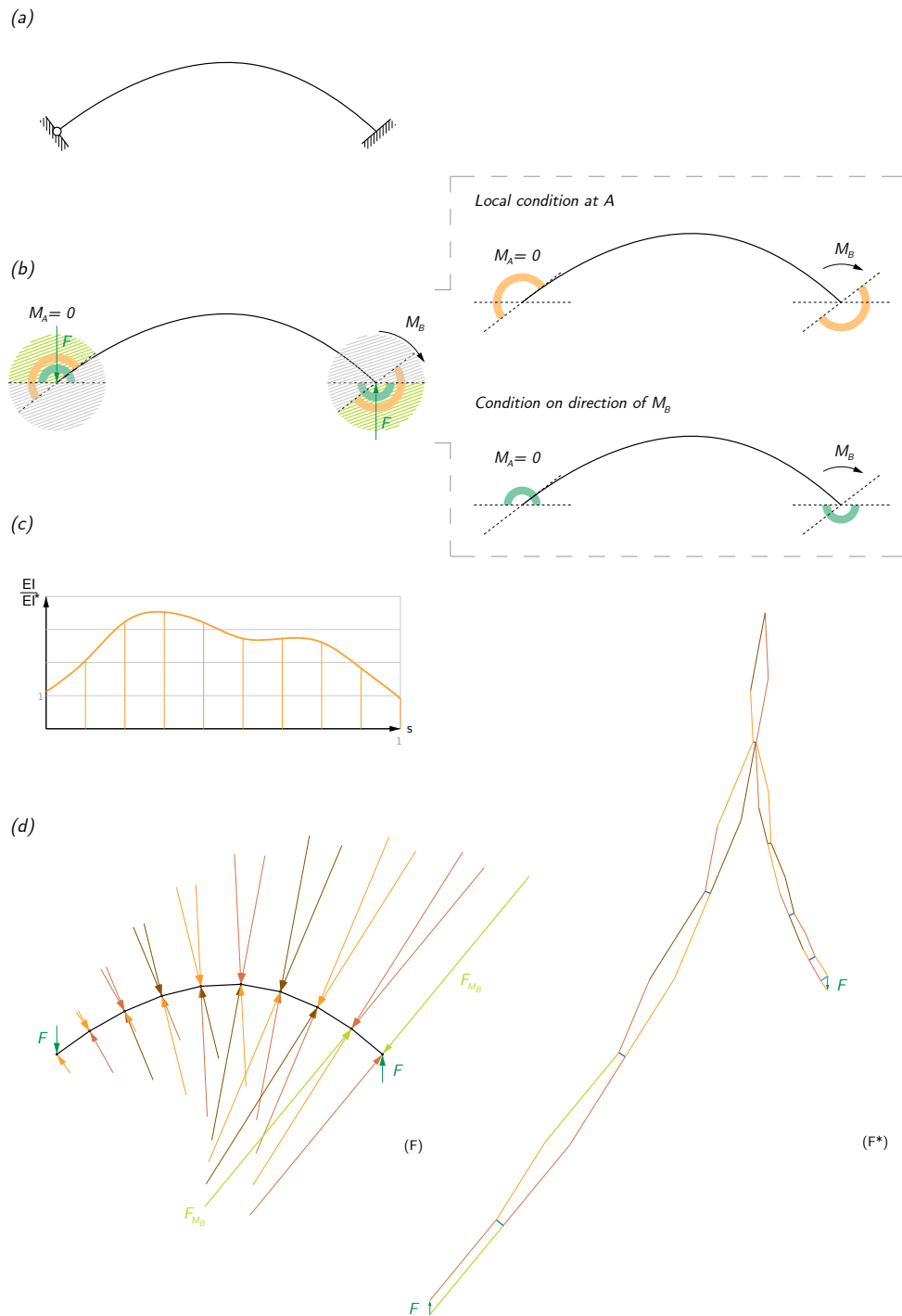


Figure 3.16: Determination of the feasible acting loads in the case of a pinned-fixed beam (Configuration 2 in Figure 3.15).

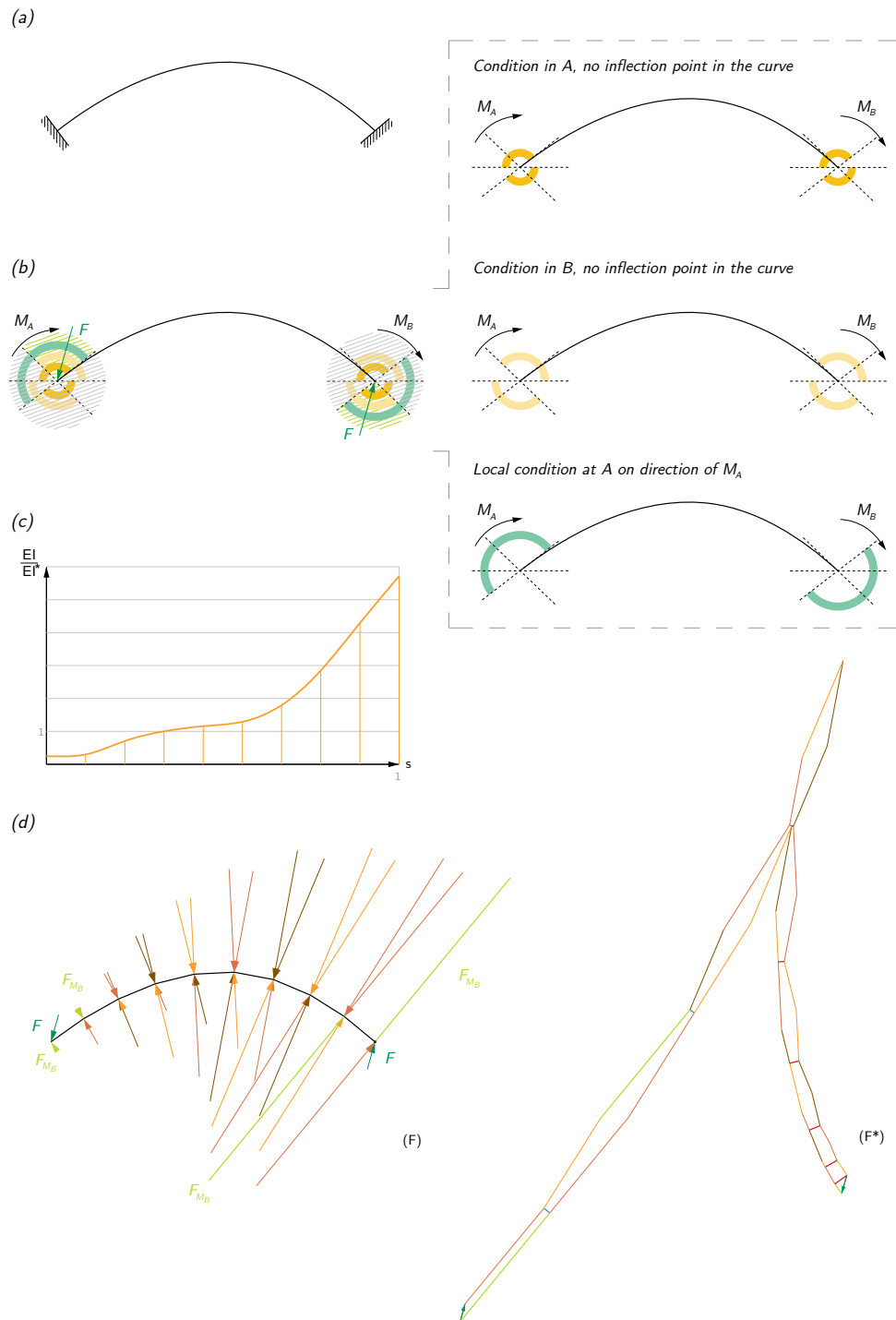


Figure 3.17: Determination of the feasible acting loads in the case of a pinned-fixed beam (Configuration 3 in Figure 3.15).

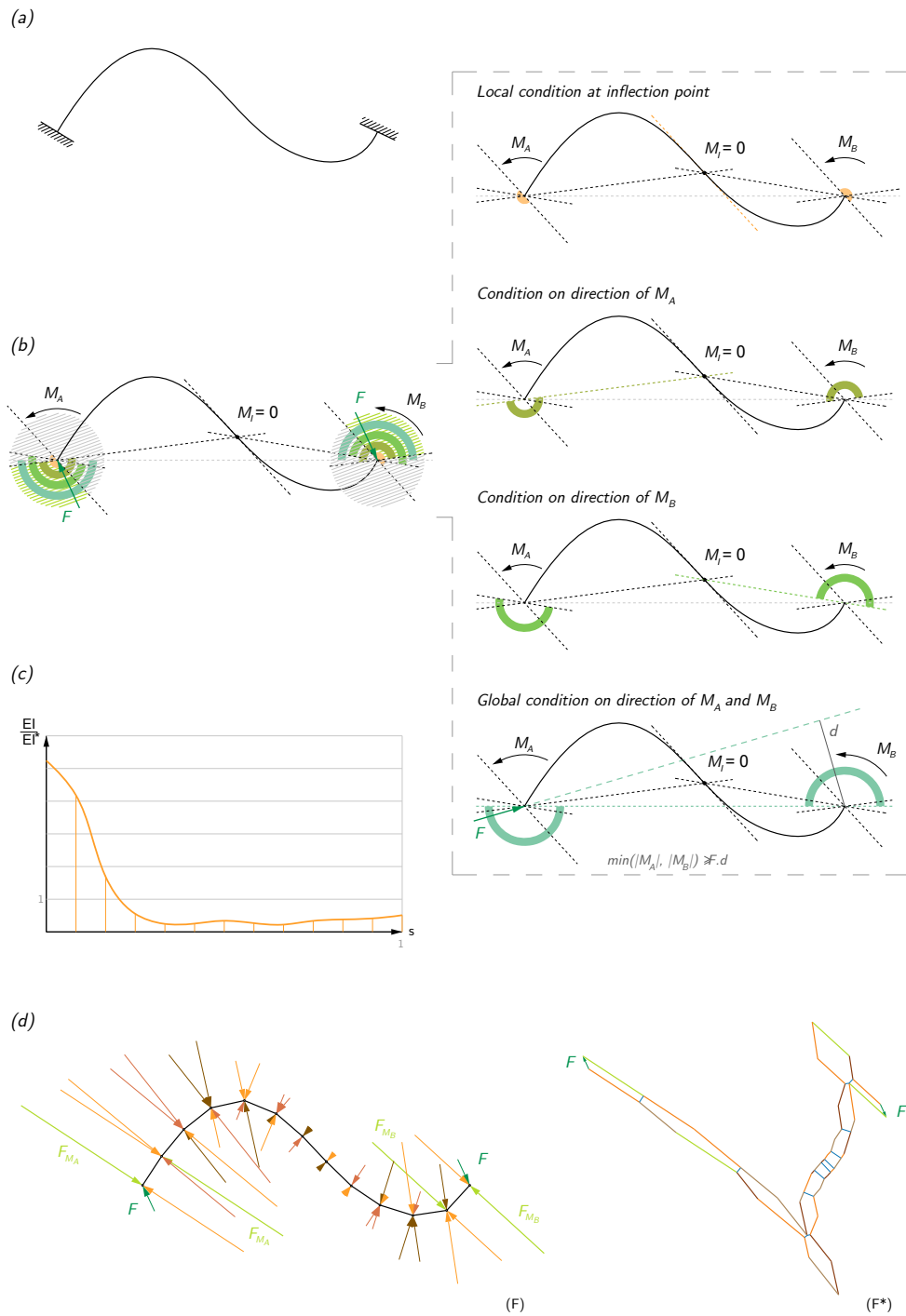


Figure 3.18: Determination of the feasible acting loads in the case of a fixed-fixed beam with an inflection point (Configuration 6 in Figure 3.15).

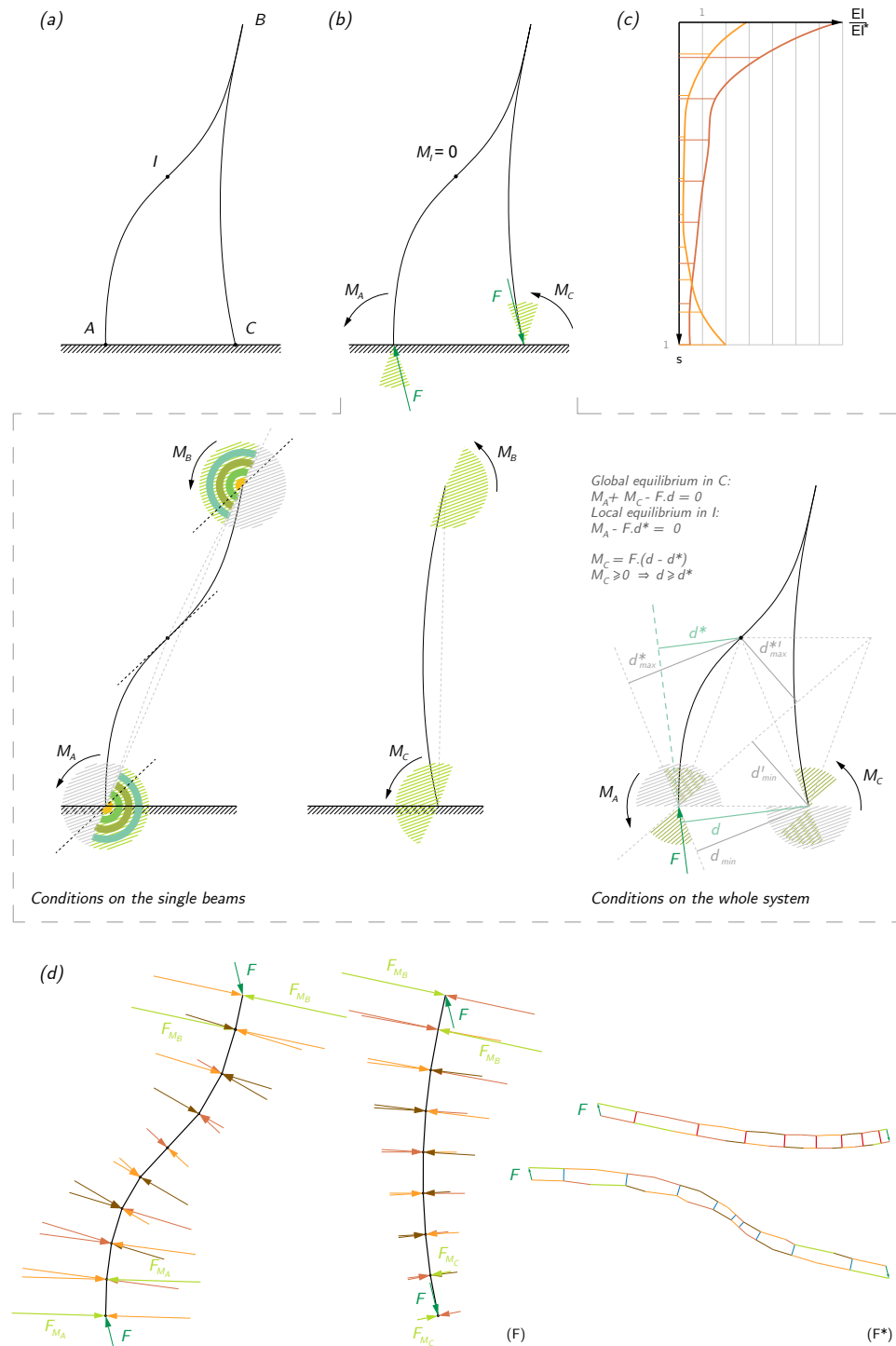


Figure 3.19: Determination of the range of feasible acting loads in the case of two interconnected beams.

3.3 Shaping bending-active beams with external restraining forces

Based on a graphical representation of the principles of static equilibrium, this section introduces a new methodology for the shaping of bending-active beams into target plane equilibrium geometries by means of additional restraining forces applied onto the beams' axis. In particular, such restraining forces can be applied onto the beams' axis in the form of external post-tensioning systems.

In the design of structures, external post-tensioning systems can indeed be used to apply additional loads to a structure in order to equilibrate its geometry which would, otherwise, not be in equilibrium or at the cost of large bending moment and cross sections. Such a principle has been used for instance in the design of the stone façade of the *Pavilion of the Future* (Seville Universal Exposition, 1992, Peter Rice) where post-tensioning cables support the funicular equilibrium of a semi-circular stone arch (Lenczner 1994). Graphic statics represents an efficient method to design and define the geometry of such post-tensioning equilibrating systems as illustrated by (Todisco et al. 2016) who present a graphical method for the design of externally post-tensioned pin-joined funicular structures. In their work, the restraining system applies to the stone structure the loads its geometry requires to behave as a funicular system, meaning that the stone structure is only under compressive forces. In regard to bending-active structures, (Alpermann and Gengnagel 2012) make use of a simplified static model to find the geometry of the cable system that forces a bending-active beam to bend into a semi-circular arch. However, this static model is based on a strong restriction due to the assumption of constant bending moment distribution over the beam's axis.

The methodology introduced in this section, on the contrary, covers the generation of restraining post-tensioning systems for the shaping of bending-active beams into any plane and continuously curved equilibrium geometry. Section 3.3.1 details how the restraining forces which are required to enforce the equilibrium of bending-active beams in target geometries are determined. This is based upon the mechanical modelling scheme of bending-active beams introduced in Section 3.1 and the geometric analysis of force diagrams. Section 3.3.2 explains the graphical construction of restraining post-tensioning systems which apply on the beams' axis appropriate restraining forces. Different design parameters are then identified and illustrated. Section 3.3.3 presents how the method of graphic statics can be used to assess the maximum load that can be applied on a triangulated post-tensioning restraining system without causing its reconfiguration into another equilibrium geometry. Eventually, in Section 3.3.4, the methodology is qualitatively validated through a physical test.

The content of Section 3.3 has been partly published in (Boulic and Schwartz 2017).

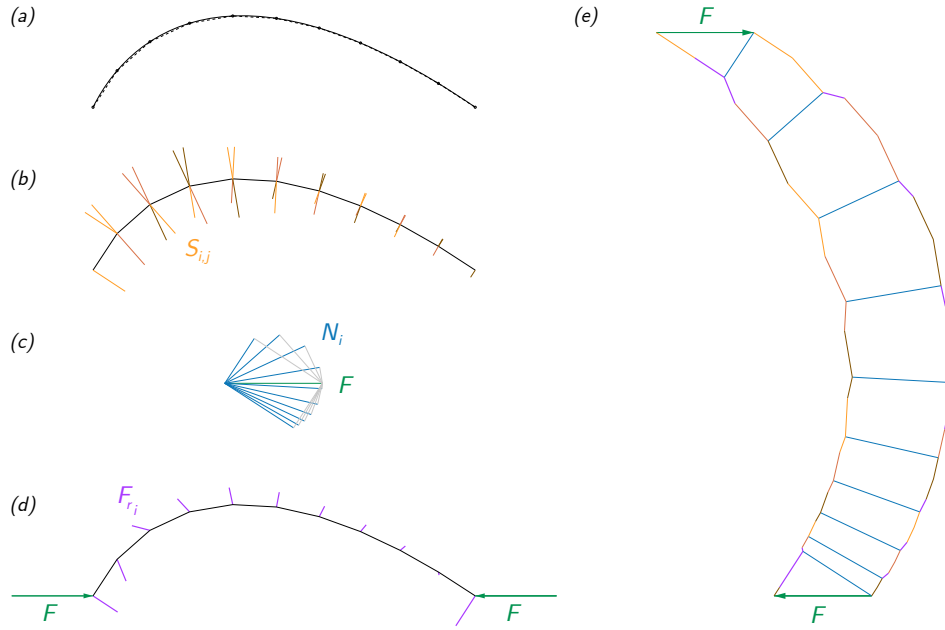


Figure 3.20: Graphical determination of the additionally required restraining forces – (a) Discretisation of the continuous target equilibrium geometry of the beam; (b) Calculation of the bending forces (orange tone) which only depend on the deformed geometry of the beam and on its bending stiffness (considered as constant along the beam's axis in this example); (c) Determination of the axial forces (blue colour) in relation with a given set of external forces (green colour) (d); (e) Determination of the missing forces (purple colour) which are additionally required to bend the beam into the target equilibrium geometry.

3.3.1 Graphical determination of the required restraining forces

Any plane continuous curve representing a target equilibrium geometry of the bending-active beam can be discretised and analysed according to the mechanical modelling scheme introduced in Section 3.1 (Figure 3.21). First, the continuous curve is discretised into bar elements. Second, the bending forces are calculated based on the relative position of the nodes and on the beam's bending stiffness at the nodes. Third, the axial forces acting along the beam's axis are deduced from the external loads which are considered to act on the beam. For each of the beam's node, internal and external forces acting at the node are assembled into a polygon of forces in the force diagram (Figure 3.20). It is most likely that these polygons do not close and that additional forces are required in order to form closed polygons and consequently ensure the equilibrium of the beam's nodes. These missing forces are the restraining forces F_{ri} which are necessary to enforce the beam to bend into the considered target geometry. They will be provided additionally and externally to the beam.

The axial forces along the beam's axis depend on the external loads which are originally considered (green forces in the diagrams). Applying onto the beam additional restraining forces amounts to modify the external forces acting on the beam, which in turn should affect the axial forces (Section 3.1.1). In fact, as

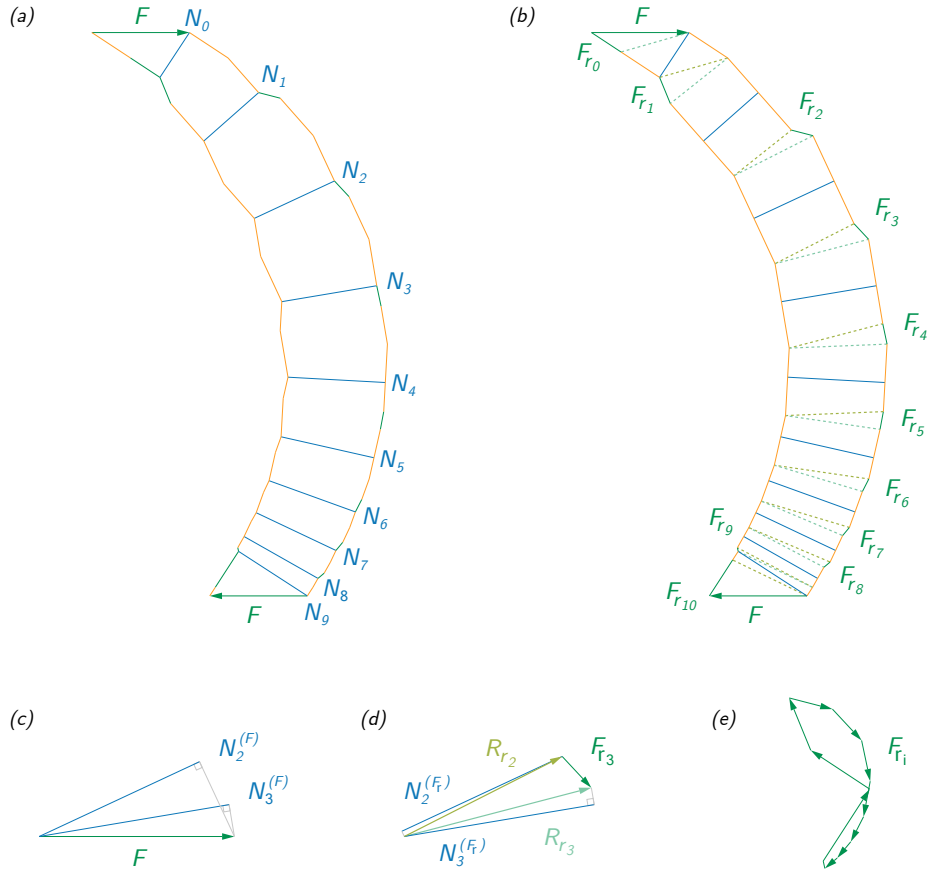


Figure 3.21: Effect of additional restraining forces on the axial forces – (a) Force diagram with forces assembled clock wise; (b) Same force diagram redrawn by permuting forces within every polygon of forces; (c) Axial forces in equilibrium with original external load F ; (d) Same axial forces in equilibrium with the added restraining forces; (e) Null resultant force of the restraining forces.

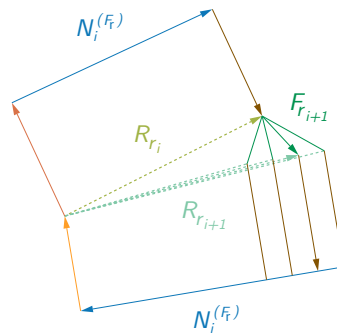


Figure 3.22: Geometric demonstration of the non-uniqueness of the required restraining forces – Polygon of the forces acting at one of the beam's node revealing the various possible restraining forces which comply with the nodal equilibrium.

graphically shown in the example of Figure 3.21, the axial forces $\mathbf{N}_i(F)$ calculated from the original external forces \mathbf{F}_i happen to correspond to the axial forces $\mathbf{N}_i(F_r)$ calculated with the restraining forces \mathbf{F}_{ri} as part of the new external forces. The force diagram can be rebuilt by permuting the order in which the forces acting on one node are assembled. It appears then clearly that the axial force \mathbf{N}_i is indeed the opposite of the projection along \mathbf{u}_i of the new sub-resultant force $\mathbf{R}_{ri} = \sum_0^i (\mathbf{F}_j + \mathbf{F}_{rj})$. Another property is also evidenced in the force diagram (e) of Figure 3.21: the resultant force of the restraining forces graphically calculated is null which means that the global equilibrium of the beam is not affected by the restraining forces.

The further study of the force diagram of the bending-active beam indicates that it is actually possible to choose the direction of the additional restraining forces. Figure 3.22 shows how the axial force \mathbf{N}_{i+1} is affected by a change of direction of the restraining force \mathbf{F}_{ri+1} and how it remains in equilibrium with the sub-resultant force $\mathbf{R}_{ri+1} = \sum_0^{i+1} (\mathbf{F}_j + \mathbf{F}_{rj})$. As a consequence, \mathbf{F}_{ri+1} can have any direction except that of \mathbf{u}_{i+1} .

3.3.2 Graphical construction of external post-tensioning restraining systems

Restraining forces can be applied to a bending-active beam by means of an external post-tensioning system consisting in several spokes connected to the beam, whether in tension or in compression, themselves connected to a bottom cable. The spokes apply onto the beam's axis the required restraining forces thanks to the effect of the prestressing forces acting in the bottom cable in relation to the length and orientation of the spokes. In turn, the bottom cable is shaped by the forces acting in the spokes. As a funicular system, the geometry of the bottom cable can easily be determined graphically by means of a geometric construction.

Geometric construction of funicular systems with graphic statics Funicular structures are structural systems with such a geometry that, at static equilibrium and for the loads for which they are designed, they are only subjected to compression-only or tension-only axial forces. A chain hanging under its self-weight or a cable tightened under the action of suspended weights are examples of simple funicular structures. It is precisely from the observation of the latter system that Varignon (Varignon 1725) establishes the existence of reciprocal relationships between the funicular polygon of the cable and the polygon of the forces acting on the cable. Such reciprocal relationships between the form and force diagrams are at the basis of graphic statics, a method developed during the 19th century (Karl-Eugen 2008) by protagonists like Culmann (Culmann 1866) and Cremona (Cremona 1872) for the solution of static problems by means of

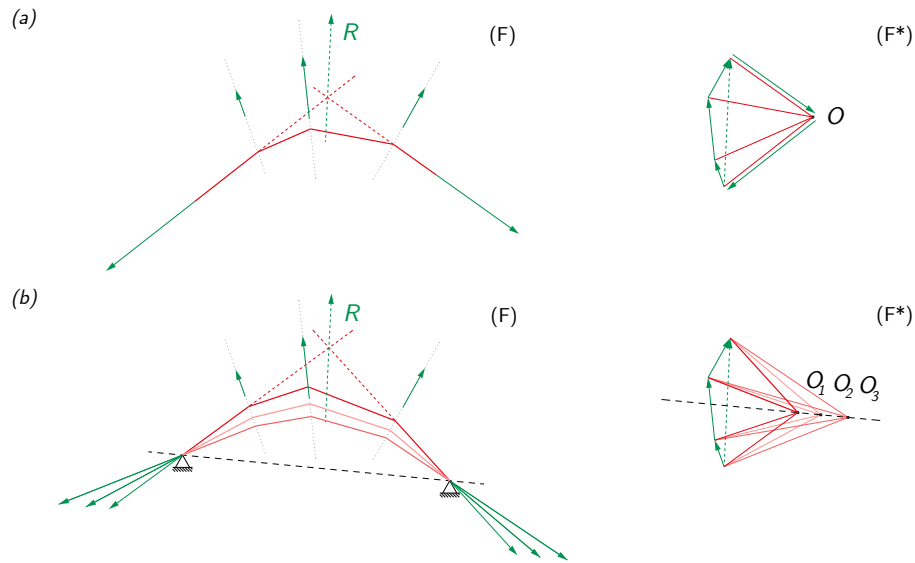


Figure 3.23: Graphical construction of a 2D funicular structure with given supports: (a) Construction of an auxiliary funicular structure to determine the line of action of the resultant force; (b) Construction of different funicular structures in equilibrium with the given supports.

geometric constructions only. It is therefore not surprising that graphic statics provides an efficient and easy-to-use method for exploring funicular forms in 2D.

The geometric construction of a simple funicular consisting of a cable under tension (or equally of an arch under compression) in equilibrium with given boundary conditions, such as the magnitude and the line of action of the applied forces and the number and location of the supports, is a well-known procedure in 2D graphic statics. The first step of this procedure consists in the definition of the resultant force of the applied loads and its line of action. This is done through the construction of an auxiliary funicular in the form diagram which satisfies the equilibrium conditions but not necessarily the geometric conditions of the supports (Figure 3.23(a)). The auxiliary funicular is derived from a force diagram constructed from the loads and from an arbitrarily chosen point on the force plane. This point is referred to as the pole of the force diagram, and will define the orientation of each segment of the funicular. When extended, the first and last segments of the auxiliary funicular intersect at a point which has the particularity of lying on the line of action of the resultant force. This line of action is fully defined from that point and the resultant force vector. The line of action of the resultant force is unique regardless the position of the pole which was chosen for the construction of the auxiliary funicular. The second step of the procedure consists in the construction of the desired funicular, which satisfies the geometric conditions of the supports. A point of the line of action of the resultant force is chosen from which the reaction forces at the supports are determined in the force diagram (Figure 3.23(b)). The new corresponding pole

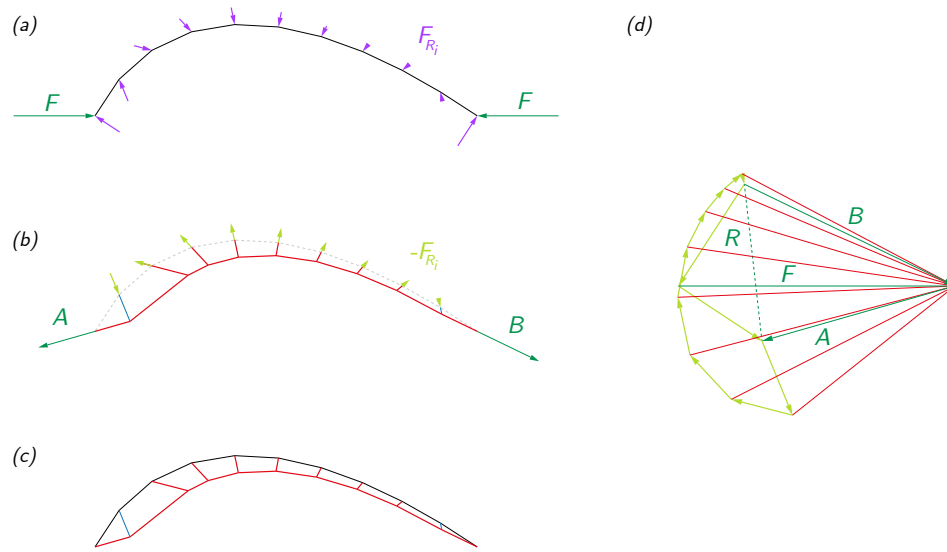


Figure 3.24: Graphical construction of the restraining system – (a) Additional restraining forces required for the equilibrium of the bending-active beam in the target equilibrium geometry; (b) Restraining system built from a force diagram (d) considering the opposite of the required restraining forces; (c) Self-stressed restrained bending-active beam.

of the force diagram is defined and from there, the entire geometry of the new funicular is established. Selecting another point along the line of action of the resultant force results in a displacement of the pole of the force diagram along a line called the closing string, which is parallel to the virtual line that connects to each other the two supports of the funicular structure.

Design of a post-tensioning restraining system The funicular geometry of the bottom cable is graphically determined based on the forces acting in the spokes, which correspond to the reverse of the restraining forces to be applied on the beam.

In the particular case in which the bending-active beam and the post-tensioning restraining system form a “closed” pre-stressed system and the system’s self-weight is neglected, the position of the supports of the bottom cable must correspond to the beam’s ends and the reaction forces at the bottom cable to the forces acting at the beam’s ends. There is then a unique funicular geometry for the bottom cable to be in equilibrium with these conditions (Figure 3.24(c)). The obtained restraining system is comprised, on the one hand, of tension and compression spokes which apply to the beam’s axis the restraining forces and, on the other hand, of a bottom cable which applies at the beam’s ends the main prestressing force responsible for the beam bending (Figure 3.24(b)).

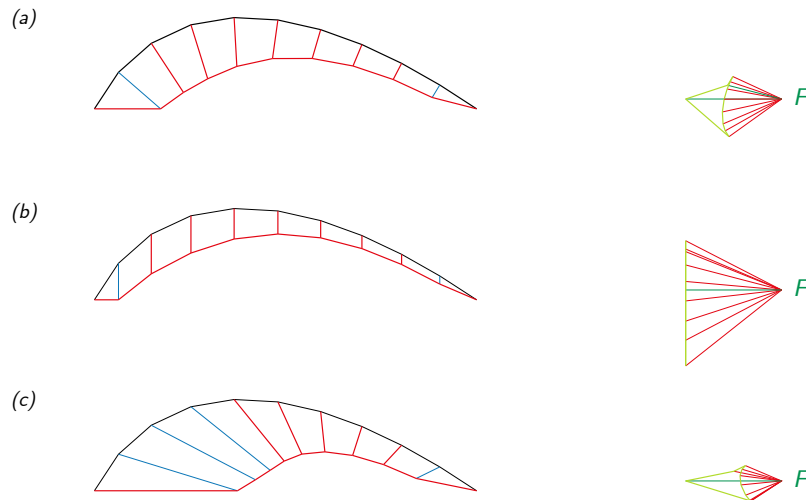


Figure 3.25: Restrained bending-active beams with variations in the direction of the restraining system's spokes – The original pre-stressing force F is kept identical in the three cases.

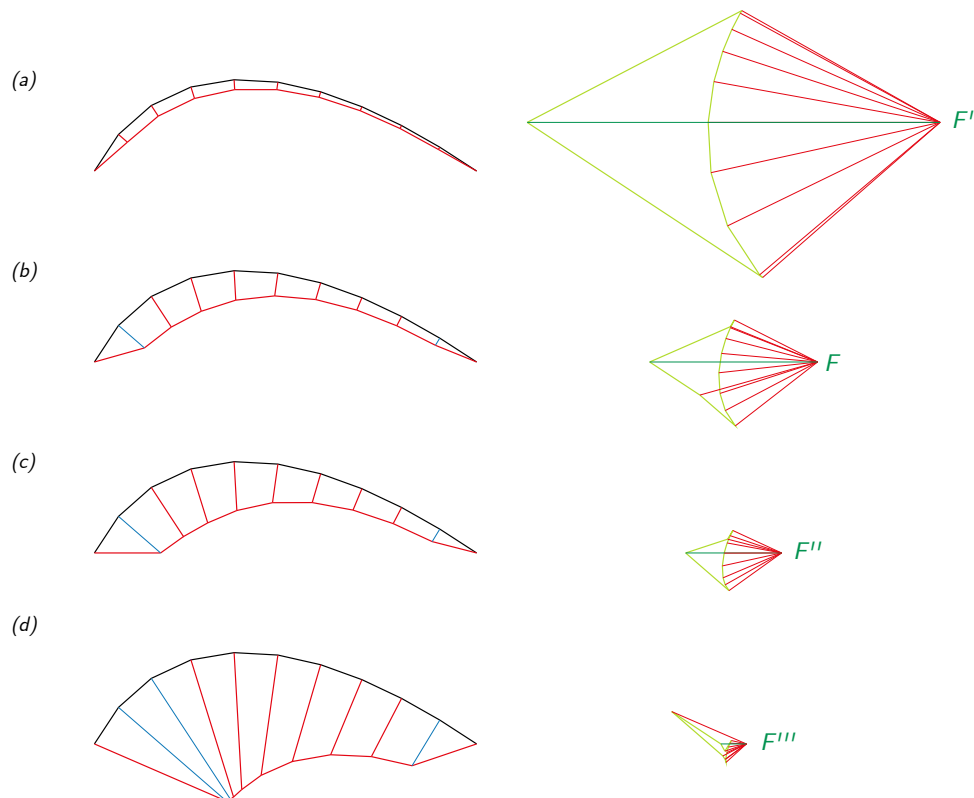


Figure 3.26: Restrained bending-active beams with variations in the original pre-stressing force F inducing a variation in the amount of pre-stressing in the restraining system – The spokes' direction is kept identical in all the four cases.

For a given bending-active beam and its target equilibrium geometry, various different restraining systems that enforce the beam's equilibrium in the target geometry can be designed. Variations of different kinds can be introduced.

Variations in the direction of the restraining spokes The possibility to freely choose the direction of the restraining forces (Section 3.3.1) can be exploited in the design of the restraining system. Figure 3.25 shows for the same equilibrium geometry of the bending-active beam different possible restraining systems resulting from different spokes's directions. One of the possible consequences of this variation is to change the force in the spokes from tension to compression or vice-versa.

Variations in the magnitude of pre-stressing forces acting in the bottom cable Another influencing parameter for the design of the restraining system is the magnitude of the pre-stressing force F applied at the ends of the beam. Modifying the magnitude of the force F affects the magnitude of the restraining forces and the funicular shape of the bottom cable. Figure 3.26 illustrates the changes induced by variations in the pre-stressing force F . The larger the force F , the closer the bottom cable is to the beam, and the larger become the forces in the restraining system, in both the spokes and the bottom cable.

Variations in the support conditions of the restraining systems Figure 3.27 illustrates the wide range of restraining systems originating from variations in the support conditions of the bottom cable. As mentioned before, one possibility is to generate a self-stressed system by connecting the bottom cable to the beam's ends and assuming that the bottom cable fully provides the prestressing force F required at the beam's ends to bend it (Figure 3.27(a)). Alternatively, it can be assumed that the restrained bending-active beam is partly pre-stressed externally at its supports (Figure 3.27(b)). Often, it turns that to obtain a self-stressed restrained bending-active beam with a tensile-only restraining system, the bottom cable has to be very close to the beam (Figure 3.26(a) and Figure 3.27(a)). Activating separately the supports of the beam and that of the restraining system makes it possible to design a wide range of bending-active tensile systems with a tensile-only restraining system. Separating the supports of the beam from the ones of the restraining system also allows for modification of the funicular's geometry (Figure 3.27(c)). The number of supports can be varied, as well as the orientation and magnitude of their reaction forces (Figure 3.27(d)-(f)).

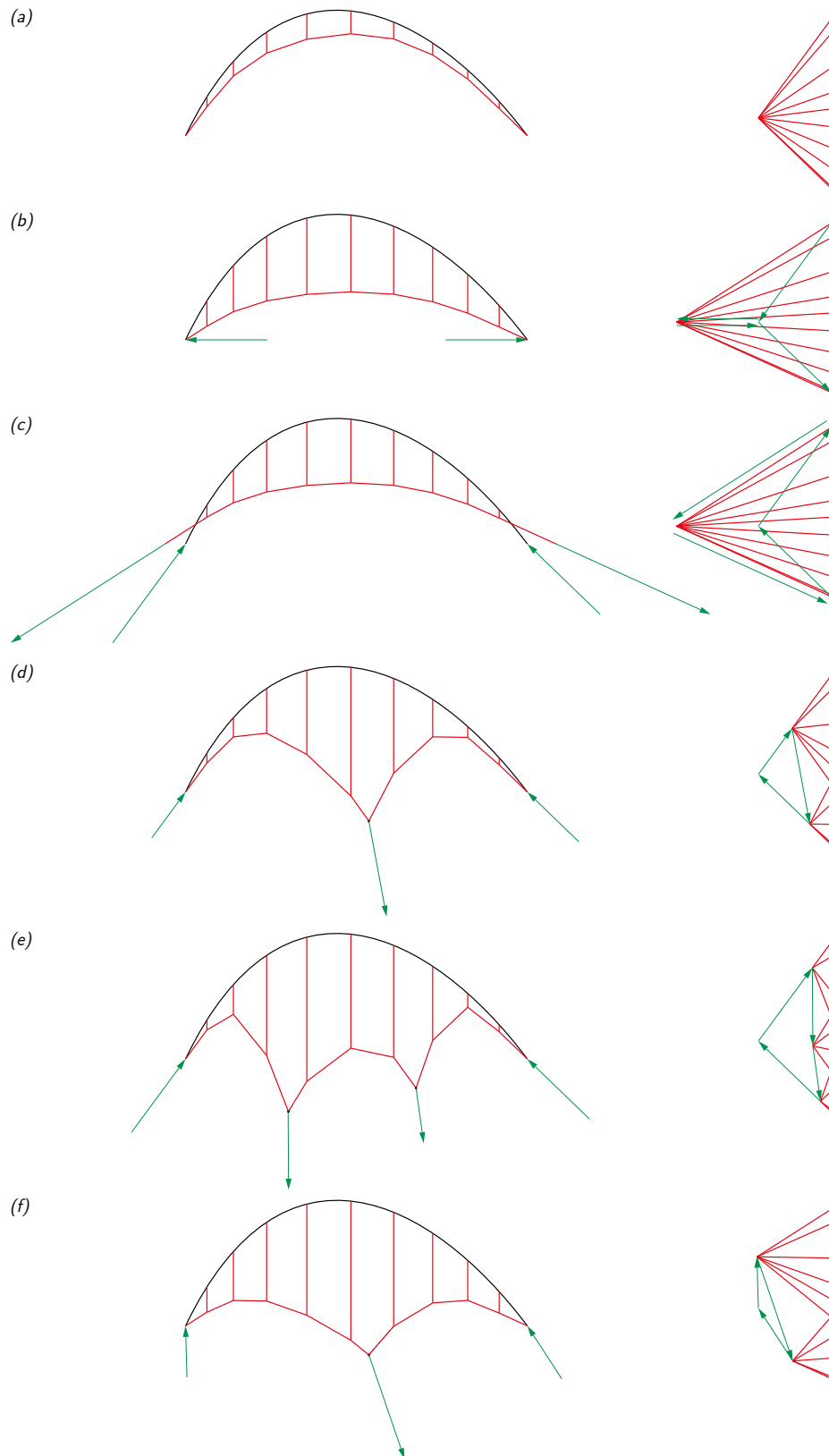


Figure 3.27: Restrained bending-active beams with variations in the support conditions – The original pre-stressing force F is kept identical in the three cases.

3.3.3 Evaluation of the maximum loads before deformation of a bending-beam restrained by a triangulated tensile system

As mentioned in Section 2.1.4, form-finding algorithms are necessary to perform a structural analysis of bending-active tensile structures under loads. In particular, under the action of loads, bending-active tensile structures tend to deform and to reach another state of equilibrium whose geometry is different from prior loading. Yet, as detailed below, in the case of a bending-active beam restrained by a triangulated restraining system, graphical methods can be used to determine the maximum loads that the bending-active tensile structure can withstand until it starts deforming.

A bending-active tensile structure consisting of a bending-active beam and a restraining tensile funicular is considered (Figure 3.28(a)). By means of subdivisions of the polygonal cells of the funicular's force diagram (Akbarzadeh et al. 2014), a new triangulated restraining system can be graphically obtained (Figure 3.28(b)). Compared to the original restraining funicular, the triangulated restraining system provides the bending-active tensile structure with an increased stability and a higher structural stiffness. The triangulated hybrid structure results to be a self-stressed structure and it is supported by a fixed support at its one end and a rolling support at its other end. A load F_0 is applied at a node of the system and its effect onto the system's equilibrium is studied. More specifically, the effect of the load on the pre-stressed tensile restraining system is evaluated.

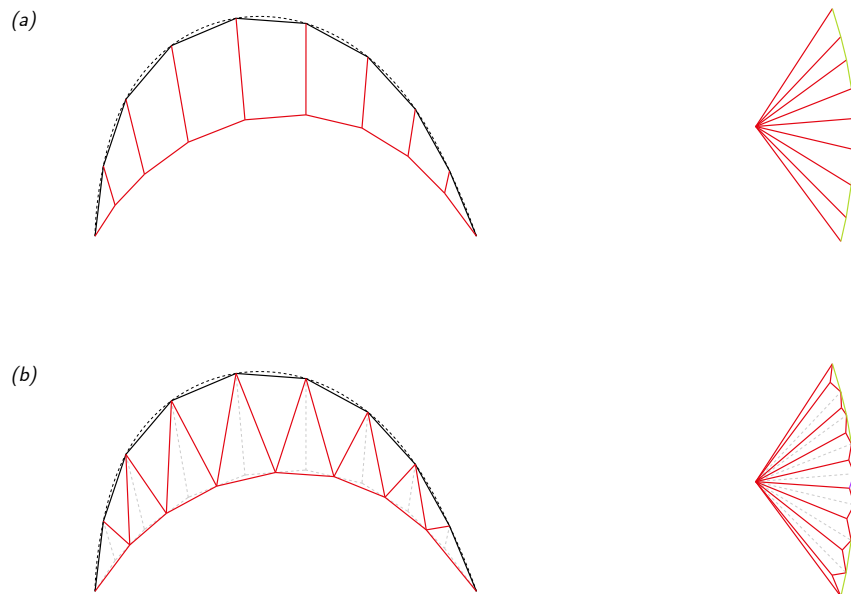


Figure 3.28: Triangulation of the restraining tensile system by subdivisions of its force diagram.

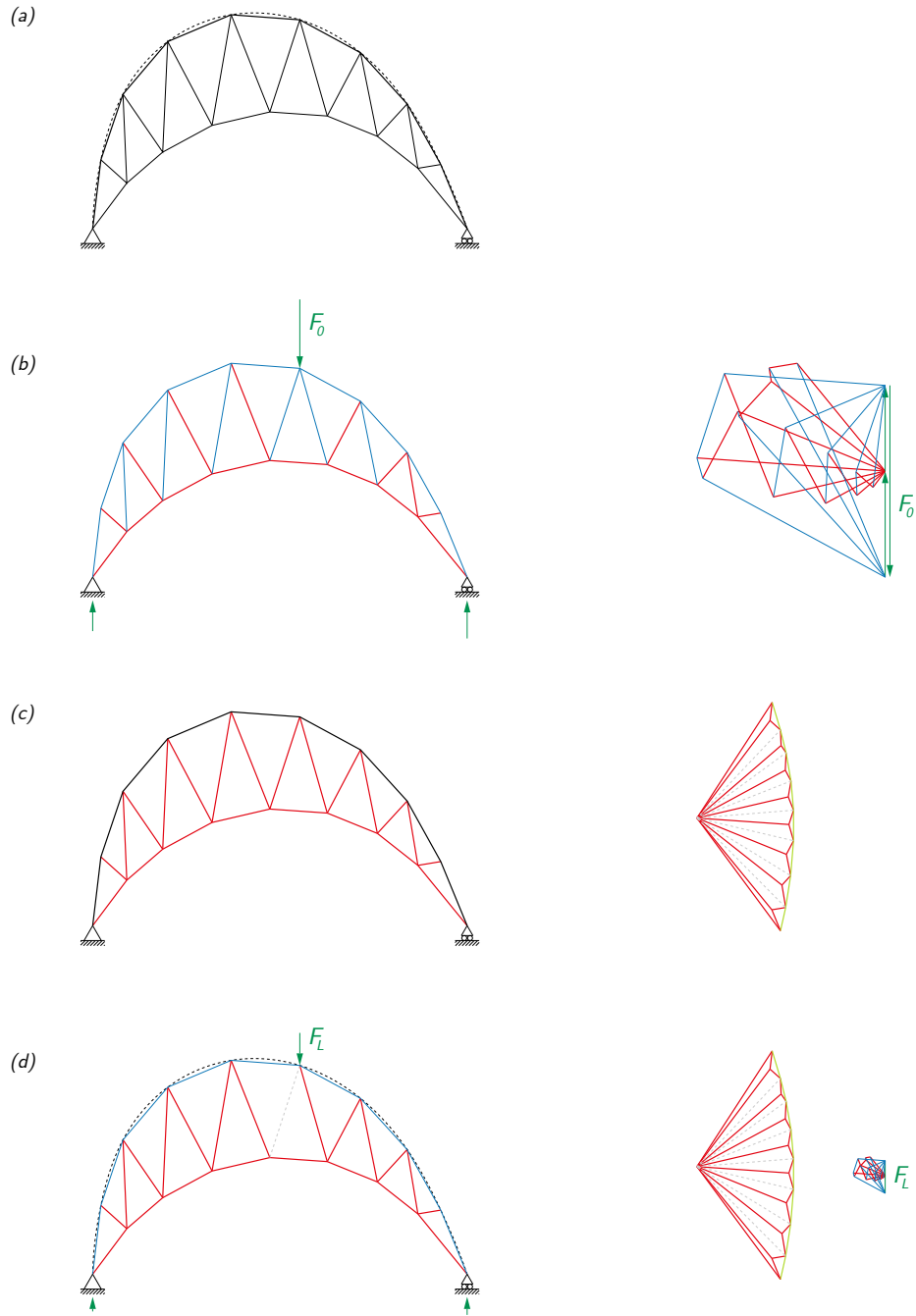


Figure 3.29: Bending-active beam restrained by a triangulated tensile system under punctual load – (a) Load acting on the truss-like restraining structure and the corresponding reaction forces, (b) Force flow within the truss-like structure for a load of magnitude F_0 , (c) Forces in the tensile restraining system before loading, (d) Updated force flow in the tensile restraining system under loading and scaled force diagram of the truss-like structure.

The proposed structural evaluation is based on the analysis of the self-stressed bending-active tensile structure as a truss structure, meaning that the bars of the beam and the cables of the restraining system can take equally tensile or compressive axial forces (Figure 3.29(a)). A load F_0 is applied at one node of the structure. In a first step, the internal force flow induced within the truss-like structure by the load is determined. It goes through the definition of the statically determinate reaction forces at the truss's supports and the construction of the force diagram of the truss (Figure 3.29(b)). The magnitude of load F_0 is arbitrary, only its line of action and its direction matter. In a second step, the bending-active tensile structure without loading and the truss-like structure under loading are combined. The tensile forces from the truss-like system add tension in the prestressed cables of the triangulated restraining system while the compressive forces have the effect to reduce the prestressing force within the cables until the prestressing force is lost. In a third step, the force diagram of the truss-like structure is scaled so that a first cable stops being active. This happens when the tensile force acting in a cable of the triangulated restraining system equals the compressive force acting in the respective bar of the truss-like structure (Figure 3.29(d)). If a cable loses its prestressing effect on the beam, the beam, and with it the whole structure, will deform until another state of equilibrium is reached. The maximal force F_L that the system can support until it deflects towards another state can then be accessed from the scaled force diagram.

3.3.4 Qualitative physical test of the proposed method

Small scale prototypes of restrained bending-active beams have been built in order to qualitatively validate the proposed method. They consist of plywood strips which are shaped into a target equilibrium curved geometry with a restraining system made of cables and sticks. The physical prototypes show a good convergence with the calculation as shown in Figure 3.30. Slight differences in geometry are noted. They could be explained by the fact the prototypes have been built at a rather small scale where the measurement uncertainties of fabrication have a stronger influence. Another reason could be that the discretisation of the equilibrium geometry is not refined enough to ensure its precise modelling.

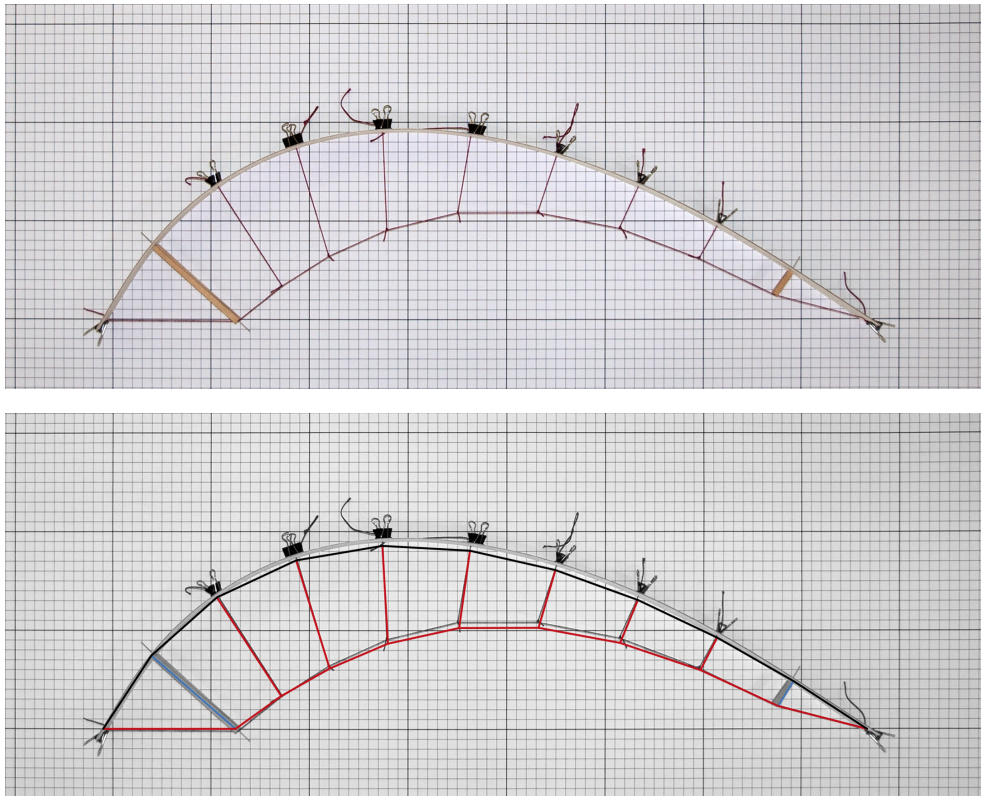


Figure 3.30: Actively bent plywood strip shaped with a restraining system – Built (top) and calculated (bottom) structures.

3.4 On the extension to 3D space

This section considers the case of slender beams which are actively bent in 3D space. As the deformations no longer occur only in the symmetry plane of the beams, torsion appears in the beams in addition to bending and influences their equilibrium geometry, as described in Section 2.1.2. Different kinematic descriptions of slender beams used for the modelling of torsion are discussed, as well as the extension of the modelling scheme presented in Sections 3.1, 3.2 and 3.3 for bending-active beams in 2D space to the case of bending-active rods in 3D space.

3.4.1 On different kinematic descriptions of slender beams considering torsion and on the use of graphic statics

A slender beam under large deformations in 3D space can be described by the position of its axis and the orientation of its cross sections in relation to its axis. For each node of the beam's axis, up to 6 degrees of freedom (DoFs) can be defined: 3 translational DoFs corresponding to the node's position and 3 rotational DoFs describing the orientation in 3D space of the beam's cross section at that node. In the literature, different frameworks can be found for the modelling of slender beams in 3D space. Most of them solve the static equilibrium of the acting loads through a similar dynamic relaxation process, but they adopt various kinematic descriptions of the beams – 3-DoF, 3-DoF with boundary, 4-DoF and 6-DoF formulations – in accordance with additional hypothesis which are specific to each of the various modelling frameworks. In practice, 4-DoF formulations are required to model accurately the behaviour in 3D space of a slender beam under external loads. Four is actually the minimal number of DoFs that enables to describe torsion in the beam.

Three different modelling frameworks are outlined and discussed below.

3-DoF-element formulation A first framework, based on a 3-DoF-element formulation, has been proposed by (Barnes et al. 2013) for the modelling of slender beams which are initially curved. The bending and torsional moments in a beam are expressed as pairs of opposite forces calculated from the relative position of four consecutive beam's nodes. An artificial calibrating factor depending on geometric parameters is required to adjust the torsional stiffness of the initially curved beam and provide satisfying results. However, in the general case of initially straight beams, this method is no longer valid. This observation is easily illustrated in the case of a bending-active flat beam, initially straight, whose ends are twisted in opposite direction, as depicted in Figure 3.31. The flat beam's axis remains straight and the relative position of the nodes unchanged while the angle of twist of the flat beam's cross sections linearly increases along

the axis, demonstrating that the single position of the nodes fails in modelling torsion inside a bending-active flat beam.

In order to do so accurately, the orientation of the beam's cross sections over deflection has indeed to be considered. In relation to Euler-Bernoulli's beam theory, as the cross sections are assumed to remain perpendicular to the axis, not all the 3 rotational DoFs are necessary. The cross sections' orientation can be defined by one scalar only: the angle of twist around the axis. The orientation of the material frame associated to the cross sections is assessed in relation to a zero-twist frame. This zero-twist frame, also referred to as a Bishop frame (Bishop 1975), is obtained from the parallel transport of an initial tangent frame along the axis of the beam (Hanson and Ma 1995). Stretching and bending of the beam are related to the deformation of the axis, while its twisting is related to the rotation of a material frame associated to each point on its axis.

3-DoF-element formulation and two boundary conditions (D'Amico et al. 2016) adopt a Bishop frame to describe the orientation of the material frame associated to the beam's cross-sections. Under the assumption of a quasi-static distribution of the angle of twist along the beam's axis, they are able to reduce to 3 translational DoFs and two boundary conditions the number of DoFs of their model. Given the cross-sections' orientation, the combined bending and twisting moment is computed. Following up the contribution of (Adriaenssens and Barnes 2001), this moment is approximated by equivalent pairs of opposite forces. The equilibrium equations are then solved by a dynamic relaxation algorithm. According to the authors, this modelling framework has proved to be a valid trade-off in terms of accuracy level and calculation time in relation to a more accurate 6-DoF-element formulation (D'Amico et al. 2014). However, two critical observations can be formulated against the application of this modelling framework to general cases.

The first observation relates to the hypothesis of quasi-static treatment of the twisting DoF, which is valid for certain configurations only. Figure 3.32 shows the case of a flat beam bent and twisted into two different configurations, and the related material and Bishop frames along the flat beam's axis. In the first configuration (Figure 3.32(a)), where the flat beam is bent into an *Elastica* whose ends would have been shifted apart orthogonally to the main bending plane, the quasi static treatment of the twisting DoF could be seen as a reasonable assumption as the angle of twist of the cross sections varies monotonically along the flat beam's axis. On the contrary, in the second configuration (Figure 3.32(b)), where the flat beam is bent into an *Elastica* whose ends have been twisted in opposite direction, the rotation of the cross sections with respect to the Bishop frame is not uniform along the axis as it increases and then decreases, which invalidates the hypothesis of quasi-static distribution of the twisting DoF. Although attractive because it reduces the number of DoFs per node and the

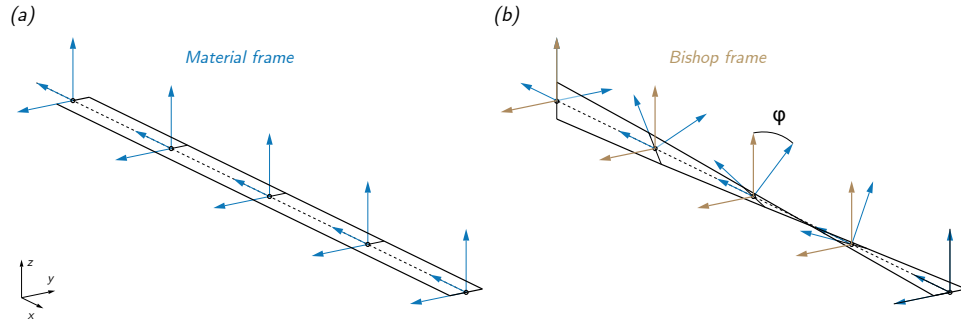


Figure 3.31: Initially straight flat beam whose ends are twisted 90° to each other – Material frames (in blue) follows the flat beam's cross-sections over the twist while the zero-twist Bishop frame (in brown) follows the flat beam's axis without twisting around it.

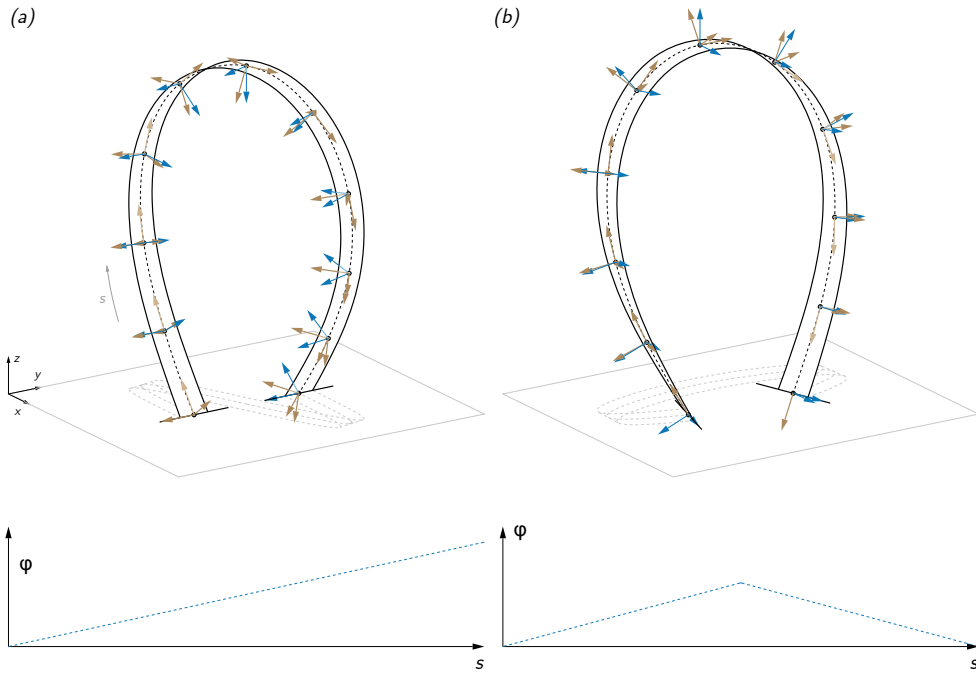


Figure 3.32: Flat beam actively bent into two spatial configurations and variation of its cross sections' angle of twist along the beam's axis – The bent geometry of the flat beam has been approximated from physical observations, but this approximation does not affect the observation made on the distribution of angle of twist along the beam's axis. Material frame in blue, and zero-twist Bishop frame in brown.

number of equations to be solved, this hypothesis seems rather inaccurate in the general case of bending-active beams in 3D space.

The second critical observation connects to the application of pairs of opposite forces at the beam's nodes as a means to generate torsional moment in the beam. Considering a finite difference modelling of three-dimensional continuous beams, and taking example onto the modelling scheme used for continuous

beams deflecting in the plane by (Adriaenssens and Barnes 2001), equivalent pairs of nodal forces are searched for in order to reproduce the combined moment acting on the beam's cross sections. In the most general case, this combined moment can be decomposed into a twisting moment, tangent to the beam's axis, and the bending moment, normal to the axis. As illustrated in Figure 3.33, a pair of opposite forces acting at the ends of a beam's segment fails to generate a twisting moment, since the resulting moment is normal to the segment. (D'Amico et al. 2014) make actually only use of the bending moment normal to the beam's segment to calculate the shear forces. Although pairs of equivalent shear forces accurately describe the bending moment only, such a modelling scheme shows an inherent limitation of nodal forces to consider torsional effect.

4-DoF-element formulation (Lefevre et al. 2017) make use of a 4-DoF-element formulation of the beams and a Bishop frame. The difference of their approach lies in the definition of the internal nodal forces and the internal moments acting at the beam's nodes. They are respectively calculated from the derivation of the elastic potential energy in respect to the nodes' position and to the cross-sectional angle of twist. A dynamic relaxation algorithm is performed on both the translational and rotational DoFs. On the one hand, a minimisation process of the translational kinematic energy based on the nodal forces allows to find the nodes' position. On the other hand, the angle of twist results from a minimisation process associated to the rotational kinematic energy and based on twisting moment. According to the authors, this modelling framework provides good results in terms of geometry and stress in comparison to FEM methods.

As a matter of fact, at least 4 DoFs are required to accurately consider torsion in bending-active beams. 4-DoF-elements means that four equations are required in order to describe and calculate the equilibrium configuration of the beams or systems of beams. Graphic statics only provides three equations in the form of the force diagram. These equations correspond to the static equilibrium of the forces acting on the structural system. One additional diagram or equation

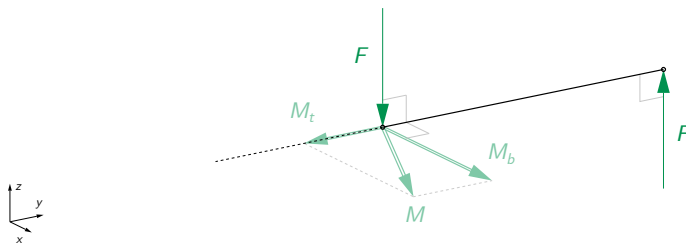


Figure 3.33: Line of action of the moment generated by a pair of opposite forces applied at the end of a beam's segment – The pair of opposite forces ($F, -F$) applied at the end of a beam's segment cannot generate a twisting moment M_t , as the resulting moment M_b is normal to the segment.

related to the twisting moment would therefore be necessary in addition to the usual force diagram. In such a case, the major interest of graphic statics of using a unique geometric object for the description of the static equilibrium of a structural system would be lost. Besides, the recourse to simplifying hypothesis such as the quasi treatment of the twisting DoF would make possible the use of a single force diagram to address the equilibrium of a beam as it reduces to 3 DoFs the kinematic formulation of the beam element but its relevance and accuracy is limited to specific configurations only.

3.4.2 Graphic statics principles applied to torsion-free rods in 3D space

Under certain conditions, the effect of torsion on the equilibrium of slender beams can be neglected in comparison to the effect of bending. In those cases, a bending-only modelling of the beams can be a good first step before further design explorations and the 3-DoF-element formulation of slender beams under large deformation presented in Section 3.1 remains valid.

Cases where torsion can be neglected More specifically, the relative effect of bending and twisting is quantified by the twist-to-bend ratio, $\eta = EI/GJ$, where EI is the bending rigidity and GJ is the torsional rigidity of the structural element. High values of η represent a structural element which can twist more easily than it can bend. For those elements, torsion have a preponderant influence on their bent geometry. (Vogel 1992) established a comparison between the twist-to-bend ratios of several structures with different cross section and material. For instance, it is illustrated that a schematic U-shape cross section of a banana leaf has a large twist-to-bend ratio of 68, while in comparison, a bar of homogeneous and isotropic material with circular cross section has a twist-to-bend ratio equal to $1 + \nu$ (Vogel 1992), equivalent to about 1.3 for a metal bar or a pultruded GFRP bar. Torsion has a limited influence onto the deformed geometry of elements with quadratic or circular cross section and can be neglected to a certain extent.

Based on this consideration, the rest of this section is limited to torsion-free slender beams with quadratic or circular cross section. These slender structural elements will be referred as torsion-free rods, according the definition given in Section 2.1.2.

Modelling scheme A torsion-free rod with a quadratic or circular cross section is considered.

Internal forces in the rod are calculated in the same way as in the case of slender beams deforming in their plane of symmetry (Section 3.1). Shear bending forces are calculated according to (Adriaenssens and Barnes 2001). The two pairs of opposite shear forces acting respectively on the nodes (i, j) and (j, k) and

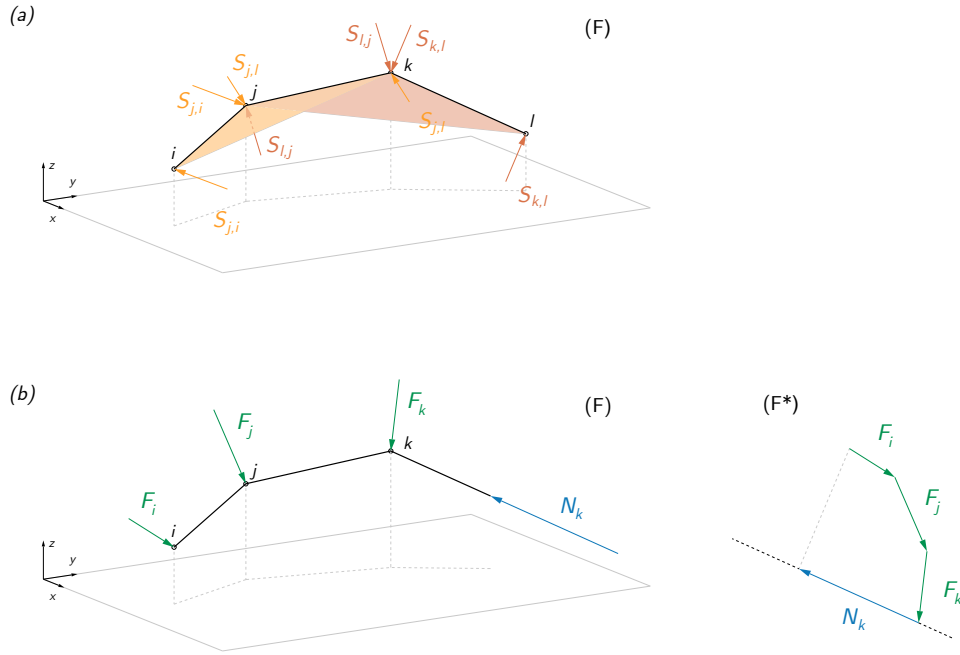


Figure 3.34: Internal forces in a torsion-free rod in 3D space – (a) Shear bending forces calculated from the relative position of three adjacent nodes of the rod, (b) Axial force in the rod's segments calculated from the projection along the segment direction of the sub-resultant force of the external forces acting on the rod.

corresponding to the bending moment \mathbf{M}_j lies on the plane defined by the nodes (i, j, k) (Figure 3.34(a)). Axial forces are calculated from the global equilibrium of a free body diagram of the rod, based on the projections along the direction of the rod's segments of sub-resultant forces of the external forces acting on the rod (Figure 3.34(b)). External forces can be of different kinds (restraining forces, punctual forces, self-weight, external torques, etc.) and are applied onto the nodes of the rod.

For each node of the rod, all the forces acting at it are assembled in a force diagram where they must form a closed polygon if the node is in static equilibrium.

Sequential construction of a torsion-free rod in equilibrium in 3D space

Following the same principle as in the case of bending-active beams deforming in 2D space, it is possible to sequentially construct a torsion-free rod in equilibrium in 3D space through a graphical procedure. The rod is built node by node, by building successively its form and force diagrams (Figure 3.35). The position of the node i of the rod's axis is determined in relation to the position of the two previous nodes $i - 1$ and $i - 2$, and from the polygon of forces corresponding to the static equilibrium of node $i - 2$. The shear force $S_{i-1,i-2}$ required to close the polygon of forces of node $i - 2$ defines the position of node i . The graphical

Figure 3.35: Sequential graphical construction of a torsion-free rod in equilibrium in 3D space— (a) Sequential construction of the form diagram and force diagram of the rod, (b) Entire rod and its corresponding 3D force diagram.

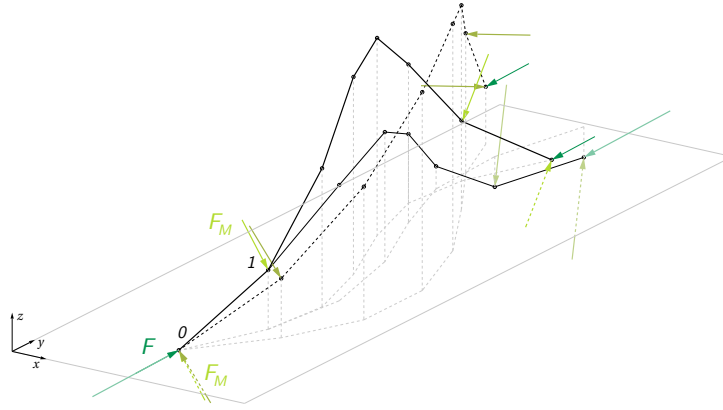


Figure 3.36: Family of 3D torsion-free rods – With respect to the generative parameters of their sequential construction: position of nodes 0 and 1, magnitude and orientation of external force at node F and magnitude and orientation of external bending torque $(F_M, -F_M)$.

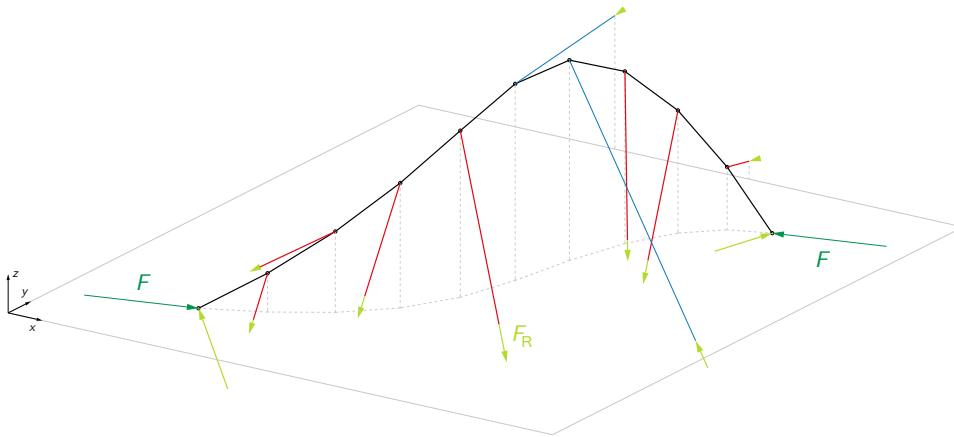


Figure 3.37: Restraining forces required in order to shape the torsion-free rod into a given 3D target equilibrium geometry under the specified external forces – Blue, respectively red, represents structural elements in compression, respectively in tension. Dark green, respectively light green, represents external forces, respectively additional restraining forces.

the segment $(0, 1)$, then the generated rod will be plane, corresponding to the scenario addressed in Sections 3.1, 3.2 and 3.3.

Equilibrating torsion-free rods in 3D space with additional restraining forces

Considering a curve in 3D space as the target equilibrium geometry of a torsion-free rod and external loads, it can be calculated from a force diagram the additional forces that are required to enforce the static equilibrium in the target geometry under such considered loads. In a similar way as in 2D space, the additional restraining forces fulfil the global equilibrium of the rod with the external

loads and the axial forces. These additional forces can be applied externally to the rod by means of connected struts and ties. In practice, the orientation in 3D space of such restraining elements, make their use difficult from a design perspective. Indeed, Figure 3.37 illustrates how the struts and ties restraining the rod might scatter.

In a similar way as in 2D space, the configuration of the polygons of forces shows that the orientation of the restraining forces can actually be chosen inside specific planes (see Figure 3.38 (left)). In theory, this property could make possible a better control of the orientation of the restraining additional elements. However, contrary to the case of beams actively bent in their plane of symmetry, the direction of the restraining forces cannot be chosen independently to each other as the different planes in which the restraining forces can be chosen depend on the orientation of the restraining forces at the other nodes of the rod. Figure 3.38 (right) illustrates this dependency.

Issues related to the use of 3D vector-based graphic statics In addition to presenting problems of visual readability, the manipulation of 3D force diagrams is ruled by the properties of 3D geometry. In particular, in 3D geometry, two non-parallel lines do not meet unless they are coplanar. This trivial observation makes impossible the scaling of shear bending forces through local adjusting of the rod bending stiffness in order to generate closed polygons of forces as proposed in Section 3.2 for the case of 2D force diagrams (Figure 3.39).

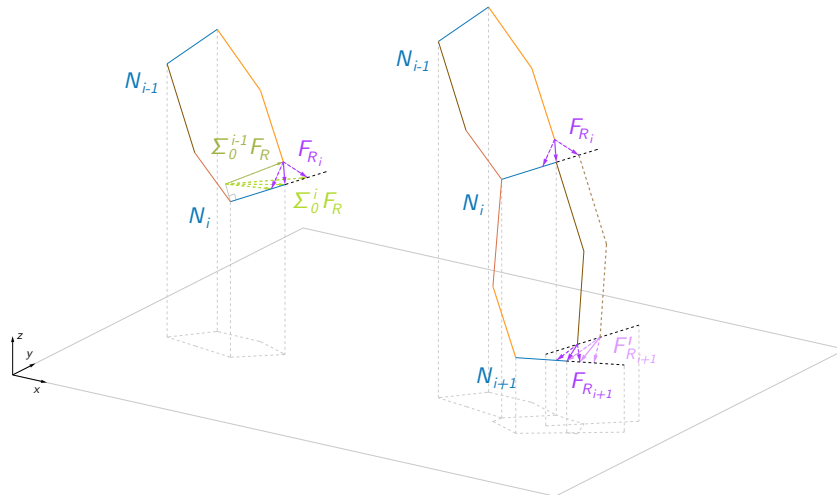


Figure 3.38: 3D polygons of forces balanced with additional restraining forces (in purple) – Different possible restraining forces can fulfil the local and global equilibrium of the torsion-free rod. At each node, these different possible restraining forces lie on a specific plane. Such plane is dependent on the orientation of the restraining forces at the other nodes of the rod.

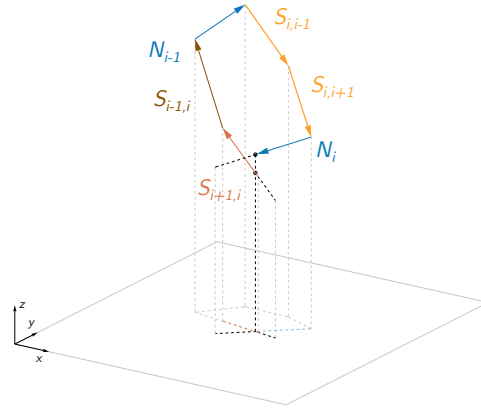


Figure 3.39: Unbalanced 3D polygon of forces – Manipulation of shear bending forces magnitude by means of bending stiffness variation fails to close the polygonal cell of forces as two non-parallel lines do not necessarily meet in 3D space.

Concluding remark The modelling scheme introduced in Section 3.1 for the modelling in 2D space of bending-active beams can be applied to the modelling of torsion-free bending-active rods in 3D space. The use of this modelling scheme in combination with force diagrams allows for the sequential construction of torsion-free rods that are actively bent in 3D space. Nevertheless, the ability and effectiveness of the graphical method to determine the conditions leading to the materialisation of a given geometric curve by the equilibrium of a slender rods actively-bent in plane is not replicated in the case of slender elements under large deformations in 3D space. For this reason, in the rest of this research work, the bending-active beams, whether flat beams or rods, will only be subjected to bending moments, they will have a plane of symmetry and will be loaded and deformed in this plane, so as to avoid torsion.

4. Design Approach

Grounded on the equilibrium of bending-active beams in 2D space, which was addressed in previous Chapter 3, this Chapter is devoted to form-driven design strategies for 3D bending-active tensile structures consisting of bending-active beams, which are bent in their plane of symmetry, and restraining tensile systems, in the form of cables and cable nets.

4.1 Form-driven design approach

Novel form-driven design approach A novel approach is introduced for the design of 3D bending-active tensile structures composed of bending-active beams, which are bent in their plane of symmetry and whose bent equilibrium geometry is plane, and 3D restraining cables and cable nets (Boulic and Schwartz 2018). The primary objective of this novel design approach is to compensate for the lack of direct control over the final deformed equilibrium geometry of bending-active tensile structures, from which existing form-finding methods suffer as explained in Sections 1.1, 2.1.3 and 2.2.1. By providing explicit control on the bent equilibrium geometry of the bending-active beams and, to a lesser extent, also on the equilibrium geometry of the restraining tensile systems, the introduced design approach intends to complement and enrich the range of existing form-finding methods for the design of bending-active tensile structures. In particular, the possibility of having such an explicit control on the equilibrium geometry of bending-active beams is considered particularly relevant during the initial design phase as it facilitates the integration of various geometry-based aspects into the design. Besides, as it is based on a simple mechanical model of slender beams (Section 3.1) and on 2D equilibrium conditions, the novel approach offers an intuitive understanding of the mechanical behaviour of bending-active tensile structures, together with the different parameters that rule their equilibrium. These two advantages are a valuable aid for the ultimate integration of architecture and structure.

The so-called form-driven approach elaborated in this Chapter differs significantly from the form-finding approaches described in Section 2.1.3. The main difference between form-finding and form-driven approaches lies on the static problem to be solved since its formulation in the two approaches is inverted

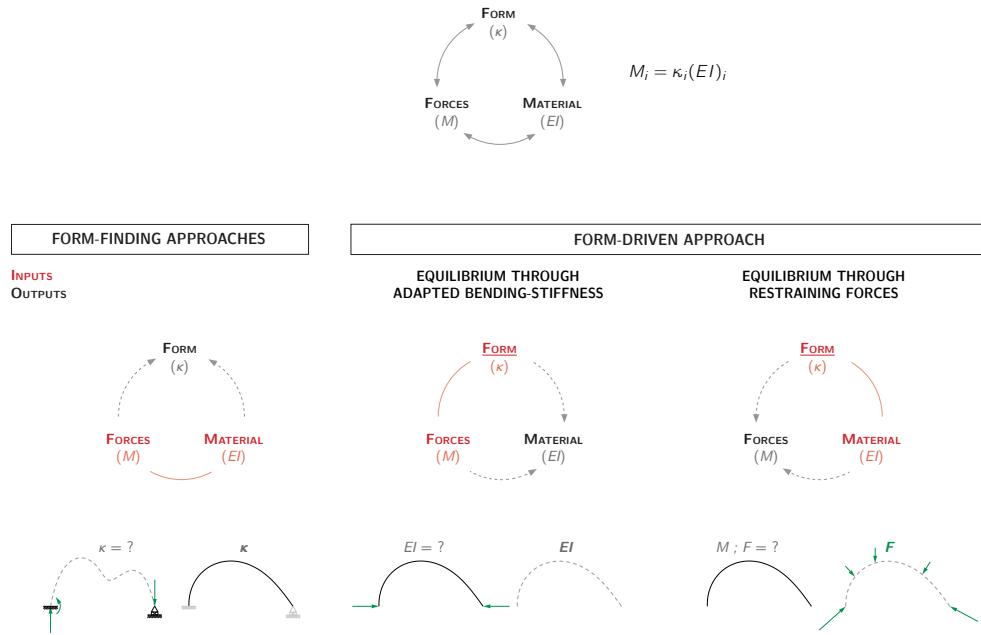


Figure 4.1: Schematic comparison between a form-finding based approach and the proposed form-driven approach in the context of active bending – L beam's length, A beam's cross sectional area, I beam's second moment of area, E beam's modulus of elasticity, ν beam's Poisson's ratio.

with respect to each other (Figure 4.1). In the form-finding approach, the goal is to find the equilibrium geometry that a given bending-active (tensile) structural system takes under imposed boundary constraints. On the contrary, in the form-driven approach, the aim is to define local and global conditions necessary to meet a given geometrical configuration of equilibrium of the bending-active structural system. That is, the length L of the slender beams, their cross-section area A and their bending stiffness EI , as well as the boundary conditions are input parameters in the form-finding approach while they are outputs of the form-driven approach. Conversely, the equilibrium geometry is the output of the form-finding algorithms while it is the input of the form-driven approach.

As opposed to most of the form-finding design approaches exposed in Section 2.1.3, in which both the geometry of the bending-active elements and the tensile elements are form-found at once, controlling the geometries of 2D bending-active beams within a 3D bending-active tensile structure is achieved by addressing successively the equilibrium of the bending-active elements and the one of the tensile elements, provided that equilibrium conditions between the two structural sub-systems are fulfilled. As an initial step, the target bent equilibrium geometry of each of the bending-active beams is defined as a plane continuous curve, considering various aspects, such as structural, functional, aesthetic and environmental criteria. The equilibrium of the beams in their target bent equilibrium geometry is achieved by combining a controlled variation of the bending

stiffness of the cross-section along the axis of the beams and additional forces along the axis of the beams through restraining systems, two concepts which have respectively been introduced in Section 3.2 and Section 3.3. Accordingly, in a second step, the global and local equilibrium of the beams is considered and a compatible set of pre-stressing elements is generated.

Different design strategies The design of bending-active tensile structure according to the form-driven approach begins with the definition in 3D space of the plane continuous curves which correspond to the desired bent equilibrium geometry of bending-active beams' axis. In order to fulfil the equilibrium of the beams in their target geometry, the restraining tensile elements must apply onto the beams' axis prestressing forces which are coplanar with their bending planes (Figure 4.2). This condition of equilibrium induces that specific compatible restraining cable nets must be generated in accordance with the beams' target equilibrium geometries. Two different strategies can then be distinguished to design such bending-active tensile structures and in particular to define such compatible restraining cables and cable nets. They are illustrated in Figure 4.3.

- **Design strategy 1 – Equilibrium of the bending-active beams through adapted bending stiffness** First, the target equilibrium geometry of each of the 2D bending-active beams is defined. Second, a compatible set of pre-stressing elements is generated, in such a way that these tensile elements apply onto the beams' axis a set of restraining forces that are coplanar with the beams' bending planes, making sure that no torsion appears in the beams. Third, for each beam, the global equilibrium is fulfilled by solving the reaction forces at the beam's supports and the local equilibrium is verified by ensuring that the applied forces generate locally a bending moment compatible with the beam's curvature. Finally, in a last step, the variable bending stiffness along the various beams' cross-sections is calculated such that the beams meet the equilibrium in the target geometries under the considered pre-stressing forces as explained in Section 3.2.
- **Design strategy 2 – Equilibrium of the bending-active beams through restraining forces** First, the target bent equilibrium geometry of each of the 2D bending-active beams is defined by the designer according various design parameters such as architectural, structural, environmental and manufacturing aspects. Second, based on the bending stiffness of the beams along their axis and on an initial set of acting loads, the restraining tensile forces required to bend the beams in their target equilibrium geometry are calculated according to the methodology presented in Section 3.3. Finally, a set of compatible pre-stressing elements is generated in such a way that these tensile elements apply onto the beams' axis the restraining forces previously calculated.

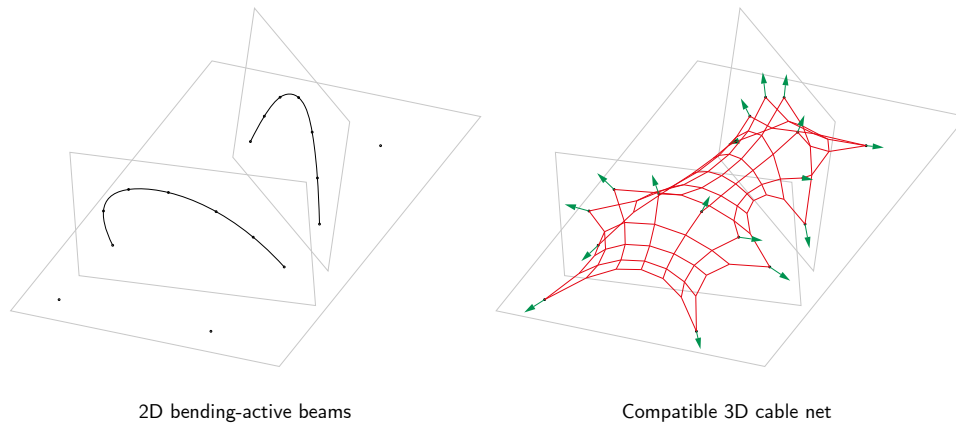


Figure 4.2: Concept of the form-driven design approach – Decoupling of the 2D bending-active beams and the 3D restraining cable nets and condition of equilibrium between the two structural subsystems.

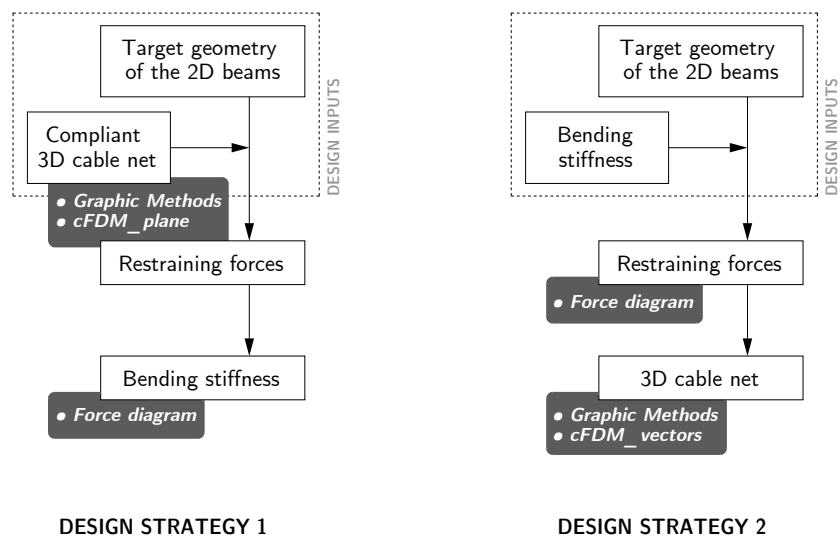


Figure 4.3: The two design strategies constituting of the form-driven approach.

Generation of compatible restraining cable net systems Different methods, both graphical and numerical, have been investigated in order to generate restraining cables and cable nets compatible with the equilibrium of the bending-active beams in their target bent geometry.

First, in Section 4.2, a graphical procedure is presented for the design of 3D funicular systems based from the transformation of an original 2D funicular system (Boulic 2020). Thanks to this graphical procedure, the results established in Section 3.3 for the shaping of single slender beams into target equilibrium geometry by restraining funicular systems are extended to the design of bending-active tensile structures consisting in single beams restrained with two 3D skew funicular systems unfolding on either side of the beams' bending plane.

Second, in Section 4.3, specific 3D arrangements of bending-active beams and pre-stressed cables that ensure the mutual equilibrium of each sub-systems have been identified thanks to the study of the form and force diagrams of continuous lines of cables. These specific patterns are based on geometric conditions and, although relatively specific, are flexible enough to allow different spatial configurations of beams and cables to be explored.

Third, in Section 4.4, a non-linear formulation of the force density method has been implemented in order to form-found the equilibrium geometry of cable nets under the design constraints imposed by the condition of equilibrium at the beams' nodes (Boulic and Schwartz 2018). The resort to this numerical method makes it possible to design bending-active tensile structures of higher complexity, regarding both the number and spatial arrangement of the bending-active beams and the topology of the cable nets.

In the form of a diagram, Figure 4.4 summarises the different graphical and numerical methods that are employed within the general form-driven design approach of bending-active tensile structures. It highlights, for each of the two design strategies – *Design strategy 1* and *Design strategy 2*, which are the graphical and numerical procedures that are employed to address, on the one hand, the equilibrium of the bending-active beams in their 2D target equilibrium geometry, and on the other hand, the generation in 3D space of tensile restraining cables and cable nets that are compliant with the 2D equilibrium of the bending-active beams.

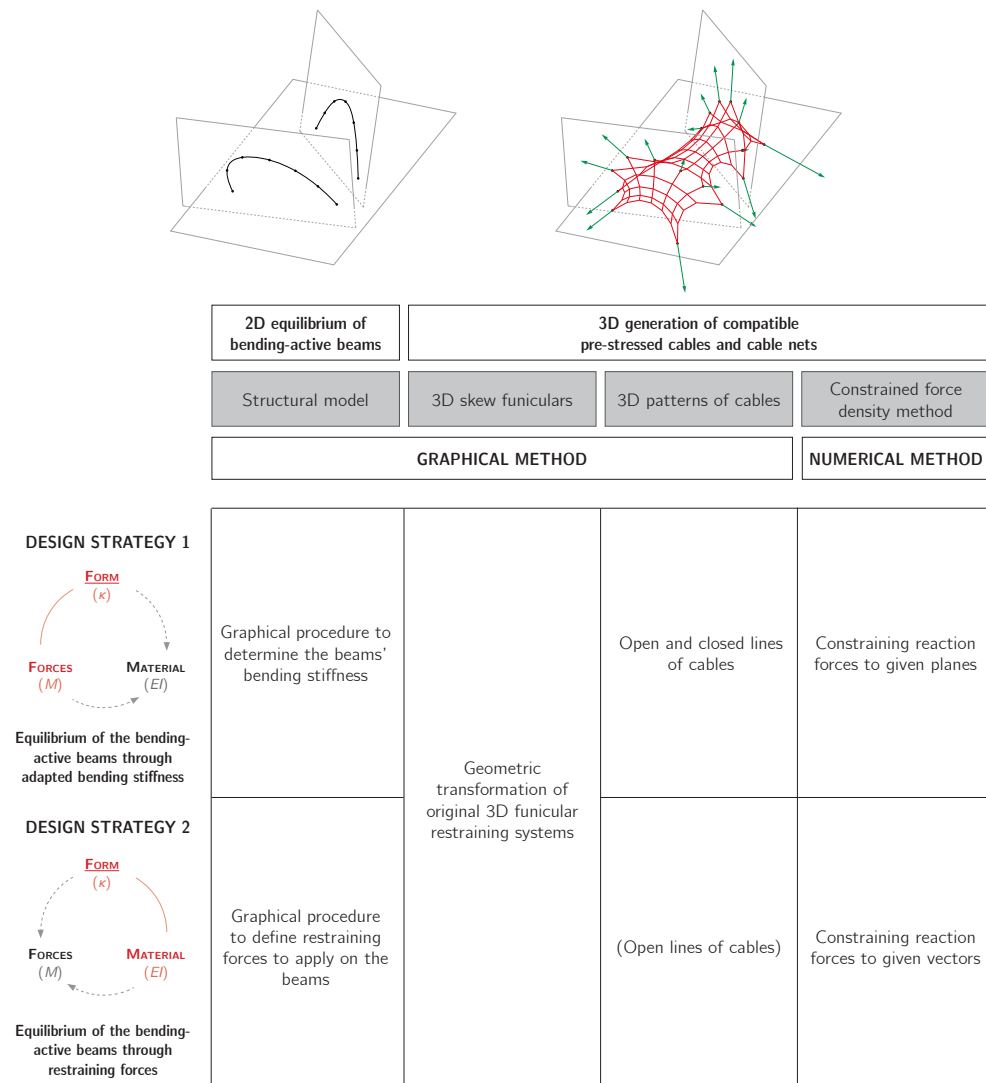


Figure 4.4: Graphical and numerical procedures employed to successively address the equilibrium of the bending-active beams and the pre-stressed cables and cable nets within a bending-active tensile structure for each of the two distinct form-driven design strategies.

4.2 Graphical construction of restraining cable nets

This section addresses the graphical construction of 3D funicular restraining systems in equilibrium with coplanar loads for the shaping of single bending-active beams which are bent in their plane of symmetry.

Considering a bending-active beam bent in its plane of symmetry, the additional restraining forces which are needed to shape the beam in its target equilibrium geometry are a set of coplanar loads. A graphical method for the construction of 3D funicular systems in equilibrium with such coplanar restraining forces is exposed. It is based on the geometric transformation of original 2D funicular systems, whose graphical construction is simple and well-established.

This section has been published with minor changes in (Boulic 2020).

4.2.1 Design of 3D funicular structures with graphical methods

3D funicular structures from the skewing of 2D funicular structures While 2D graphic statics efficiently allows the construction of 2D funicular structures for the transfer of a set of given loads to specified supports (Section 3.3.2), it does not offer, in most cases, such an elegant and straightforward procedure for solving the same problem in 3D space. Some of the methods used instead to address similar 3D funicular structures (Block 2009, Lachauer and Block 2012, Ohlbrock et al. 2017) share common principles with graphic statics, but couple these principles to numerical simulation tools. On the contrary, in particular cases, specific fully-graphical procedures can be defined: for example, a graphical method using polyhedron-based 3D graphic statics has been proposed for the construction of constrained funicular forms for a simple, determinate boundary condition (Akbarzadeh et al. 2015, 2016).

As demonstrated by Rankin (Huerta 2010) when applied to simple structural systems, geometric operations capable of transforming a structure while preserving its static equilibrium allow the generation of more complex systems at a lower cost. This paper focuses on the construction of 3D funicular structures from original 2D funicular structures, in a purely geometric manner, with vector-based 3D graphic statics. More specifically, the paper deals with the generation of 3D funicular structures, in equilibrium with given coplanar loads and supports located on either side of the plane of the loads, from the spatial transformation of original 2D funiculars, designed in the plane of the loads (Figure 4.5).

The construction of such 3D funicular structures involves the following steps: first, an original 2D funicular in equilibrium with the coplanar loads that are considered is designed following the methodology described above (Figure 4.5(a)); then, this 2D funicular is split into two superimposed funiculars (Figure 4.5(b)); and finally, each of these funiculars and the spokes that transfer the loads onto them are deployed into a 3D funicular structure on one side of the plane of the

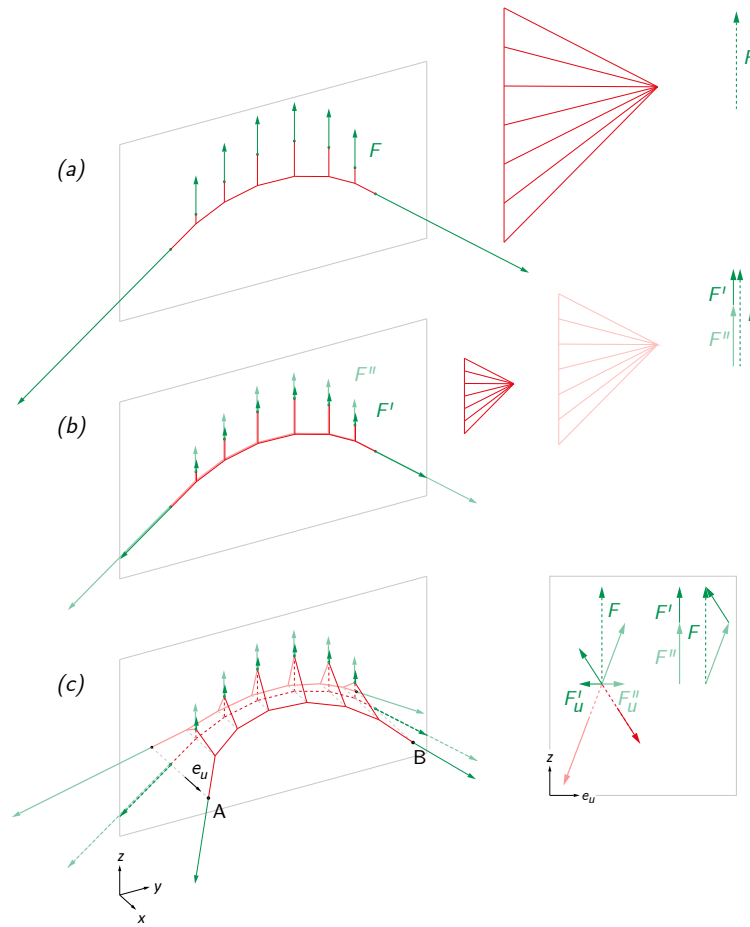


Figure 4.5: Pair of 3D skew funiculars from a transformed 2D funicular – (a) Original 2D funicular, (b) Superimposed 2D funicular subsystems, (c) Funicular subsystems unfolded on either side of the loading plane, along direction \mathbf{e}_u .

loads, to the supports that are considered, while the position of the points of application of the loads is kept unchanged (Figure 4.5(c)).

The applied geometric transformation is such that the 2D funicular is the projection of the nodes of the 3D funiculars onto the plane of the loads along the direction of projection \mathbf{e}_u , meaning that the nodes of the 3D funiculars are obtained by moving the nodes of the 2D funicular along the direction \mathbf{e}_u . It results that the equilibrium of the internal forces along the original plane is preserved over the transformation and that the force diagram of the 2D funicular is the projection of the force diagram of the 3D funiculars along the direction \mathbf{e}_u . The two newly constructed 3D funiculars including the various spokes are not plane anymore but skew, unless their new supports and the points of application of the loads are coplanar. The exact position of the 3D funiculars' nodes, which relates to the inclination of the spokes that connect the points of application of the loads to the skew funicular, is determined with the force diagram, ensuring the

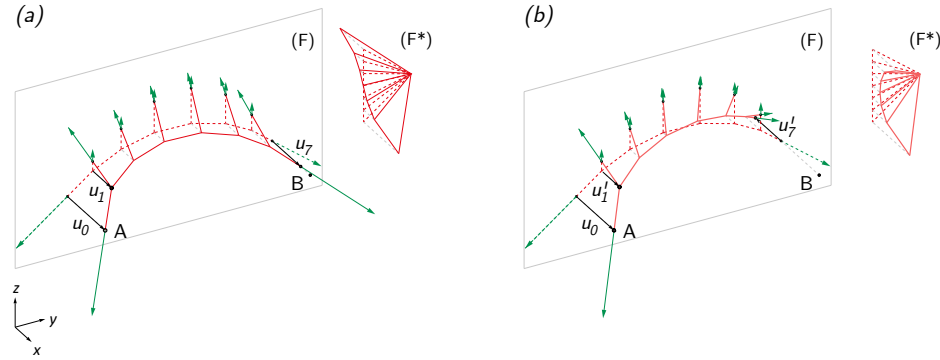


Figure 4.6: Skew funicular from a transformed 2D funicular – Construction of skew funicular subsystems from the arbitrary translation of 2 adjacent nodes along direction \mathbf{e}_u .

equilibrium of the internal forces of the structure along the direction of projection \mathbf{e}_u . Additionally, the two skew funiculars are unfolded on either side of the plane of the loads in such proportions that the equilibrium of the internal forces along \mathbf{e}_u is preserved at the points of application of the loads (Figure 4.5(c)).

The two skew funiculars can be built graphically by successively solving the equilibrium of their various nodes (Figure 4.6). Considering one skew funicular only, the position of its nodes is determined by the arbitrarily translation along \mathbf{e}_u of two adjacent nodes (translations \mathbf{u}_0 and $\mathbf{u}_1^{(l)}$ in Figure 4.6). Unfortunately, the position of the funicular' supports (translation $\mathbf{u}_7^{(l)}$ in Figure 4.6) cannot be controlled directly with this procedure. In a digital and parametric environment, it is possible to vary the translation vector of the two initiating nodes until the boundary conditions are met. The aim of the contribution is to establish a fully graphical procedure that allows the direct construction of the skew funiculars in equilibrium with given supports.

More generally, geometric transformations of 3D structural systems which preserve static equilibrium are of growing interest. (Fivet 2016) enumerates projective transformations which can be applied onto the form diagram of a structure in equilibrium while (D'Acunto et al. 2017) elaborate on the geometric transformations which can be performed on the force diagram of a structure in equilibrium in the context of vector-based 3D graphic statics.

4.2.2 Graphical method

A graphical procedure is proposed in order to transform 2D funiculars into pairs of skew funiculars which are in equilibrium with coplanar loads and supports whose position is controlled. This procedure keeps the simplicity of the graphical construction of a 2D funicular in the plane, by making use of the reciprocal and linear relationships between the form and force diagrams of the funicular structure over the investigated geometric transformation.

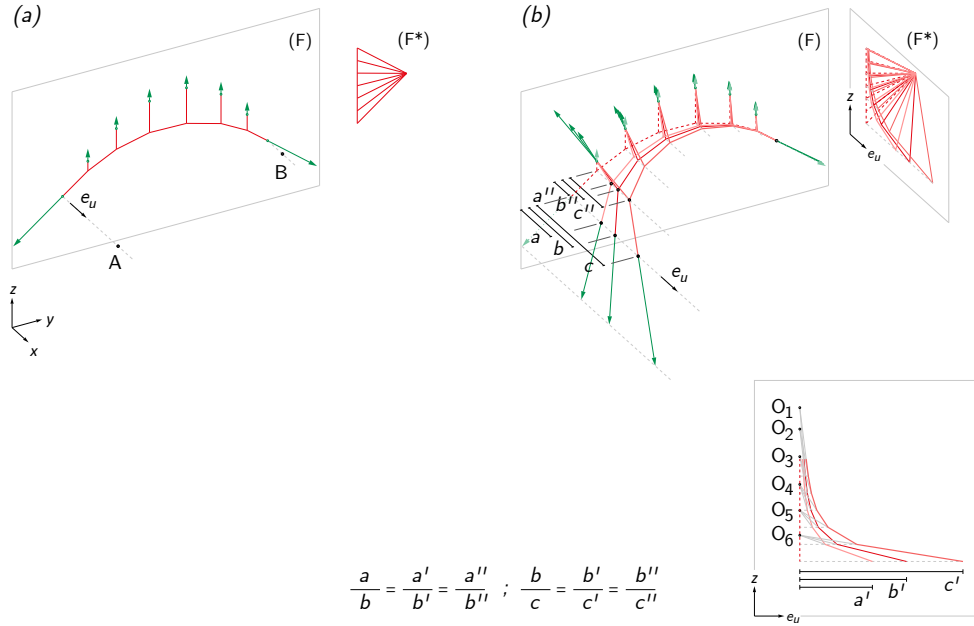


Figure 4.7: Three funiculars originating from one support and the linear relation they share, expressed through *spokes' poles* O_i in the force diagram.

Linear relationships over the transformation: graphical demonstration For the sake of clarity, especially regarding the readability of the force diagrams, only the skewing of one of the two superimposed 2D funiculars is considered in the following paragraphs.

Three distinct skew funiculars, originating from one of the specified supports and based on the skewing of the considered 2D funicular subsystem, are built node by node with the help of a force diagram (Figure 4.7). It can then be noted that these three skew funiculars, as well as their corresponding force diagrams, are connected to each other geometrically. Considering that their force diagrams are located in the force space (F^*) such that they are aligned which each other along the direction \mathbf{e}_u , such that the poles of the three force diagrams overlay for example, the segments corresponding to the forces within the funiculars' spokes are extended with straight lines. Three by three, these lines intersect at a unique point, referred to as a *spokes' pole*, which reflects some linear relationships over the geometric transformation of the force and form diagrams. For each node of the force and form diagrams, the coefficient of linearity of the translation operation from the original 2D funicular differs; however, the points of the force diagrams, as well as the nodes of the skew funiculars, move along the direction \mathbf{e}_u in the same relative proportion (Figure 4.7(b)). Besides, the location of the *spokes' poles* depends on geometric parameters of the original 2D funicular and on how the diagrams are placed in relation to each other in the force space (F^*).

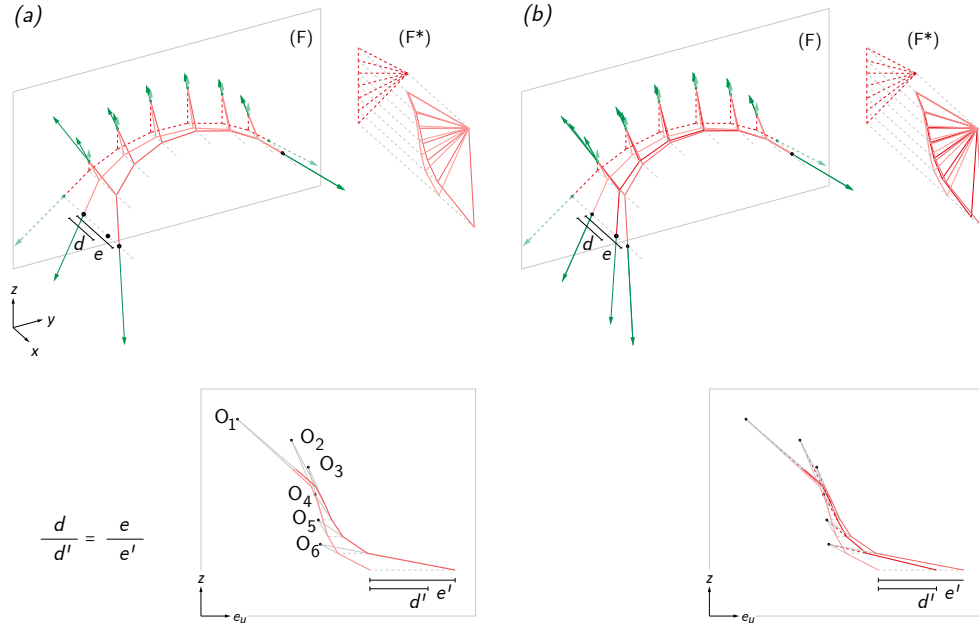


Figure 4.8: Construction of a skew funicular with given supports through auxiliary skew funiculars.

Procedure From that observation, if the geometry of two skew funiculars originating from one of the desired supports is known, the skew funicular ending at the second desired support, together with its force diagram, can be deduced from the relative position of the skew funiculars' ending supports (Figure 4.8). In a similar way as in 2D, where an auxiliary funicular is required to build a funicular through two given supports, two auxiliary skew funiculars are needed in 3D to build a skew funicular through two given supports.

For the sake of simplification, the system shown in Figure 4.7 and Figure 4.8 is such that \mathbf{e}_u is parallel to the x axis and that loads are parallel with each other and along the z axis. Under those conditions, and if the loads are equally distributed between the two skew funiculars, a symmetric structure ensures that the forces along \mathbf{e}_u , which are generated at the points of application of the loads by the two skew funiculars, cancel each other. However, any skewing direction \mathbf{e}_u can be chosen as long as $(\mathbf{e}_u \wedge \mathbf{e}_y) \wedge (\mathbf{e}_u \wedge \mathbf{e}_z) \neq \mathbf{0}$ (Figure 4.11), the loads do not need to be parallel with each other (Figure 4.10) and the proportion of loads taken by each of the two skew funiculars can be unequal (as illustrated in the asymmetric configurations of Figure 4.9). Obviously, any 2D funicular structure with more than two supports can also be extended to the third dimension thanks to this graphical procedure. The position of the supports can be freely chosen for one of the two skew funiculars and the relative position of the supports of the two skew funiculars on the either side of the plane of the loads is directly related to the proportion of the original loads taken by each skew funicular (Figure 4.9).

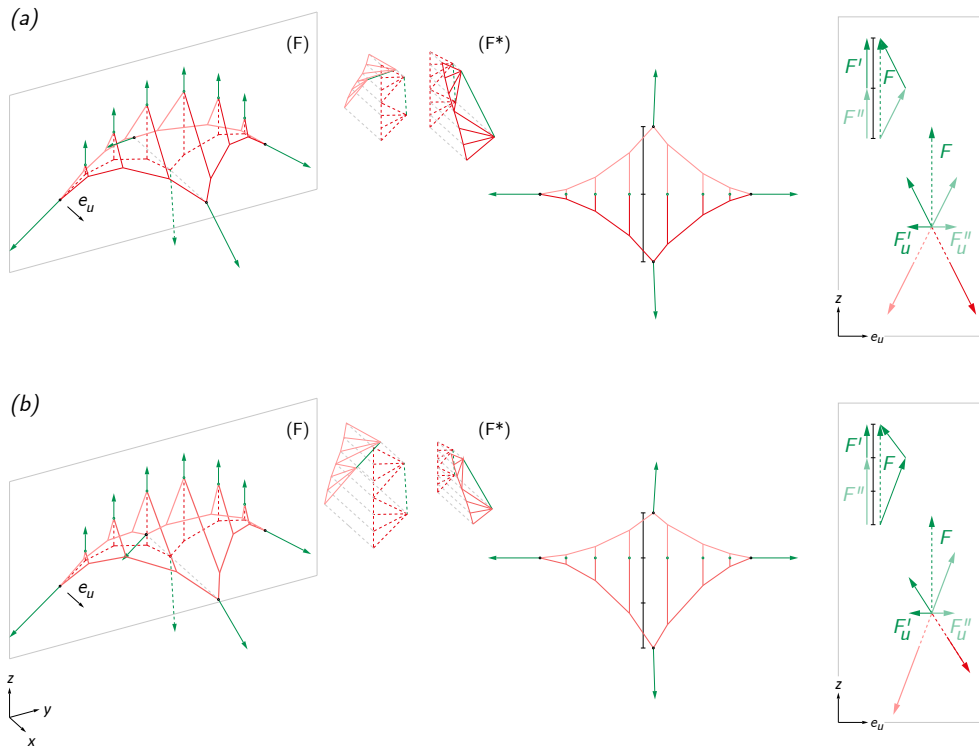


Figure 4.9: Symmetric and asymmetric 3D funicular systems with intermediate supports – The relative location along direction e_u of the supports of either skew funicular is in opposite proportion to that of the relative amount of the original loads take by either skew funicular.

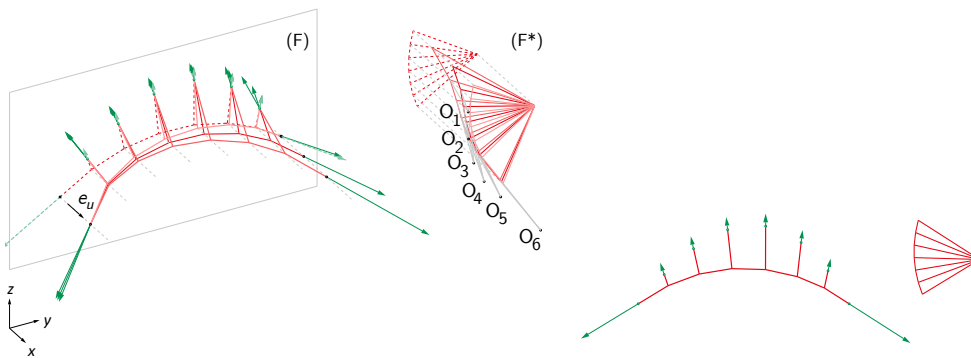


Figure 4.10: Skew funicular with non parallel spokes – Original coplanar loads are not parallel and the spokes' poles of the force diagram do not lie in a plane.

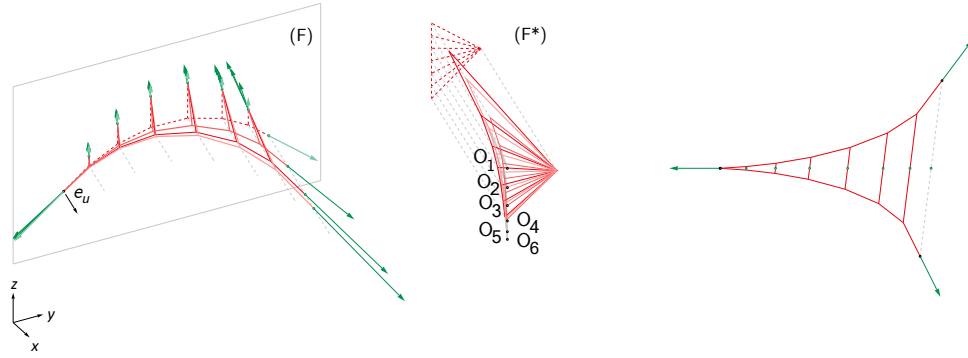


Figure 4.11: Skewing of a 2D funicular along an arbitrary skewing direction \mathbf{e}_u not coplanar to the loading plane.

Linear relationships over the transformation: analytical demonstration

The linearity of the skewing transformation is demonstrated here analytically. A skew funicular structure can be regarded as a network structure composed of n free nodes, which are not loaded, n_f fixed nodes, which are the supports of the structure and the points of application of the loads, and m branches, which connect the nodes to each other. According to the force density method (Schek 1974), which is introduced with further detail in Section 4.4.1, the coordinates $\mathbf{x}, \mathbf{y}, \mathbf{u}$ of the free nodes within the coordinate system $(\mathbf{e}_x, \mathbf{e}_y, \mathbf{e}_u)$ can be deduced from the coordinates $\mathbf{x}_f, \mathbf{y}_f, \mathbf{u}_f$ of the fixed nodes, based on the following relations:

$$\begin{aligned} \mathbf{x} &= -(\mathbf{C}^T \mathbf{Q} \mathbf{C})^{-1} \mathbf{C}^T \mathbf{Q} \mathbf{C}_f \mathbf{x}_f \\ \mathbf{y} &= -(\mathbf{C}^T \mathbf{Q} \mathbf{C})^{-1} \mathbf{C}^T \mathbf{Q} \mathbf{C}_f \mathbf{y}_f \\ \mathbf{u} &= -(\mathbf{C}^T \mathbf{Q} \mathbf{C})^{-1} \mathbf{C}^T \mathbf{Q} \mathbf{C}_f \mathbf{u}_f \end{aligned} \quad (4.1)$$

where \mathbf{C} is the $[m \times n]$ connectivity matrix of the free nodes, \mathbf{C}_f the $[m \times n_f]$ connectivity matrix of the fixed nodes and \mathbf{Q} the $[m \times m]$ diagonal matrix of the force density of the branches.

A translation of \mathbf{u}'_A and \mathbf{u}'_B of the supports' positions along direction \mathbf{e}_u results in new fixed nodes coordinates $\mathbf{x}'_f = \mathbf{x}_f$, $\mathbf{y}'_f = \mathbf{y}_f$ and $\mathbf{u}'_f = (\mathbf{u}'_A, \mathbf{u}'_B, 0, \dots, 0)$. Let's be \mathbf{A} the $[n \times n_f]$ matrix $-(\mathbf{C}^T \mathbf{Q} \mathbf{C})^{-1} \mathbf{C}^T \mathbf{Q} \mathbf{C}_f$. From equation 4.1, the new coordinates of the free nodes are:

$$\mathbf{x}' = \mathbf{x}, \quad \mathbf{y}' = \mathbf{y}, \quad \mathbf{u}'/i \in \langle 1, n_f \rangle, \quad \mathbf{u}'_i = A_{i1} \mathbf{u}'_A + A_{i2} \mathbf{u}'_B \quad (4.2)$$

Equation 4.2 shows the linear dependency to \mathbf{u}'_A and \mathbf{u}'_B of the nodes' translation along direction \mathbf{e}_u . It also shows that the coefficient of proportionality is different for each free node and depends on the connectivity and force density matrices.

4.2.3 Increasing topological complexity through force diagram subdivisions

One of the properties of funicular structures is their ability to derive many other funicular structures from the subdivision of the polygonal cells of their force diagram. These new structures share the same boundary conditions as the original structure but have a more complex topology. The subdivision operation results in a redistribution of the internal force flow by branching original members of the structure with newly created members. This structural and geometric property has been illustrated in the case of 2D structures with nodes connecting at least three branches (Akbarzadeh et al. 2014), and in the case of 3D structures with nodes connecting at least four branches (Akbarzadeh et al. 2015).

Subdividing vector-based force diagrams is being investigated in the context of skew funiculars in order to explore the graphical construction of systems which are topologically more complex than the original 2D funicular.

There are two ways to divide a polygonal cell: by a point in its convex domain, or by its edges. The subdivision by an inner point of the cell preserves the boundary conditions of the corresponding node while creating new branches from the original branches (Figure 4.12(b)). On the contrary, a subdivision of

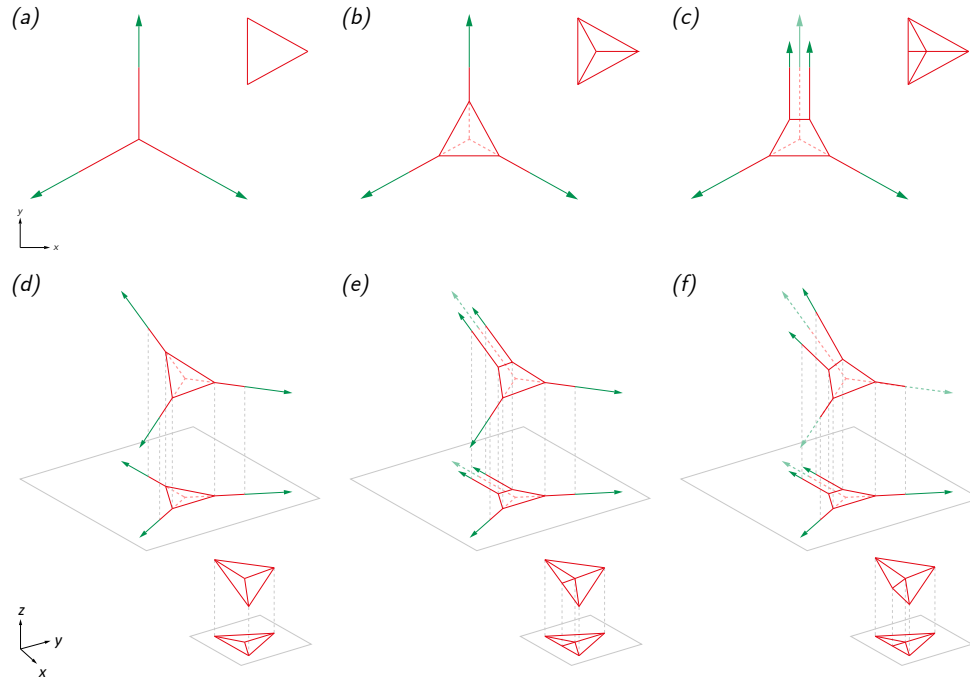


Figure 4.12: Subdivisions of a 3-branch node and its triangular polygon of forces in 2D and their projection in 3D – (a) Original 3-branch node (F) and its corresponding triangular cell (F^*), (b) Subdivision of the cell by its centre and (d) its projection in 3D which remains plane, (c) Subdivision of the cell involving an edge subdivision and its (e) plane and (f) skew projection in space.

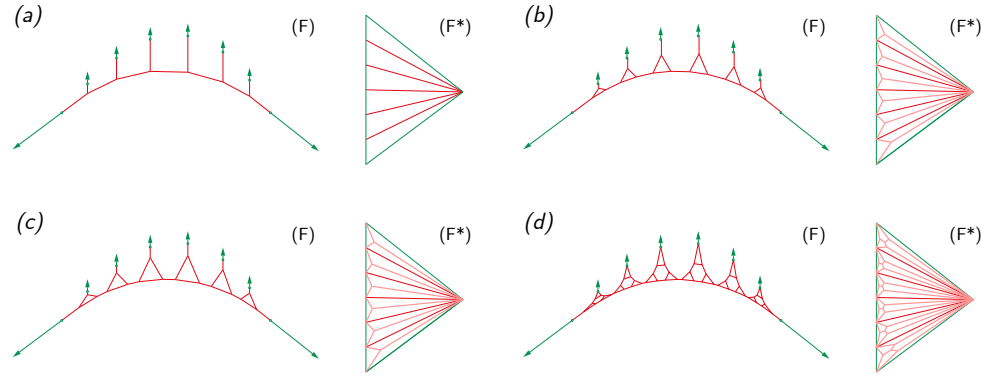


Figure 4.13: Generation of 2D complex structures through centre-vertexes subdivisions of the force diagram – (a) Initial funicular configuration, (b) a first centre-vertexes subdivision of the polygonal cells (F^*) and two possible corresponding branched funicular (F), (c) and (d) a second centre-vertexes subdivision of the cells (F^*) and a possible branched funicular (F).

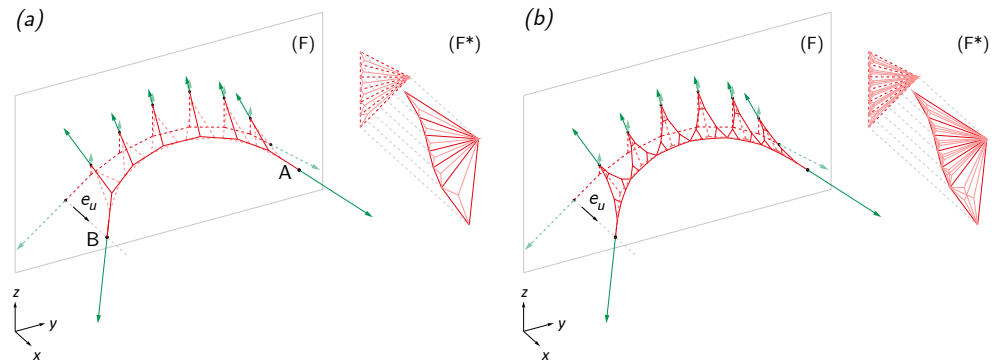


Figure 4.14: Generation of 3D funicular systems through centre-vertexes subdivisions of the force diagram – (a) Original 2D funicular configuration, (b) centre-vertexes subdivision of the polygonal cells (F^*) and a corresponding branched funicular (F), (c) and (d) subdivisions operated on the 3D skew funicular directly.

the cell involving the subdivision of an edge of the cell provokes the duplication of the branches corresponding to the divided edges (Figure 4.12(c)) and therefore affects the boundary conditions of the corresponding node.

Centre-vertexes subdivision In the case of an original triangular cell, a division by an inner point of the cell generates three sub-cells that are themselves triangular, and consequently new nodes in the form diagram with three branches (Figure 4.12(a)(b)). The newly created nodes and branches are located in the plane of the original branches. Therefore, transformation of the form and form diagram of a funicular with only 3-valent nodes involving only this kind of subdivision can equally be performed on the original 2D funicular or on the skew funiculars, according to the procedure detailed by (Akbarzadeh et al. 2014).

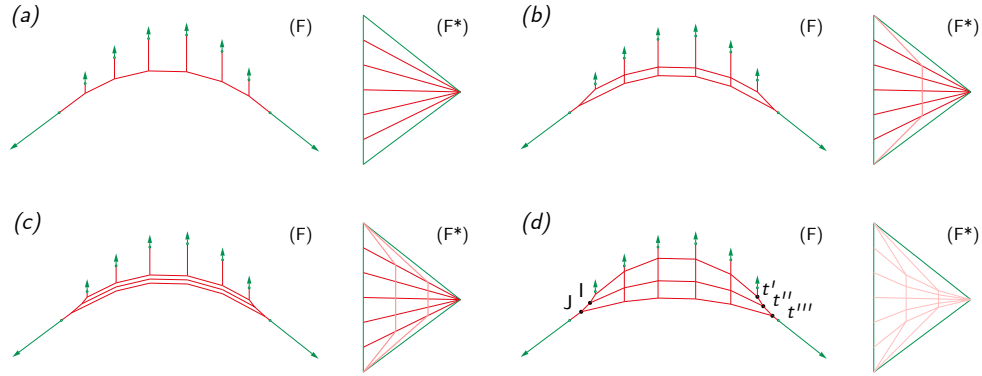


Figure 4.15: Generation of 2D complex structures through edge subdivisions of the force diagram – (a) Initial funicular configuration, (b) edge-edge subdivision of the polygonal cells – the cells' edges are divided in half, (c) edge-edge subdivision of the polygonal cells – the cells' edges are divided in three equal parts, and (d) internal nodes of the diagram (F*) are moved in order to widen the cable net (F).

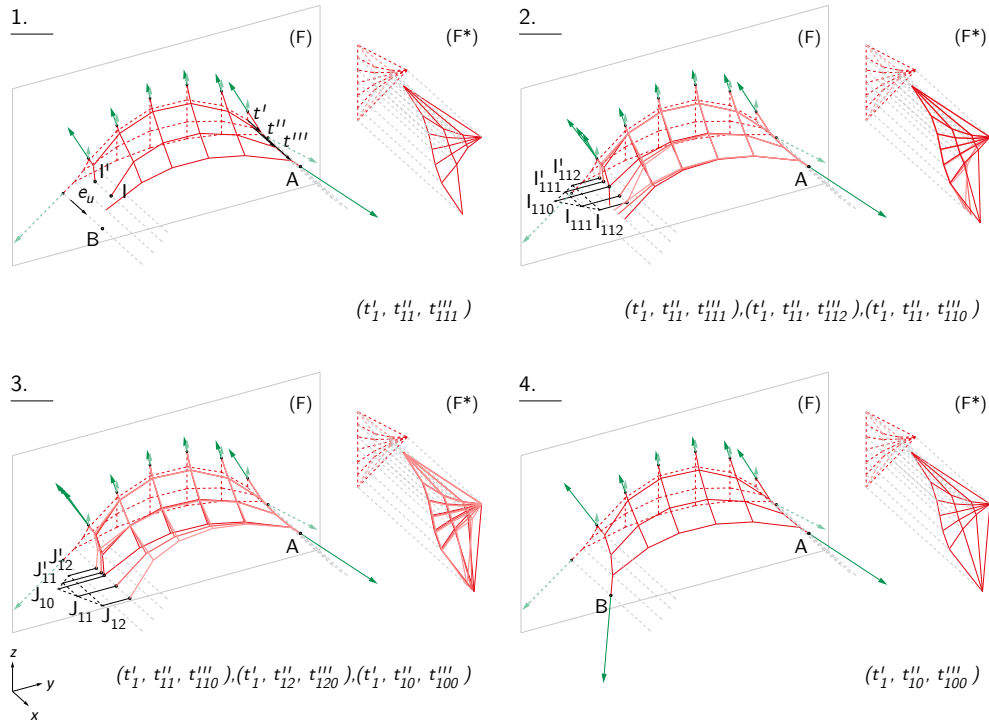


Figure 4.16: Generation of 3D funicular systems through edge subdivisions of the force diagram – Iterative construction of the 3D skew branched structure thanks to auxiliary systems.

Figure 4.13 shows a 2D funicular structure originating from successive subdivisions of the force diagram's cells by an inner point and Figure 4.13 illustrates how the subdivisions can equally be performed directly on the 3D skew funicular or performed on the original 2D funicular and then projected onto the 3D skew funicular.

Edges subdivision When a cell division involves subdividing an edge of the cell (Figure 4.12(c)), the new resulting branches might not remain coplanar with the original projected branches when projected in space (Figure 4.12(e)(f)). This is because the funicular surface generated by the new branches has the characteristic to be doubly curved. Therefore, when a transformation of the original network involves edge subdivision, it is not possible to subdivide on the force diagram of the skew funicular directly. It is necessary to subdivide first the 2D funicular (Figure 4.15) and then build the corresponding skew structure (Figure 4.16).

To graphically construct such a skew funicular structure node by node, the translation of a certain number of nodes along the skewing direction \mathbf{e}_u has to be chosen arbitrarily (parameters (t', t'', t''') in Figure 4.15 and Figure 4.16). However, the incorrect position of these nodes leads to a divergence of the system: at some point of the construction, branches in the form diagram do not intersect while they should (nodes I and I' in Figure 4.16(1)). As a consequence, their correct position has to be found iteratively through the construction of auxiliary systems. In the example of Figure 4.16, for given translations (t'_1, t'_{11}) , two values of t' , t'_{111} and t'_{112} , are arbitrarily chosen from which are built two auxiliary systems with non-intersecting branches, respectively nodes I_{110} and I'_{111} and nodes I_{112} and I'_{112} , and the translation t'_{110} making branches to meet at node I_{110} is determined through a linear interpolation which can be done graphically, and satisfies:

$$\frac{t'_{111} - t'_{110}}{t'_{112} - t'_{110}} = \frac{I'_{111} I_{110} \cdot \mathbf{e}_u}{I'_{112} I_{110} \cdot \mathbf{e}_u} = \frac{I_{111} I_{110} \cdot \mathbf{e}_u}{I_{112} I_{110} \cdot \mathbf{e}_u} \quad (4.3)$$

Still, branches of the skew funicular structure do not meet at J . The same procedure is repeated for translations (t''_1, t''_{12}) . From the auxiliary systems $(t'_1, t'_{11}, t'_{110})$ and $(t''_1, t''_{12}, t'_{120})$, the translation t''_{10} is found allowing branches to intersect at I and J . The translations t''_{10} and t'_{100} are such that:

$$\frac{t''_{11} - t''_{10}}{t''_{12} - t''_{10}} = \frac{J'_{11} J_{10} \cdot \mathbf{e}_u}{J'_{12} J_{10} \cdot \mathbf{e}_u} = \frac{J_{11} J_{10} \cdot \mathbf{e}_u}{J_{12} J_{10} \cdot \mathbf{e}_u} = \frac{t'_{110} - t'_{100}}{t'_{120} - t'_{100}} \quad (4.4)$$

A total of 6 auxiliary constructions is needed to build a complete skew funicular structure derived from edge-edge subdivision of the original 2D funicular, and 14 auxiliary constructions would be required in order to find the skew structure $(t'''_1, t''_{11}, t'_{110})$ reaching the second support at a specified position (it would be done by repeating the same procedure as above for a new arbitrarily chosen translation t'''_2 and a linear interpolation). Obviously, in a numerical and parametric environment, it is possible to automate these graphical constructions.

4.2.4 Examples of design application

Funicular systems made of pairs of skew funiculars in equilibrium with coplanar loads, and whose graphical construction has been detailed in Sections 4.2.2 and 4.2.3, can be applied to the conceptual design of bending-active tensile structures in which they allow restraining single bending-active beams which are bent in their plane of symmetry. More widely, such 3D funicular structures can be applied to the conceptual design of any other load bearing structures in which the design loads are coplanar. In order to illustrate such possibilities, two design applications have been developed.

The first example investigates the use of tensile funicular systems to restrain bending-active beams which are bent in their plane of symmetry. The hybrid structure shown in Figure 4.17 consists of two slender beams, actively bent into arches and restrained by means of a cable net. According to the form-driven design method of bending-active tensile systems presented in Section 4.1, the restraining forces required to enforce the beam to bend into the target equilibrium geometry that is considered are graphically calculated (Figure 4.17(a)) and applied to the beam by means of a restraining cable net (Figure 4.17(b)), a 3D tensile funicular system, that unfolds on each side of the bending-active beam and generates an enclosed space (Figure 4.17(c)). The developed bending-active tensile structure results from the spatial assembly of two beam/skew funicular systems and the addition of a compressive strut which provides the cable net with an additional support necessary for the equilibrium of the whole structure (Figure 4.17(top)). Subdivisions of the cable net's force diagram have been operated in order to densify the number of cables and give a stronger feeling of space enclosure.

The second example consists of a deck arch bridge in which the self-weight of the deck is transferred to two skew compressive arches through inclined columns. The bridge, depicted in Figure 4.18, rests on three supports. The resultant of the self-weight of the deck has been first considered, therefore acting along the plane of symmetry of the deck. A compressive 2D funicular has then been designed in the plane of the loads. From there, two skew funiculars in equilibrium with half of the self-weight of the deck have been graphically built after which they have been shifted apart from each other in order that the deck is supported by two rows of inclined columns. Consequently, the deck has been structurally activated either in tension or in compression in relation to the inclination of the supporting columns.

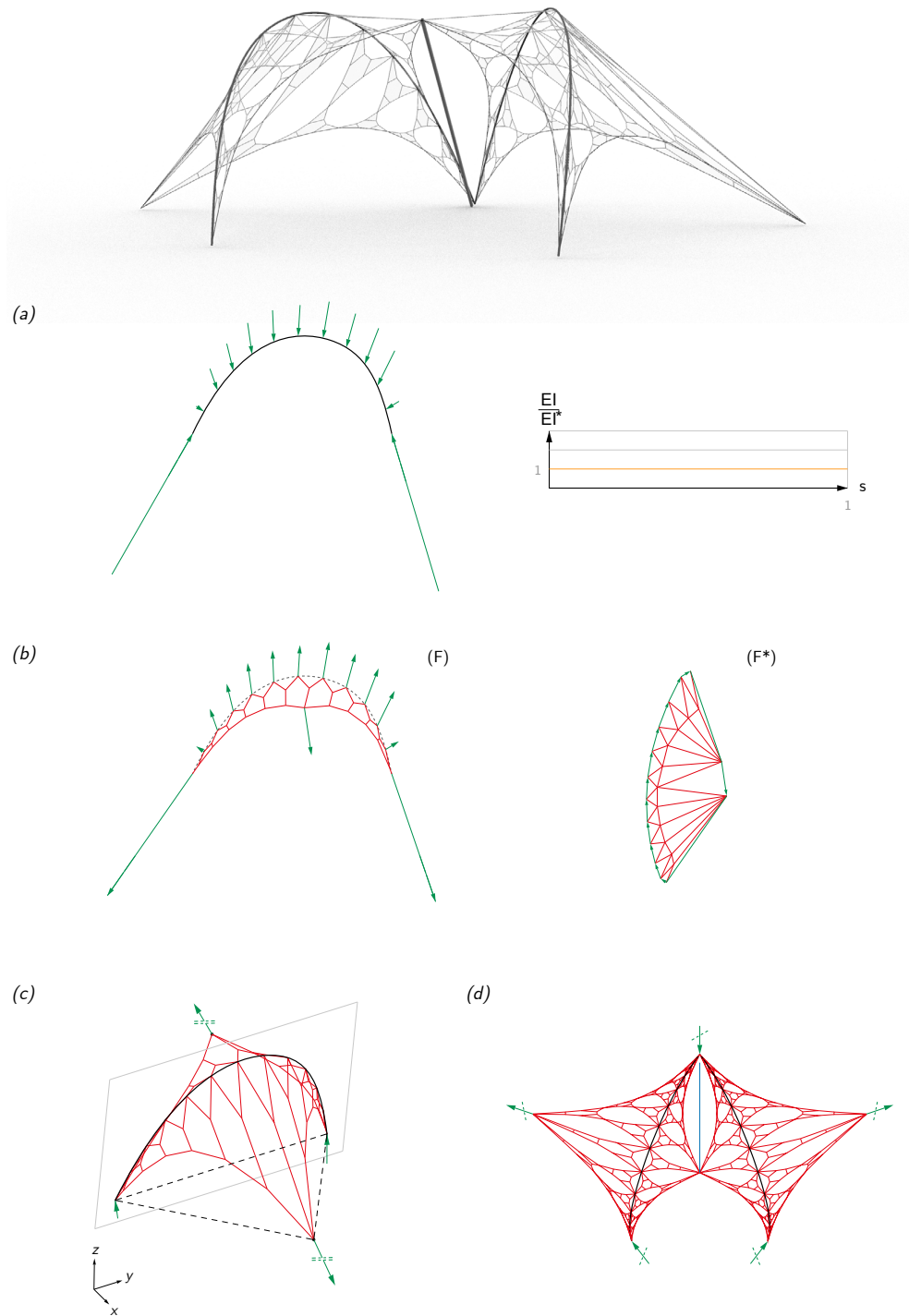
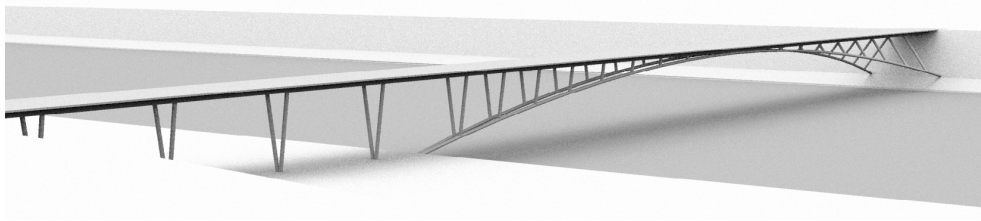
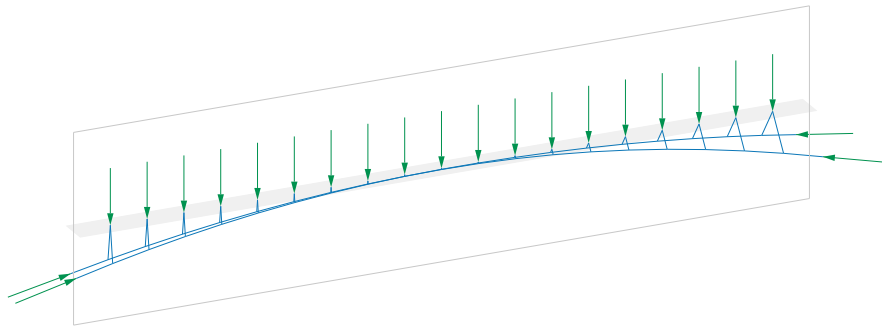


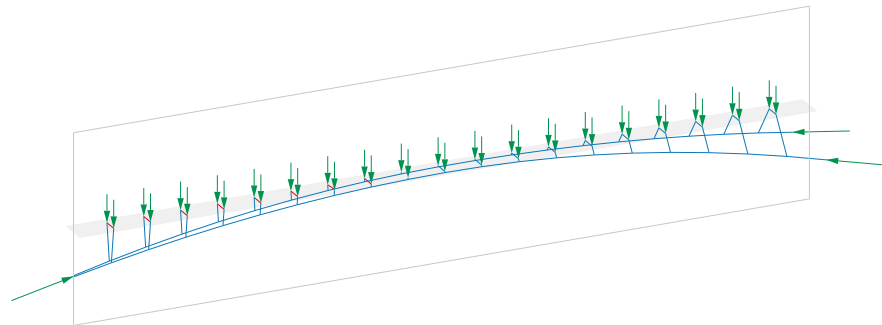
Figure 4.17: Bending-active tensile structure – (a) Restraining forces required to bend the beam into its target equilibrium geometry given that its bending stiffness is constant bending stiffness along their axis; (b) Plane restraining funicular system providing the beam the restraining forces it requires; (c) Spatially unfolded restraining funicular system; (d) Spatial assembly of two arched beams restrained by 3D funiculars with a compressive strut.



(a)



(b)



(c)

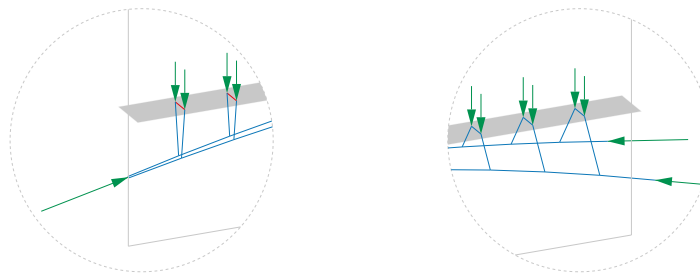


Figure 4.18: Deck arch bridge with three supports – (a) Skewing of a plane columns-arch system; (b) Shift of the two skew sub-systems along skewing direction; (c) Activation of the deck.

4.3 Geometric patterns of restraining cables

In this section, graphical methods have been further explored in order to graphically generate restraining tensile systems able to connect in 3D space several bending-active beams, which are bent in their plane of symmetry, while ensuring their static equilibrium in their 2D target geometry. In particular, several geometric configurations of pre-stressed cables have been established to connect bending-active beams together while applying onto their axes forces which are coplanar with their bending planes.

4.3.1 Condition of equilibrium between the beams and the cables

In a bending-active tensile structure composed of pre-stressed cables and bending-active beams that are bent in their plane of symmetry, the cables must apply onto the beams' axis forces which are coplanar with the beams' bending planes. This is the condition for not generating torsion around the beams' axes and making possible the static equilibrium of the beams in their 2D target geometries.

This translates into the following geometric constraint: at any point of a beam's axis where cables are connected, the cables must be either one, and in this case, the single cable must lie in the beam's bending plane (Figure 4.19(a)), or at least two, and in this case, at least two of the cables must be laid on either side of the beam's bending plane (Figure 4.19(b)). Under this condition, it is possible indeed to decompose the restraining force \mathbf{F}_r acting on the beam's axis into two pre-stressing forces \mathbf{F}_c and \mathbf{F}'_c applied each by one of the two cables, or conversely, it is possible to adjust the prestressing force \mathbf{F}_c and \mathbf{F}'_c in each of the two cables so as to obtain a resultant force in the beam's bending plane:

$$(\mathbf{F}_c + \mathbf{F}'_c) \wedge \mathbf{n} = \mathbf{F}_r \wedge \mathbf{n} = \mathbf{0} \quad (4.5)$$

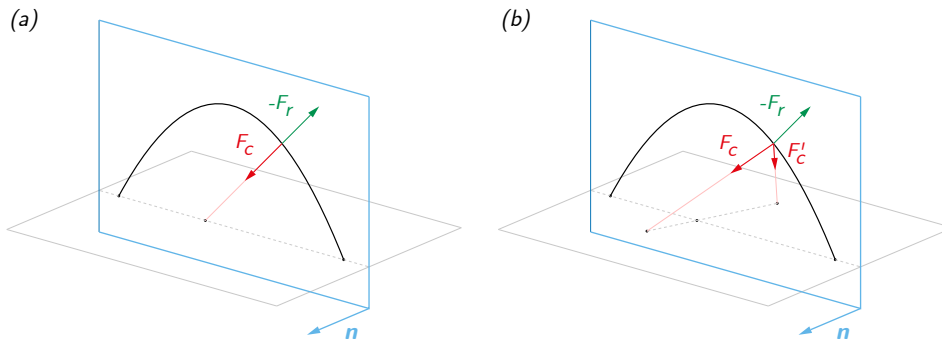


Figure 4.19: Geometric conditions of equilibrium between the beam and the pre-stressed cables.

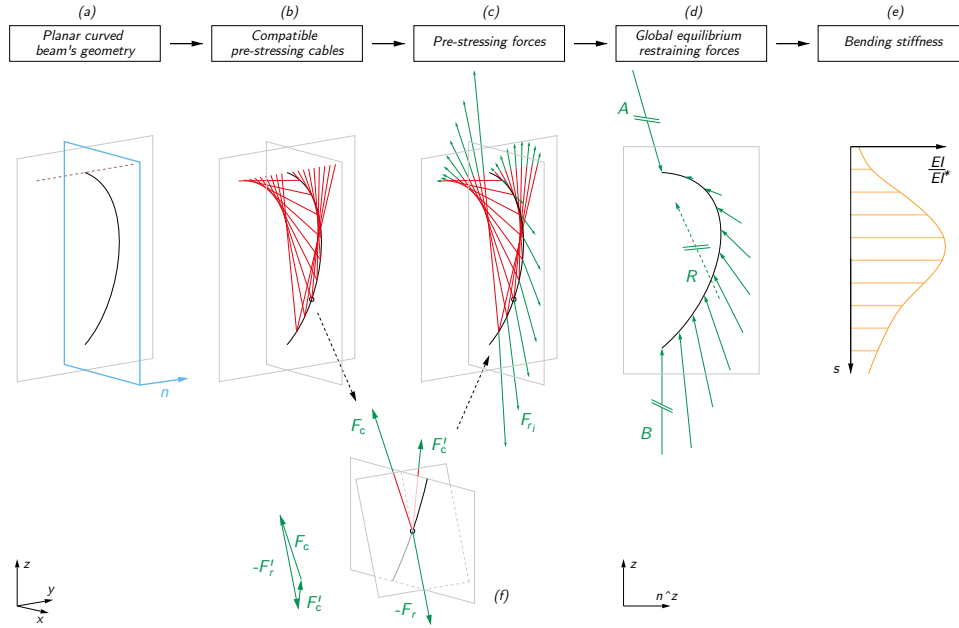


Figure 4.20: Design methodology of a bending-active tensile structure based on open lines of restraining cables.

4.3.2 Lines of cables

A set of n pre-stressed cables assembled end-to-end is considered. They form a line of cables which connects successively several beams to each other while meeting the geometric condition of equilibrium explained in Section 4.3.1. Because the forces applied by the cables on the beams' axis must be in the beams' bending planes, the prestressing force acting in one of the cables of the line determines the distinct prestressing forces in the other cables of the line. As a result, the several restraining forces applied by a line of cables to the various beams it connects cannot be defined independently from each other. For this reason, the design of tensile bending-active structures based on lines of cables follows *Design strategy 1* as defined in Section 4.1 in which the restraining forces applied to the beams' axis are defined first and the beams' bending stiffness is adjusted afterwards. The methodology consists in these steps:

- First, definition of the 2D target equilibrium geometry of the beams as plane continuous curves (Figure 4.20(a));
- Second, definition of the lines of cables meeting the geometric constraint related to the 2D equilibrium of the beams (Section 4.1) (Figure 4.20(b));
- Third, definition of the prestressing forces in the lines of cables (one input prestressing force per line of cables) (Figure 4.20(c));
- Fourth, solving the global equilibrium of the beams considering all the restraining forces applied to them (Figure 4.20(d));

- Fifth, calculating the distribution of bending stiffness along the beams' axis which matches to the beams' target equilibrium geometry and their boundary conditions (Figure 4.20(e)).

Two distinct configurations of lines have to be distinguished. The first situation corresponds to open lines of cables, meaning that the first and last cables of the line are not connected to each other (Figure 4.21(a)). The second situation corresponds to closed line of cables: the first cable is connected end-to-end to the last cable in such a way that the line of cables forms a loop on itself (Figure 4.21(b)).

Open lines of cables In the case of open lines of cables, any geometric configuration of the cables and the beams that satisfies the above geometric condition of 2D equilibrium of the beams is valid. It must, of course, be ensured that the forces applied by the lines of cables on the beams meet the local equilibrium conditions related to the curved geometry of the beams, which are detailed in Section 3.2.2. The design of bending-active tensile structures with open lines of cables follows the above steps and is further detailed in Chapter 5 which presents the design of a façade bending-active tensile structure based on this approach.

Closed lines of cables In the case of closed lines of cables, the first cable and last cable must produce on the beam to which they are connected a resultant force which lies on the beam's bending plane (Figure 4.21(b)). This additional condition implies more specific conditions regarding the relative arrangement of the beams' bending planes and the lines of cables. Different specific spatial configurations that meet this additional condition have been identified. Figure 4.22 shows two different configurations involving a closed line of cables in equilibrium with forces that, two by two, are coplanar.

The first configuration is a closed line of four cables which connects four arbitrary points in 3D space. As shown in Figure 4.22(a) (top), a closed line

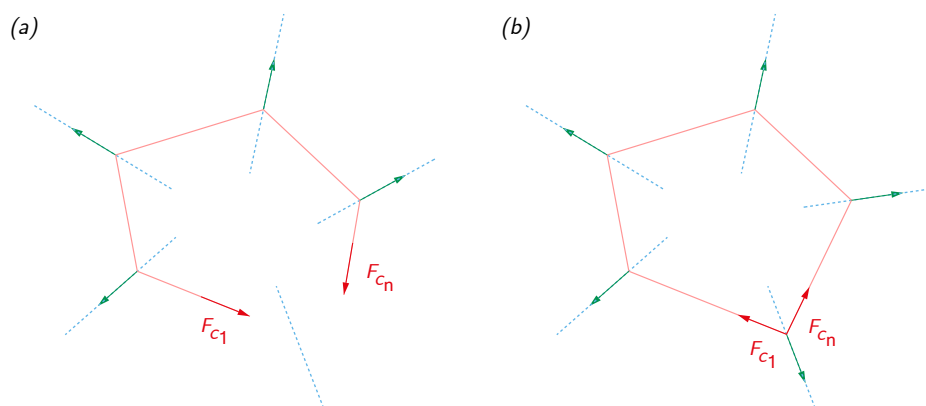


Figure 4.21: Open (a) and closed (b) lines of restraining cables.

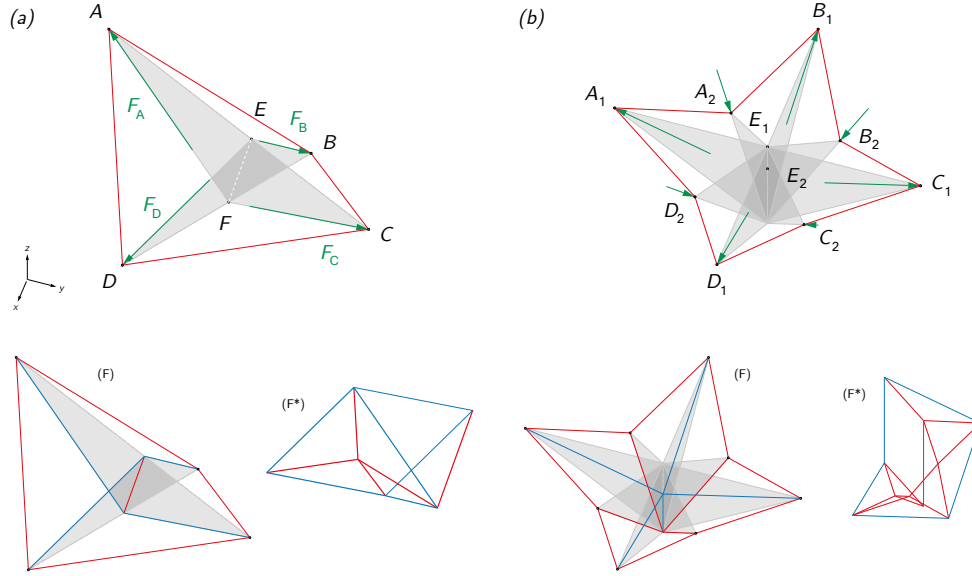


Figure 4.22: Equilibrium of closed lines of 4 and 8 cables with pairs of coplanar forces – (top) Equilibrium of the cables with the coplanar forces and (bottom) corresponding self-stressed structures and their force diagram.

of four cables which connects four points (A, B, C, D) is indeed in equilibrium with two pairs of coplanar forces ($\mathbf{F}_A, \mathbf{F}_C$) and ($\mathbf{F}_B, \mathbf{F}_D$). The orientation and magnitude of forces $\mathbf{F}_A, \mathbf{F}_C, \mathbf{F}_B$ and \mathbf{F}_D depend on the position of the points (E, F), which belong respectively to segments AC and BD . The resultant force of \mathbf{F}_A and \mathbf{F}_C is the reverse of the resultant force of \mathbf{F}_B and \mathbf{F}_D and both resultant forces lie on the same line of action, the line connecting E and F . This allows to build a self-stressed structure as shown in Figure 4.22(a) (bottom).

In particular, this configuration can be applied to a closed line of four cables connecting four points located on the half axes of two beams, which are bent in their respective plane of symmetry and intersected in their central part, as illustrated in Figure 4.23. Given that points E and F are on the intersection of the two beams' bending planes, forces ($\mathbf{F}_A, \mathbf{F}_C$) and ($\mathbf{F}_B, \mathbf{F}_D$) will be in the beams' bending planes. The position of points A and C along respectively the first and the second halves of first beam and the position of points B and D along respectively the first and the second halves of the second beam can be any. This makes the pattern of cables flexible to implement and allows multiple variations of restraining tensile systems in the case of two bending-active beams that intersect as evidenced in Figure 4.23.

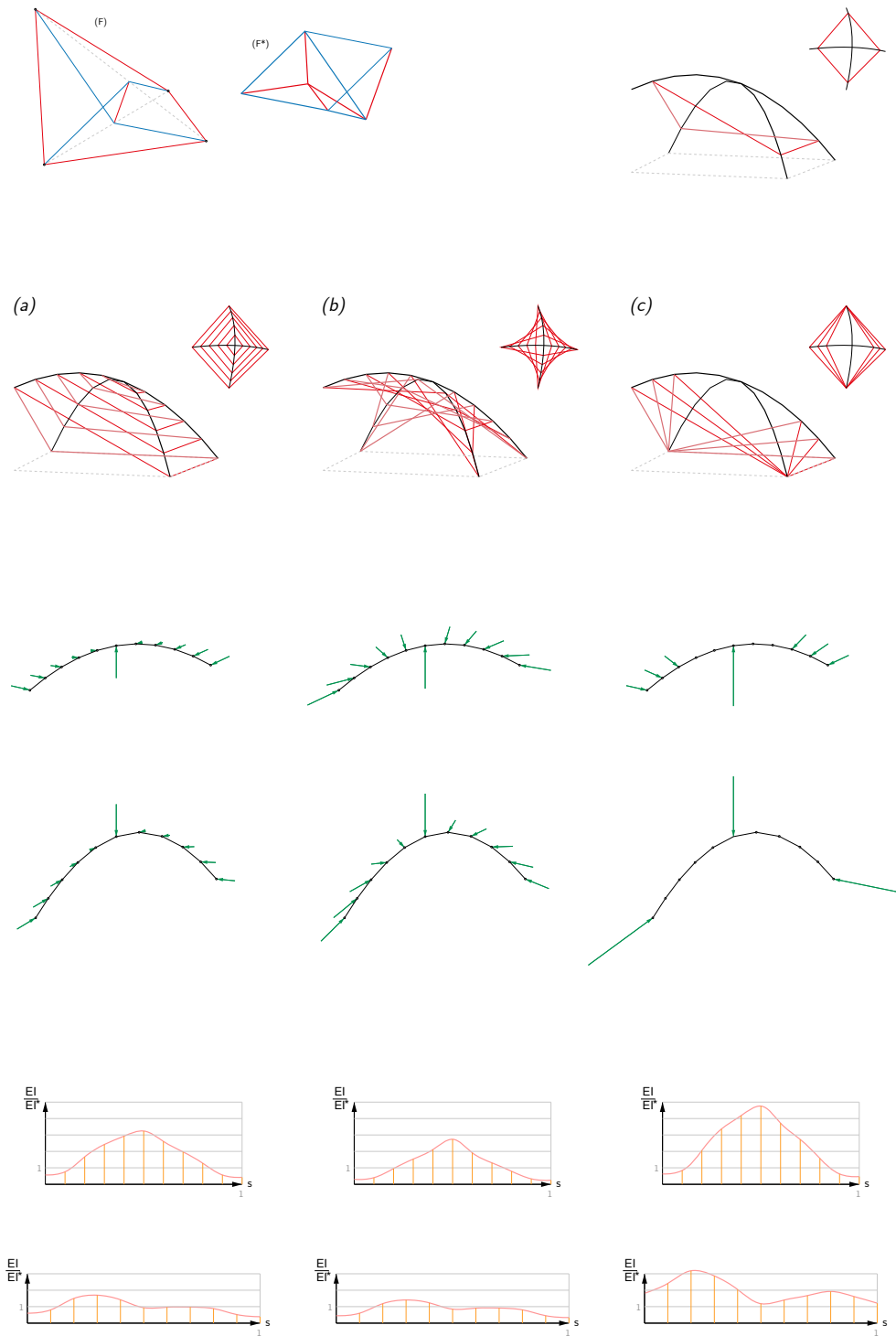


Figure 4.23: Equilibrium of bending-active tensile structures from two intersecting bending-active beams and closed lines of four restraining cables.

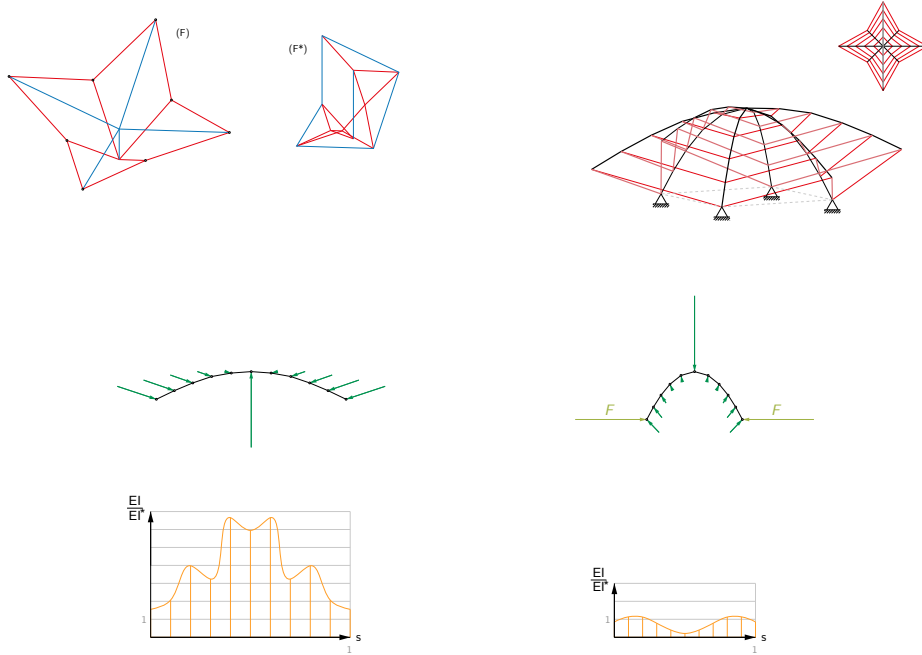


Figure 4.24: Equilibrium of a bending-active tensile structure from four intersecting bending-active beams and closed lines of eight restraining cables

The second configuration (Figure 4.22(b)) considers the case of a closed line of eight cables connecting eight points in 3D space ($A_1, A_2, B_1, B_2, C_1, C_2, D_1, D_2$). These points are the vertices of two squares (A_1, B_1, C_1, D_1) and (A_2, B_2, C_2, D_2) of different sizes, which are oriented at 45 degrees with respect to one another and belong to parallel planes, and whose centres E_1 and E_2 are aligned according to the normal to their plane. The pre-stressing force in each cable of the line is constant and is balanced at each point by a force which is in the plane defined by the point and the squares' centres.

Figure 4.24 shows a structure composed of four beams of two different lengths that intersect in their middle. They are arranged in radial symmetry by alternating the long and short beams. The bending planes of these four beams intersect along a single straight line. The eight-cable line pattern detailed above is used to connect the beams together and apply restraining forces to them. Five lines of chains are defined and the constant pre-stressing force in each of them is set. Globally, for each beam, the restraining forces applied by the cables are in equilibrium. However, for the short beams, the restraining forces are not compatible with the curvature of their target equilibrium geometry and additional forces are added at the ends of the short beams in the form of either a closed line of four cables or fixed supports to reach the local condition of equilibrium of the beams. Once the external forces acting on the beams are compatible with their global and local equilibrium, the bending stiffness along the beams' axis is calculated.

4.4 Form-finding of restraining cable nets

In this Section a non-linear formulation of the force density method is proposed to form-found cable nets compatible with the equilibrium of bending-active beams which are bent in their plane of symmetry. The content of this Section has been published in (Boulic and Schwartz 2018).

4.4.1 Force density method

The force density method is a numerical method for the form-finding of general pin-jointed network structures, which was developed by Schek (Schek 1974). It is based upon the introduction, for each of the network's branches, of the force-length ratio, which is referred to as the force density. The assumption that the force densities remain constant during the form-finding process makes it possible to linearise the geometrically non-linear equations of static equilibrium that rule general network structures, and thus solving them directly in one go.

In particular, the force density method allows to form-find pin-jointed network structures based on the network's topology, nodal loads, force densities, and fixed supporting nodes. In the linear formulation of the method, the coordinates of the network's free nodes are linearly calculated from the force density vector, the position of the network's fixed supporting nodes, the network's connectivity matrix and the nodal loads (Figure 4.25).

Similar to graphic statics, the force density method is a geometric stiffness method which only involves geometric parameters in the equilibrium definition of a structure, the way how the structure is materialised has not an explicit influence on the equilibrium definition. In particular, according to the linearised governing equations, the equilibrium position of a free node of the network corresponds to the barycentre position of its adjacent nodes weighted by the force density of the connecting branches (Figure 4.26). From this point of view, the existence

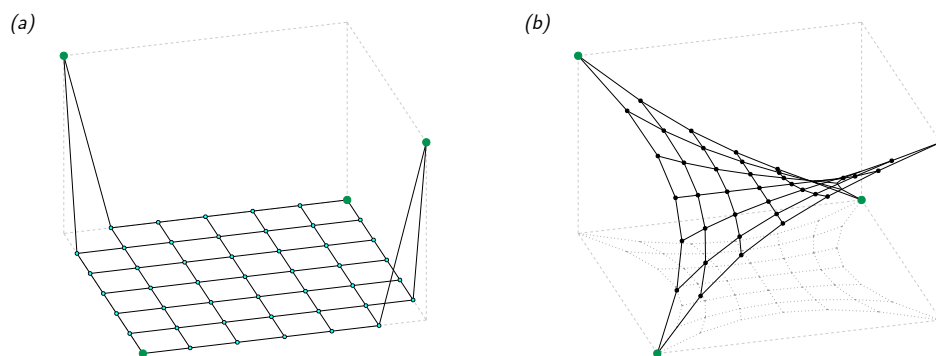


Figure 4.25: Form-finding of a cable net with the force density method – (a) Arbitrary initial configuration of the net prior to form-finding; (b) Equilibrium configuration of the cable net after form-finding. Green dots are fixed nodes while black dots are free nodes.

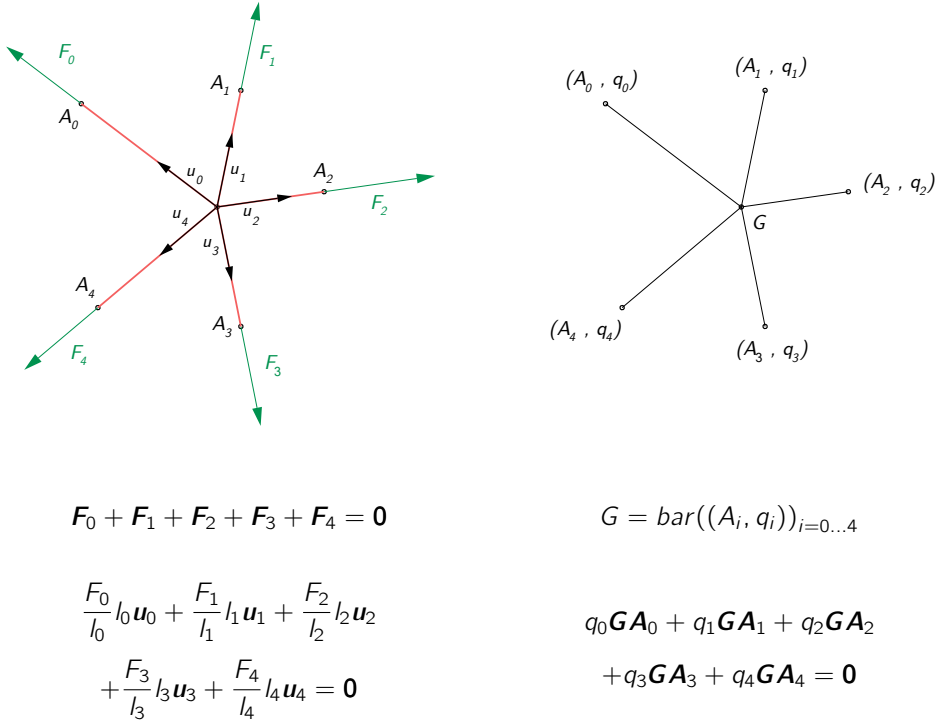


Figure 4.26: Equilibrium position of a single node within a pin-jointed network – (a) Equilibrium of branch forces acting on one free node; (b) Barycentre of adjacent nodes weighted by the force density of the connecting branches.

of a solution to the equations is assured as long as the branches of the network have all a positive force density or all a negative force density. In this case, in the network's equilibrium configuration, the free nodes remain in the convex hull defined by the fixed nodes.

Form-finding networks under additional given constraints necessitates to extend the original linear formulation of the method to a non-linear formulation, meaning that, on top of the regular equilibrium equations, additional constraints have to be satisfied. For that purpose, a new force density vector, which fulfils these additional constraints, is searched for, based on an iterative minimisation process. Such additional constraints can consist for instance in imposing the length of a branch (Schek 1974), constraining a free node of the network to a given plane, line or point (Lachauer and Block 2014), or imposing the intensity of the reaction force at a fixed node (Malerba et al. 2012). In the case of the form-finding of cable nets compatible with the equilibrium of bending-active beams which are bent in their plane of symmetry, the nodes of the cable nets which are connected to the beams are fixed nodes of the networks, and the reaction forces at these fixed nodes need to be constrained to the beams' bending planes or to prescribed restraining forces, coplanar with these planes.

The following paragraphs introduce further the linear formulation of the force density method and present two non-linear formulations of the force density method for the form-finding of cable nets with constraints onto the reaction forces at some fixed nodes.

Linear formulation of the force density method For a detailed description of the method, one can refer to (Schek 1974). Here, the general notations are introduced and the equations are shown. For a given network composed of n_s nodes (n free nodes and n_f fixed nodes) connected by m branches, the following matrices and vectors can be defined:

- \mathbf{C}_s , $[m \times n_s]$, connectivity matrix (also called branch-node matrix) describing the topology of the net. If branch k connects node i to node j , then $\mathbf{C}_s(k, i)$ equals 1 and $\mathbf{C}_s(k, j)$ equals -1 ; all other elements of \mathbf{C}_s are 0. \mathbf{C}_s can be portioned into two matrices: \mathbf{C} , $[m \times n]$, connectivity matrix of the free nodes, and \mathbf{C}_f , $[m \times n_f]$, connectivity matrix of the fixed nodes;
- \mathbf{x}_s , \mathbf{y}_s , \mathbf{z}_s , $[n_s \times 1]$, coordinates of the nodes projected along the usual orthonormal coordinate system $(\mathbf{e}_x, \mathbf{e}_y, \mathbf{e}_z)$, and its sub-vectors \mathbf{x} , \mathbf{y} , \mathbf{z} , $[n \times 1]$, coordinates of the free nodes, and \mathbf{x}_f , \mathbf{y}_f , \mathbf{z}_f , $[n_f \times 1]$, coordinates of the fixed nodes;
- \mathbf{f}_x , \mathbf{f}_y , \mathbf{f}_z , $[n \times 1]$, nodal loads projected respectively along \mathbf{e}_x , \mathbf{e}_y , \mathbf{e}_z ;
- \mathbf{r}_x , \mathbf{r}_y , \mathbf{r}_z , $[n_f \times 1]$, reactions forces at the fixed nodes projected respectively along \mathbf{e}_x , \mathbf{e}_y , \mathbf{e}_z ;
- \mathbf{l} , $[m \times 1]$, length of the branches, $\mathbf{L} = \text{diag}(\mathbf{l})$;
- \mathbf{t} , $[m \times 1]$, forces in the branches;
- $\mathbf{u} = \mathbf{C}_s \mathbf{x}_s$, $\mathbf{v} = \mathbf{C}_s \mathbf{y}_s$, $\mathbf{w} = \mathbf{C}_s \mathbf{z}_s$, $[m \times 1]$, coordinate differences per branch;
- $\mathbf{U} = \text{diag}(\mathbf{u})$, $\mathbf{V} = \text{diag}(\mathbf{v})$, $\mathbf{W} = \text{diag}(\mathbf{w})$;
- $\mathbf{q} = \mathbf{L}^{-1} \mathbf{t}$, $[m \times 1]$, force density of the branches, $\mathbf{Q} = \text{diag}(\mathbf{q})$;
- $\mathbf{D} = \mathbf{C}^T \mathbf{Q} \mathbf{C}$ and $\mathbf{D}_f = \mathbf{C}_f^T \mathbf{Q} \mathbf{C}_f$.

It results from the partition of the matrix \mathbf{C}_s that:

$$\mathbf{u} = \mathbf{C}_s \mathbf{x}_s + \mathbf{C}_f \mathbf{x}_f, \quad \mathbf{v} = \mathbf{C}_s \mathbf{y}_s + \mathbf{C}_f \mathbf{y}_f, \quad \mathbf{w} = \mathbf{C}_s \mathbf{z}_s + \mathbf{C}_f \mathbf{z}_f \quad (4.6)$$

The $3n_s$ equilibrium equations can be expressed by the following system:

$$\mathbf{f}_x = \mathbf{C}^T \mathbf{U} \mathbf{L}^{-1} \mathbf{t}, \quad \mathbf{f}_y = \mathbf{C}^T \mathbf{V} \mathbf{L}^{-1} \mathbf{t}, \quad \mathbf{f}_z = \mathbf{C}^T \mathbf{W} \mathbf{L}^{-1} \mathbf{t} \quad (4.7)$$

By introducing the matrices $\mathbf{D} = \mathbf{C}^T \mathbf{Q} \mathbf{C}$ and $\mathbf{D}_f = \mathbf{C}_f^T \mathbf{Q} \mathbf{C}_f$, and by combining equations 4.6 and 4.7, the system of equilibrium equations becomes:

$$\mathbf{D} \mathbf{x} = \mathbf{f}_x - \mathbf{D}_f \mathbf{x}_f, \quad \mathbf{D} \mathbf{y} = \mathbf{f}_y - \mathbf{D}_f \mathbf{y}_f, \quad \mathbf{D} \mathbf{z} = \mathbf{f}_z - \mathbf{D}_f \mathbf{z}_f \quad (4.8)$$

whose solution is:

$$\mathbf{x} = \mathbf{D}^{-1}(\mathbf{f}_x - \mathbf{D}_f \mathbf{x}_f), \quad \mathbf{y} = \mathbf{D}^{-1}(\mathbf{f}_y - \mathbf{D}_f \mathbf{y}_f), \quad \mathbf{z} = \mathbf{D}^{-1}(\mathbf{f}_z - \mathbf{D}_f \mathbf{z}_f) \quad (4.9)$$

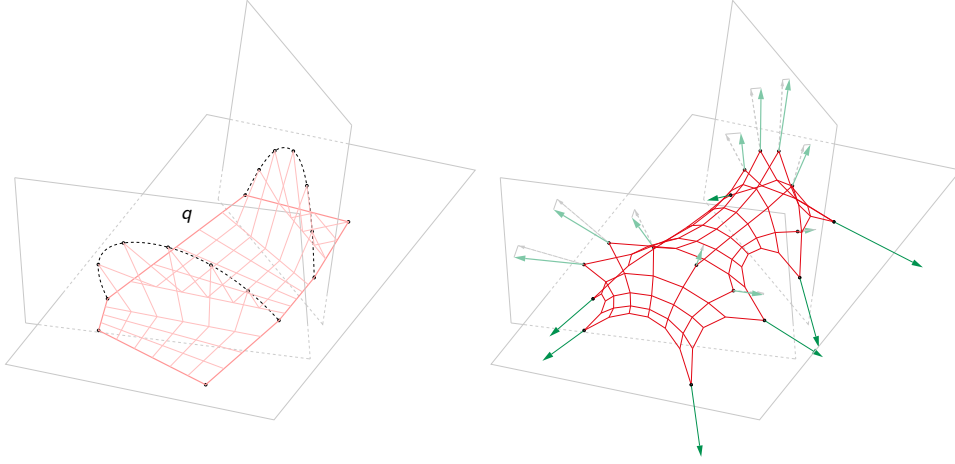


Figure 4.27: Linear formulation of the force density method – Form-finding of a cable net based on its topology, the vector \mathbf{q} of the force density of its branches and the fixed position of the support nodes. The reaction forces of the cable net at the beams' nodes are not coplanar with the beams' bending planes.

Non-linear formulation of the force density method In the extension of the force density method to the form-finding of network under constraints, the additional constraints which have to be fulfilled by the network have to be formulated in the form of a general equation:

$$\mathbf{g}(\mathbf{x}(\mathbf{q}), \mathbf{y}(\mathbf{q}), \mathbf{z}(\mathbf{q}), \mathbf{q}) = \mathbf{0} \quad (4.10)$$

The function \mathbf{g} is referred to as the objective function. The vector \mathbf{q} that solutions equation 4.10, is iteratively searched for following the Newton method. For that, an initial force density vector $\mathbf{q}^{(0)}$ is chosen and a vector $\Delta\mathbf{q}$ satisfying the following linearised condition is searched for:

$$\mathbf{g}(\mathbf{q}^{(0)}) + \frac{\partial \mathbf{g}(\mathbf{q}^{(0)})}{\partial \mathbf{q}} \Delta\mathbf{q} = \mathbf{0} \quad (4.11)$$

By introducing the matrix \mathbf{G} and the vector $\boldsymbol{\rho}$ as:

$$\mathbf{G}^T = \frac{\partial \mathbf{g}(\mathbf{q}^{(0)})}{\partial \mathbf{q}} \quad \text{and} \quad \boldsymbol{\rho} = -\mathbf{g}(\mathbf{q}^{(0)}) \quad (4.12)$$

equation 4.11 becomes:

$$\mathbf{G}^T \Delta\mathbf{q} = \boldsymbol{\rho} \quad (4.13)$$

Equation 4.13 is underdetermined and admits an infinite number of solutions. Among these solutions, the solution $\Delta\mathbf{q}$ which has the minimum norm is searched for (Schek 1974, Malerba et al. 2012). It is given by the equation:

$$\Delta\mathbf{q} = \mathbf{G}(\mathbf{G}^T \mathbf{G})^{-1} \boldsymbol{\rho} \quad (4.14)$$

The vector $\Delta\mathbf{q}$ is then used to define a new density vector $\mathbf{q}^{(k+1)}$

$$\mathbf{q}^{(k+1)} = \mathbf{q}^{(k)} + \Delta\mathbf{q} \quad (4.15)$$

and the method is iterated until $|\Delta\mathbf{q}| < \epsilon$.

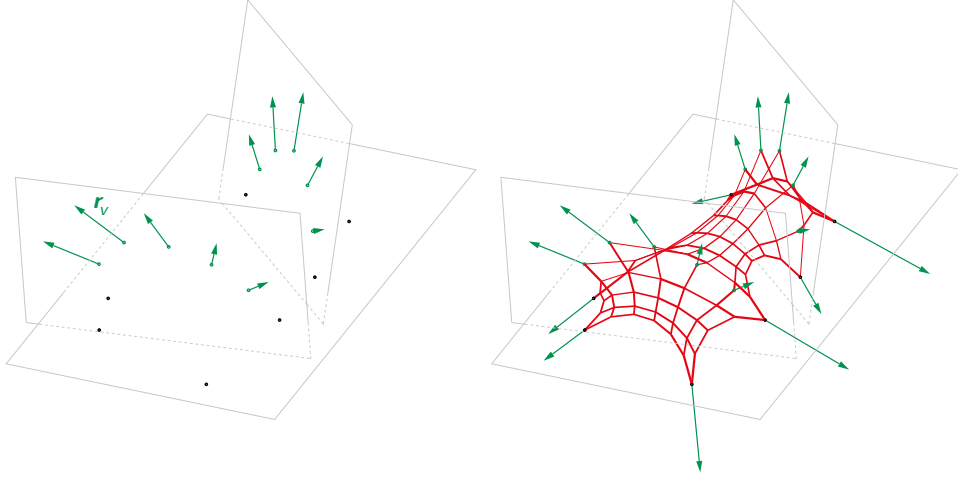


Figure 4.28: Non-linear formulation of force density method with reaction forces constrained to given vectors – Form-finding of a cable net with reaction forces at some fixed nodes constrained to given vectors. The thickness of the cable net branches is proportional to their force density, which illustrates the redistribution of force density within the network.

4.4.2 Constraining reaction forces of a cable net

Constraining reaction forces to given vectors Extending the force density method to the form-finding of network structures with prescribed reactions forces (Figure 4.28) has been proposed by (Malerba et al. 2012). The corresponding equations are:

$$g_x = \bar{C}_f^T U q - r_{vx} = 0 \quad (4.16)$$

$$g_y = \bar{C}_f^T V q - r_{vy} = 0 \quad (4.17)$$

$$g_z = \bar{C}_f^T W q - r_{vz} = 0 \quad (4.18)$$

where r_{vx} , r_{vy} and r_{vz} are the prescribed reactions forces at the constrained fixed nodes projected respectively along e_x , e_y and e_z .

The Jacobian matrixes of the objective functions are given by:

$$G_x^T = \bar{C}_f^T U - \bar{C}_f^T Q C D^{-1} C^T U \quad (4.19)$$

$$G_y^T = \bar{C}_f^T V - \bar{C}_f^T Q C D^{-1} C^T V \quad (4.20)$$

$$G_z^T = \bar{C}_f^T W - \bar{C}_f^T Q C D^{-1} C^T W \quad (4.21)$$

Finally, the vector Δq can be calculated from:

$$\Delta q = -G(G^T G)^{-1} g(q) \quad (4.22)$$

with:

$$G = \begin{bmatrix} G_x & G_y & G_z \end{bmatrix} \quad \text{and} \quad g = \begin{bmatrix} g_x \\ g_y \\ g_z \end{bmatrix} \quad (4.23)$$

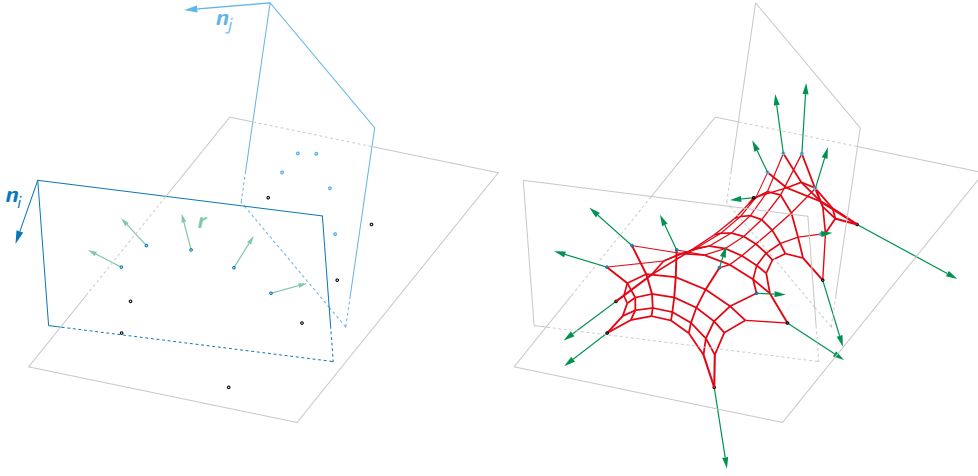


Figure 4.29: Non-linear formulation of force density method with reaction forces constrained to given planes – Form-finding of a cable net with reaction forces at some fixed nodes constrained to given planes. Thickness of the cable branches proportional to their force density illustrating the redistribution of force density within the network.

Constraining reaction forces to given planes The reaction forces $\mathbf{r} = (r_x, r_y, r_z)$ at the network's fixed nodes satisfy the equilibrium equations:

$$\mathbf{r}_x = \mathbf{C}^T \mathbf{U} \mathbf{L}^{-1} \mathbf{t}, \quad \mathbf{r}_y = \mathbf{C}^T \mathbf{V} \mathbf{L}^{-1} \mathbf{t}, \quad \mathbf{r}_z = \mathbf{C}^T \mathbf{W} \mathbf{L}^{-1} \mathbf{t} \quad (4.24)$$

It is supposed that the reaction forces of a set of p_i fixed nodes are constrained to be in the plane π_i , which is defined by its normal $\mathbf{n}_i = (n_{ix}, n_{iy}, n_{iz})$. Being $\bar{\mathbf{r}}_{ix}$, $\bar{\mathbf{r}}_{iy}$, $\bar{\mathbf{r}}_{iz}$ the sub-vectors of the reaction forces at the p_i nodes along \mathbf{e}_x , \mathbf{e}_y and \mathbf{e}_z , the coplanarity condition takes the form of the following equation:

$$\mathbf{g}_i = n_{ix} \mathbf{I}_{p_i} \bar{\mathbf{r}}_{ix} + n_{iy} \mathbf{I}_{p_i} \bar{\mathbf{r}}_{iy} + n_{iz} \mathbf{I}_{p_i} \bar{\mathbf{r}}_{iz} = \mathbf{0} \quad (4.25)$$

Considering r similar conditions, the reactions forces of the p_i nodes ($i \in \langle 1, r \rangle$) of r sets of points are assumed to be constrained to r different planes. Additionally, it is assumed that the r sets of p_i constrained points ($i \in \langle 1, r \rangle$) are mutually disjointed and that $\sum_i p_i = n_c \leq n_f$. By introducing the diagonal matrices \mathbf{N}_x , \mathbf{N}_y , \mathbf{N}_z , $[n_c \times n_c]$, and the sub-vectors $\bar{\mathbf{r}}_x$, $\bar{\mathbf{r}}_y$, $\bar{\mathbf{r}}_z$, $[n_c \times 1]$, of the reactions forces of the n_c constrained fixed nodes, all the coplanarity conditions can be written in the general form:

$$\mathbf{g}(\mathbf{x}(\mathbf{q}), \mathbf{y}(\mathbf{q}), \mathbf{z}(\mathbf{q}), \mathbf{q}) = \mathbf{N}_x \bar{\mathbf{r}}_x + \mathbf{N}_y \bar{\mathbf{r}}_y + \mathbf{N}_z \bar{\mathbf{r}}_z = \mathbf{0} \quad (4.26)$$

where:

$$\bar{\mathbf{r}}_x = \bar{\mathbf{C}}_f^T \mathbf{U} \mathbf{q}, \quad \bar{\mathbf{r}}_y = \bar{\mathbf{C}}_f^T \mathbf{V} \mathbf{q}, \quad \bar{\mathbf{r}}_z = \bar{\mathbf{C}}_f^T \mathbf{W} \mathbf{q} \quad (4.27)$$

The Jacobian matrix \mathbf{G} of \mathbf{g} is given by:

$$\mathbf{G}^T = \frac{\partial \mathbf{g}}{\partial \mathbf{q}} = \frac{\partial \mathbf{g}}{\partial \mathbf{x}} \frac{\partial \mathbf{x}}{\partial \mathbf{q}} + \frac{\partial \mathbf{g}}{\partial \mathbf{y}} \frac{\partial \mathbf{y}}{\partial \mathbf{q}} + \frac{\partial \mathbf{g}}{\partial \mathbf{z}} \frac{\partial \mathbf{z}}{\partial \mathbf{q}} + \frac{\partial \mathbf{g}}{\partial \mathbf{q}} \quad (4.28)$$

It is shown in (Malerba et al. 2012) that:

$$\frac{\partial \mathbf{x}}{\partial \mathbf{q}} = -\mathbf{D}^{-1} \mathbf{C}^T \mathbf{U}, \quad \frac{\partial \mathbf{y}}{\partial \mathbf{q}} = -\mathbf{D}^{-1} \mathbf{C}^T \mathbf{V}, \quad \frac{\partial \mathbf{z}}{\partial \mathbf{q}} = -\mathbf{D}^{-1} \mathbf{C}^T \mathbf{W} \quad (4.29)$$

Besides, the partial derivatives of \mathbf{g} regarding \mathbf{x} , \mathbf{y} and \mathbf{z} are:

$$\frac{\partial \mathbf{g}}{\partial \mathbf{x}} = \mathbf{N}_x \bar{\mathbf{C}}_f^T \mathbf{Q} \mathbf{C}, \quad \frac{\partial \mathbf{g}}{\partial \mathbf{y}} = \mathbf{N}_y \bar{\mathbf{C}}_f^T \mathbf{Q} \mathbf{C}, \quad \frac{\partial \mathbf{g}}{\partial \mathbf{z}} = \mathbf{N}_z \bar{\mathbf{C}}_f^T \mathbf{Q} \mathbf{C} \quad (4.30)$$

This comes from:

$$\begin{aligned} \frac{\partial \bar{\mathbf{r}}_x}{\partial \mathbf{x}} &= \frac{\partial}{\partial \mathbf{x}} (\bar{\mathbf{C}}_f^T \mathbf{U} \mathbf{L}^{-1} \mathbf{t}) = \bar{\mathbf{C}}_f^T \frac{\partial}{\partial \mathbf{x}} (\mathbf{U} \mathbf{L}^{-1} \mathbf{t}) = \bar{\mathbf{C}}_f^T \frac{\partial}{\partial \mathbf{x}} (\mathbf{U} \mathbf{q}) \\ &= \bar{\mathbf{C}}_f^T \frac{\partial}{\partial \mathbf{x}} (\mathbf{Q} \mathbf{u}) = \bar{\mathbf{C}}_f^T \mathbf{Q} \frac{\partial}{\partial \mathbf{x}} (\mathbf{u}) = \bar{\mathbf{C}}_f^T \mathbf{Q} \mathbf{C} \end{aligned} \quad (4.31)$$

and:

$$\begin{aligned} \frac{\partial \bar{\mathbf{r}}_y}{\partial \mathbf{x}} &= \frac{\partial}{\partial \mathbf{x}} (\bar{\mathbf{C}}_f^T \mathbf{V} \mathbf{L}^{-1} \mathbf{t}) = \bar{\mathbf{C}}_f^T \frac{\partial}{\partial \mathbf{x}} (\mathbf{V} \mathbf{L}^{-1} \mathbf{t}) = \bar{\mathbf{C}}_f^T \frac{\partial}{\partial \mathbf{x}} (\mathbf{V} \mathbf{q}) \\ &= \bar{\mathbf{C}}_f^T \frac{\partial}{\partial \mathbf{x}} (\mathbf{Q} \mathbf{v}) = \bar{\mathbf{C}}_f^T \mathbf{Q} \frac{\partial}{\partial \mathbf{x}} (\mathbf{v}) = 0 \end{aligned} \quad (4.32)$$

And similarly:

$$\frac{\partial \bar{\mathbf{r}}_y}{\partial \mathbf{y}} = \bar{\mathbf{C}}_f^T \mathbf{Q} \mathbf{C} \text{ and } \frac{\partial \bar{\mathbf{r}}_z}{\partial \mathbf{z}} = \bar{\mathbf{C}}_f^T \mathbf{Q} \mathbf{C} \quad (4.33)$$

and:

$$\frac{\partial \bar{\mathbf{r}}_y}{\partial \mathbf{z}} = 0, \quad \frac{\partial \bar{\mathbf{r}}_x}{\partial \mathbf{y}} = 0, \quad \frac{\partial \bar{\mathbf{r}}_x}{\partial \mathbf{z}} = 0, \quad \frac{\partial \bar{\mathbf{r}}_z}{\partial \mathbf{x}} = 0, \quad \frac{\partial \bar{\mathbf{r}}_z}{\partial \mathbf{y}} = 0 \quad (4.34)$$

The last term of the Jacobian matrix is given by:

$$\frac{\partial \mathbf{g}}{\partial \mathbf{q}} = \mathbf{N}_x \frac{\partial \bar{\mathbf{r}}_x}{\partial \mathbf{q}} + \mathbf{N}_y \frac{\partial \bar{\mathbf{r}}_y}{\partial \mathbf{q}} + \mathbf{N}_z \frac{\partial \bar{\mathbf{r}}_z}{\partial \mathbf{q}} = \mathbf{N}_x \bar{\mathbf{C}}_f^T \mathbf{U} + \mathbf{N}_y \bar{\mathbf{C}}_f^T \mathbf{V} + \mathbf{N}_z \bar{\mathbf{C}}_f^T \mathbf{W} \quad (4.35)$$

Finally, the Jacobian matrix can be expressed as follows:

$$\begin{aligned} \mathbf{G}^T &= \mathbf{N}_x \bar{\mathbf{C}}_f^T \mathbf{U} + \mathbf{N}_y \bar{\mathbf{C}}_f^T \mathbf{V} + \mathbf{N}_z \bar{\mathbf{C}}_f^T \mathbf{W} \\ &\quad - \mathbf{N}_x \bar{\mathbf{C}}_f^T \mathbf{Q} \mathbf{C} \mathbf{D}^{-1} \mathbf{C}^T \mathbf{U} - \mathbf{N}_y \bar{\mathbf{C}}_f^T \mathbf{Q} \mathbf{C} \mathbf{D}^{-1} \mathbf{C}^T \mathbf{V} - \mathbf{N}_z \bar{\mathbf{C}}_f^T \mathbf{Q} \mathbf{C} \mathbf{D}^{-1} \mathbf{C}^T \mathbf{W} \end{aligned} \quad (4.36)$$

The vector $\boldsymbol{\rho}$ can be calculated :

$$\begin{aligned} \boldsymbol{\rho} &= -\mathbf{q}(\mathbf{q}) = \mathbf{N}_x \bar{\mathbf{r}}_x + \mathbf{N}_y \bar{\mathbf{r}}_y + \mathbf{N}_z \bar{\mathbf{r}}_z \\ &= \mathbf{N}_x \bar{\mathbf{C}}_f^T \mathbf{U} \mathbf{q} + \mathbf{N}_y \bar{\mathbf{C}}_f^T \mathbf{V} \mathbf{q} + \mathbf{N}_z \bar{\mathbf{C}}_f^T \mathbf{W} \mathbf{q} \end{aligned} \quad (4.37)$$

as well as the vector $\Delta \mathbf{q}$:

$$\Delta \mathbf{q} = \mathbf{G}(\mathbf{G}^T \mathbf{G})^{-1} (\mathbf{N}_x \bar{\mathbf{C}}_f^T \mathbf{U} \mathbf{q} + \mathbf{N}_y \bar{\mathbf{C}}_f^T \mathbf{V} \mathbf{q} + \mathbf{N}_z \bar{\mathbf{C}}_f^T \mathbf{W} \mathbf{q}) \quad (4.38)$$

4.4.3 Design examples

Three bending-active tensile structures have been developed as examples to illustrate how the constrained force density method for the generation of compatible cable nets is combined to the form-driven design approach and what are the design possibilities it offers.

Vaulted structure The first example illustrates the two different strategies of implementation of the form-driven approach presented in Section 4.1: *Design strategy 1* – Equilibrium of the bending-active beams through an adapted bending stiffness, which is associated with the force density method with constraints on the forces applied by the cable net to the beams to prescribed planes, and *Design strategy 2* – Equilibrium of the bending-active beams through restraining forces, which is associated with the force density method with constraints on the forces applied by the cable net to the beams to prescribed vectors. Starting from the same target equilibrium geometry of two bending-active arched beams, two distinct bending-active tensile structures are designed following each of the two strategies. Figure 4.30 details for each of the two strategies the successive design steps and the final result. In addition to sharing the same target equilibrium geometry of the two beams, the two structures have in common a cable net with same topology and fixed points. On the contrary, the two cable nets which are form-found with the force density method under constraints have a different equilibrium geometry, the forces in the beams are different as well as the beams' bending stiffness. In both strategies, certain parameters can be adjusted in order to generate design variations while keeping the equilibrium geometry of the beams unchanged: the initial force density vector to start the iterative search of the non-linear solution of the cable net, the reactions forces at the beams' supports, the amount of the pre-stressing force in the beams, the beams' bending stiffness and the lines of action of the restraining forces in *Design strategy 2*.

Structure with six cantilevering beams The second design example implements the form-driven design approach through *Design strategy 1*, in which the equilibrium of the beams in their target geometry is achieved through an adapted bending stiffness. The bending-active tensile structure consists of six beams radially clamped in the ground at one of their ends and support for a wrapping prestressing cable net pulled in its centre downward (Figure 4.31). In turn, the cable net bends the beams in their planes of symmetry towards the centre of the structure. The beams have a non-constant bending-stiffness which is adjusted in order to match the target equilibrium geometry of the beams under the restraining forces which are applied to them by a cable net form-found with the force density method under the constraint that the restraining forces are coplanar with the plane of the beams. Once the cable net with restraining forces coplanar with the beams' planes has been form-found, each beam' bending stiff-

ness is calculated. It has to be checked that the restraining forces transferred by the cable net to the beams fulfil the local and global conditions of equilibrium discussed in Section 3.2.2. If not the case, the initial force density vector, the topology of the cable net, the target equilibrium geometry of the beams, and the boundary conditions of the structure might be iteratively adjusted in order to reach a possible state of equilibrium.

Structure with two arched beams The third structure consists in a prestressed cable net supported by two bending-active arched beams (Figure 4.32). The design of this tent-like structure was carried out according to *Design strategy 2*, in which the equilibrium of the bending-active beams in their target geometry is achieved through appropriate restraining forces. The beams' bending stiffness, which is considered as constant along their axis, constitutes an initial input of the design as well as the equilibrium geometry of the arched beams. The additional restraining forces required to bring the beams into equilibrium in the desired geometry in relation to an initial set of loads at the beams' supports is calculated. As demonstrated in Section 3.3.1, the lines of action of the restraining forces can be adjusted by the designer. Finally, as its topology and the fixed position of its supports are defined, the geometry of the cable net is generated through a constrained force density method where the prestressing forces applied by the cable net to the beams' axis are constrained to the reverse of the restraining forces required for the equilibrium of the beams.

The form-finding of such a cable net with a non-linear formulation of the force density method is initiated from a linear solution, calculated itself from an initial force density vector of the cable net's branches. Two variations of the cable net have been produced to show the impact of the initial force density vector onto the equilibrium geometry of the cable net, and how the force densities are redistributed within the cable net branches in order to meet the imposed constraints. Eventually, it is illustrated through these two variations how different cable nets can be explored while keeping unchanged the equilibrium geometry of the beams.

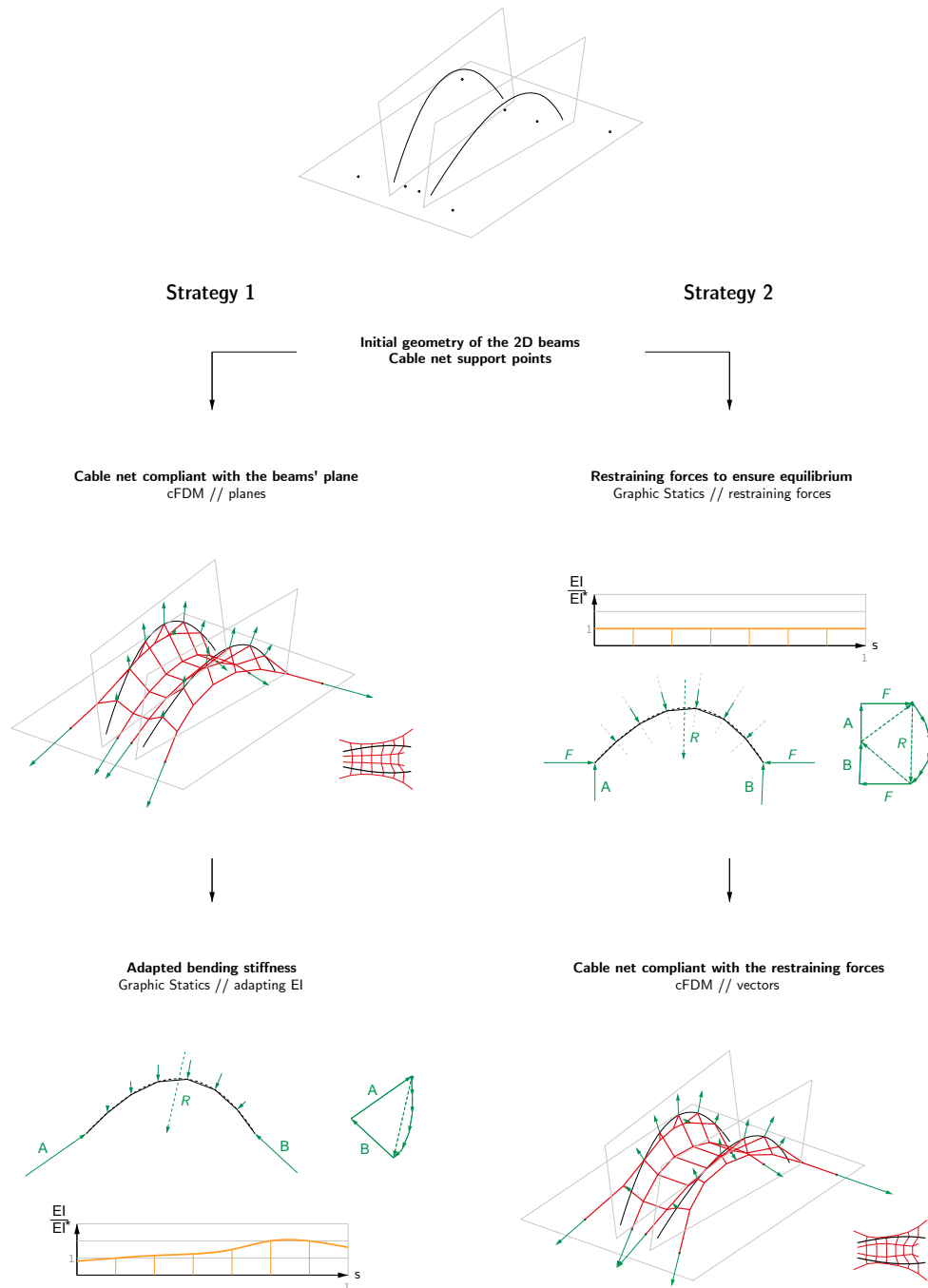


Figure 4.30: Design of a vaulted structure following each of the two possible form-driven design strategies.

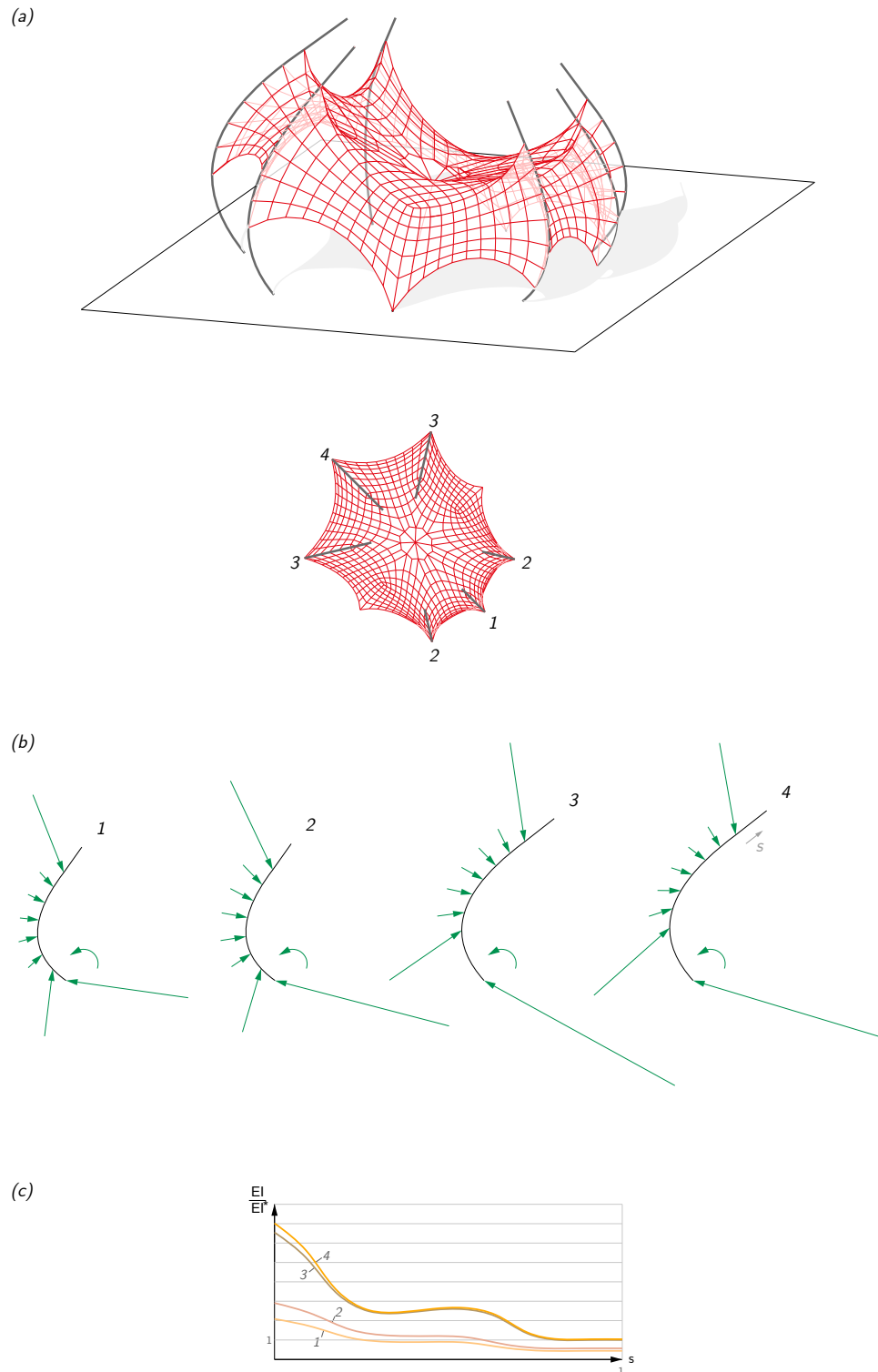


Figure 4.31: Bending-active tensile structure with six cantilevering beams – (a) Axonometric and top view of the beams and the form-found cable net (restraining forces constrained to planes); (b) Forces acting on the beams; (c) Distribution of the cross sectional bending stiffness along the beams' axis.

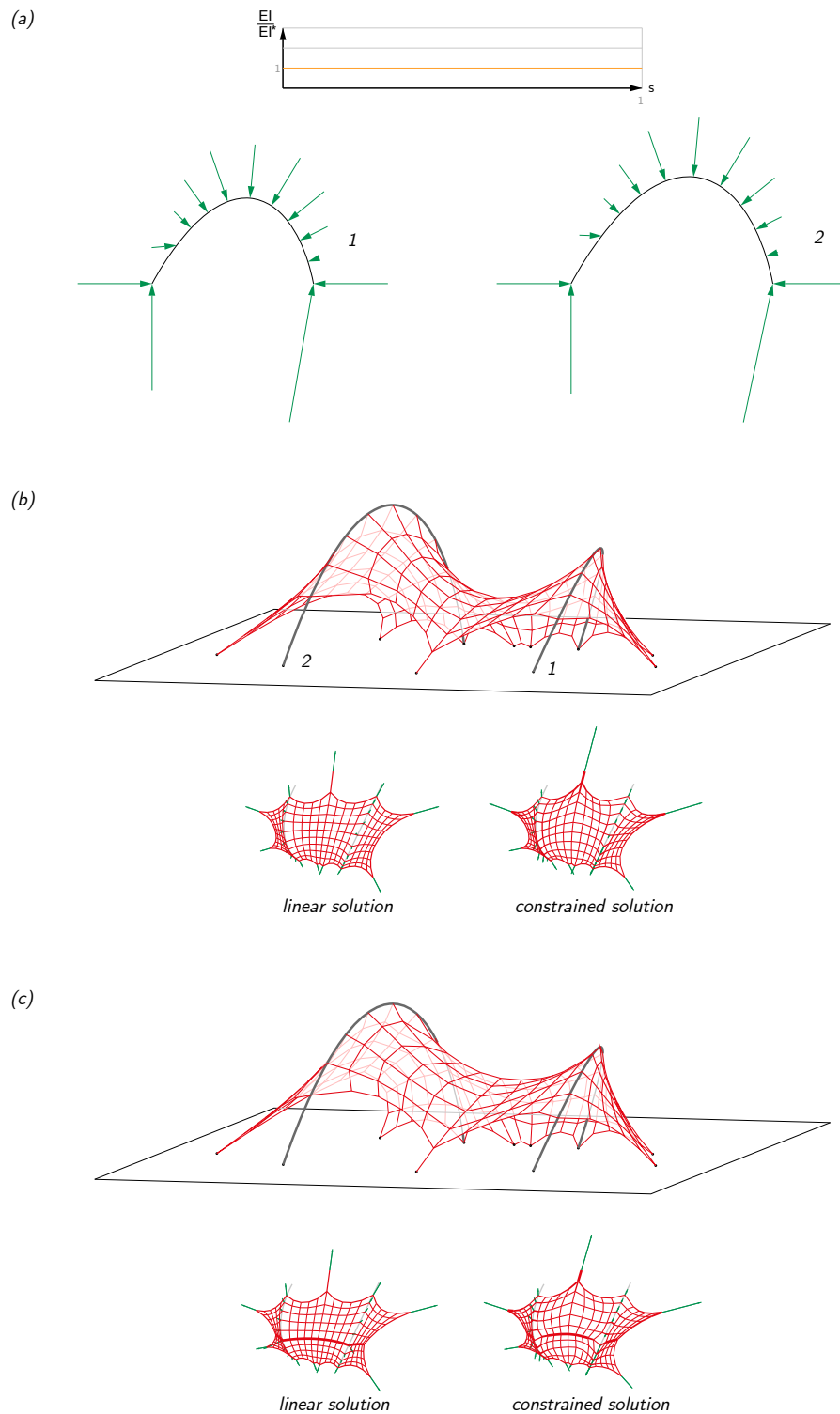


Figure 4.32: Bending-active tensile structure with two arched beams – (a) Restraining forces required to bent the beams into their target equilibrium geometry according to their bending stiffness; (b),(c) Axonometric view of the structure and top view of the cable net for the initial linear solution and the final solution for two different initial force density vectors. In the top view, the thickness of the cable net branches is proportional to the their force density.

5. Design Application

This Chapter presents an architectural application of the form-driven design approach elaborated in Chapter 4. Through this architectural application, the objective is to highlight the strengths of the form-driven approach in comparison to conventional form-finding approaches, especially for those design scenarios in which it is more convenient to consider the bent equilibrium geometry of the structure as the input rather than the output of the design process. In this regard, a self-supporting sun-shading façade system is used as a case study since both structural and sun-shading requirements, which strongly rely on the geometry of that system, have to be addressed simultaneously. The conventional way to design bending-active tensile structures through form-finding does not offer a direct control over the final bent shape, which would be beneficial during the conceptual design phase of such sun-shading system as the geometry strongly influence the sun-shading performance of the structure.

The sun-shading façade system was developed in 2018 by the author in collaboration with Pierluigi D'Acunto (ETH Zurich, Chair of Structural Design) and Federico Bertagna (University of Pisa, Department of Civil and Industrial Engineering), based on an original idea of the author, Pierluigi D'Acunto and Juan José Castellón (ETH Zurich, Chair of Structural Design / Rice University, School University). The physical experiments and the manufacturing of the prototype were undertaken by the author and Federico Bertagna. Special thanks go to Alessandro Tellini and Denizay Apusoglu (ETH Zurich, Rapid Prototype Laboratory) who provided support during the development of the experiments and the manufacturing of the prototype, and to Artai Sanchez for his help with the visualisations.

This Chapter has been published with minor changes in (Boulic et al. 2020).

5.1 A bending-active tensile sun-shading façade system

The case study developed in this Chapter consists in the conceptual design of a static, self-standing, sun-shading façade system, which is exemplarily applied to the glass curtain wall of the HIB office building of the ETH Science City Campus in Zurich (Switzerland), with the aim of improving the thermal and visual comfort of the building's occupants. The HIB office building has indeed fully glazed façades which allows maximising the visual connection between indoor and outdoor spaces but, in turn, increases the risk of thermal overheating and glare inside the building, thus affecting its occupants with potential thermal and visual discomfort. In order to overcome these issues, external sun-shading systems can be effectively used as a way to protect the exposed façades.

In architecture, bending-active structures can be very valuable solutions for the design of external sun-shading façade systems. This has been effectively demonstrated in relation to kinetic structures made of bending-active plates (Lienhard et al. 2011, Knippers et al. 2012, Lienhard, Riederer, Jungjohann, Oppe and Knippers 2013, Körner et al. 2018). Regarding static bending-active tensile structures, various aspects motivate their use in the context of façade design. First of all, bending-active tensile structures are remarkably lightweight systems, as they take advantage of the mutual interaction between actively bent elements and tensile elements and make efficient use of the structural performance of both subsystems. This property allows bending-active tensile structures to be used for building façade retrofitting. Second, bending-active tensile structures provide integrated solutions where both actively bent and tensile elements can perform for various functional purposes other than the structural one, such as sun-shading or more generally protection from the elements (Lienhard and Knippers 2012, De Laet et al. 2013, Lienhard, Ahlquist, Menges and Knippers 2013). Third, from an architectural standpoint, bending-active tensile structures are generally endowed with distinctive aesthetic connotations and are characterised by a strong formal expression.

The proposed sun-shading system is made of slender beams that are actively bent and a series of pre-stressed strips working in tension (Figure 5.1). The pre-stressed strips fulfil two functions: on the one hand, they shape and stabilise the actively bent beams; and on the other hand, they act as sun-louvers preventing the sun beams to hit the glazed façades (Figure 5.6). Each beam is anchored at its ends to the frame of the curtain wall. Its shape is dependent, on the one hand, on its bending stiffness, which varies along its axis due to a variable cross-section geometry, and on the other hand, on the restraining effect of the pre-stressing strips, which, in turn, bring additional stability and stiffness to the construction. The global geometry of the structure is informed by a solar analysis to prevent

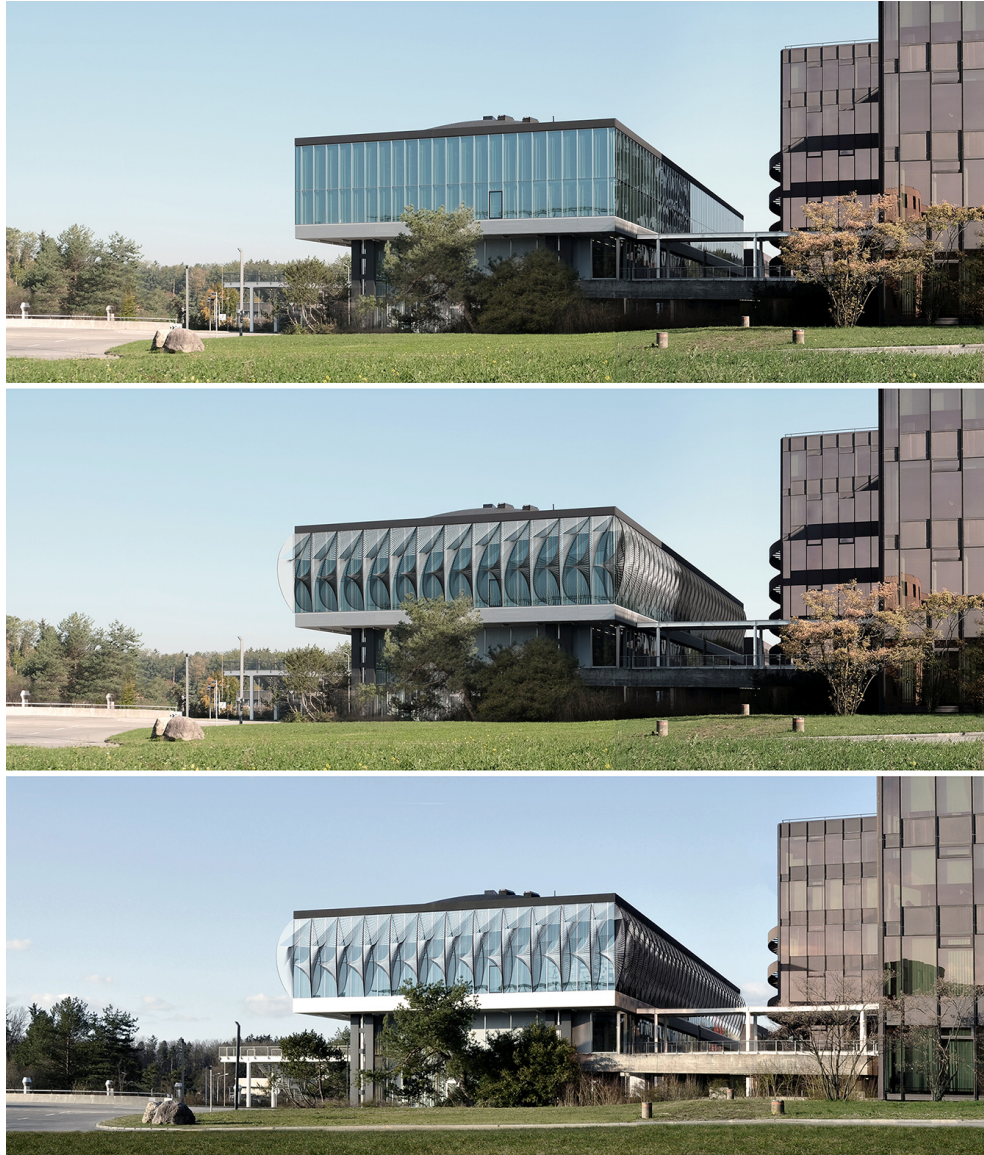


Figure 5.1: South-west façade of the HIB building at ETH Science City Campus in Zurich: photograph of the current state (top); collages with the proposed sun-shading bending-active tensile structure at two distinct times of the year: March 28, 14:30 (middle) and October 5, 11:45 (bottom).

overheating and glare inside the building, while maintaining appropriate internal lighting conditions (illuminance levels within an acceptable range of 100 - 3000 lux and reduction of the glaring risk on the work plane).

The conventional way to design bending-active tensile structures is through form-finding. This approach, however, does not offer an explicit control over the final equilibrium geometry of structure which would be beneficial during the design phase as the geometry directly impact the sun-shading performance of the system. On the contrary, the sun-shading façade system designed here takes

advantage of the form-driven design approach. Thanks to it, the bending-active beams can be directly designed in the equilibrium geometry that best fulfils the sun-shading purposes of the façade system, and the solar and visual analysis – a geometry-based analysis – can be performed independently of the structural analysis. An integral design framework is introduced which is grounded on the form-driven design approach for bending-active tensile structures and on different parametric models. In particular, this integral design framework makes it possible for multiple factors to be considered within the design process. As a result, the global geometry of the sun-shading façade system can be informed by both structural and functional requirements, including, among others, the protection from direct solar radiation and the visual connection between the interior and the exterior of the building.

The rest of the Chapter is structured as follows. Section 5.2 synthetically describes the form-driven method that has been employed to generate the geometry of the bending-active tensile façade system. Moreover, this section gives an overview on how the proposed integral design framework articulates the different steps of the design process. Section 5.3 defines the indoor comfort evaluation criteria used for the visual and thermal assessment of the designed façade system. This section also outlines the iterative design process based on a thorough solar and visual analysis, which informed the geometry of the proposed sun-shading system. Section 5.4 explains in detail the different parametric models on which the proposed integral design framework is based upon. Finally, Section 5.5 presents the construction of a 1:2 scale prototype of the façade, with a focus on the related material and fabrication investigations.

5.2 Application of the form-driven design approach

5.2.1 Form-driven design methodology

As presented in Section 4.1, in the form-driven approach, the control of the 2D geometry of bending-active beams within a 3D bending-active tensile structure is achieved by addressing successively the equilibrium of the bending-active beams and the one of the tensile elements, provided that equilibrium conditions between the two structural sub-systems are fulfilled. Two different strategies for implementing the form-driven design approach are described in Section 4.1. The strategy that is implemented in the design of the sun-shading bending-active tensile structure corresponds to *Design strategy 1* in which the equilibrium of the bending-active beams in their target geometry is achieved by adjusting their bending stiffness along their axis. It is summarised in Figure 5.2:

- In the first step (Figure 5.2(a)), the desired curved target equilibrium geometry of each of the 2D bending-active beams is defined, considering various aspects, such as structural, functional, and environmental criteria;
- In the second step (Figure 5.2(b)-(c)), a compatible set of pre-stressing elements is generated, in such a way that these tensile elements apply a series of forces $\mathbf{F}_{r,i}$ onto the axis of the beams; these forces are in the beams' planes and do not generate any torsion on the beams;
- In the third step (Figure 5.2(d)), the global equilibrium of each beam is fulfilled by ensuring that the applied forces generate locally a bending moment compatible with the curvature of the beam; in particular, this step involves the solution of the reaction forces at the beam's supports;
- Finally, in the last step (Figure 5.2(e)), the variable bending stiffness along the various beams' cross-sections is calculated such that the beams meet the equilibrium in the target geometries under the considered pre-stressing forces.

5.2.2 Open lines of cables

In order to fully control the equilibrium configuration of the hybrid structure, the geometry of the tensile elements can be directly designed in its equilibrium configuration as well. This is done through specific compatible arrangement of cables as described in Section 4.3, and, in particular, open lines of cables are used for the design of the sun-shading façade system. For each node of the beam to be restrained, two straight pre-stressing cables are introduced that connect the actively bent beam to their neighbouring beams or to the system's boundaries (Figure 5.2(b)-(c)). The pre-stressing forces \mathbf{F}_c and \mathbf{F}'_c in each of the two cables are assigned so that their resultant force \mathbf{F}_r lies on the beam's

plane (Figure 5.2(f)), which corresponds to:

$$(\mathbf{F}_c + \mathbf{F}'_c) \wedge \mathbf{n} = \mathbf{F}_r \wedge \mathbf{n} = \mathbf{0} \quad (5.1)$$

where \mathbf{n} is the normal vector of the beam's bending plane. As explained in Section 4.3, the condition of equilibrium between the beam and the cables is achieved independently for each node.

5.2.3 Integral design framework

Within its scope of applicability, the form-driven approach involving open lines of cables as described above allows decoupling the generation of the geometry of a bending-active tensile structure from the assessment of its static equilibrium. This makes it possible to first focus on the generation of feasible bending-active tensile structures whose shape can be easily controlled and adjusted according to geometry-dependent criteria, before integrating further structural and manufacturing aspects into the design. Figure 5.3 summarises the integral design framework described above, which relies on the use of three parametric models: the first one (*Geometric parametric model* – Section 5.4.1) defines the geometry of the bending-active tensile structure, the second one (*Structural parametric model* – Section 5.4.2) performs the structural evaluation, and the last one (*Manufacturing parametric model* – Section 5.4.3) addresses questions related to fabrication.

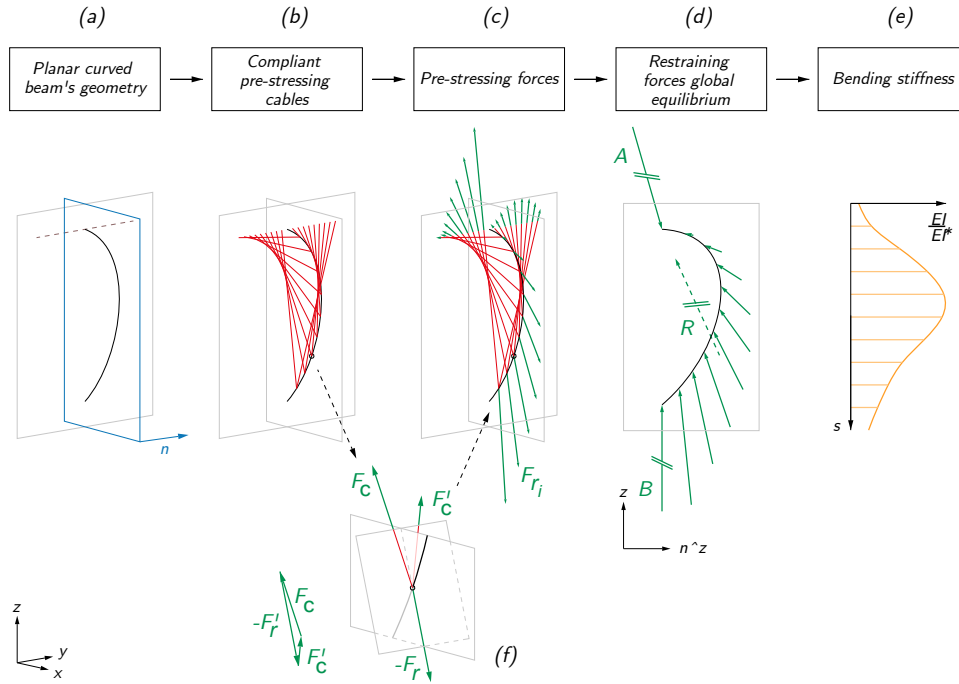


Figure 5.2: Form-driven design methodology of the bending-active tensile sun-shading façade system.

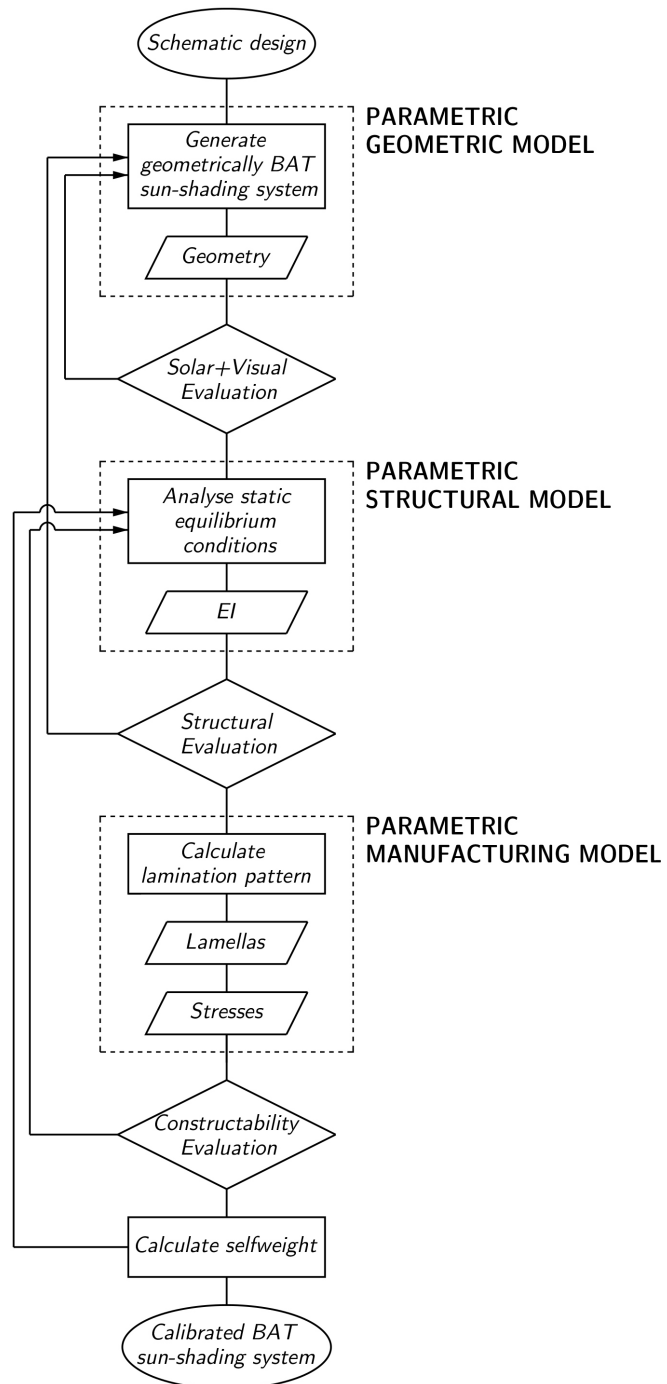


Figure 5.3: Integral design framework based on three different parametric models.

5.3 Geometric studies

The design of a sun-shading system that protects a glazed building façade should respond to sometimes-contradictory requirements for the thermal and visual comfort of the building's occupants. On the one hand, the solar gain through direct sun exposure of the façade should be reduced during summer and to a less extent, over spring and autumn, in order to prevent the internal overheating of the building and to reduce the energy consumption of active cooling systems. Moreover, during winter, daylight glare discomfort of the building's occupants caused by the low position of the sun in the sky should be eliminated. On the other hand, the visual comfort of the building's occupants should be satisfied throughout the year, by preserving as much as possible suitable lighting conditions as well as the views to the outside offered by the glazed façade.

5.3.1 Description of the case study and definition of the indoor comfort evaluation criteria

The sun-shading façade system used as a case study in this work has been designed for an office building located in Zurich (Switzerland) at the ETH Science City Campus. The building consists of a main volume containing office spaces, sitting on top of a smaller volume with workshops and technical rooms. At present, the building lacks an external sun-shading system. Considering the orientation of the building and the fact that the surrounding buildings naturally generate shadow, the most exposed façades of the building that require sun protection are the south-west façade and part of the south-east one (Figure 5.4). The indoor zones located behind the exposed façades are distributed on two floors and consist of one circulation space and two different workspaces (Figure 5.5).

In order to evaluate the indoor comfort of the building's occupants, several evaluation criteria were defined in relation to thermal, lighting, and visual connectivity aspects. Since the thermal comfort in an indoor space strongly depends on the amount of solar radiation that enters the building through its façades, the related metric which was considered is the following:

- *Solar radiation* [kWh]: The total incident direct solar radiation received by the glazed façades over a day.

Regarding the indoor visual comfort, three different aspects were considered: the illuminance level, the risk of glare and the visual connection to the outside. They are respectively evaluated according to the following metrics:

- *Illuminance level* [h]: The average time of a working day (9am-6pm) for which the illuminance value [lux] of an ideal horizontal work plane, positioned at 0.9m above the floor, remains within the acceptable range of 100 - 3000 lux (Mardaljevic et al. 2012);

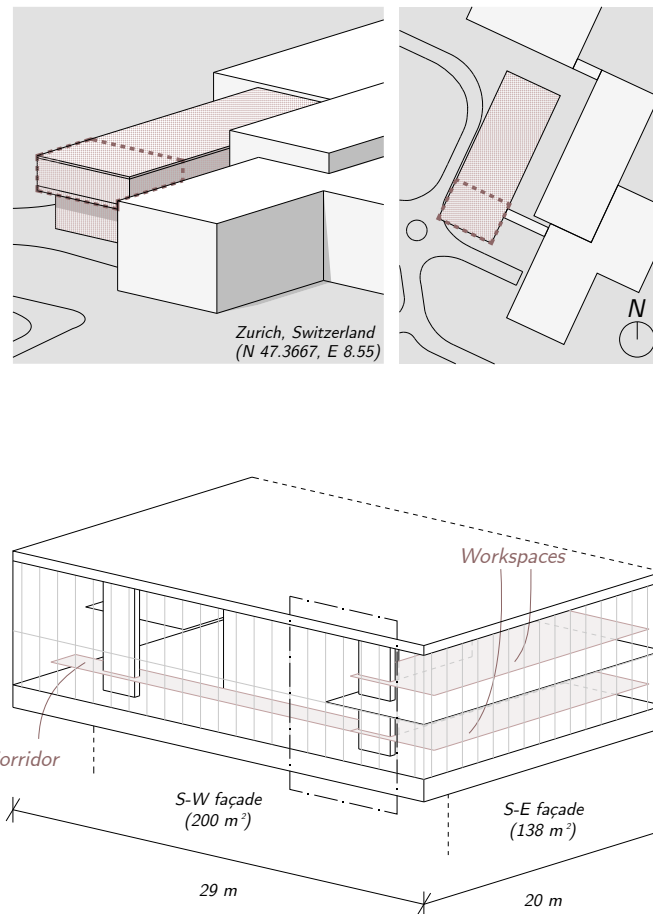


Figure 5.4: HIB office building chosen as a case study – (top) Situation and orientation of the building; (Bottom) Axonometry of the part of the building used for the solar and visual analysis.

- *Glare level* [h]: The average time of a working day (9am-6pm) for which an ideal horizontal work plane, positioned at 0.9m above the floor, is under direct sunlight. This measure is directly related to the glare risk;
- *Visual occlusion level* [%]: The percentage of visual occlusion of the horizon surface from a grid of points inside the building located 1.2m above the floor, which corresponds to an ideal eye height when sitting.

The metrics were assessed for the different indoor zones with the *Grasshopper's* (Rutten 2009) plug-in *Ladybug* (LLC 2013) in the *Rhinoceros* CAD environment (Robert McNeel & Associates n.d.) Figure 5.5 presents the average values over the calculation area. The solar analysis of the building in its current configuration – without sun-shading system – allowed clarifying the needs of the building in terms of solar protection, and in particular, to identify the most critical times of the year and of the day when major indoor discomfort occurs. It helped to initialise the step-by-step design development presented below. Above all, it

served as a reference to weigh the benefits brought by the distinct sun-shading systems explored below in relation to the considered metrics.

5.3.2 Design development

The shape of the bending-active tensile sun-shading structure to retrofit the previously described building has been obtained through successive transformations of a generic sun-shading system, considering the above thermal and lighting criteria. Through this progressive geometric definition, starting from simple configurations, the complexity of the structure has been gradually increased in iterative steps and new geometric parameters have been introduced (Figure 5.5). The following paragraphs offer an overview of this parametric study, while a complete description of the parametric model used in step 3 is presented in Section 5.4.

Step 1: Combination of horizontal and vertical brise-soleils In the first step, different modular configurations, combining conventional vertical and horizontal rectangular brise-soleils, were explored in order to assess the general dimensions of the structure – i.e. the relative spacing, depth and orientation of the sun-shading elements (Figure 5.5, cases 1.a and 1.b).

Step 2: Introduction of curved sun-shading elements in place of the vertical brise-soleils In the second step, the vertical brise-soleils were replaced by curved sun-shading elements. The upper horizontal sun-shading elements were then adjusted accordingly. An investigation was conducted to determine the geometry of the curved elements that contributes the greatest to the reduction of the solar radiation on the façade and the risk of glare (Figure 5.5, cases 2.a and 2.b).

Step 3: Transition to a bending-active tensile system In the third step, the geometry resulting from the previous step was modelled in the form of a bending-active tensile structure following the rules presented in Section 5.2.2. To simplify the calculations, the tensile elements were replaced with a continuous ruled surface. Multiple parameters were used to describe the geometry of the sun-shading structure (Section 5.4.1) and different variations of these parameters were tested to produce various spatial configurations, such as those ones in Figure 5.5. At last, additional parameters were introduced to enable the top down control of the global geometry of the sun-shading structure at the building scale, and thus break the modularity of the structure. This additional differentiation of the system allowed for a better negotiation of the different design requirements. Moreover, the above continuous ruled surfaces were replaced with wide strips, whose widths were adjusted to balance the conflicting requirements for sun protection and internal illuminance level.

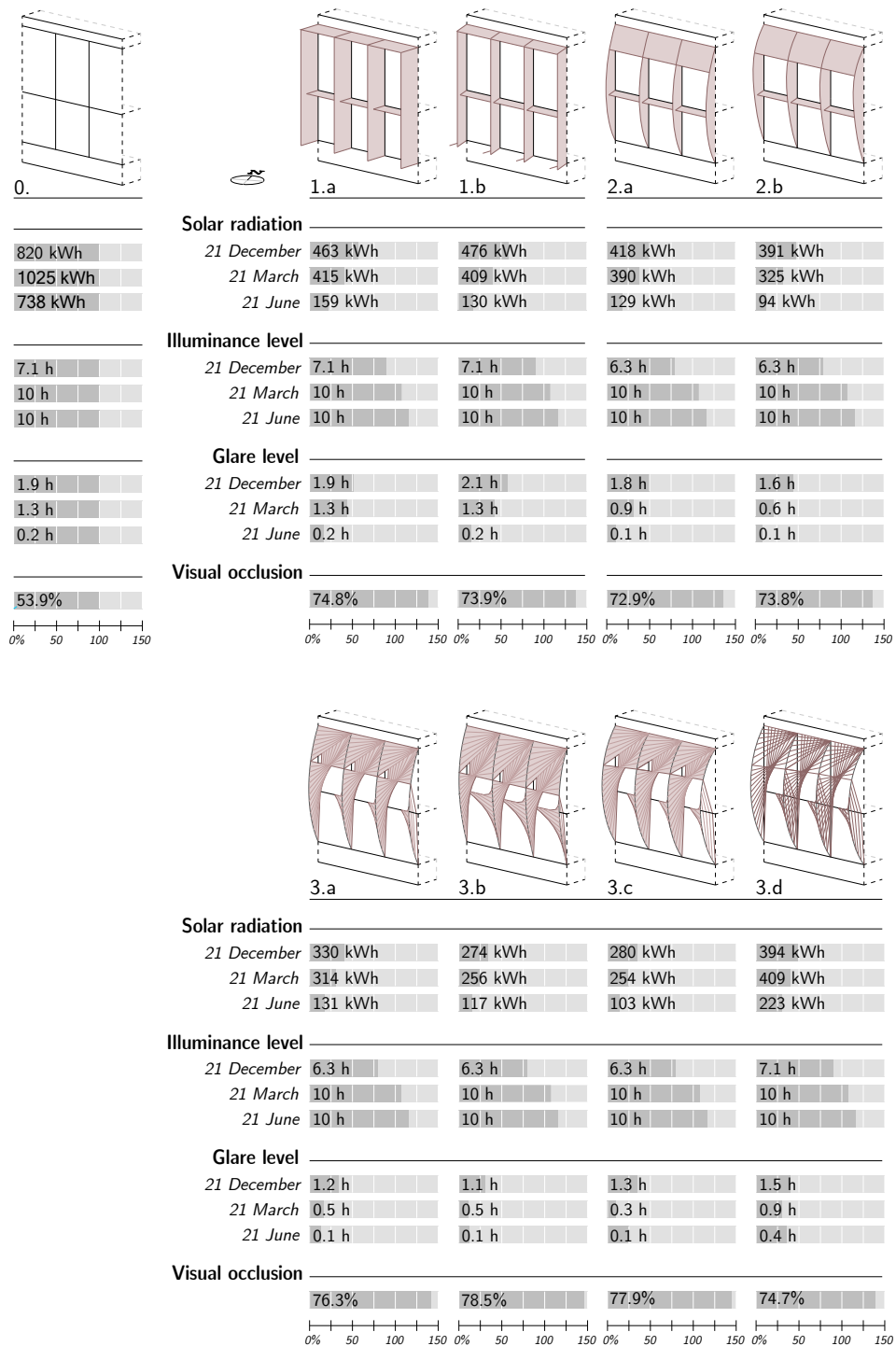


Figure 5.5: Solar and visual analysis and design development.



Figure 5.6: Interior view of the office with the proposed sun-shading system applied on the façade.

5.3.3 Design outcome

Through geometric variations along the two façades of the building, the designed bending-active tensile sun-shading façade system offers a global solution to a time dependent issue. The different requirements in terms of visual and thermal comfort, which are sometimes conflicting over time, are negotiated through an appropriate geometry of the system. In particular, the proposed system is more open at the level of the workspaces in order to maximise the visual connection of the occupants to the outside, while preventing the risk of glare (Figure 5.6). On the contrary, in other parts of the façade, particularly on the south-western side where the corridors are located, the system is more closed. From a structural standpoint, neighbouring beams are interconnected with the sun-shading strips that work in tension, overall generating a continuous structure along the façades.

In relation to the considered indoor comfort evaluation criteria, the designed sun-shading façade system performs in a similar manner as conventional sun-shading configurations (as case 1.a and 1.b.). However, in the proposed system, unlike in conventional systems, the structure and the sun-shading function are fully integrated. The sun-shading tensile strips unfolding on either side of the beams are structurally active and offer an integrated solution for wind bracing, while the resort to discrete cables decreases the system's windage. The resort to active bending allows to activate thin sections of material.

5.4 Parametric models

As explained in Section 5.2.3, the integral design framework involves three different parametric models, which are detailed below.

5.4.1 Parametric geometric model

In accordance with Sections 5.2.1 and 5.2.2, each actively bent beam and the related tensile elements of a beam-cables cluster are defined geometrically one after the other and can be adjusted any of the two at any time.

Figure 5.7(a)-(b) shows the different geometric parameters involved in the generation of the bending-active beams. The planes where the beams' axes are located are oriented with an angle $\alpha_i^{(l)}$ with respect to the façade. The beams are modelled as NURBS curves, each of which is defined by 4 control points: two points located on the façade, at the level of the frames, $(M_i^{(l)}, P_i^{(l)})$, and two other points, $N_i^{(l)}$ and $O_i^{(l)}$, resulting from the intersection of the beam's bending plane and two straight lines (resp. $N^{(l)}N$ and $O^{(l)}O$).

As for the straight cables, they are geometrically arranged in 3D space to reproduce the global geometrical features of sun-shading configuration 2.b, as it was found to be a satisfying solution with regards to the considered thermal and lighting metrics. The spatial layout of the cables emerges from the progressive transformation of a simple planar system consisting of a beam restrained with radial cables as detailed in Figure 5.7(b), while preserving the conditions for a 2D equilibrium of the beams. For each cluster, the position of points A , B , C , D , E and F of Figure 5.7(b) can be adjusted, as well as the distribution of the anchorage points of the cables along the curves AP , BD , CE , BF .

Finally, the parameters related to both the beams and the cables layout are integrated resulting in the complete geometric model of the sun-shading structure (Figure 5.7(c)). Global and local parametric variations can then be implemented.

5.4.2 Parametric structural model

Once the overall system geometry is established, pre-stressing forces are assigned to the cables. Given equilibrium equation 5.1, for each two cables connected to a node of the beam, a pre-stressing force F_c is assigned to one of the two cables (Figure 5.8(a)) and the pre-stressing force F'_c in the other cable and the resulting restraining force F_r are derived accordingly (Figure 5.8(b)). Besides, pre-stressing forces in each pair of cables can be adjusted independently. Regarding the support conditions of the beams, it was decided that each beam was pinned to the façade. Because of the static indeterminacy of the system, the reaction forces at the supports balancing the forces applied by the cables cannot be uniquely determined but are defined based on their overall resultant force

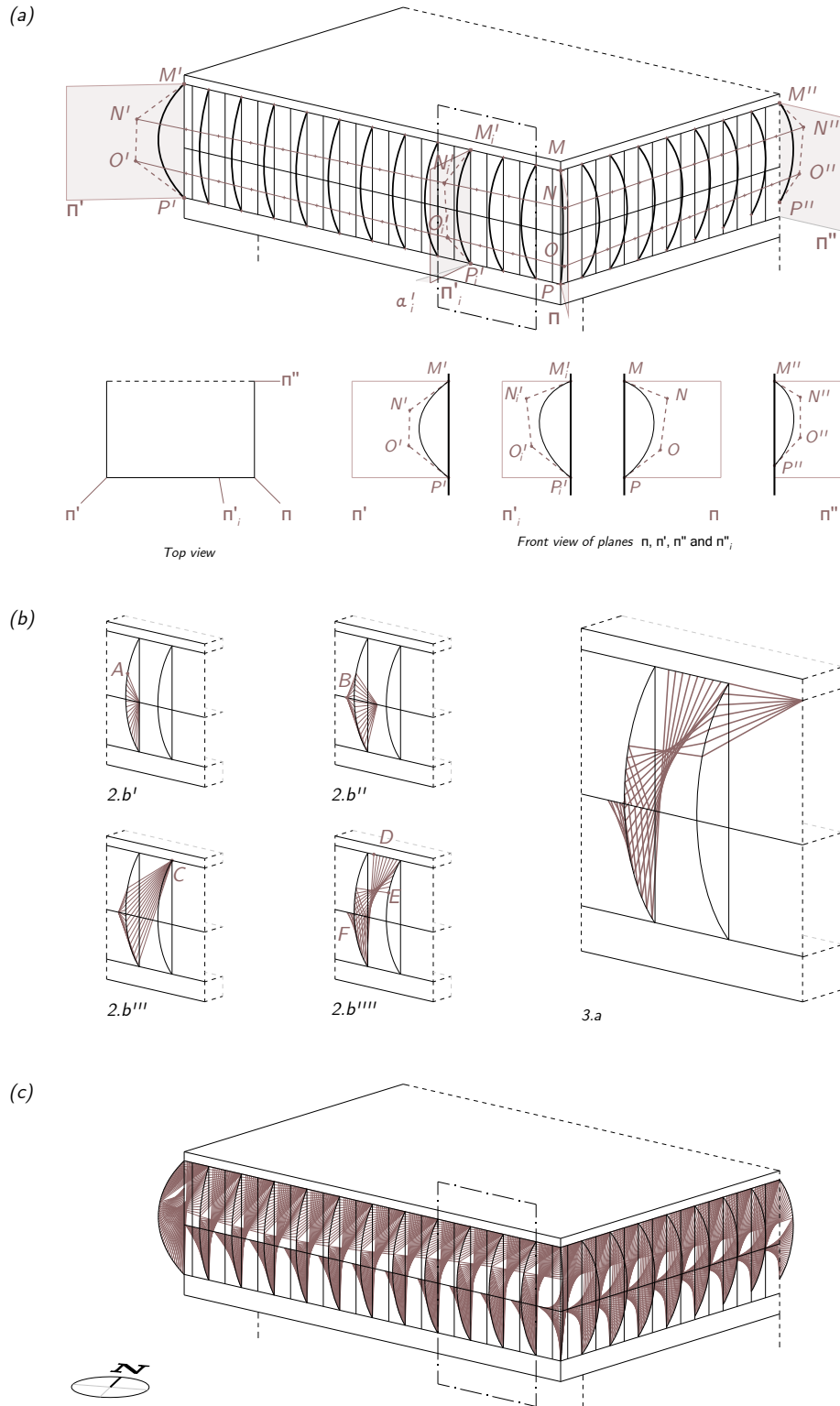


Figure 5.7: Parametric geometric model – (a) Parametric definition of the actively-bent beams as NURBS curves; (b) Generation of the parametric volumetric tensile sun-shading sub-system, from a planar configuration and preserving the planar static equilibrium of the beams; (c) Final geometry of the bending-active tensile sun-shading structure obtained thanks to the global parametric geometric model.

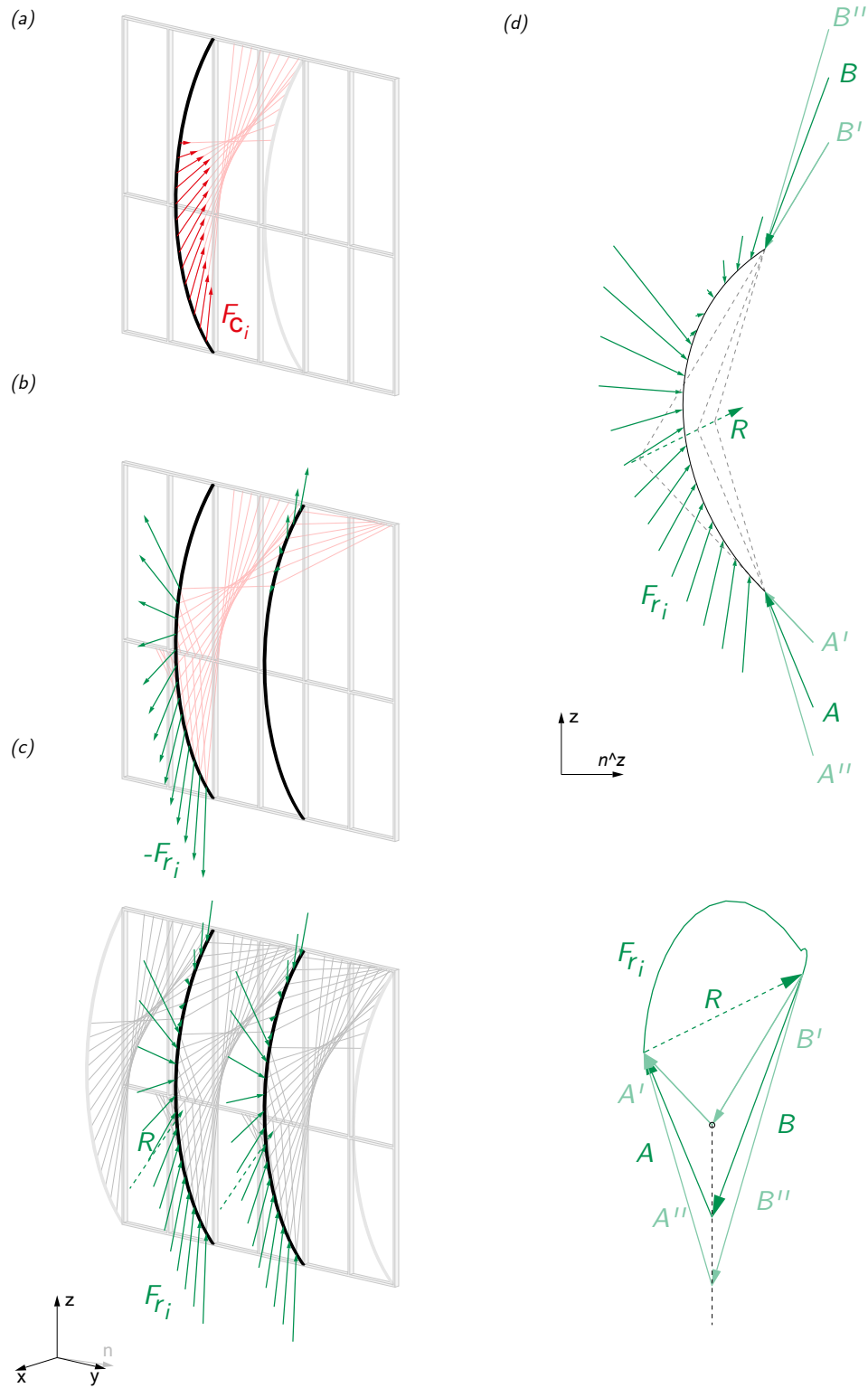


Figure 5.8: Structural evaluation of the bending-active tensile structure – (a) Assignment of pre-stressing forces in the cables, (b)-(c) Calculation of restraining forces, (d) Solving of global equilibrium through reaction forces.

(Figure 5.8(d)). The reaction forces component along the direction that connects the two beam's ends together (along z here), governs in which proportion the target geometry of the beam at equilibrium is reached through an adaptation of the beam's cross sectional bending stiffness or through the restraining effect of the pre-stressing cables.

Finally, for each beam, a non-constant bending stiffness is determined according to the graphical method proposed in Section 3.2, in such a way that the beam bends into the previously defined equilibrium geometry under the action of the previously defined pre-stressing forces (Figure 5.9(b)).

5.4.3 Parametric manufacturing model

The calculated bending stiffness El is not constant and varies along the axis of the beam. Since a differentiation of the elastic modulus E along the beam is rather difficult to implement even if possible (Bechert et al. 2016), such variations are obtained here by tailoring the geometry of its cross-section and thus the quadratic moment of inertia I along the bending axis. One possible way to produce beams with variable cross-sectional areas is to laminate the beams out of individual elastic lamellas, with variable width and length but constant mechanical properties. To keep the position of the main axis of inertia constant, the lamellas are assembled symmetrically with respect to the axis of the beam. For example, in the case of a section composed of 5 symmetrical layers (Figure 5.9(c)), the quadratic moment is given by the following formula:

$$I_x = \frac{e_0^3 b_0}{12} + 2 \left(\frac{e_1^3 b_1}{12} + \left(\frac{e_0 + e_1}{2} \right)^2 e_1 b_1 \right) + 2 \left(\frac{e_2^3 b_2}{12} + \left(\frac{e_0 + 2e_1 + e_2}{2} \right)^2 e_2 b_2 \right) \quad (5.2)$$

where e_0 , b_0 , e_1 , b_1 , e_2 , b_2 are respectively the width and the height of lamellas 0, 1, 1', 2, and 2'. In the case that $e_0 = e_1 = e_2 = e$, equation 5.2 can be simplified to:

$$I_x = \left(\frac{1}{12} b_0 + \frac{13}{6} b_1 + \frac{49}{6} b_2 \right) e^3 \quad (5.3)$$

Different lamination configurations can produce the same quadratic moment of inertia since for a given number of lamellas of known thickness, there is an infinity of widths ($b_0(x)$, $b_1(x)$, $b_2(x)$) satisfying equation (3). In addition, the same quadratic moment can also be obtained by using a different number of lamellas. In this parametric model, the number of lamellas, their thickness and their width, can vary in order to provide different lamination patterns (Figure 5.9(c)). When choosing the number of lamellas and their thickness, the maximum stress in the beam, which is directly related to the thickness of the beam, is a determining factor (see Equation 5.7). It is worth mentioning that in this study the effect of self-weight is ignored. In fact, adapting the section of the element affects its

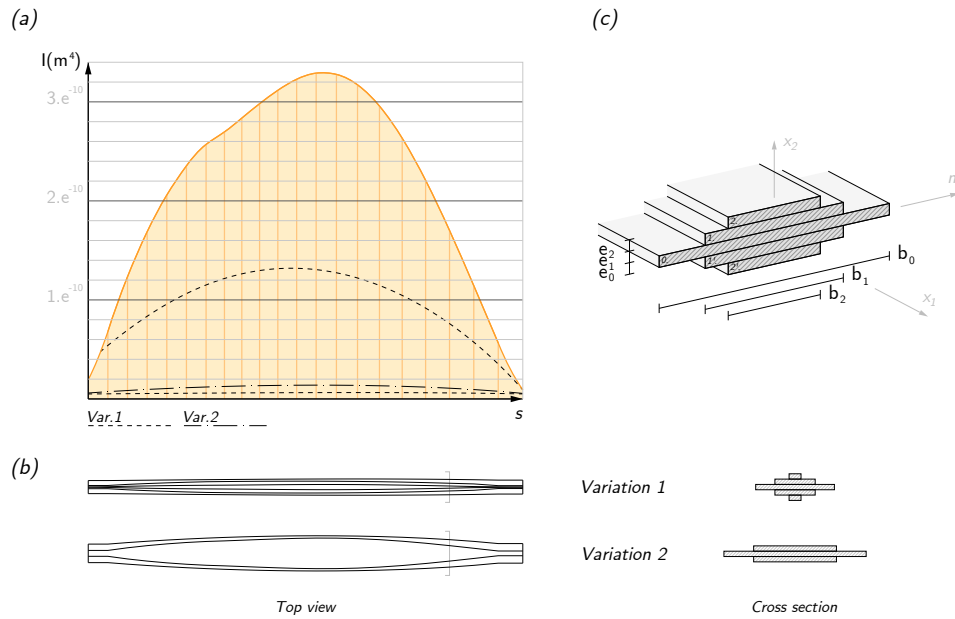


Figure 5.9: Manufacturing parametric model – Parametric generation of lamination patterns for producing beams with variable bending stiffness along their axis.

own weight, and so the loads initially considered for the calculation. Iterations are necessary to consider this change in self-weight into the global equilibrium of the system and to recalculate the stiffness resulting from this change.

5.5 Material investigation

5.5.1 Structural prototype

A prototype of the sun-shading structure was built at 1:2 scale to provide a qualitative validation of the structural model and to check the applicability of the design approach to a real construction. An exemplary portion of the entire bending-active tensile structure, which was made of four actively bent beams, was built (Figure 5.10). The beams at the sides of the prototype have been materialised in the form of rigid frames.

5.5.2 Fabrication of beams with variable bending stiffness

Plywood lamellas 1-mm-thick birch plywood made of 3 plies was chosen for the lamellas in the laminated beams. Due to its high flexural strength and its moderate stiffness, plywood is an ideal material to resist large elastic deformations without failing (Kotelnikova-Weiler et al. 2013), thus appropriate for the realisation of bending-active structures (Weinand and Hudert 2010, Fleischmann et al. 2012, D'Acunto and Kotnik 2013, Bechert et al. 2016, La Magna et al. 2016, Brancart et al. 2019).

The mechanical characteristics of the chosen 1-mm-thick birch plywood have been estimated by simple mechanical tests. A series of plywood lamellas (width b : 40mm, length l : 1000mm, thickness e : 1mm), with their longitudinal axis aligned with the grain direction of the outer plies, were bent with a cable into different *Elastica*, and the corresponding buckling force was measured. From these measures and based on the theoretical values of the buckling force / bending stiffness ratio (Timoshenko and Gere 1961, 76–82), the average elastic modulus E of the 1-mm-thick birch plywood lamellas along the grain direction could be estimated to 9.6GPa (Figure 5.11(a)). This value was afterwards validated through a simple 3-point bending test performed on the same samples (Figure 5.11(c)). Additionally, the average yield strength $f = Ee/2\rho_{min} = 37\text{MPa}$ along the grain direction was estimated after measuring the minimal radius ρ_{min} at which the above series of plywood lamellas started to crack under bending (Figure 5.11(b)). The measured values are both in line with the reference values of the Swiss norm (*SIA 265/1:2009 Construction en bois - Spécifications complémentaires* 2009).

Fabrication of laminated beams With regard to the manufacturing of the different lamellas, they were laser cut from panels of the above 1-mm-thick plywood. Due to the limited bed size of the laser cutter, the lamellas had to be segmented into shorter elements, which were subsequently glued and mechanically connected (Figure 5.14(a)). Joints with a dovetail geometry were used to ensure the transfer of tensile forces within the bent beams, while the transfer



Figure 5.10: 1:2 scale structural prototype of an exemplary portion of the sun-shading structure.

of compressive forces was ensured by contact between the lamellas' segments. The behaviour of the joints as a function of their geometry and their distribution in the beam was studied through a series of physical tests (Figure 5.12). From one lamella to another, the discontinuities caused by the joints were shifted to avoid the generation of mechanical weakness along the beam (Figure 5.14(a)). The use of mechanical fasteners prevented the delamination of the lamellas in the most critical areas, whether under compression or tension.

5.5.3 Steel cables

In the prototype, the tensile elements, representing the sun-shading strips, were materialised as steel cables. In addition, at this stage of the design process, the elongation of metal cables was negligible, whereas the use of a textile material, for example, would require a more in-depth knowledge of its mechanical properties. The length of the cables was controlled by shaft collars.

5.5.4 Calibration of restraining forces and lamellas pattern according to mechanical properties

The calibration of the internal forces within the structure has been carried out over four successive steps as depicted in the flow chart of Figure 5.3 (*Analysis of structural equilibrium, Calculation of number of lamellas in the beam, Generation of lamination pattern and Integration of self-weight in the calculation*) and has involved both material and fabrication related parameters.

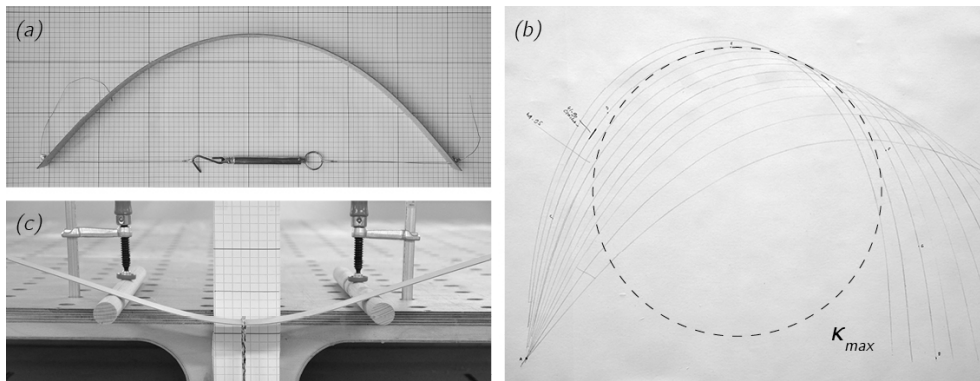


Figure 5.11: Simple physical tests to characterise the mechanical properties of 1mm-thick birch plywood lamella – Estimation of the modulus of elasticity (a) and of the yield strength (b). Additional converging 3-point bending test to estimate the modulus of elasticity (c).



Figure 5.12: Investigation on the geometry of the dove tail joints and their distribution in the beams.

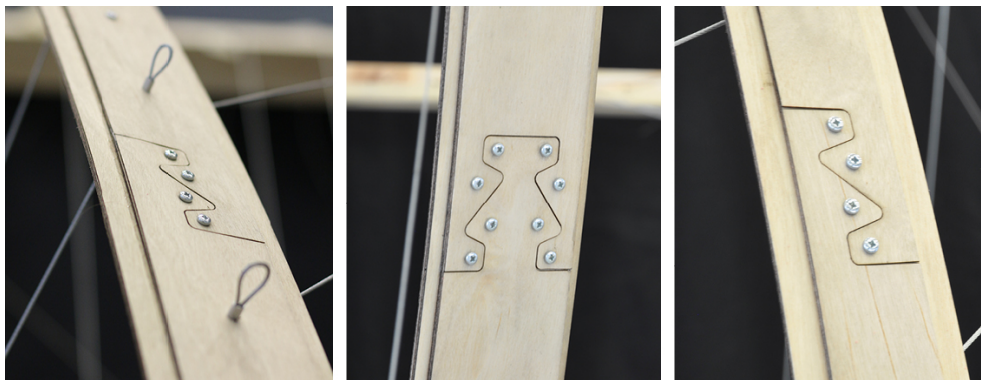


Figure 5.13: Details of the designed joints between the segmented lamellas.

Pre-stressing forces and reaction forces were adjusted in such a way that the cables were stretched evenly, the internal stresses remained within the allowed values, and the shape of the different lamellas satisfied the fabrication requirements.

Regarding the determination of the number of lamellas constituting each of the different beams, this value has been calculated so that the axial stress

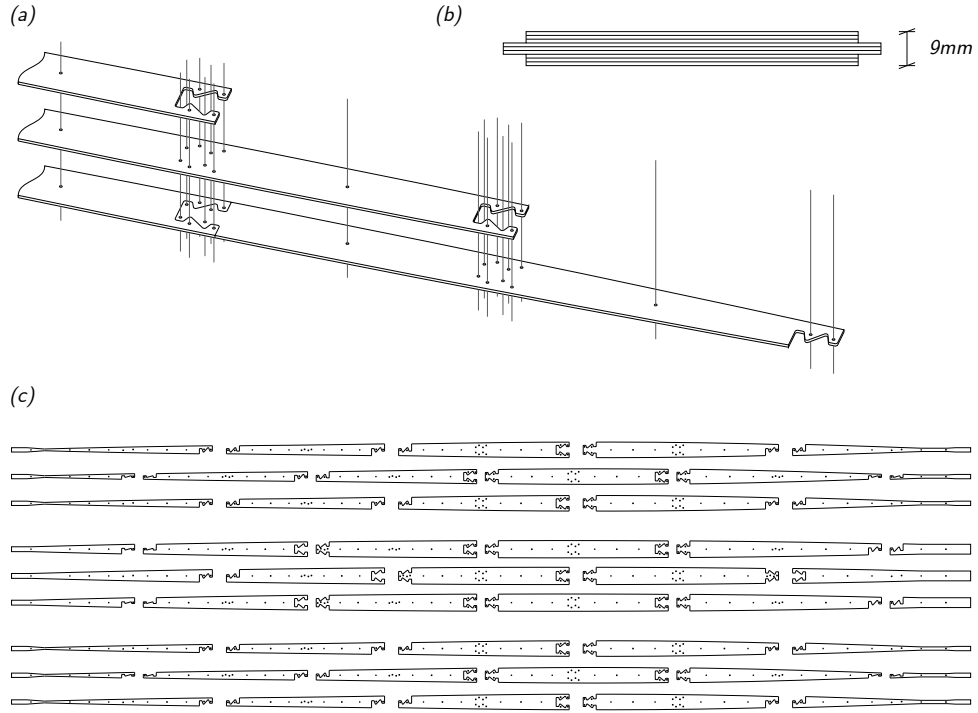


Figure 5.14: Laminated beams – (a) Assembly logic of a laminated beam from segmented lamellas, (b) laminated beam cross section from 9 lamellas and (c) pattern of the constituting lamellas of one of the two beams.

in the beam reaches at maximum 75% of the material maximal capacity. In this way, the beam gains enough stiffness through the prestressing effect of active bending without risking material failure. Given a beam under pure flexural bending in the xy plane and y and z the principal axis of inertia of its cross-sections, and provided that planar cross-sections of the beam remain planar, the flexural bending moment is:

$$M_z = EI_z \kappa_z \quad (5.4)$$

The normal stress acting on the beam's cross section is given by:

$$\sigma_x(y) = \frac{N}{S} - \frac{M_z}{I_z} y \approx -\frac{M_z}{I_z} y \quad (5.5)$$

After substitution, it simplifies to:

$$\sigma_x(y) \approx -E \kappa_z y \quad (5.6)$$

which leads to the maximal value of the normal stress in the beam:

$$\sigma_{x_{max}} \approx -E \kappa_{z_{max}} y_{max} \quad (5.7)$$

The thickness of each beam, therefore the number of lamellae which are layered, is calculated as such:

$$y_{max} = \frac{0.75f}{E \kappa_{z_{max}}} \quad (5.8)$$

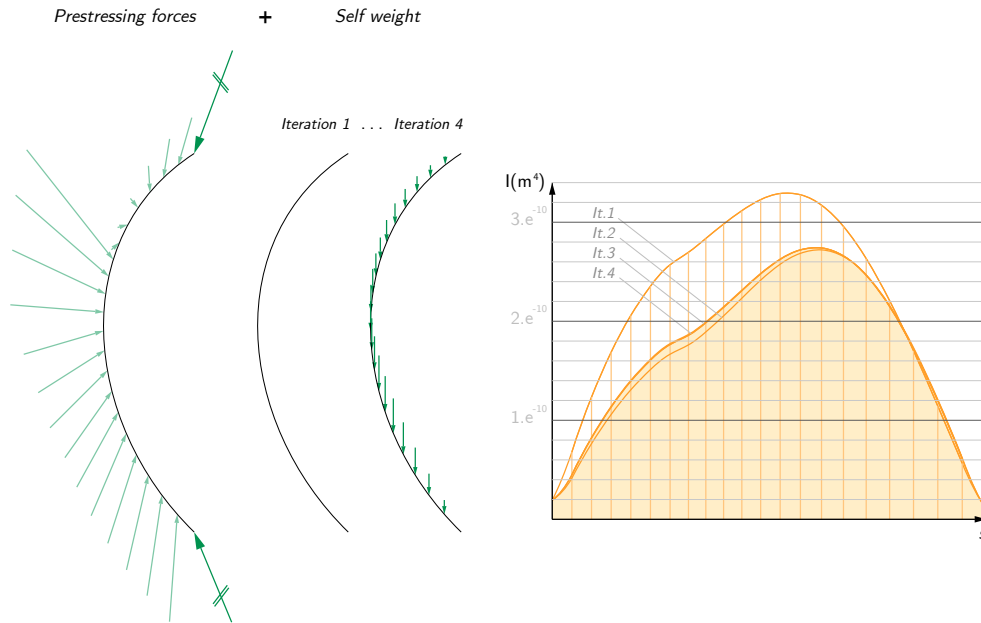


Figure 5.15: Integration of self-weight effect in the beam's bending-stiffness calculation.

In the case of the two beams of the prototype, this gives respectively a beam height of 9.5mm and 9.9mm that correspond in both beams to 9 lamellas of 1 mm of thickness (Figure 5.14(b)). Finally, the self-weight of the beam was introduced in the calculation based on a material density of the plywood lamellas of 650 kg/m^3 . The four above steps were repeated until the dimensions of the beam cross section converge to a unique configuration (Figure 5.15). Ultimately, the lamination pattern of each beam could be produced and the lamellas laser cut (Figure 5.14(c)).

5.5.5 Prototype assembly

A timber frame was first built to replicate the curtain wall of the façade. Once manufactured according to the lamination patterns, the two beams were progressively and slowly bent until their extremes could be connected to the frame, on free rotating supports. As the deflection was increasing, water was spread several times onto the stretched face of the beams to release stresses and prevent failure. Afterward, all the cables have been connected loosely to the beams and the frame, and the cables providing the strongest restraining forces were adjusted first (Figure 5.16). Iteratively the length of all the cables were adjusted until the required pre-stressing force was achieved. The staggered positioning of the joints within the different laminates of the beams allowed for a smooth curvature of the bent elements (Figure 5.13).

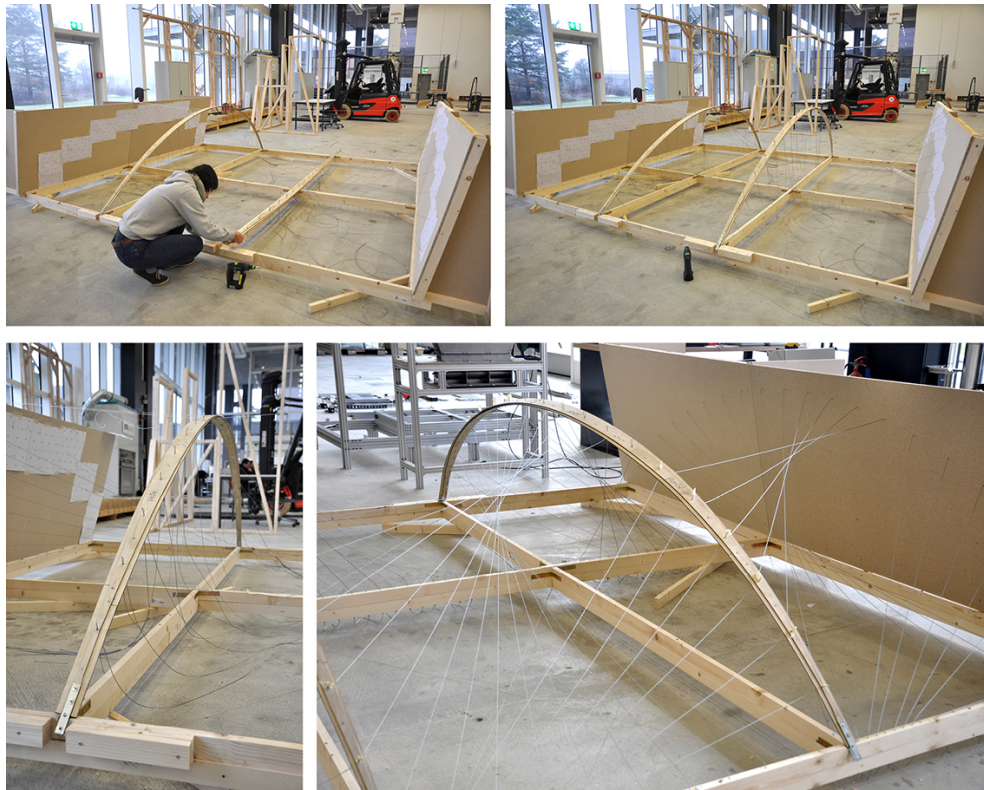


Figure 5.16: Bending and assembly process.

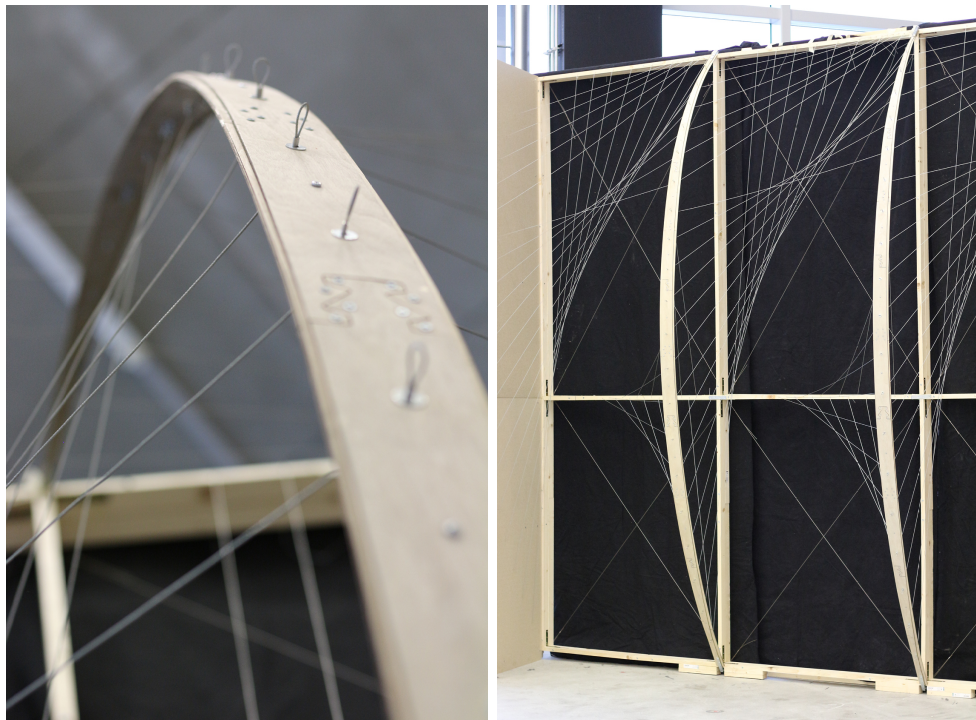


Figure 5.17: Details of the 1:2 scale structural prototype



Figure 5.18: 1:2 scale structural prototype of an exemplary portion of the sun-shading structure.

5.6 Observations

Through the exemplary design of a façade sun-shading system, it has been demonstrated how the proposed form-driven approach to bending-active tensile structures, unlike conventional form-finding methods, allows having explicit control over the equilibrium geometry of the hybrid system. Such direct geometric control is particularly beneficial in those design applications in which structure is not the only parameters to be considered but also architectural, environmental and manufacturing considerations are at stake. Thanks to the form-driven approach, an integral design framework which includes all these aspects has been proposed based on a parametric geometry-based definition of the bending-active tensile structure. Eventually, through the variation of the system's geometry along the façades and the variation of the beams' bending stiffness along their axis, a negotiation between all the parameters that influence the geometry of the system has been possible.

Further considerations can be made in relation to the effectiveness of the design process. In particular, throughout the process, various parameters were adjusted manually. One could imagine an automation of the process to refine the distribution of prestressing forces and internal stresses in the system, and to consider manufacturing constraints. Besides, Finite Element Analysis would be helpful in assessing the behaviour of the system more thoroughly, after its geometry has been designed using the form-driven approach.

The structural prototype established a first step towards the development of a complete façade system, and it provided valuable information regarding the forces calibration procedure. The fabrication of the prototype gave a first qualitative validation of the theoretical digital model, although a more thorough assessment of the physical model would be required to draw a deeper conclusion.

With regards to the fabrication itself, further developments should be implemented. On the one hand, the current pre-stressing steel cables, which are supposed to work as sun-louvers, should be substituted by tensile strips, such as coated fabric strips. The possibility to slightly stretch the material would facilitate the tensioning of the tensile elements. On the other hand, further research is required to defined a proper material system that can be effectively used for the manufacturing of the beams at full scale. Composite materials and industrial lamination manufacturing processes could be explored to improve the fabrication of beams with non-constant bending stiffness along their length and avoid the resort to mechanical joints and fasteners.

6. Conclusion

This Chapter provides a summary of the various contributions of this thesis, presents the current limitations of the research and proposes suggestions for future developments. It finally reflects on the overall content of the research.

6.1 Contributions

With the aim to overcome some of the limitations of the current form-finding methods, especially in terms of geometry control, the main contribution of this research has been to introduce a novel form-driven approach for the design of bending-active tensile structures, which provides the designer with more control over their final equilibrium geometry.

The elaboration of the proposed form-driven design approach has entailed the development of several models and procedures, including the definition of a structural model (Chapter 3), the formulation of a design process (Chapter 4), and the design of a bending-active tensile structure as an architectural application of the approach (Chapter 5). In the following paragraphs, contributions related to each of these points are reported.

6.1.1 Structural model

Different frameworks have been proposed in the literature for the modelling of bending-active tensile structures (Sections 2.1.2, 2.1.3 and 3.4.1). They are based on distinct mechanical models of slender elastic beams under large deformations but all make use of numerical methods to form-find the equilibrium geometry of the structures. The resort to form-finding approaches implies for the designer a limited control over the geometry of the form-found bending-active tensile structures and therefore a lack of intuitive strategies to implement his/her design intentions.

An alternative structural model for bending-active beams in 2D space has been developed. It is based on a simplified mechanical model of the beam-active beams and on graphic statics.

- A simplified mechanical model has been proposed for the description of the large elastic deformations of slender beams in their plane of symmetry

(Section 3.1.1). In this model, internal forces do not relate to the infinitesimal deformation of the beams' cross-sections but to the global deflected geometry of the beams. Combined with the use of form and force diagrams (Section 3.1.2), this mechanical model facilitates the understanding of the mechanisms involved in the static equilibrium of a bending-active, in particular thanks to the visual dimension of the diagrams. Grounded on this mechanical model, two graphical procedures have been introduced in order to evaluate and control the static equilibrium of bending-active beams. More precisely, these procedures allow to deduce the internal and external forces that must act on a beam so that, at equilibrium, the beam bends into a target geometry which has been previously defined by the designer as a plane continuous curve.

- A first graphical procedure consisting in rebuilding the beam's force diagram has been formulated to determine the appropriate distribution of bending stiffness along its axis a beam requires so that it bends into the target equilibrium geometry (Section 3.2.1).
- A second graphical procedure based on the study and manipulation of the beam's force diagram provides the different possible external actions that enforce the equilibrium of the beam into the target equilibrium geometry (Section 3.3.1).

Finally, as a natural development of this last graphical procedure, the following contribution has been achieved:

- The shaping of single bending-active beams by external restraining systems into target curved equilibrium geometry by means of geometric constructions has been presented (Section 3.3.2). The different design parameters of such 2D bending-active tensile systems, which can perform as building components for instance, have been identified and illustrated, highlighting the design possibilities opened by the graphical approach with regard to bending-active tensile structures.

6.1.2 Form-driven design approach

Built upon the above structural model, a novel general approach for the design of bending-active tensile structures has been conceived. More specifically, this approach allows the creation of bending-active tensile structures composed of bending-active beams bent in their plane of symmetry and pre-stressed cables and cable nets. The singularity of the approach lies in the fact that the bending-active beams are generated directly in their own target equilibrium geometry, as plane continuous curves. The local and global conditions of their static equilibrium in the target geometry are deduced afterwards and informs the geometry of the pre-stressed cables and cable nets that restrain the beams. Thanks to such a control over the equilibrium geometry of the bending-active beams, the proposed

form-driven approach displays valuable advantage over the existing form-finding methods especially during the conceptual design phase in which the focus is given to the overall geometry of the bending-active tensile structures. In relation to the proposed approach, the following contribution has been made:

- A global design process based on the successive consideration of the bending-active beams and the pre-stressed cables and cable nets has been formulated (Section 4.1). It is composed of two distinct design strategies which are each based on the three following design operations: (1) definition of the equilibrium geometry of the beams as plane continuous curves, (2) solving of the equilibrium of the beams and (3) generation of the pre-stressed restraining cables and cable nets.

The equilibrium of the bending-active beams in their target geometry is addressed according to the structural model previously introduced. As for the generation of pre-stressed restraining elements that are compatible with the equilibrium of the beams in their target geometry, specific methods have been developed which correspond to the following contributions:

- A graphical procedure has been formulated for the generation of 3D tensile restraining systems in equilibrium with coplanar loads and supports whose position is controlled from the spatial transformation of original 2D tensile restraining systems (Section 4.2). This procedure allows to graphically built 3D tensile restraining systems for the curve shaping of single bending-active beams in their plane of symmetry. More widely, the proposed procedure can be applied to the design of 3D tension-only or compression-only structures in equilibrium with coplanar loads.
- Specific 3D geometric patterns of cables which apply onto the beams' axis restraining forces that are in the beams' bending plane have been identified (Section 4.3). In combination with the proposed design strategies, such patterns of cables make it possible to address the design of bending-active tensile structures in a purely geometric way. Deriving from simple conditions of 2D equilibrium, the highlighted patterns of cables allow a large geometric exploration of bending-active tensile structures while ensuring that boundary conditions and mechanical properties of the beams can be found retrospectively so that static equilibrium can be reached in the geometric configurations so generated.
- A non-linear formulation of the force density method has been implemented and further elaborated for the form-finding of the cable nets compatible with the equilibrium of bending-active beams in their bending planes (Section 4.4). This constrained force density method makes it possible to address the design of bending-active tensile structures with complex geometry in terms of both the topology of the cable nets and the spatial arrangement of the beams.

6.1.3 Design application

The proposed approach for the form-driven design of bending-active tensile structures has been tested by means of a design case study. In particular, a lightweight bending-active tensile structure serving as an external sun-shading façade system has been developed in response to a given design task, with its own specifications and defined boundary conditions. Overall, the case study has proven the relevance and effectiveness of the proposed approach when applied to a real design scenario. With this regard, two main contributions have been made:

- The validity and relevance of the form-driven approach to conceptually design bending-active tensile structures in a design scenario where the geometry of the structures needs to be finely controlled and adjusted to fulfil their design purpose has been demonstrated.
- An integral design framework has been proposed, it is based on a parametric geometry-based definition of the bending-active tensile structures, thus allowing to efficiently integrate into the designed structures structural, architectural, manufacturing and other geometry-based considerations.

6.2 Limitations and further developments

Although the application of the proposed form-driven design approach for bending-active tensile structures to a real design scenario has established the strengths of the developed approach, this latter presents several limitations in its current implementation. These limitations relate simultaneously to the structural model, the design approach and the case study, and are underlined in the following paragraphs. In addition, in order to overcome these limits, various possibilities for improvement are suggested.

6.2.1 Structural model

The proposed structural model of bending-active beams is based on a series of assumptions on the mechanical behaviour of slender elastic beams. While these assumptions allow to make the model simple to understand and to implement, they also restrict its scope of applicability. The following limitations can be pointed out, and further developments can be suggested:

- The structural analysis which is used to determine the internal and external conditions allowing the equilibrium of a beam in a given target equilibrium geometry has a certain sensitivity with respect to the geometry of the plane continuous curves to which it is applied. A slight variation in the target equilibrium geometry can sometimes produce significantly different distributions of the bending stiffness or required restraining forces along the beam's axis. In order to take this dependence into consideration, different alternative curves near the original target equilibrium geometry could be automatically tested. This would allow, for instance, to have a distribution of bending stiffness that is more compatible with manufacturing constraints or to more controlled restraining forces, while keeping the global equilibrium geometry of the beams close to the original target.
- Another limiting aspect of the structural model is that it only applies to beams that deform in their plane of symmetry and are subjected to a bending moment only. This is due to the fact that the model does not describe torsion in the beams. It has been shown that it is not possible to model the effect of torsion using nodal forces applied to the discretised axis of the beams and the use of a unique force diagram. Future work would include further investigation to define a simple yet valid model to describe torsion in slender elastic beams.

6.2.2 Form-driven design approach

In relation to the form-driven design approach itself, the following limitations can be highlighted, and possible improvements suggested:

- During the various design operations of the proposed design approach, the value of a number of parameters has to be manually adjusted by the designer. Explicitly defining these parameters contributes to the intentional and controlled generation of bending-active tensile structures which is characteristically supported by this research. However, as the complexity of the structures increases, the number and interdependence of these parameters also increases. In order to support the designer in this task and to improve the effectiveness of the design process, automated procedures could then be considered to evaluate different values of these parameters which, although they all result in the same equilibrium geometry of the bending-active beams, have an influence on the structural state of equilibrium of the overall structures.
- The proposed form-driven design approach efficiently allows the creation of bending-active tensile structures which are in static equilibrium with the loads for which they have been designed. However, the use of form-finding methods remains necessary when it comes to assessing the behaviour of the structures of under load, determining their new equilibrium or evaluating the deformations occurring during their erection process. Such structural evaluation of the bending-active tensile structures is important and would need to be integrated to the proposed methodology to inform the design.
- The bending-active tensile structures which are designed with the proposed form-driven approach consists of bending-active beams and prestressed cables or cable nets. However, for architectural and structural reasons, it may be appropriate to use membranes instead of cables and cable nets. To this end, the non-linear force density method under constraints which has initially been formulated for cable nets (Section 4.4) would need to be extended to membrane elements (Maurin and Motro 1998).

In addition, it might be interesting to extend the form-driven approach originally formulated in this thesis for the design of bending-active tensile structures to other types of bending-active structures:

- A form-driven approach could thus be developed for the design of bending-active structures like grid-shells. The physical nature of the connections between the grid's bending-active beams will, however, condition the relevance of the approach as torsional moments can be generated in the structure if bending and torsional moments are transmitted from one beam to another (Nabaei et al. 2010, Du Peloux et al. 2015).

6.2.3 Design application

Although the case study of a bending-active tensile sun-shading façade system has demonstrated the potentials and strengths and of the form-driven approach for conceptual architectural design and the built structural prototype has

established a first step towards the development of the complete façade system, the further development of the system towards its full scale fabrication should be carried out in order to better assess the effectiveness of the proposed approach as part of a complete architectural design process and to integrate even more material and manufacturing constraints in the design process. In this context, Finite Element Analysis would be helpful in validating the results obtained with the form-driven approach and assessing more thoroughly the behaviour of the structure after its geometry has been designed.

Besides, the development of additional design experiments with the proposed form-driven approach would provide the chance to test the relevance and effectiveness of the approach in various design scenarios and at various scales.

Overall, the fabrication of a half scale structural prototype of the sun-shading façade system has highlighted the general need to further investigate the fabrication of bespoke structural components with non-uniform mechanical properties, be it at the geometric or material level. With this regard, future developments include the following suggestions:

- Composite materials and industrial lamination manufacturing processes could be explored in order to improve the bespoke fabrication of bending-active beams with non-constant bending stiffness along their length.
- The design of bending-active tensile structures with membranes according to the non-linear formulation of force density method suggested above would result in highly differentiated membranes whose materialisation could be addressed through knitting technology. The fabrication of bespoke architectural and structural knitted membranes is currently under active investigation and constitutes one of the development directions taken by current research on bending-active tensile structures (Ahlquist 2015, Popescu et al. 2018, Ramsgaard Thomsen et al. 2019).

6.3 Overview and final discussion

During the design process of bending-active tensile structures, the initiative and degree of influence of the designer is being limited by the physical laws which underlie the structures' equilibrium and by the nature and lack of transparency of the form-finding methods currently used to determine the structures' equilibrium geometry - a geometry that is not predictable other than by these methods. This lack of influence makes it difficult to control the structures' geometry and, consequently to integrate contextual, spatial, structural, functional, manufacturing and environmental consideration into the design in a direct and explicit way. This research was motivated by the observation that, in order to make the design process of bending-active tensile structures more intentional, it is desirable for the designer to gain more control during the design process, particularly at a geometric level. Aiming at a stronger integration of architectural and structural design, this thesis has shown, with the introduction of a novel design approach, that, despite the complex nature of bending-active tensile structures, it is possible to give the designer a leading role in the generation of these hybrid structures.

By breaking down the complex problem of form-finding of bending-active tensile structures into simpler sub-problems, i.e. by successively addressing the equilibrium of their bending-active elements and the equilibrium of their prestressed elements, the approach developed in this thesis gives the designer the possibility to have a direct control on the equilibrium geometry of the hybrid structures that are generated. In particular, it allows him/her to fully control the equilibrium geometry of the bending-active elements and to partially control the geometry of the tensile elements. Thanks to this geometric control, it becomes easier for the designer to give form to his/her intentions than with the use of conventional form-finding tools.

The proposed approach is aimed to be alternative and complementary to the form-finding methods that are commonly used. These methods are themselves varied and complementary to each other during the design process, none of them being well suited to address all the design phases of bending-active tensile structures. The so-called form-driven approach has valuable advantages during the early design phase since it gives more significance to the final equilibrium geometry, overcoming in this way the limitations of the form-finding methods in this respect.

The proposed form-driven approach has relied on graphical methods which, in combination with a simplified mechanical model of slender beams under bending, have demonstrated their ability to describe, generate and control the equilibrium of bending-active tensile structures.

In particular, in 2D space, force diagrams allow a simple and transparent understanding of the mechanisms involved in the equilibrium of bending-active

beams by offering a visualisation of the reciprocal dependencies between geometry, forces and mechanical quantities at play in their equilibrium. Force diagrams highlight indeed how bending stiffness, boundary conditions and applied loads relate to the equilibrium geometries of bending-active beams, and thus provide valuable guidance to the designer. In particular, through the construction and manipulation of force diagrams, the designer has the possibility to generate the bending-active beams of a bending-active tensile structure directly in their equilibrium geometry.

Apart from addressing the equilibrium of the bending-active beams, graphical methods also provide a relevant approach to generate the equilibrium of the tensile elements of bending-active tensile structures. Moreover, when necessary, graphical methods can be complemented by numerical methods with which they can be well combined.

Overall, the graphical methods developed in this research foster the intuitive and intentional design of bending-active tensile structures and make possible a better integration of the various architectural, structural, aesthetic, environmental and material aspects involved in the design process.

Besides its graphical nature, the form-driven approach is characterised by the introduction of gradients of mechanical and geometric properties within the bending-active tensile structures. As a matter of fact, in the context of structural systems whose form derives from the mechanical and geometric characteristics of their elements, the differentiation within the systems of these characteristics makes it possible to mediate and negotiate the structural and formal aspects of design. Thus, in order to achieve the desired structures' equilibrium geometry, it has been proposed to introduce, on the one hand, differences in bending stiffness along the beams' axis and, on the other hand, differences in force density within the cable nets. The introduction of mechanically and geometrically differentiated non-standard structural elements naturally raises the question of their manufacturing. The possibilities opened up by the field of digital fabrication provide a first solution to this issue and current advances and research point to a vast and promising field of exploration.

Paradoxically, although the structural principle of active bending originates in the elastic deformations of slender elements, these deformations are neglected in the mechanical model of slender elastic beams and the design approach proposed in this thesis. Indeed, the main focus is not so much on the elastic deformations occurring at the microscopic scale as on their effect at the macroscopic scale, that of the beams. This is the reason why the large deformations of the bending-active beams are described more by geometric quantities than by mechanical quantities. The variations in beams' bending stiffness which participate in the geometric control of the structures can also be generated and governed by geometric quantities, namely their quadratic moment of inertia. Moreover, similar as for the bending-active beams, for cables and cable nets

the graphical and numerical methods which have been developed and used in this thesis are based only on geometric quantities and neglect the microscopic deformation of the elements under tension.

In this way, by extracting the geometric quantities at play in the equilibrium of bending-active tensile structures, while playing on differentiation of their mechanical quantities, this research has shown that it is possible under certain conditions to describe and generate bending-active tensile structures entirely in a geometric manner, a first approximation that is well suited to the initial phase of the design. Mechanical properties which are related to the materialisation of the structures are involved in the calibration of the forces and the calculation of the maximum stresses.

Moreover, in addition to allowing a geometric control of the generated structures, the proposed approach has the advantage of not providing the designer with a unique solution to the design problem which is addressed, as it is the case with a traditional form-finding tool. Conversely, the approach opens up a range of various design possibilities. To do this, it takes advantage of the fact that, as evidenced by the study of its force diagram, in the plane, a curve can be materialised by distinct bending-active beams. Such multiplicity of solutions makes it possible to efficiently mediate the various contextual, spatial, structural, functional, constructive and environmental aspects of the design, a mediation necessary to a holistic approach to design.

Overall, thanks to the rapprochement of architectural and structural design it promotes, it is hoped that the form-driven approach elaborated in this thesis for the design of bending-active tensile structures in architecture will contribute to the development of their full potential as lightweight architectural structures like spatial installations, temporary or mobile housings, or architectural façade components.

References

- Addis, B.: 2007, *Building: 3000 Years of Design Engineering and Construction*, Phaidon, London & New-York.
- Adriaenssens, S. and Barnes, M. R.: 2001, Tensegrity Spline Beam and Grid Shell Structures, *Engineering Structures* **23**, 29–36.
- Ahlquist, S.: 2015, Integrating Differentiated Knit Logics and Pre-Stress in Textile Hybrid Structures Hybrid Structures, *Modelling Behaviour, Design Modelling Symposium 2015*, Copenhagen, Denmark, pp. 101–111.
- Ahlquist, S., Kampowski, T., Torghabehi, O. O., Menges, A. and Speck, T.: 2015, Development of a Digital Framework for the Computation of Complex Material and Morphological Behavior of Biological and Technological Systems, *Computer-Aided Design* **60**, 84–104.
- Ahlquist, S., Lienhard, J., Knippers, J. and Menges, A.: 2013, Exploring Material Reciprocities for Textile-Hybrid Systems as Spatial Structures, in M. Stacey (ed.), *Prototyping Architecture: The Conference Papers*, London, pp. 187–210.
- Ahlquist, S. and Menges, A.: 2013, Frameworks for Computational Design of Textile Micro-Architectures and Material Behavior in Forming Complex Force-Active Structures, *Proceedings of ACADIA 2013: Adaptive Architecture*, Cambridge, Canada, pp. 281–292.
- Akbarzadeh, M., Van Mele, T. and Block, P.: 2014, Compression-only Form Finding through Finite Subdivision of the Force Polygon, *Proceedings of the IASS-SLTE 2014 Symposium: Shells, Membranes and Spatial Structures: Footprints*, Brasilia, Brazil.
- Akbarzadeh, M., Van Mele, T. and Block, P.: 2015, Three-Dimensional Compression Form Finding through Subdivision, *Proceedings of the International Association for Shell and Spatial Structures (IASS) Symposium 2015: Future Visions*, Amsterdam, The Netherlands.
- Akbarzadeh, M., van Mele, T. and Block, P.: 2016, Three-Dimensional Graphic Statics : Initial Explorations with Polyhedral Form and Force Diagrams, *International Journal of Space Structures* **31**(2), 217–226.

- Aldinger, L., Margariti, G., Körner, A., Suzuki, S. and Knippers, J.: 2018, Tailoring Self-Formation Fabrication and Simulation of Membrane-Actuated Stiffness Gradient Composites, *Proceedings of the IASS Symposium 2018*, Boston, MA.
- Alpermann, H. and Gengnagel, C.: 2012, Shaping Actively-Bent Elements by Restraining Systems, *Proceedings of the IASS-APCS 2012: From Spatial Structures to Space Structures*, Seoul, Korea.
- Alpermann, H. and Gengnagel, C.: 2013, Restraining Actively-Bent Structures by Membranes, *Structural Membranes 2013: VI International Conference on Textile Composites and Inflatable Structures*, Munich, Germany.
- Alvarez, M. E., Martínez-Parachini, E. E., Baharlou, E., Krieg, O. D., Schwinn, T., Vasey, L., Hua, C., Menges, A. and Yuan, P. F.: 2018, Tailored Structures, Robotic Sewing of Wooden Shells, *Robotic Fabrication in Architecture, Art and Design 2018*, Zurich, Switzerland, pp. 405–420.
- Audoly, B. and Pomeau, Y.: 2010, *Elasticity and Geometry, From Hair Curls to the Non-Linear Response of Shells*, Oxford University Press, Oxford, UK.
- Bamboo Structure Project / Pouya Khazaeli Parsa: 2010. <https://www.archdaily.com/93922/bamboo-structure-project-pouya-khazaeli-parsa/> (Accessed: 2019-07-29).
- Barnes, M. R.: 1975, Applications of Dynamic Relaxation to the Design and Analysis of Cable, Membrane and Pneumatic Structures, *2nd International Conference on Space Structure*, Guildford, UK, pp. 74–94.
- Barnes, M. R.: 1980, Non-Linear Numerical Solution Methods for Static and Dynamic Analysis of Tension Structures, *Air-supported Structures: the State of the Art, Institution of Structural Engineers Symposium*, London, UK, pp. 8–56.
- Barnes, M. R.: 1999, Form Finding and Analysis of Tension Structures by Dynamic Relaxation, *International Journal of Space Structures* **14**(2), 89–104.
- Barnes, M. R.: 2000, Form and Stress Modeling of Tension Structures, in M. R. Barnes and M. Dickson (eds), *Widespan Roof Structures*, Thomas Telford, pp. 21–40.
- Barnes, M. R., Adriaenssens, S. and Krupka, M.: 2013, A Novel Torsion / Bending Element for Dynamic Relaxation Modeling, *Computers and Structures* **119**, 60–67.
- Bauer, A. M., Längst, P., La Magna, R., Lienhard, J., Piker, D., Quinn, G., Gengnagel, C. and Bletzinger, K.-U.: 2018, Exploring Software Approaches

-
- for the Design and Simulation of Bending Active Systems, *Proceedings of the IASS Symposium 2018*, Boston, USA.
- Bauer, A. M., Längst, P., Wüchner, R. and Bletzinger, K.-U.: 2017, Isogeometric Analysis for Modeling and Simulation of Building Processes, *Proceedings of the IASS Annual Symposium 2017*, Hamburg, Germany.
- Bechert, S., Knippers, J., Krieg, O. D., Menges, A., Schwinn, T. and Sonntag, D.: 2016, Textile Fabrication Techniques for Timber Shells - Elastic Bending of Custom-laminated Veneer for Segmented Shell Construction Systems, *Advances in Architectural Geometry 2016*, Zurich, Switzerland, pp. 154–169.
- Bergman, C. A. and McEwen, E.: 1997, Sinew-Reinforced and Composite Bows, Technology, Function and Social Implications, in H. Knecht (ed.), *Projectile Technology*, Springer, Boston, USA, chapter 6, pp. 143–160.
- Bernoulli, J.: 1694, *Curvatura Laminae Elasticae. Ejus identitas com curvatura lintei a pondere inclusi fluidi expansi. Radii circulatorum osculantium in terminis simplicissimis exhibiti; una cum novis quibusdam theormatis huc pertinentibus, etc.*, Acta Eruditorum, Lipsiae.
- Bessai, T.: 2013, Bending-Active Bundled Structures: Preliminary Research and Taxonomy towards an Ultra-Light Weight Architecture of Differentiated Components, *Proceedings of Annual Conference of the Association for Computer-Aided Design in Architecture - ACADIA 2013: Adaptive Architecture*, Cambridge, Ontario, Canada, pp. 293–300.
- Bessini, J., Lázaro, C. and Monleón, S.: 2017, A Form-Finding Method Based on the Geometrically Exact Rod Model for Bending-Active Structures, *Engineering Structures* **152**, 549–558.
- Beukers, A. and van Hinte, E.: 2005, *Lightness, The Inevitable Renaissance of Minimum Energy Structures*, fourth rev edn, 010 publishers, Rotterdam.
- Bishop, R. L.: 1975, There Is More than One Way to Frame a Curve, *The American Mathematical Monthly* **82**, 246–251.
- Bletzinger, K.-U. and Ramm, E.: 1999, A General Finite Element Approach to the Form Finding of Tensile Structures by the Updated Reference Strategy, *International Journal of Space Structures* **14**(2), 131–145.
- Block, P.: 2009, *Thrust Network Analysis, Exploring Three-dimensional Equilibrium*, PhD thesis, Massachusetts Institute of Technology, Cambridge, MA, USA.
- Bouaziz, S., Deuss, M., Schwartzburg, Y., Weise, T. and Pauly, M.: 2012, Shape-Up: Shaping Discrete Geometry with Projections, *Eurographics Symposium on Geometry Processing 2012*, Vol. 31.

- Boulic, L.: 2020, Graphical Method for the Construction of Pairs of 3D Skew Funiculars in Equilibrium with Coplanar Loads and Controlled Supports' Positions, *Structural Concrete* . (Accepted for publication).
- Boulic, L., D'Acunto, P., Bertagna, F. and Castellón, J.: 2020, Form-Driven Design of a Bending-Active Tensile Façade System, *International Journal of Space Structures* . (Accepted for publication).
- Boulic, L. and Schwartz, J.: 2017, Graphic Statics Principles for the Design of Actively Bent Elements Shaped with Restraining Systems, *Proceedings of the IASS Annual Symposium 2017*, Hamburg, Germany.
- Boulic, L. and Schwartz, J.: 2018, Design Strategies of Hybrid Bending-Active Systems Based on Graphic Statics and a Constrained Force Density Method, *Journal of the International Association for Shell and Spatial Structures* **59**(4), 267–275.
- Brancart, S., Popovic Larsen, O., De Laet, L. and De Temmerman, N.: 2019, Rapidly Assembled Reciprocal Systems with Bending-Active Components: the ReciPlyDome, *Journal of the International Association for Shell and Spatial Structures* **60**(1), 65–77.
- Brütting, J., Körner, A., Sonntag, D. and Knippers, J.: 2017, Bending-Active Segmented Shells, *Proceedings of the IASS Annual Symposium 2017*, Hamburg, Germany.
- Burhardt, B. (ed.): 1978, *IL13 - Multihalle Mannheim*, Institut für leichte Flächentragwerke, Stuttgart.
- Cataldi, G.: 1997, Structural Types, in P. Oliver (ed.), *Encyclopedia of Vernacular Architecture of the World, Volume 1 - Theories and Principles*, Cambridge University Press, pp. 644–654.
- Cremona, L.: 1872, *Le Figure Reciproche nella Statica Grafica*, Tipografia di Giuseppe Bernardoni, Milano.
- Culmann, K.: 1866, *Die Graphische Statik*, Meller & Zeller, Zurich.
- Cuvilliers, P., Yang, J. R., Coar, L. and Mueller, C.: 2018, A Comparison of Two Algorithms for the Simulation of Bending-Active Structures, *International Journal of Space Structures* **33**(2)(73-85).
- D'Acunto, P., Jasienski, J.-P. and Ohlbrock, P. O.: 2017, Vector-Based 3D Graphic Statics : Transformations of Force Diagrams, *Proceedings of the IASS Annual Symposium 2017*, Hamburg, Germany.
- D'Acunto, P. and Kotnik, T.: 2013, AA / ETH Pavilion, *Proceedings of the TensiNet Symposium 2013*, Istanbul, Turkey, pp. 99–108.

- D'Amico, B., Kermani, A. and Zhang, H.: 2014, Form Finding and Structural Analysis of Actively Bent Timber Grid Shells, *Engineering Structures* **81**, 195–207.
- D'Amico, B., Zhang, H. and Kermani, A.: 2016, A Finite-Difference Formulation of Elastic Rod for the Design of Actively Bent Structures, *Engineering Structures* **117**, 518–527.
- Day, A.: 1965, An Introduction to Dynamic Relaxation, *Engineer* **219**, 218–221.
- Day, A. and Bunce, J.: 1969, The Analysis of Hanging Roofs, *The Arup Journal* **4**(3), 30–31.
- De Laet, L., Slabbinck, E., Van Mele, T., Block, P. and Mollaert, M.: 2013, Case Study: A Modular, Self-Tensioned, Bending-Active Canopy, *Proceedings of the IASS Annual Symposium 2013*, Wroclaw, Poland.
- Deleuran, A. H., Schmeck, M., Quinn, G., Gengnagel, C., Tamke, M. and Thomsen, M. R.: 2015, The Tower: Modelling, Analysis and Construction of Bending-Active Tensile Membrane Hybrid Structures, *Proceedings of the IASS Annual Symposium 2015*, Amsterdam, The Netherlands.
- Dieringer, F., Philipp, B., Wüchner, R. and Bletzinger, K.-U.: 2013, Numerical Methods for the Design and Analysis of Hybrid Structures, *International Journal of Space Structures* **28**(3&4), 149–160.
- Dill, E. H.: 1992, Kirchhoff's Theory of Rods, *Archives for History of Exact Sciences* **44**(1), 1–23.
- Douthe, C., Baverel, O. and Caron, J.-F.: 2006, Form-Finding of a Grid Shell in Composite Materials, *Journal of the International Association for Shell and Spatial Structures* **47**(150), 53–62.
- Du Peloux, L., Tayeb, F., Baverel, O. and Caron, J.-F.: 2016, Construction of a Large Composite Gridshell Structure: A Lightweight Structure Made with Pultruded Glass Fibre Reinforced Polymer Tubes, *Structural Engineering International* **26**(2), 160–167.
- Du Peloux, L., Tayeb, F., Lefevre, B., Baverel, O. and Caron, J.-F.: 2015, Formulation of a 4-DoF Torsion / Bending Element for the Form-Finding of Elastic Gridshells, *Proceedings of the IASS Annual Symposium 2015*, Amsterdam, The Netherlands.
- Engel, H.: 1967, *Tragsysteme Structure Systems*, 1997 edn, Verlag Gerd Hatje.
- Euler, L.: 1744, *Methodus inveniendi, Lineas curvas, Maximi Minimive proprietate gaudentes, Additamentum I, 'De curvis elasticis'*.

- Fearson, A.: 2012, Wind and Water Bar by Vo Trong Nghia. <https://www.dezeen.com/2012/09/03/wind-and-water-bar-by-vo-trong-nghia/>, (Accessed: 2019-07-30).
- Fivet, C.: 2016, Projective Transformations of Structural Equilibrium, *International Journal of Space Structures* **31**(2-4), 135–146.
- Fleischmann, M., Knippers, J., Lienhard, J., Menges, A. and Schleicher, S.: 2012, Material Behaviour: Embedding Physical Properties in Computational Design Processes, *Architectural Design, Material Computation: Higher Integration in Morphogenetic Design* **82**(2), 44–51.
- Fleischmann, M. and Menges, A.: 2011, ICD / ITKE Research Pavilion: A Case Study of Multi-disciplinary Collaborative Computational, *Proceedings of the Design Modeling Symposium 2011*, Berlin, Germany, pp. 239–248.
- Frey, P.: 2010, *Learning from Vernacular, towards a New Vernacular Architecture*, Actes Sud, Arles.
- Fuller, R. B.: 1975, *Synergetics, Explorations in the Geometry of Thinking*, Macmillan Publishing Co., New-York.
- Gass, S.: 1990, *IL 25 - Form Force Mass 5 - Experiments*, Institut für leichte Flächentragwerke, Stuttgart.
- Haber, R. and Abel, J.: 1982, Initial Equilibrium Solution Methods for Cable, *Computer Methods in Applied Mechanics and Engineering* **30**, 263–284.
- Hamilton, B.: 2017, The North Face and R. Buckminster Fuller Special Connection - Part 2: Oval Intention – The Epistemic Tent. <https://www.outinunder.com/content/north-face-and-r-buckminster-fuller-special-connection-part-2> (Accessed: 2019-07-30).
- Hanson, A. J. and Ma, H.: 1995, Parallel Transport Approach to Curve Framing, *Technical report*, Department of Computer Science, Indiana University.
- Harris, R., Romer, J., Kelly, O. and Johnson, S.: 2003, Design and Construction of the Downland Gridshell, *Building Research and Information* **31**(6), 427–454.
- Harris, R. and Roynon, J.: 2008, The Savill Garden Gridshell Design and Construction, *Structural Engineer* **86**(17), 27–34.
- Haug, E.: 1972, *Finite Element Analysis of Nonlinear Membrane Structures*, PhD thesis, University of Berkeley, California.
- Hudert, M. and Weinand, Y.: 2011, Timberfabric : Innovative Lightweight Structures, *IABSE-IASS Symposium 2011*, London, UK.

- Huerta, S.: 2006, Structural Design in the Work of Gaudí, *Architectural Science Review* **49**(4), 324–339.
- Huerta, S.: 2010, Designing by Geometry: Rankine's Theorems of Transformation of Structures, in P. Cassinello, S. Huerta, J. M. de PradaPoole and R. S. Lampreave (eds), *Geometry and Proportion in Structural Design, Essays in Ricardo Aroca's Honour*, Editorial Lampreave, Madrid, pp. 263–285.
- Hughes, T. J., Cottrell, J. A. and Bazilevs, Y.: 2005, Isogeometric Analysis: CAD, Finite Elements, NURBS, Exact Geometry and Mesh Refinement, *Computer Methods in Applied Mechanics and Engineering* **194**, 4135–4195.
- Karl-Eugen, K.: 2008, *The History of the Theory of Structures From Arch Analysis to Computational Mechanics*, Ernst & Sohn, Berlin.
- Kelly, O., Harris, R., Dickson, M. and Rowe, J.: 2001, Construction of the Downland Gridshell, *The Structural Engineer* **79**(17), 25–33.
- Kilian, A.: 2014, Steering of Form, in S. Adriaenssens, P. Block, D. Veenendaal and C. Williams (eds), *Shell Structures for Architecture, Form Finding and Optimization*, Routledge, New-York, pp. 131–139.
- Kilian, A. and Ochsendorf, J.: 2005, Particule-Spring Systems for Structural Form Finding, *Journal of the International Association for Shell and Spatial Structures* **46**(147).
- Knippers, J., Scheible, F., Oppe, M. and Jungjohann, H.: 2012, Bio-inspired Kinetic GFRP-façade for the Thematic Pavilion of the EXPO 2012 in Yeosu, *IASS-APCS Symposium 2012: From Spatial Structures to Space Structures*, Seoul, Korea.
- Körner, A., Born, L., Mader, A., Sachse, R., Saffarian, S., Wertermeier, A. S., Poppinga, S., Bischoff, M., Gresser, G. T., Milwich, M., Speck, T. and Knippers, J.: 2018, Flectofold - A Biomimetic Compliant Shading Device for Complex Free Form Facades, *Smart Materials and Structures* **27**.
- Kotelnikova-Weiler, N., Douthe, C., Lafuente Hernandez, E., Baverel, O., Gengnagel, C. and Caron, J.-F.: 2013, Materials for Actively-Bent Structures, *International Journal of Space Structures* **28**(3 & 4).
- Kwok, N.: 2015a, Vo Trong Nghia Constructs Conference Hall Using Two Types of Bamboo in Vietnam. <https://www.designboom.com/architecture/vo-trong-nghia-architects-conference-hall-naman-spa-and-resort-vietnam-10-19-2015/> (Accessed: 2019-07-30).
- Kwok, N.: 2015b, Vo Trong Nghia's Naman Beach Bar Combines Bamboo, Thatch and Stone. <https://www.designboom.com/architecture/vo-trong-nghia-architects-conference-hall-naman-spa-and-resort-vietnam-10-19-2015/>

- nghia-architects-naman-retreat-beach-bar-danang-vietnam-09-25-2015/*
(Accessed: 2019-07-30).
- La Magna, R., Fragkias, V., Längst, P., Lienhard, J., Noël, R., Baranovskaya, Y., Tamke, M. and Thomsen, M. R.: 2018, Isoropia: an Encompassing Approach for the Design, Analysis and Form-Finding of Bending-Active Textile Hybrids, *Proceedings of the IASS Symposium 2018*, Boston, USA.
- La Magna, R., Schleicher, S. and Knippers, J.: 2016, Bending-Active Plates: Form and Structure, *Advances in Architectural Geometry 2016*, pp. 170–186.
- Lachauer, L. and Block, P.: 2012, Compression Support Structures for Slabs, in L. Hesselgren, S. Sharma, J. Wallner, N. Baldassini, P. Bompas and J. Raynaud (eds), *Proceedings of Advances in Architectural Geometry 2012*, Springer Vienna, Paris, France.
- Lachauer, L. and Block, P.: 2014, Interactive Equilibrium Modelling, *International Journal of Space Structures* **29**(1).
- Längst, P., Bauer, A. M., Michalski, A. and Lienhard, J.: 2017, The Potentials of Isogeometric Analysis Methods in Integrated Design Processes, *Proceedings of the IASS Annual Symposium 2017*, Hambourg, Germany.
- Lázaro, C., Bessini, J. and Monleón, S.: 2018, Mechanical Models in Computational Form Finding of Bending-Active Structures, *International Journal of Space Structures* **33**(2), 86–97.
- Le Ricolais, R.: 1973, Interviews with Robert Le Ricolais - 'Things themselves are lying, and so are their images', in J. Bryan and R. Sauer (eds), *Structures Implicit and Explicit - VIA*, Vol. 2, Graduate School of Fine Arts, University of Pennsylvania, Philadelphia, pp. 80–109.
- Lefevre, B., Tayeb, F., Du Peloux, L. and Caron, J.-f.: 2017, A 4-Degree-of-Freedom Kirchhoff Beam Model for the Modeling of Bending – Torsion Couplings in Active-Bending Structures, *International Journal of Space Structures* **32**(2), 69–83.
- Lenczner, E. A. R.: 1994, The Design of the Stone Facade to the Pavilion of the Future, Expo'92, Seville, *The Structural Engineer* **72**(11), 171–177.
- Levien, R.: 2008, The Elastica: a Mathematical History, *Technical report*, University of California at Berkeley.
- Lienhard, J.: 2014, *Bending-Active Structures: Form-Finding Strategies Using Elastic Deformation in Static and Kinematic Systems and the Structural Potentials Therein*, PhD thesis, Universität Stuttgart, Stuttgart.

- Lienhard, J., Ahlquist, S., Menges, A. and Knippers, J.: 2013, Extending the Functional and Formal Vocabulary of Tensile Membrane Structures Through the Interaction with Bending-Active Elements, *Proceedings of the TensiNet Symposium 2013*, Istanbul, Turkey.
- Lienhard, J., Alpermann, H., Gengnagel, C. and Knippers, J.: 2013, Active Bending, a Review on Structures where Bending is used as a Self-Formation Process, *International Journal of Space Structures* **28**(3 & 4).
- Lienhard, J., Bergmann, C., La Magna, R. and Runberger, J.: 2017, A Collaborative Model for the Design and Engineering of a Textile Hybrid Structure, *Proceedings of the IASS Annual Symposium 2017*, Hamburg, Germany.
- Lienhard, J. and Gengnagel, C.: 2018, Recent Developments in Bending-Active Structures, *Proceedings of the IASS Annual Symposium 2018*, Boston, USA.
- Lienhard, J. and Knippers, J.: 2012, Permanent and Convertible Membrane Structures with Intricate Bending-Active Support Systems, *Proceedings of the International IASS Symposium 2012*, Seoul, Korea.
- Lienhard, J. and Knippers, J.: 2013, Considerations on the Scaling of Bending-Active Structures, *International Journal of Space Structures* **28**(3-4), 137–147.
- Lienhard, J. and Knippers, J.: 2015, Bending-Active Textile Hybrids, *Journal of the International Association for Shell and Spatial Structures* **56**(1), 37–48.
- Lienhard, J., La Magna, R. and Knippers, J.: 2014, Form-Finding Bending-Active Structures with Temporary Ultra-elastic Contraction Elements, *WIT Transactions on the Built Environment* **136**, 107–116.
- Lienhard, J., Riederer, J., Jungjohann, H., Oppe, M. and Knippers, J.: 2013, Multifunctional Adaptive Facade at IBA 2013, *Structural Membranes 2013: VI International Conference on Textile Composites and Inflatable Structures*, Munich, Germany.
- Lienhard, J., Schleicher, S. and Knippers, J.: 2015, Bio-inspired, Flexible Structures and Materials, in F. Pacheco Torgal, J. Labrincha, M. Diamanti, C.-P. Yu and H. Lee (eds), *Biotechnologies and Biomimetics for Civil Engineering*, Springer International Publishing, chapter 11, pp. 275–296.
- Lienhard, J., Schleicher, S., Poppinga, S., Masselter, T., Milwich, M., Speck, T. and Knippers, J.: 2011, Flectofin: A Hingeless Flapping Mechanism Inspired by Nature, *Bioinspiration and Biomimetics* **6**(4).
- Linkwitz, K. and Schek, H.-J.: 1971, Einige Bemerkungen zur Berechnung von vorgespannten Seilnetzkonstruktionen, *Ingenieur-Archiv* **40**(3), 145–158.

- Liuti, A., Mazzola, C. and Zanelli, A.: 2018, Where Design Meets Construction: a Review of Bending-Active Structures, *Proceedings of the IASS Annual Symposium 2018*, Boston, USA.
- LLC, L. T.: 2013, Ladybug Tools. <https://www.ladybug.tools> (Accessed: 2019-07-08).
- Mairs, J.: 2017, Arched Bamboo Trusses Left Exposed in Chiang Mai Sports Hall to Create a "Feast to the Eye". <https://www.dezeen.com/2017/08/21/chiangmai-life-architects-construction-sports-hall-panyaden-international-school-thailand-arching-bamboo-trusses/> (Accessed: 2019-07-29).
- Malcolm, C. W.: 1914, *A Text Book on Graphic Statics*, first edit edn, M.C. Clark Publishing Co., New-York and Chicago.
- Malerba, P. G., Patelli, M. and Quagliaroli, M.: 2012, An Extended Force Density Method for the Form Finding of Cable Systems with New Forms, *Structural Engineering & Mechanics* **42**(2), 191–210.
- Mardaljevic, J., Andersen, M., Roy, N. and Christoffersen, J.: 2012, Daylighting, Artificial Lighting and Non-Visual Effects Study for a Residential Building, *Technical report*.
- Marks, R. W.: 1960, *The Dymaxion World of Buckminster Fuller*, Reinhold Publishing Corporation, New-York.
- Maurin, B. and Motro, R.: 1998, The Surface Stress Density Method as a Form-Finding Tool for Tensile Membranes, *Engineering Structures* **20**(8), 712–719.
- Mazzola, C., Stimpfle, B., Zanelli, A. and Canobbio, R.: 2019, TemporActive Pavilion: First Loop of Design and Prototyping of an Ultra-Lightweight Temporary Architecture, *Proceedings of the TensiNet Symposium 2019*, Milan, Italy, pp. 390–401.
- Menges, A.: 2012, Material Resource Fullness, Activating Material Information in Computational Design, *Architectural Design - Material Computation: Higher Integration in Morphogenetic Design* **82**(2), 34–43.
- Motro, R.: 2009, An Approach to Structural Morphology, in R. Motro (ed.), *An Anthology of Structural Morphology*, World Scientific, Singapour, pp. 15–32.
- Nabaei, S. S., Baverel, O. and Weinand, Y.: 2010, Form Finding of Twisted Interlaced Structures: a Hybrid Approach, *Advances in Architectural Geometry 2010*, pp. 127–143.
- Nabaei, S. S., Baverel, O. and Weinand, Y.: 2013, Mechanical Form-Finding of the Timber Fabric Structures with Dynamic Relaxation Method, *International Journal of Space Structures* **28**(3-4), 197–214.

- Nabaei, S. S., Baverel, O. and Weinand, Y.: 2015, Form-Finding of Interlaced Space Structures Using Constrained Nonlinear Optimization, *International Journal of Space Structures* **30**(3-4), 273–285.
- nARCHITECTS: 2006, Windshape. <http://narchitects.com/work/windshape-2/> (Accessed: 2019-07-29).
- nARCHITECTS: 2016, Polycentric Pavilion. <http://narchitects.com/work/polycentric-pavilion/> (Accessed: 2019-07-29).
- Navier, H.: 1826, *Résumé des leçons données à l'École des Ponts et Chaussées sur l'Application de la Mécanique à l'Établissement des Constructions et des Machines*, Firmin-Didot, Paris.
- Nicholas, P. and Tamke, M.: 2012, Engaging a Bespoke Material Practice in Digitally Designed Materials, *Physical Digitality: Proceedings of the 30th eCAADe Conference*, Vol. 2, pp. 681–690.
- Niiranen, J.: 2013, Radical Wood Pavilion, *PUU Wood magazine*.
- Off, R.: 2010, New Trends on Membrane and Shell Structures - Examples of Bat-Sail and Cushion-Belt Technologies, in P. J. S. Cruz (ed.), *Structures and Architecture: Proceedings of the First International Conference on Structures and Architecture*, Guimarães, Portugal, pp. 25–28.
- Ohlbrock, P. O., D'Acunto, P., Jasienski, J.-P. and Fivet, C.: 2017, Constraint-Driven Design with Combinatorial Equilibrium Modelling, *Proceedings of the IASS Annual Symposium 2017*, Hambourg, Germany.
- Otter, J. and Day, A.: 1960, Tidal Flow Computations, *Engineer* **209**, 117–182.
- Otto, F.: 1990, Preface, *IL 25 - Form Force Mass 5 - Experiments*, Institut für leichte Flächentragwerke, Stuttgart, p. 0.6.
- Oxman, N.: 2012, Material computation, in B. Sheil (ed.), *Manufacturing the Bespoke, Making and Prototyping Architecture*, ad reader edn, John Wiley & Sons Ltd, pp. 256–265.
- Philipp, B. and Bletzinger, K.-U.: 2013, Hybrid Structures - Enlarging the Design Space of Architectural Membranes, *Journal of the International Association for Shell and Spatial Structures* **54**(178), 281–291.
- Piker, D.: n.d., Kangaroo3d. <http://kangaroo3d.com/> (Accessed: 2019-07-05).
- Pirazzi, C. and Weinand, Y.: 2006, Geodesic Lines on Free-Form Surfaces: Optimized Grids for Timber Rib Shells, *9th World Conference on Timber Engineering*, pp. 72–79.

- Pone, S., Colabella, S., Parenti, B., Lancia, D., Fiore, A., D'Amico, B., Portioli, F., Landolfo, R., D'Aniello, M. and Ceraldi, C.: 2013, Construction and Form-Finding of a Post-Formed Timber Grid-Shell, *International Conference on Structures and Architecture*, number July, pp. 245–252.
- Popescu, M., Reiter, L., Liew, A., Van Mele, T., Flatt, R. J. and Block, P.: 2018, Building in Concrete with an Ultra-lightweight Knitted Stay-in-place Formwork: Prototype of a Concrete Shell Bridge, *Structures* **14**, 322–332.
- Purpura, W. T.: 2018, Bamboo Club + Cafe by VTN Architects Takes Center Stage in the Heart of Vietnam. <https://www.designboom.com/architecture/vtn-architects-bamboo-club-cafe-vietnam-vinh-06-21-2018/>, (Accessed: 2019-07-30).
- Puystiens, S., Van Craenenbroeck, M., Van Hemelrijck, D., Van Paepegem, W., Mollaert, M. and De Laet, L.: 2019a, Implementation of Bending-Active Elements in Kinematic Form-Active Structures – Part I: Design of a Representative Case Study, *Composite Structures* **216**(March), 436–448.
- Puystiens, S., Van Craenenbroeck, M., Van Hemelrijck, D., Van Paepegem, W., Mollaert, M. and De Laet, L.: 2019b, Implementation of Bending-Active Elements in Kinematic Form-Active Structures – Part II: Experimental Verification, *Composite Structures* **213**(January), 1–13.
- Quinn, G., Deleuran, A. H., Piker, D., Brandt-Olsen, C., Tamke, M., Thomsen, M. R. and Gengnagel, C.: 2016, Calibrated and Interactive Modelling of Form-Active Hybrid Structures, *Proceedings of the IASS Annual Symposium 2016*, Tokyo, Japan.
- Ramsgaard Thomsen, M., Sinke Baranovskaya, Y., Monteiro, F., Lienhard, J., La Magna, R. and Tamke, M.: 2019, Systems for Transformative Textile Structures in CNC Knitted Fabrics – Isoropia, *Proceedings of the TensiNet Symposium 2019*, Milan, Italy, pp. 95–110.
- Ritter, W. and Culmann, K.: 1900, *Anwendungen der Graphischen Statik nach Professor Dr. C. Culmann*, Meller & Zeller, Zürich.
- Robert McNeel & Associates: n.d., Rhinoceros. <https://www.rhino3d.com/> (Accessed: 2019-07-05).
- Roland, C.: 1965, *Frei Otto - Spannweiten: Ideen und Versuche zum Leichtbau*, Ullstein, Frankfurt am Main.
- Rombouts, J., Lombaert, G., De Laet, L. and Schevenels, M.: 2018, On the Equivalence of Dynamic Relaxation and the Newton-Raphson Method, *International Journal for Numerical Methods in Engineering* **113**(9), 1531–1539.

- Rutten, D.: 2009, Grasshopper - Algorithmic Modeling for Rhino. <https://www.grasshopper3d.com/> (Accessed: 2019-07-05).
- Schek, H.-J.: 1974, The Force Density Method for Form Finding and Computation of General Networks, *Computer Methods in Applied Mechanics and Engineering* **3**, 115–134.
- Schleicher, S., La Magna, R. and Zabel, J.: 2017, Bending-Active Sandwich Shells: Studio One Research Pavilion 2017, *Disciplines and Disruption - Proceedings Catalog of the 37th Annual Conference of the Association for Computer Aided Design in Architecture, ACADIA 2017*, pp. 544–551.
- Schwartz, J.: 2010, Bending and Confusion: The Long Development of Bending Theory and its Impact on the Design and Construction of Beams, in M. Rinke and J. Schwartz (eds), *Before Steel: The Introduction of Structural Iron and its Consequences*, Niggli, Zürich, pp. 193–209.
- SIA 265/1:2009 *Construction en bois - Spécifications complémentaires*: 2009, Norm, Société Suisse des Ingénieurs et des Architectes.
- Sistaninia, M., Hudert, M., Humbert, L. and Weinand, Y.: 2013, Experimental and Numerical Study on Structural Behavior of a Single Timber Textile Module, *Engineering Structures* **46**, 557–568.
- Slabbinck, E., Suzuki, S., Solly, J., Mader, A. and Knippers, J.: 2017, Conceptual Framework for Analyzing and Designing Bending-Active Tensile Hybrid Structures, *Proceedings of the IASS Annual Symposium 2017*.
- SoFiSTiK AG: n.d., SoFiSTiK. <https://www.sofistik.com> (Accessed: 2019-10-23).
- Stevin, S.: 1586, *De Beghinselen der Weeghconst*, Raphelengius, Leiden.
- Suzuki, S. and Knippers, J.: 2017, ElasticSpace: A Computational Framework for Interactive Form-Finding of Textile Hybrid Structures through Evolving Topology Networks, *International Journal of Parallel, Emergent and Distributed Systems* **32**(sup1), 4–14.
- Suzuki, S., Körner, A. and Knippers, J.: 2018, IGUANA : Advances on the Development of a Robust Computational Framework for Active-Geometric and -Topologic Modeling of Lightweight Structures., *Proceedings of the IASS Symposium 2018*, Boston, MA.
- Tamke, M., Baranovskaya, Y., Deleuran, A. H., Monteiro, F., Fanguero, R. M. E. S., Stranghöfner, N., Uhlemann, J., Schmeck, M., Gengnagel, C. and Thomsen, M. R.: 2016, Bespoke Materials For Bespoke Textile Architecture, *Proceedings of the IASS Annual Symposium 2016*, Tokyo, Japan.

- Tamke, M., Nicholas, P., Ramsgaard Thomsen, M., Jungjohann, H. and Markov, I.: 2012, Graded Territories: Towards the Design, Specification, and Simulation of Materially Graded Bending-Active Structures, *Acadia 2012: Synthetic Digital Ecologies*, pp. 79–86.
- Tamke, M., Stasiuk, D. and Ramsgaard Thomsen, M.: 2013, The Rise: Material Behaviour in Generative Design, *Proceedings of ACADIA 2013: Adaptive Architecture*, pp. 379–388.
- Tamke, M., Zwierzycki, M., Deleuran, A. H., Baranovskaya, Y. S., Tinning, I. K. F. and Thomsen, M. R.: 2017, Lace Wall: Extending Design Intuition through Machine Learning, *Fabricate 2017*, pp. 98–105.
- Temporärer Pavillon in Noda / Temporary Pavilion in Noda*: 2012, *DETAIL* (10), 1086–1088.
- Thompson, D. W.: 1917, *On Growth and Form*, University Press, Cambridge.
- Thomsen, M. R., Tamke, M., Deleuran, A. H., Tinning, I. K. F., Evers, H. L., Gengnagel, C. and Schmeck, M.: 2015, Hybrid Tower, Designing Soft Structures, *Modelling Behaviour: Design Modelling Symposium 2015*, Copenhagen, Denmark.
- Timoshenko, S. P. and Gere, M. J.: 1961, *Theory of Elastic Stability*, McGraw - Hill Book Company.
- Todisco, L., Peiretti, H. C. and Mueller, C.: 2016, Funicularity through External Post-Tensioning : Design Philosophy and Computational Tool, *Journal of Structural Engineering* **142**(2), 1–9.
- Tornabell, P., Soriano, E. and Sastre, R.: 2014, Pliable Structures with Rigid Couplings for Parallel Leaf-Springs: A Pliable Timber Torus Pavilion, *Mobile and Rapidly Assembled Structures IV*, Vol. 136, WIT Transactions on the Built Environment, pp. 117–128.
- Tournès, D.: 2003, Junius Massau et l'Intégration Graphique, *Revue d'histoire des mathématiques* **9**, 181–252.
- Van Mele, T., De Laet, L., Veenendaal, D., Mollaert, M. and Block, P.: 2013, Shaping Tension Structures with Actively Bent Linear Elements, *International Journal of Space Structures* **28**(3-4), 127–136.
- Varignon, P.: 1725, *Nouvelle Mécanique ou Statique*, Joubert, Paris.
- Vogel, S.: 1992, Twist-to-bend ratios and cross-sectional shapes of petioles and stems, *Journal of Experimental Botany* **43**(11), 1527–1532.
- Weinand, Y. and Hudert, M.: 2010, Timber Fabric, Applying Textile Principles on a Building Scale, *Architectural Design - Structuralism* **80**(4), 102–107.

Wolfe, W. S.: 1921, *Graphical Analysis; a Text Book on Graphic Statics*, McGraw- Hill Book Company, New York.

Zhang, A. and Chen, G.: 2013, A Comprehensive Elliptic Integral Solution to the Large Deflection Problems of Thin Beams in Compliant Mechanisms, *Journal of Mechanisms and Robotics* **5**.

List of Figures

(Only figures that are not original by the author are listed)

Figure 1.1 Lightweight structures

Hyperbolic tower by Vladimir Shukhov (1922): [Online Image] Available from: <http://theconstructivistproject.com/en/object/7/shukhov-tower> (Accessed 2019-10-19) [Photo credits: Natalia Melikova 2014].

Los Manantiales shell structure by Félix Candela (1958): [Online Image] Available from: <https://www.archdaily.com/496202/ad-classics-los-manantiales-felix-candela/> (Accessed 2019-10-15) [Photo credits: unknown].

Models by Robert Le Ricolais (1945): Langlois, G.-A.: 2017, *À Yaoundé, la halle APLEX ultime de Robert Le Ricolais*. [Photo credits: D. R.].

Figure 1.2 Physical form-finding models

Hanging models by Heinz Isler (1981): [Online Image] Available from: <http://www.explorations-architecturales.com/data/upload/images/hst93.jpg> (Accessed 2019-10-15) [Photo credits: unknown]

Textile membranes and rope nets model for the *German Pavillon 67* by Frei Otto: Hanselka, H., Schielke, J.E., Vrachliotis, G., Kurz, P., (eds): 2017, *Frei Otto. Denken in Modellen*, Leipzig: Spector Books, p. 45.

Figure 1.3 Classification of self-forming processes according to the generating forces by Frei Otto

Gass, S.: 1990, *IL 25 Form Force Mass 5 Experiments*, Institut für leichte Flächentragwerke, p. 2.17.

Figure 1.4 Bending as a self-forming process

Construction of a traditional mudhif house from plant stems (Iraq): Frey, P.: 2010, *Learning from vernacular, towards a new vernacular architecture*, Actes Sud, Arles. [Photo credits: Wilfred Thesiger].

Elastica curve by Euler: Euler, L.: 1744, *Methodus inveniendi, Lineas curvas, Maximi Minimive proprietate gaudentes, Additamentum I, 'De curvis elasticis'*.

Figure 1.5 Lightweight hybrid structural systems

Tensegrity sphere hold by Buckminster Fuller (1979): [Online Image] Available from: <https://www.flickr.com/photos/esquaredfashion/8548434198> (Accessed 2019-10-15) [Photo credits: Bill Ingraham/AP].

Temporary pavilion in Noda by Kazuhiro Kojima + Kojima Laboratory, Tokyo University of Science (2011): [Online Image] Available from: <https://inspiration.detail.de/temporaerer-pavillon-in-noda-100959.html> (Accessed 2019-10-15) [Photo credits: Sadao Hotta].

Figure 1.6 Hybrid bending-active tensile structures

Geodome 4 tent by the North Face company (2018): [Online Image] Available from: <https://www.insidehook.com/article/gear/north-face-geodesic-geodome-4-tent> (Accessed 2019-10-22) [Photo credits: unknown].

Isoropia structure by CITA and collaborators (2018): [Online Image] Available from: <https://kadk.dk/en/case/isoropia> (Accessed 2019-10-22) [Photo credits: Rasmus Hjortshøj].

Figure 1.7 Asian composite bow illustrating how a differentiated bending stiffness along the limb of the bow affects its form in relation to functional aspects

Bergman, C. A. and McEwen, E.: 1997, Sinew-Reinforced and Composite Bows, Technology, Function and Social Implications, in Knecht, H. (ed.), *Projectile Technology*, Springer, Boston, MA, chapter 6, pp. 143–160.

Figure 1.8 Static equilibrium of weights hanging on a cable analysed through graphic statics

Varignon, P.: 1725, *Nouvelle Mécanique ou Statique*, Paris: Joubert.

Figure 2.2 Vernacular bending-active structures

Traditional mudhif collective house by Madans people in Iraq: Frey, P.: 2010, *Learning from vernacular, towards a new vernacular architecture*, Actes Sud, Arles. [Photo credits: Wilfred Thesiger].

Traditional hut by Dorze people in Ethiopia: [Online Image] Available from: <https://www.nomads.org/dorze.html> (Accessed 2019-10-15) [Photo credits: Gordon Clarke].

Figure 2.3 Bending-active arched structures

Forest Pavilion by nArchitects (2011): [Online Image] Available from: https://www.archdaily.com/165393/forest-pavilion-narchitects?ad_medium=gallery (Accessed 2019-10-15) [Photo credits: Iwan Baan].

AA/ETH Pavilion (2011): [Photo credits: AA(EmTech) and Chair of Structural Design, ETH Zurich].

Figure 2.4 Bending-active grid-shells

Mannheim Multihalle by Carlfried Mutschler & Partners, Frei Otto and Ove Arup & Partners (1975): [Online Image] Available from: <https://mannheim-multihalle.de/en/blog-2/the-architects/> (Accessed 2019-10-15).

Pannikar Pavilion by CODA (2014): [Online Image] Available from: <http://coda-office.com/work/Panikkar> (Accessed 2019-10-15).

UWE Pavilion by the University of West of England and Format Engineers (2016): [Online Image] Available from: <https://formatengineers.com/research/UWE-pavilion.html> (Accessed 2019-10-15).

Figure 2.5 Bending-active shells

Geodesic Plydome by Buckminster Fuller (1957): Fuller, R. B.: 1975, *Synergetics, Explorations in the Geometry of Thinking*, Macmillan Publishing Co., New-York.

ICD/ITKE Research Pavilion 2010 by ICD/ITKE University of Stuttgart (2010): Knippers, J.: 2011, Digital Technologies for Evolutionary Construction, in C. Gengnagel, A. Kilian, N. Palz, F. Scheurer (eds), *Computational Design Modelling*, Springer, pp. 47–54. [Photo credits: Roland Halbe].

Bend9 pavilion by Riccardo La Magna: Schleicher, S. and La Magna, R.: 2016, Bending-active plates: Form-Finding and Form-Conversion, *Posthuman Frontiers: Data, Designers, and Cognitive Machines - Proceedings of the 36th Annual Conference of the Association for Computer Aided Design in Architecture, ACADIA 2016*, pp. 260–269.

Figure 2.6 Bamboo bending-active frames and trusses

Sports hall in Thailand by Chiangmai Life Architects and Construction (2017): [Online Image] Available from: <https://www.dezeen.com/2017/08/21/chiangmai-life-architects-construction-sports-hall-panyaden-international-school-thailand-arching-bamboo-trusses/> (Accessed 2019-10-15) [Photo credits: Alberto Cosi].

Conference hall in Da Nang by in Vietnam by Vo Trong Nghia (2015): [Online Image] Available from: <https://www.designboom.com/architecture/vo-trong-nghia-architects-conference-hall-naman-spa-and-resort-vietnam-10-19-2015/> (Accessed 2019-10-15) [Photo credits: Hiroyuki Oki].

Figure 2.7 Bending-active tensile structures

Isoropia structure by CITA and collaborators (2018): [Online Image] Available from: <https://kadk.dk/en/case/isoropia> (Accessed 2019-10-22) [Photo credits: Rasmus Hjortshøj].

Hybrid structure by MPDA19 Studio 2, BarcelonaTech (2019): [Online Image] Available from: <https://www.mpda.upc.edu/studio-2> (Accessed 2019-10-22) [Photo credits: Andrés Flajszer].

Form Follows Tension installation by Chair of Structural Design, Technische Universität München (2015): Schling, E. et al.: 2015, Bending-Activated Tensegrity, *Proceedings of the IASS Symposium 2015*, Amsterdam, The Netherlands. [Photo credits: Matthias Kestel].

Figure 2.9 Bending-active tensile structures with coated woven membranes

Permanent umbrella in Marrakech by the Institute of Building Structures and Structural Design, University of Stuttgart (2011): [Online Image] Available from: <https://www.itke.uni-stuttgart.de/archives/portfolio-type/biegeaktives-membrandach> (Accessed 2019-10-22).

Bending-active textile hybrid sculpture by Lienhard, Hafen City University Hambourg (2017): [Online Image] Available from: <https://www.kiwi3d.com/theory/> (Accessed 2019-10-22).

Modular self-tensioned bending-active canopy by Vrije Universiteit Brussel (2013): De Laet, L. et al.: 2013, Case study: A modular, self-tensioned, bending-active canopy, *Proceedings of the IASS Annual Symposium 2013*, Wroclaw, Poland.

Figure 2.10 Bending-active tensile structures with a bespoke knitted membrane

sensoryPLAYSCAPE (v1.0) by Taubman College of Architecture and Urban Planning, University of Michigan (2015): [Online Image] Available from: <http://www.materialarchitectures.com/social-sensory> (Accessed 2019-10-22).

Hybrid Tower by CITA, The Royal Danish Academy of Fine Arts (2014): [Online Image] Available from: <https://www.complexmodelling.dk/?p=1088> (Accessed 2019-10-22) [Photo credits: Anders Ingvarlsen].

Figure 2.11 Bending-active elements restrained with cables

Windshape installation by nArchitects (2006): [Online Image] Available from: https://www.archdaily.com/4608/windshape-narchitects/500ef62028ba0d0cc7000fe1-windshape-narchitects-image?next_project=no [Accessed 22/10/19] [Photo credits: nArchitects].

Lace Wall installation by CITA (2016): [Online Image] Available from: <https://www.facebook.com/citacph/photos/pcb.1474692905878367/1474701375877520/?type=3&theater> (Accessed 2019-10-22).

TemporActive pavilion by Politecnico di Milano (2019): Mazzola, C. et al.: 2019, TemporActive Pavilion: first loop of design and prototyping of an ultra-lightweight temporary architecture, *Proceedings of the TensiNet Symposium 2019*, Milan, Italy, pp. 390–401.

Figure 2.12 Form-finding of the *Multihalle Mannheim* elastic grid-shell

Hanging chain model (1975): [Online Image] Available from: <https://www.detail-online.com/article/research-development-and-daring-frei->

otto-wins-the-pritzker-prize-26524/ (Accessed 2019-10-22) [Photo credits: Atelier Frei Otto Warmbronn].

Comparison between *Elastica* and catenary curves: Lienhard, J.: 2014, *Bending-Active Structures: Form-finding strategies using elastic deformation in static and kinematic systems and the structural potentials therein*, PhD thesis, Universität Stuttgart, Stuttgart.

Figure 2.19 Form-finding of bending-active plate structures based on a finite element analysis

Classical mesh-based approach with *SoFiSTiK*'s software: Schleicher, S. et al.: 2015, Form-Finding and Design Potentials of Bending-Active Plate Structures, in *Modelling Behaviour: Design Modelling Symposium 2015*, Springer, p. 53–63.

Isogeometric analysis with *Kiwi!3D* new plugin for *Grasshopper*: [Online Image] Available from: <https://www.kiwi3d.com/theory/> (Accessed 2019-10-22).

Figure 2.20 Design of *Isoropia* structure by CITA, Royal Danish Academy of Fine Arts, and collaborators (2018)

Picture on the left: [Online Image] Available from: <https://www.designboom.com/architecture/danish-pavilion-possible-spaces-venice-biennale-05-30-2018/> (Accessed 2019-10-22) [Photo credits: Rasmus Hjortshøj].

Figures on the right: La Magna, R. et al.: 2018, *Isoropia: an Encompassing Approach for the Design, Analysis and Form-Finding of Bending-Active Textile Hybrids*, *Proceedings of the IASS Annual Symposium 2018*, Boston, USA.

Figure 2.21 Physical models used as a generative driver of the design of bending-active structures

Model of the arched roof of *Isoropia* structure by CITA, Royal Danish Academy of Fine Arts, and collaborators (2018): La Magna, R. et al.: 2018, *Isoropia: an Encompassing Approach for the Design, Analysis and Form-Finding of Bending-Active Textile Hybrids*, *Proceedings of the IASS Annual Symposium 2018*, Boston, USA.

Exploration of bending-active arched structures by IACC and CITA (2014): [Online Image] Available from: <https://cargocollective.com/efilenabaseta/Adaptive-Self-parametrisation/> (Accessed 2019-10-22).

Conceptual model for the design of the *Lace Wall* installation by CITA, Royal Danish Academy of Fine Arts (2016): [Online Image] Available from: <https://kadm.dk/case/lace-wall> (Accessed 2019-10-22).

Figure 2.22 Construction of bending moment diagrams and elastic curves with graphic statics by Karl Culmann

Addis, B.: 2007, *Building: 3000 Years of Design Engineering and Construction*, Phaidon, London & New-York, p. 372.

Acknowledgments

First of all, I would like to thank my supervisor, Prof. Dr. Joseph Schwartz, who supervised my work throughout this doctoral thesis. I am deeply grateful to him for giving me the opportunity to be part of the research and teaching team he heads as the Chair of Structural Design at the ETH Zurich. Throughout my work, I felt supported by his enthusiasm for my research, the quality of his scientific inputs, and by the freedom he gave me in pursuing my interests. All this demonstrates his trust and open-mindedness towards my work. Moreover, I would like to express my sincere appreciation for his very caring attitude when encouraging and accompanying me in my professional and personal development.

Furthermore, I would like to express my deep gratitude to my co-director, Ass. Prof. Dr. Juan José Castellón, for his relevant remarks and the very inspiring discussions which enriched my work. He was able to share his enthusiasm and his stimulating vision of architecture. I was particularly receptive to his availability and the constant attention he paid to my questions.

I would like to thank all my colleagues at the Chair of Structural Design who, through shared teaching activities, discussions and convivial moments have supported me over the years, each in their own way. In particular, I would like to thank Pierluigi D'Acunto for his encouragement and sincere interest in my work and who, together with Juan José Castellón and Federico Bertagna, whom I would also like to thank, took part in the development of the project presented in Chapter 5 of this thesis. I would also like to warmly thank Katerina Chalvatzi, Roshanak Haddadi, Giulia Boller and Davide Tanadini for their daily friendly support and Lukas Ingold who translated the abstract of this thesis into German.

My sincere appreciation goes to Alessandro Tellini, from the Rapid Laboratory of Fabrication, ETH Zurich, for his generous help whenever I needed support and advice to build physical models and prototypes.

I gratefully acknowledge the grant received towards my doctoral studies from the Doctoral Program in Architecture & Technology of the Institute of Technology in Architecture, ETH Zurich, which has partially funded my research. Special thanks go to Yvonne Mossmann for her kindness and her support in any administrative steps.

I am extremely grateful to Prof. Dr. Delia Dumitrescu who introduced me to the world of Textile Design by generously inviting me to attend a knitting

technology course at the Swedish School of Textile, University of Borås, Sweden, in the autumn of 2017. These very inspiring weeks allowed me to discover the wide range of possibilities offered by knitted textiles and in particular the potential of their use in bending-active tensile systems as well as more widely in architecture.

Finally, I would like to give my warmest thanks to my family and close friends for their invaluable support and continuous encouragement.

